

# Analytical and Numerical Investigation of the Ultra-Relativistic Euler Equations

## Dissertation

zur Erlangung des akademischen Grades

doctor rerum naturalium  
(Dr. rer. nat.)

von **Mahmoud Abdelaziz Elbiomy Abdelrahman**  
geb. am 26.02.1983 in Elmansoura, Egypt

genehmigt durch die Fakultät für Mathematik  
der Otto-von-Guericke-Universität Magdeburg

Gutachter:

Prof. Dr. Matthias Kunik

Prof. Dr. h.c. Hans-Dieter Alber

Eingereicht am: 04. 09. 2013

Verteidigung am: 04. 11. 2013



## Acknowledgements

Praise be to ALLAH the lord of the world, Eternal Guardian of the heavens and earth. I praise Him for His favors and ask Him to increase His grace.

Firstly, I would like to express my thankfulness and gratitude to my country Egypt for supporting me during my research to finish Ph.D degree.

I would like to express my deep appreciation and gratitude to my supervisor **Prof. Dr. Matthias Kunik** for giving me an initiative to this research. He introduced me to the interesting field of conservation laws. His inspiring guidance, remarkable suggestions, encouragement, continuous guidance, and friendly discussions enabled me to complete the research work and this thesis efficiently. He spared a lot of his priceless time in advising and helping me throughout the research work.

I am also very grateful to **Prof. Dr. Gerald Warnecke** for constant encouragement, remarkable suggestions during my studies. In his group I have found a very good atmosphere to do research. Due to his generous support, I attended many international conference and workshops in Europe and Canada.

Further acknowledgment goes to **Prof. Dr. Hans-Dieter Alber** who accepted to review my thesis, for his repetitive support and for valuable comments and suggestions.

Many thanks go to all members of the research group of **Prof. Warnecke**, with special thanks go to **Dr. Walfred Grambow** and **Mrs. Stephanie Wernicke** for their helping. I also would like to thank **Robin Gröpler** and **Carlos Cueto Camejo** for the interesting scientific discussions and for their friendly support.

I wish to express my deep obligation to my parents for their sacrifices during the pursuance of my education. It is indeed of the prayers of my parents and well wishers that I have been able to complete my Ph.D. studies. Their encouragement and inspiration have always been with me.

I would like to take this opportunity to express my warm thankfulness to my mother **Nabiha Mowafi**, to my brothers **Ahmed** and **Mohamed**, my sister **Mona** and to every member in my extended family for their unconditional love and support.

Last but not least I am heartily thankful to my wife **Yasmin Omar**, to my son **Ahmed** and my daughter **Nour**. Their love, care, support and advice have encouraged me to work hard for this degree.

Finally I would like to dedicate this thesis to the soul of my father, he was there for the beginning of this degree, and did not make it to the end. His love, support, and constant care will never be forgotten. He is very much missed.

**Mahmoud Abdelaziz Elbiomy Abdelrahman**  
**Magdeburg, Germany**

## Abstract

In this thesis we study the ultra-relativistic Euler equations for an ideal gas, which is a system of nonlinear hyperbolic conservation laws. These equations are described in terms of the pressure  $p$ , the spatial part  $\mathbf{u} \in \mathbb{R}^3$  of the dimensionless four-velocity and the particle density  $n$ . We analyze the single shocks and rarefaction waves and give the solution of the Riemann problem in a constructive way. We also prove that this solution is unique. Especially we develop an own parametrization for single shocks, which will be used to derive a new explicit shock interaction formula. We use this formula to give an interesting example for the non-backward uniqueness of our hyperbolic system. The cone-grid scheme presented here is based on the Riemann solution for the ultra-relativistic Euler equations, it is unconditionally stable, i.e. no Courant-Friedrichs-Levy (CFL) condition is needed. This cone-grid scheme guarantees a positive pressure and particle density for all later times, provided that these positivity properties are satisfied for the initial data.

We present a new function, which measures the strengths of the waves of the ultra-relativistic Euler equations, and derive sharp estimates for these strengths. The interpretation of the strength for the Riemann solution is also given. This function has the important implication that the strength is non increasing for the interactions of waves for our system. This study of interaction estimates also allows us to determine the type of the outgoing Riemann solutions. It is also plays an important role in order to estimate the total variations of solutions. We have not seen a similar function for other hyperbolic systems. In the most studies about the hyperbolic systems of conservation laws a more classical approach is familiar, which uses the change of Riemann invariants as a measure of wave strength.

Further, we present a new front tracking technique for the ultra-relativistic Euler equations in one space dimension. The basic ingredient for our new scheme is the front tracking Riemann solution. In this Riemann solution we approximate the continuous rarefaction waves by a finite collection of discontinuities, so called non-entropy shocks (fronts). Most standard front tracking methods allow some non-physical waves, i.e. the Rankine-Hugoniot conditions are not satisfied in general. In contrast, our new front tracking technique for the ultra-relativistic Euler equations gives only exact weak solutions.

For the comparison of the numerical results, we give the results of exact Riemann solution, cone-grid and front tracking schemes for the one-dimensional ultra-relativistic Euler equations. The CFL condition in the ultra-relativistic case is very simple and independent from the initial data, which is  $\Delta t = \frac{\Delta x}{2}$ . This CFL condition comes out automatically due to the structure of light cones, since every signal speed is bounded by the velocity of light, which is normalized to one in dimensionless form. The numerical examples show excellent accuracy of the schemes as well as sharp resolution of the solutions.

Finally, we study the interaction estimates of the generalized shocks (entropy and non-entropy shocks) of the ultra-relativistic Euler equations and the outgoing asymptotic Riemann solution.

## Zusammenfassung

In dieser Arbeit studieren wir die ultrarelativistischen Eulergleichungen für ein ideales Gas, ein System nichtlinearer hyperbolischer Erhaltungsgleichungen. Diese sind Gleichungen für den Druck  $p$ , den räumlichen Anteil  $\mathbf{u} \in \mathbb{R}^3$  der Vierergeschwindigkeit und der Teilchenzahldichte  $n$ . Nach dem Studium einzelner Stoßwellen und Verdünnungsfächer lösen wir das Riemannsche Anfangswertproblem explizit. Wir zeigen die Eindeutigkeit der Lösungen. Wir entwickeln für die Beschreibung von Stoßwellen-Interaktionen eine eigene Parametrisierung, die für verschiedene Familien von Stößen auf eine explizite Druckformel nach der Stoßinteraktion führt. Wir verwenden diese Formel, um ein interessantes Beispiel für "non backward uniqueness" der ultrarelativistischen Eulergleichungen anzugeben. Ein hier vorgestelltes numerisches Kegelschema basiert auf Riemann-Lösungen für dieses System, es ist stabil, erfüllt die CFL-Bedingung und erhält Positivität von Druck und Teilchenzahldichte.

Wir führen eine neue Funktion ein, die die Stärke der elementaren Wellen beschreibt, und leiten hierzu scharfe Ungleichungen ab. Die Interpretation der Stärke Riemannscher Anfangsdaten ist ebenfalls gegeben. Diese Funktion hat die wichtige Eigenschaft, dass die Stärke auch für beliebige Wellen-Interaktionen unseres Systems monoton fallend mit der Zeit ist. Dieses Studium der Welleninteraktion gestattet auch die Bestimmung des Types der transmittierten Wellen. Es kann dazu verwendet werden, eine natürliche Totalvariation der Lösungen zu jeder Zeit zu definieren. Wir haben für andere hyperbolische Systeme ein vergleichbares Resultat noch nicht gesehen. In den meisten Arbeiten über hyperbolische Erhaltungsgleichungen ist stattdessen ein eher klassischer Zugang üblich, der Änderungen der Riemann-Invarianten als ein Maß für die Stärke der Wellen verwendet.

Weiterhin präsentieren wir eine neue Front-Tracking Methode für die ultrarelativistischen Eulergleichungen in einer Raumdimension. Der wichtigste Baustein hierfür ist ein eigener Riemann-Löser. Der Front-Tracking Riemann-Löser approximiert einen kontinuierlichen Verdünnungsfächer durch eine endliche Anzahl von Verdünnungsstößen (non entropy shocks). Während andere Front-Tracking Methoden auch nicht physikalische Lösungen gestatten, die die Rankine-Hugoniot Gleichungen verletzen, ist dies bei unserem Front-Tracking Riemann-Löser nicht der Fall. Wir erhalten somit exakte schwache Lösungen, deren Entropieverletzung kontrollierbar bleibt.

Wir vergleichen die exakte Riemann-Lösung mit den Lösungen vom Kegelschema und unserer Front-Tracking Methode für die ultrarelativistischen Eulergleichungen in einer Raumdimension. Die CFL-Bedingung ist hierbei sehr einfach, und unabhängig von den Anfangsdaten gegeben durch

$$\Delta t = \frac{1}{2} \Delta x.$$

Sie kommt aus der Invarianz der Lichtgeschwindigkeit unter Lorentz-Transformationen. Die numerischen Beispiele zeigen sehr gute Übereinstimmung und eine scharfe Auflösung.

Schliesslich studieren wir die Welleninteraktionen auch mit verallgemeinerten Stössen, die die Rankine-Hugoniot Gleichungen erfüllen, aber nicht unbedingt die Entropiegleichung.



---

# Contents

<b>1</b>	<b>Introduction</b>	<b>1</b>
1.1	Overview . . . . .	1
1.2	New results . . . . .	4
1.3	Outline . . . . .	6
<b>2</b>	<b>The Relativistic Euler Equations</b>	<b>9</b>
2.1	Lorentz-transformations . . . . .	9
2.2	Vectors and tensors . . . . .	11
2.2.1	Tensor calculus . . . . .	12
2.3	Light cone . . . . .	14
2.3.1	Einstein velocity addition . . . . .	15
2.4	Notions on conservation laws . . . . .	16
2.4.1	Hyperbolic systems of conservation laws . . . . .	16
2.4.2	The Riemann problem . . . . .	18
2.5	Relativistic Euler equations . . . . .	20
<b>3</b>	<b>Ultra-Relativistic Euler Equations</b>	<b>23</b>
3.1	Introduction . . . . .	23
3.2	The $(p, u)$ system . . . . .	25
3.2.1	Jump conditions . . . . .	29
3.3	Parametrizations of single shocks and rarefaction waves . . . . .	32
3.3.1	Single shocks . . . . .	32
3.3.2	Rarefaction waves . . . . .	38
3.4	Solution of the Riemann problem . . . . .	40
3.5	Riemann invariants . . . . .	43
3.6	Cone-grid scheme for the one-dimensional ultra-relativistic Euler equations	47
3.6.1	The computational domain . . . . .	48
3.6.2	The construction of the solution . . . . .	50
3.6.3	Formulation of the cone-grid scheme . . . . .	51
3.6.4	Positivity of pressure and particle density for the cone-grid scheme .	52
3.7	The hyperbolic four-field system . . . . .	53
3.7.1	The corresponding with the ultra-relativistic Euler equations . . . .	54
3.7.2	Numerical examples . . . . .	55

# CONTENTS

---

<b>4</b>	<b>The Uniqueness Problem for the Ultra-Relativistic Euler Equations</b>	<b>57</b>
4.1	Introduction . . . . .	57
4.2	Uniqueness of the Riemann solutions . . . . .	57
4.3	Shock interaction . . . . .	60
4.4	Non-backward uniqueness for nonlinear hyperbolic conservation laws . . . . .	63
4.4.1	Burgers equation . . . . .	63
4.4.2	Ultra-relativistic Euler equations . . . . .	65
<b>5</b>	<b>The Interaction of Waves for the Ultra-Relativistic Euler Equations</b>	<b>71</b>
5.1	Introduction . . . . .	71
5.2	Strength of the waves . . . . .	72
5.2.1	Strength function $S(\alpha, \beta)$ . . . . .	74
5.2.2	Interpretation of $S(\alpha, \beta)$ for general Riemannian initial data: . . . . .	80
5.3	Wave interactions with non increasing strength . . . . .	82
5.3.1	The cases with conservation of strength . . . . .	83
5.3.2	The cases with strictly decreasing strength . . . . .	90
<b>6</b>	<b>The Front Tracking Scheme</b>	<b>103</b>
6.1	Introduction . . . . .	103
6.2	Front tracking scheme . . . . .	106
6.2.1	Single non-entropy shocks . . . . .	106
6.2.2	The discretization of rarefaction waves . . . . .	108
6.2.3	Front tracking Riemann solution . . . . .	111
6.3	Numerical results . . . . .	115
<b>7</b>	<b>Basic Estimates for the Front Tracking Algorithm for the Ultra-Relativistic Euler Equations</b>	<b>125</b>
7.1	Introduction . . . . .	125
7.2	Interaction estimates . . . . .	127
7.2.1	The cases with conservation of strength . . . . .	128
7.2.2	The cases with strictly decreasing strength . . . . .	133
7.2.3	The cases with conservation of strength in the limit . . . . .	143
<b>8</b>	<b>Conclusions and Outlook</b>	<b>151</b>
<b>A</b>	<b>The Lorentz Invariance of the Ultra-Relativistic Euler Equations</b>	<b>155</b>
<b>B</b>	<b>Mathematical Properties of the <math>3 \times 3</math> Ultra-Relativistic Euler Equations</b>	<b>161</b>
<b>C</b>	<b>Front Tracking Algorithm</b>	<b>165</b>
	<b>Bibliography</b>	<b>167</b>
	<b>Curriculum Vitae</b>	<b>176</b>

---

# Chapter 1

## Introduction

### 1.1 Overview

Hyperbolic systems describe the propagation of waves with finite velocities, which in special relativity are naturally bounded by the speed of light. This fact is reflected in the beautiful and interesting mathematical structure of the relativistic Euler equations. Nevertheless the relativistic Euler equations considered here seem to look complicated, an intensive study shows a simpler mathematical behavior than the corresponding classical Euler equations. For example, even the solution of the standard shock tube or Riemann problem for the classical Euler equations of gas dynamics may lead to a vacuum region within the shock tube that complicates a rigorous mathematical analysis for the general initial value problem. However, we will see that at least for the so called ultra-relativistic Euler equations this behavior will not occur.

Euler's equations (relativistic or classic) deal with an ideal gas in local equilibrium, in which mean free paths and collision free times are so short that perfect isotropy is maintained about any point moving with the gas. For more details we refer to the textbook of Weinberg [79, Chapter 10] which gives a short introduction to special relativity and relativistic hydrodynamics with further literature also for the imperfect fluid (gas), see for example the papers of Eckart [31, 32, 33].

There is another interesting model which is equivalent to the ultra-relativistic Euler equations. This system of hyperbolic conservation laws describes a phonon-Bose gas in terms of the energy density  $e$  and the heat flux  $Q$ . This system has specific applications in physics, see [26, 27, 28, 29, 30, 42, 45].

A system of usually nonlinear hyperbolic conservation laws in one spacial dimension is a first order quasilinear system of partial differential equations of the form

$$U_t + F(U)_x = 0, \tag{1.1}$$

where  $U = (U_1, \dots, U_n)$  are the conserved quantities and  $F(U) = (F_1(U), \dots, F_n(U))$  the

## CHAPTER 1. INTRODUCTION

---

fluxes. A primary example is provided by the nonlinear Euler equations describing the evolution of a compressible, non viscous fluid:

$$\begin{cases} \rho_t + (\rho v)_x = 0 & \text{(conservation of mass),} \\ (\rho v)_t + (\rho v^2 + p)_x = 0 & \text{(conservation of momentum),} \\ E_t + v(E + p)_x = 0 & \text{(conservation of energy),} \end{cases} \quad (1.2)$$

where the total energy  $E$  is given by

$$E = \frac{p}{\gamma - 1} + \frac{\rho v^2}{2}, \quad 1 < \gamma < 3, \quad (1.3)$$

here  $\gamma$  is the ratio of specific heats,  $\rho$  is the density and  $v$  is the velocity. Also due to the  $\gamma$ -gas law the specific internal energy  $e$  and pressure  $p$  are related as  $p = (\gamma - 1)\rho e$ . These differential equations are a particular example of a system of conservation laws, which constitute a strictly hyperbolic system with the characteristic velocities

$$\lambda_1 = -\sqrt{\gamma \frac{p}{\rho}}, \quad \lambda_2 = v, \quad \lambda_3 = \sqrt{\gamma \frac{p}{\rho}}. \quad (1.4)$$

It is well known that even for smooth initial data, discontinuities form in the fluid variables in the solution to the Cauchy problem in finite time, [21]. The differential equations (1.2) are not sufficient if we take into account shock discontinuities. Therefore we choose a weak integral formulation with a piecewise  $C^1$ -solution  $\rho, v, p : (0, \infty) \times \mathbb{R} \mapsto \mathbb{R}$ ,  $\rho, p > 0$ , which is given due to Oleinik [66] by curve integrals in time and space, namely

$$\begin{aligned} \oint_{\partial\Omega} \rho \, dx - (\rho v) \, dt &= 0, \\ \oint_{\partial\Omega} (\rho v) \, dx - (\rho v^2 + p) \, dt &= 0, \\ \oint_{\partial\Omega} E \, dx - v(E + p) \, dt &= 0. \end{aligned} \quad (1.5)$$

Here  $\Omega \subset \mathbb{R}_0^+ \times \mathbb{R}$  is a convex set in space-time with piecewise smooth, positive oriented boundary.

Note that this weak formulation takes discontinuities into account, since there are no derivatives of the field involved. If we apply the Gaussian divergence theorem to the weak formulation (1.5) in space-time regions where the solution is regular we come back to

the differential form of the Euler equations (1.2). Furthermore we require that the weak solution (1.5) must also satisfy the entropy-inequality

$$\oint_{\partial\Omega} h dx - \phi dt \geq 0, \quad (1.6)$$

with positive oriented  $\partial\Omega$ . Where the entropy density  $h$  and the entropy flux  $\phi$  are given by

$$h(\rho, p) = \frac{\rho}{\gamma - 1} \ln \left( \frac{p}{\rho^\gamma} \right) + \frac{\rho}{\gamma - 1} (1 + \ln 2\pi), \quad \phi(\rho, v, p) = v \cdot h(\rho, p). \quad (1.7)$$

The early work on the general structure of hyperbolic systems of conservation laws was presented by Lax [50]. Lax's results provided the foundation necessary for Glimm to give the first general existence result in 1965. More precisely, Glimm proved existence of solutions with small total variations to general systems of strictly hyperbolic conservation laws (1.1) with genuinely non-linear or linearly degenerate characteristic fields [36]. For an extensive overview for the theory of the hyperbolic system of conservation laws, we refer to Dafermos [24], Evans [34], Friedrichs [35], Godlewski and Raviart [37], LeVeque [52, 53], Majda [61], Serre [73] and Smoller [74]. We refer to these authors for details on the theory of conservation laws and related issues. A particular feature of the non-linear hyperbolic systems of conservation law is the appearance of shock waves.

An alternative way to construct approximate solutions to the general Cauchy problem is by front tracking method. This method was first proposed by Dafermos [22] to study scalar conservation laws, then adapted by DiPerna [25] to the case of  $2 \times 2$  systems and extended in [10, 12, 70] to general  $N \times N$  systems with genuinely nonlinear or linearly degenerate characteristic fields.

The idea of front tracking method is simple. We require approximate solutions which are piecewise constant, having jumps along a finite number of straight lines in the  $t - x$  plane. For this purpose, at initial time  $t = 0$  we start with an initial data which is piecewise constant. At each point of jump, we construct a piecewise constant approximate solution of the corresponding Riemann problem. Piecing together these local solutions, we obtain a solution  $u = u(t, x)$ , which is well defined until the first time  $t_1$  where the interaction of two lines of discontinuity take place. In this case, the solution can be further prolonged in time by solving the new Riemann problem determined by the interaction. This yields an approximate solution valid up to the next time  $t_2 > t_1$  where two more fronts interact. Again we solve the corresponding Riemann problem, thus extending the solution further in time, and so on. Early applications of the front tracking method to special systems are found in the papers of Alber [4, 5], Lin [54] and Wendroff [80].

In the theory of the classical Euler equations one has to assume a bound for the characteristic speeds, which depend on the choice of the initial data in order to obtain a CFL-condition for the numerical schemes. In the relativistic theory every signal speed is bounded by the velocity of light, independent from the choice of the initial data. Hence

## CHAPTER 1. INTRODUCTION

---

the CFL condition in the ultra-relativistic case is very simple, namely  $\frac{1}{2}\frac{\Delta x}{\Delta t} = 1$  for the dimensionless speed of the light. This CFL condition follows automatically due to the natural structure of light cones.

It is known that many numerical methods developed for the relativistic Euler equations are based on a macroscopic continuum description. The reason is, that they solved a phenomenological form of the relativistic Euler equations, see Kunik et al. [49] and Martí et al. [41, 62, 63]. These are the relativistic Euler equation which can be obtained by using the classical constitutive relation for the internal energy density and gamma-gas law. Since these equations are in Lorentz invariant form, they are still relativistic Euler equations.

### 1.2 New results

In this thesis, we are concerned with analytical and numerical investigation of the ultra-relativistic Euler equations. The equations that describe the relativistic gas dynamics are system of nonlinear hyperbolic conservation laws. We study the relativistic equations for a perfect fluid in Minkowski space-time, which can be written in the following form by using Einstein's summation convention in [79]:

$$\frac{\partial T^{\alpha\beta}}{\partial x^\beta} = 0, \quad \frac{\partial N^\alpha}{\partial x^\alpha} = 0, \quad (1.8)$$

where

$$T^{\alpha\beta} = -pg^{\alpha\beta} + 4pu^\alpha u^\beta \quad (1.9)$$

denotes the energy-momentum tensor for the ideal ultra-relativistic gas. Here  $p$  represents the pressure,  $\underline{u} \in \mathbb{R}^3$  is the spatial part of the four-velocity  $(u^0, u^1, u^2, u^3) = (\sqrt{1 + |\underline{u}|^2}, \underline{u})$  and  $g^{\alpha\beta}$  denotes the flat Minkowski metric, which is

$$g^{\alpha\beta} = \begin{cases} +1, & \alpha = \beta = 0, \\ -1, & \alpha = \beta = 1, 2, 3, \\ 0, & \alpha \neq \beta, \end{cases} \quad (1.10)$$

and

$$N^\alpha = nu^\alpha \quad (1.11)$$

denotes particle-density four-vector, where  $n$  is the proper particle density. For more details see [79, Part one, pg. 47-52]. In this thesis we study the spatially one dimensional case in detail see Appendix A and B.

We first analyze the single shocks and rarefaction waves of the ultra-relativistic Euler equations and solve the Riemann problem in a constructive way. Whereas the basic ingredients for Riemann solutions are the parametrizations of shocks and rarefaction waves. We also prove that the solution of the Riemann problem is unique. Especially we develop

an own parametrization for single shocks, which will be used to derive a new explicit shock interaction formula. This shock interaction formula plays an important role in the study of the ultra-relativistic Euler equations. One application will be presented in Chapter 4, namely the construction of explicit solutions including shock fronts, which gives an interesting example for the non-backward uniqueness of our hyperbolic system. Backward uniqueness problem is reviewed, it means the following: If we know the solution at one time, then we can reconstruct the solution in the past. The transformation  $t \rightarrow -t$  does not leave the weak form of the equations including entropy inequality invariant. In Smoller [74, Chapter 15, §E] one can find a simple example for non-backward uniqueness for the nonlinear scalar conservation laws, Burgers equation. To show this for the ultra-relativistic Euler equations uses a similar idea, but is much more complicated to realize. We give a counterexample to show that there is no backward uniqueness for the ultra-relativistic Euler equations. Whereas the other application will present in Chapters 6 and 7.

In this thesis we give a new function, which measures the strengths of the waves in the Riemann solution in a natural way, and derive sharp estimates for these strengths. We obtain formulas for the strength of the elementary waves, which are given in explicit algebraic expressions. We also give the interpretation of the strength for the Riemann solution for the ultra-relativistic Euler equations. This function has interesting applications, one of this is presented in Section 5.3. It is also plays an important role in order to estimate the total variations of solutions. We have not seen a similar function for other hyperbolic systems. In the most papers about hyperbolic systems of conservation laws a more classical approach is familiar, which uses the change of Riemann invariants as a measure of wave strength, see [25, 67, 81] and references therein.

We are interested in the interaction estimates of nonlinear waves for the ultra-relativistic Euler system. More precisely, we consider the interaction of two shocks, of a shock and a centered rarefaction wave and of two centered rarefaction waves producing transmitted waves. Our study of interaction of waves also allows us to determine the type of the outgoing Riemann solutions. In fact our strength function enables us to show that the strength after interactions of single waves is non increasing.

In this thesis, we present two schemes in order to solve the initial value problems of the ultra-relativistic Euler equations, namely a cone-grid and a new front tracking schemes. The cone-grid scheme is based on the Riemann solution for the ultra-relativistic Euler equations, it is unconditionally stable. This cone-grid scheme preserve the properties like conservations laws, entropy inequality, positivity. This scheme gives sharp shock resolution.

The new front tracking technique for the ultra-relativistic Euler equations is based on the front tracking Riemann solution. In this Riemann solution we discretize a continuous rarefaction waves by a finite collection of discontinuities, so called non-entropy shocks (fronts). We call entropy and non-entropy shocks by the generalized shocks. So the

## CHAPTER 1. INTRODUCTION

---

scheme is based on approximations to the solutions of the local Riemann problems, where the solution is represented by constant states separated by straight line shock segments. The solution procedure for an initial value problem takes care for the interaction of these shock segments of the neighbored local Riemann problems. At each intersection point the discontinuous solution is again equal to the initial conditions of a new local Riemann problem. The straight line shocks can again intersect with each other and so on.

Most standard front tracking methods [10, 12, 13] allow some non-physical waves, i.e. the Rankine-Hugoniot conditions are not satisfied in general. On the other hand, our new front tracking technique for the ultra-relativistic Euler equations gives only exact weak solutions. It is well known that the vacuum state cannot be connected to another state by a single shock satisfying the Rankine-Hugoniot conditions. However, we can prove that the vacuum state cannot appear for the ultra-relativistic Euler equations, provided it is not presented in the initial data. This is not the case with the classical Euler equations, where the vacuum states may give several complications in analysis as well as numerics.

Since the front tracking technique based on the interaction of the discontinuities (generalized shocks). We study the interaction of these discontinuities. We formulate and prove the fundamental estimates for the interaction of discontinuities.

### 1.3 Outline

The contents of this thesis are organized as follows:

In Chapter 2 we present the basic definitions of the relativistic Euler equations, namely Lorentz-transformations, vectors and tensors, the light cone, Einsteins velocity addition. Since the relativistic Euler system is hyperbolic we present the basic facts of the mathematical theory for hyperbolic systems of conservation laws.

In Chapter 3 we consider the ultra-relativistic Euler equations. These equations are written in differential form as well as in a weak integral form. An entropy inequality is given in weak integral form with an entropy function which satisfies the Gibbs equation, see [45, Section 4.4]. The Rankine-Hugoniot jump conditions and the entropy inequality were used in order to derive a simple parameter representation for the admissible shocks. In Subsection 3.2.1 we start with Lemma 3.2.6, which gives a very simple characterization for the Lax entropy conditions of single shock waves. This lemma is needed to develop a new parametrization for single shocks of our system, namely Proposition 3.3.6, which turns out to be very useful in order to describe shock interaction in Section 4.3. For later purposes we also need some other known parametrizations for single shocks and rarefaction waves, which are also given in this chapter. Also parametrization for the rarefaction fan has been derived here. In Section 3.4 we use these shock and rarefaction parametrizations in order to derive an exact Riemann solution for the one-dimensional ultra-relativistic Euler equations. In Section 3.5 we also compute the Riemann invariants



for the ultra-relativistic Euler equations. In Section 3.6 we introduce a new cone-grid scheme in order to solve the one-dimensional ultra-relativistic Euler equations. We prove that this cone-grid scheme strictly preserves the positivity of pressure and particle density for all later times. In Section 3.7 we present a system of hyperbolic system of conservation laws, which is equivalent to the ultra-relativistic Euler equations. This equivalent system describes a phonon-Bose gas in terms of the energy density  $e$  and the heat flux  $Q$ . Then we present numerical test cases for the solution of the phonon-Bose equations.

In Chapter 4 we consider the uniqueness of the solution of the Riemann problem. We study the uniqueness problem of the Riemann solution as well as the problem of non-backward uniqueness of the ultra-relativistic Euler equations. First we give an important formula for the interaction of shock waves from different families by using the results given in Chapter 3. In this formula the states before shock interaction determine explicitly given algebraic expressions for the intermediate state after the interaction. We have not seen a similar result for other hyperbolic systems. This formula has interesting applications, one of this is presented in Section 4.4 of this chapter. It also plays an important role to obtain sharp shock interaction estimates in Chapter 5. In Section 4.4 we present explicit solutions to give an interesting example of the non-backward uniqueness of the ultra-relativistic Euler equations. This example is one application of the new shock interaction formula given in Section 4.3. The corresponding result for the scalar equation is simple and very well known, but turns out to be much more complicated for our system.

In Chapter 5 we are concerned in the interaction estimates of nonlinear waves for the ultra-relativistic Euler system. In Section 5.2 we introduce the new strength function, which measures the strengths of the waves of the ultra-relativistic Euler equations in a natural way, and derive sharp estimates for these strengths in Proposition 5.2.7. The strength of the waves are given in explicit algebraic expressions. We also give the interpretation of the strength for the Riemann solution for our system. In Section 5.3 we derive the formula (5.1) for the interaction of waves from different families in Propositions 4.3.1 and 5.3.3. We study the interactions between shocks and rarefaction waves in terms of the new strength function and obtain that the strength after interactions is non increasing. The cases where the strength is conserved after interaction is given in Propositions 5.3.4, and the other cases of strictly decreasing strength are considered in Proposition 5.3.5.

In Chapter 6 we present a new front tracking technique for the ultra-relativistic Euler equations in one space dimension. In Section 6.2 we give the parametrizations for the non-entropy shocks, namely Lemma 6.2.3, which turns out to be very useful in order to describe the discretization of rarefaction waves as well as the generalized shocks interaction in Chapter 7. In Subsection 6.2.3 we give the front tracking Riemann solution, which consider the heart for our new scheme. In Section 6.3 we present numerical test cases for the solution of the ultra-relativistic Euler equations. For the comparison we use exact Riemann solution, cone-grid and front tracking schemes. We also calculate the experimental order of convergence and numerical  $L^1$ -stability of these schemes. In this chapter, the front tracking method is considered as a numerical tool to solve the initial

## CHAPTER 1. INTRODUCTION

---

value problem for the ultra-relativistic Euler equations. In fact this method will also serve as an analytical tool.

In Chapter 7 we formulate and prove the fundamental estimates for the interaction of the generalized shocks. We consider the interaction of generalized shocks and the outcoming asymptotic Riemann solution.

Chapter 8 presents a summary to the results and some general conclusions. Some suggestions for future work is also given.

Parts of Chapters 3 and 4 will appear as

- M.A.E. Abdelrahman and M. Kunik. The Ultra-Relativistic Euler Equations, submitted for publication, 2012. Also available as preprint at

[www-ian.math.uni-magdeburg.de/~abdelrah/abdelrahman\\_kunik\\_preprint.pdf](http://www-ian.math.uni-magdeburg.de/~abdelrah/abdelrahman_kunik_preprint.pdf)

A condensed form appear as

- Mahmoud Abdelrahman, Matthias Kunik and Gerald Warnecke, On the Ultra-Relativistic Euler Equations. Proc. Appl. Math. Mech, Darmstadt, Germany 12, 597 - 598 (2012).

Chapter 5 will appear as

- M.A.E. Abdelrahman and M. Kunik. The Interaction of Waves for the Ultra-Relativistic Euler Equations. J. Math. Anal. Appl, 409 (2014), 1140-1158.

Chapter 6 will appear as

- M.A.E. Abdelrahman and M. Kunik. A new Front Tracking Scheme for the Ultra-Relativistic Euler Equations, submitted for publication, 2013. Also available as preprint at

[http://www-ian.math.uni-magdeburg.de/~abdelrah/ultra\\_relativistic.pdf](http://www-ian.math.uni-magdeburg.de/~abdelrah/ultra_relativistic.pdf)

---

## Chapter 2

# The Relativistic Euler Equations

Albert Einstein introduced his theory of special relativity in 1905. Within this framework one can generalize the classical Euler equations to obtain equations that convenient within the theory of relativity. In other words, the relativistic Euler equations are a generalization of the classical Euler equations that account for the effects of special relativity. In the textbook of Weinberg [79, Chapter 10] one can find a short introduction to special relativity and relativistic hydrodynamics. For more details also for the imperfect fluid (gas), see for example the papers of Eckart [31, 32, 33] for the classical and relativistic thermodynamics.

In this chapter we present the basic framework of general relativity. In particular we introduce the Lorentz-transformations, vectors, light cone. Then a short review of mathematical concepts and theory concering hyperbolic system of conservation laws is presented. For an extensive overview for the theory of the general relativity, we refer to Weinberg [79, Part two], Wald [78] and Reintjes [69]. In the last section we study the main features of the relativistic Euler equations. This chapter is of interest on its own, but it also provides the necessary tools for the ultra-relativistic Euler equations presented in Chapter 3. Important input for this chapter came from the textbooks of Weinberg [79, Chapter 10], LeVeque [52, 53], Kunik [45], Qamar [68] and Smoller [74].

### 2.1 Lorentz-transformations

In special relativity the laws of nature are invariant under a particular group of space-time coordinate transformations, called Lorentz-transformations. In order to formulate our theory in a Lorentz-invariant form, we make use of the notations for the tensor calculus used in the textbook of Weinberg [79], with only slight modifications:

1. **The time space coordinates** may be rewritten in terms of a four quantity

$$\tilde{x} = (x^0, x^1, x^2, x^3)$$

according to

$$x^0 = ct, \quad x^1 = x, \quad x^2 = y, \quad x^3 = z. \quad (2.1)$$

## CHAPTER 2. THE RELATIVISTIC EULER EQUATIONS

---

$\tilde{x}$  describe an event in time and space. We may identify  $\tilde{x}$  with this event.

2. **The metric tensor** is

$$g_{\mu\nu} = g^{\mu\nu} = \begin{cases} +1, & \mu = \nu = 0, \\ -1, & \mu = \nu = 1, 2, 3, \\ 0, & \mu \neq \nu. \end{cases} \quad (2.2)$$

In matrix form it can be written as

$$G = \begin{pmatrix} +1 & 0 & 0 & 0 \\ 0 & -1 & 0 & 0 \\ 0 & 0 & -1 & 0 \\ 0 & 0 & 0 & -1 \end{pmatrix}. \quad (2.3)$$

3. **The proper Lorentz-transformations** are linear transformations  $\Lambda^\alpha_\beta$  from one system of space-time with coordinates  $x^\alpha$  to another system  $x'^\alpha$ . They must satisfy

$$x'^\alpha = \Lambda^\alpha_\beta x^\beta, \quad g_{\mu\nu} = \Lambda^\alpha_\mu \Lambda^\beta_\nu g_{\alpha\beta}, \quad \Lambda^0_0 \geq 1, \quad \det\Lambda = +1. \quad (2.4)$$

The conditions  $\Lambda^0_0 \geq 1$  and  $\det\Lambda = +1$  are necessary in order to exclude inversion in time and space. Then the following quantity forms a tensor with respect to proper Lorentz-transformations, the so called Levi-Civita tensor:

$$\epsilon_{\alpha\beta\gamma\delta} = \begin{cases} +1, & \alpha\beta\gamma\delta \text{ even permutation of } 0123, \\ -1, & \alpha\beta\gamma\delta \text{ odd permutation of } 0123, \\ 0, & \text{otherwise.} \end{cases} \quad (2.5)$$

Note that in the textbook of Weinberg [79] this tensor as well as the metric tensor both have the opposite sign to the notation used here.

4. **Einstein's summation convention:** Here a Greek index like  $\mu, \nu$  will always run over the four numbers 0, 1, 2, 3. In this chapter we make use of Einstein's summation convention, i.e. any index, like  $\mu, \nu$  that appears twice once as a subscript and once as a superscript, is understood to be summed over, if not otherwise noted. For spatial indices, which are denoted by Latin indices like  $i, j, k$  we will not apply this summation convention.

**Proposition 2.1.1.** *Define the Minkowskian matrix  $G$  as in (2.3). Then the following statements are equivalent for any matrix  $\Lambda \in \mathbb{R}^{4 \times 4}$ :*

- (i) *The Lorentz-matrix  $\Lambda$  leaves the Einstein-Minkowski metric  $Q(x) = x^T G x$  invariant.*
- (ii) *The matrix  $\Lambda$  is regular and has the inverse matrix  $\Lambda^{-1} = G \Lambda^T G$ .*
- (iii) *We have  $G = \Lambda^T G \Lambda$ , i.e. the matrix  $\Lambda$  leaves the wave operator  $\square$  invariant.*

*Proof.* Let  $I$  be the unit matrix in  $\mathbb{R}^{4 \times 4}$ . We obtain

$$\begin{aligned} G &= \Lambda G \Lambda^T \iff \\ I &= G^2 = \Lambda(G \Lambda^T G) \iff \\ \Lambda^{-1} &= G \Lambda^T G \iff \\ I &= \Lambda^{-1} \Lambda = G \Lambda^T G \Lambda \iff \\ G &= G^2 \Lambda^T G \Lambda = \Lambda^T G \Lambda. \end{aligned}$$

□

**Definition 2.1.2.** A constant matrix  $\Lambda \in \mathbb{R}^{4 \times 4}$  which satisfies the equivalent conditions (i), (ii), (iii) in Proposition (2.1.1) is called a **Lorentz-matrix**.

A Lorentz-matrix  $\Lambda$  and a constant four-quantity  $\tilde{a} \in \mathbb{R}^4$  describe a Lorentz-transformation

$$x \implies \tilde{x} = \Lambda x + a \tag{2.6}$$

of the four space-time coordinates. The Lorentz-transformation is called homogeneous if  $\tilde{a} = 0$ .

A familiar example of the homogeneous Lorentz-transformation is

$$t' = \frac{t - \frac{vx}{c^2}}{\sqrt{1 - \frac{v^2}{c^2}}}, \quad x' = \frac{x - vt}{\sqrt{1 - \frac{v^2}{c^2}}}, \quad y' = y, \quad z' = z \tag{2.7}$$

with velocity  $v = v_x$  along the  $x$ -axis, which reduces for  $|v| \ll c$  to the classical Galilean transformation

$$t' = t, \quad x' = x - vt. \tag{2.8}$$

## 2.2 Vectors and tensors

Any quantity that transforms like  $f'^\alpha = \Lambda^\alpha_\beta f^\beta$  is called four-vector.

**Contravariant four-vector:** is a vector with single upper index having the following Lorentz-transformation property

$$V^\alpha(x) \rightarrow V'^\alpha(x') = \Lambda^\alpha_\beta V^\beta(x). \tag{2.9}$$

**Covariant four-vector:** is a quantity with a single lower index having transformation

$$U_\alpha(x) \rightarrow U'_\alpha(x') = \Lambda^\beta_\alpha U_\beta(x), \tag{2.10}$$

where

$$\Lambda_\beta^\alpha = g_{\beta\gamma} g^{\alpha\delta} \Lambda^\gamma_\delta. \tag{2.11}$$

The matrix  $g^{\alpha\delta}$  introduced here is numerically the same as  $g_{\alpha\delta}$ , that is

$$g^{\alpha\delta} = g_{\alpha\delta}. \tag{2.12}$$

## CHAPTER 2. THE RELATIVISTIC EULER EQUATIONS

---

Also note that

$$g^{\alpha\delta}g_{\delta\beta} = \begin{cases} +1, & \alpha = \beta, \\ 0, & \alpha \neq \beta. \end{cases} \quad (2.13)$$

This means that  $\Lambda^\alpha_\beta$  is the inverse of the matrix  $\Lambda^\beta_\alpha$ , that using (2.3) and (2.11)

$$\Lambda^\gamma_\alpha \Lambda^\alpha_\beta = g_{\alpha\delta} g^{\gamma\eta} \Lambda^\delta_\eta \Lambda^\alpha_\beta = g_{\eta\beta} g^{\gamma\eta} = \delta^\gamma_\beta. \quad (2.14)$$

It follows that the scalar product of a contravariant with a covariant four-vector is invariant with respect to Lorentz-transformation (2.11), that is,

$$U'_\alpha V'^\alpha = \Lambda^\gamma_\alpha \Lambda^\alpha_\beta U_\gamma V^\beta = U_\beta V^\beta. \quad (2.15)$$

To every contravariant four-vector  $V^\alpha$  there corresponds a covariant four-vector

$$V_\alpha = g_{\alpha\beta} V^\beta \quad (2.16)$$

and to every covariant  $U_\alpha$  there corresponds a contravariant

$$U^\alpha = g^{\alpha\beta} U_\beta. \quad (2.17)$$

A covariant or contravariant vector is a tensor with one index, and scalar (invariant expression) is a tensor without indices.

Note that raising the index on  $V_\alpha$  simply gives back  $V^\alpha$ , and lowering the index on  $U^\alpha$  simply gives back  $U_\alpha$ ,

$$g^{\alpha\beta} V_\beta = g^{\alpha\beta} g_{\beta\gamma} V^\gamma = V^\alpha, \quad (2.18)$$

$$g_{\alpha\beta} U^\beta = g_{\alpha\beta} g^{\beta\gamma} U_\gamma = U_\alpha. \quad (2.19)$$

### 2.2.1 Tensor calculus

Here we are looking for simple rules which enables us to construct new tensors from the old ones. These rules may be combined with each others under certain constraints to obtain every possible tensor. In fact these rules play an important role in order to show that the relativistic Euler equations are Lorentz-invariant.

**Rule I: Linear combinations:** A linear combination of two tensors  $R$  and  $S$  with the same upper and lower indices is a new tensor  $T$  with these indices, for example let be

$$T_\alpha^\beta = a R_\alpha^\beta + b S_\alpha^\beta$$

with given tensors  $R_\alpha^\beta$ ,  $S_\alpha^\beta$ . Then  $T_\alpha^\beta$  is also a tensor according to

$$\begin{aligned} T'^\alpha_\beta &= a R'^\alpha_\beta + b S'^\alpha_\beta \\ &= a \Lambda^\alpha_k \Lambda^\beta_\mu R_k^\mu + b \Lambda^\alpha_k \Lambda^\beta_\mu S_k^\mu \\ &= \Lambda^\alpha_k \Lambda^\beta_\mu T_k^\mu. \end{aligned}$$

**Rule II: Direct products:** The product of two tensors  $R$  and  $S$  is a new tensor  $T$  whose upper and lower indices consists of all the upper and lower indices of the original tensors, for example let be

$$T_{\beta}^{\alpha \gamma} = R^{\alpha} S_{\beta}^{\gamma}$$

with given tensors  $R^{\alpha}$ ,  $S_{\beta}^{\gamma}$ . Then  $T_{\beta}^{\alpha \gamma}$  is also a tensor according to

$$\begin{aligned} T'_{\beta}^{\alpha \gamma} &= R'^{\alpha} S'_{\beta}^{\gamma} \\ &= \Lambda^{\alpha}_k R^k \Lambda_{\beta}^{\nu} \Lambda^{\gamma}_{\mu} S_{\nu}^{\mu} \\ &= \Lambda^{\alpha}_k \Lambda_{\beta}^{\nu} \Lambda^{\gamma}_{\mu} T^k_{\nu}{}^{\mu}. \end{aligned}$$

**Rule III: Contractions:** Setting an upper and lower index of a tensor equal and summing it over its values 0,1,2,3 we obtain a new tensor without these two indices. For example, let  $T_{\beta\alpha\gamma}^{\alpha}$  be a tensor. Then

$$T_{\beta\gamma} = T_{\beta\alpha\gamma}^{\alpha}$$

is also a tensor according to

$$\begin{aligned} T'_{\beta\gamma} &= T'_{\beta\alpha\gamma} \\ &= \Lambda^{\alpha}_k \Lambda_{\beta}^{\lambda} \Lambda_{\alpha}^{\mu} \Lambda_{\gamma}^{\nu} T^k_{\lambda\mu\nu} \\ &= \delta^{\mu}_k \Lambda_{\beta}^{\lambda} \Lambda_{\gamma}^{\nu} T^k_{\lambda\mu\nu} \\ &= \Lambda_{\beta}^{\lambda} \Lambda_{\gamma}^{\nu} T^{\mu}_{\lambda\mu\nu} \\ &= \Lambda_{\beta}^{\lambda} \Lambda_{\gamma}^{\nu} T_{\lambda\nu}. \end{aligned}$$

**Rule IV: Differentiation:** Differentiation of a tensor with respect to  $x^{\alpha}$  yields a tensor with an additional covariant index  $\alpha$ . For example, let  $T_{\gamma}^{\beta}$  be a tensor and define

$$T_{\alpha \gamma}^{\beta} = \frac{\partial T_{\gamma}^{\beta}}{\partial x^{\alpha}}.$$

Then  $T_{\alpha \gamma}^{\beta}$  is also a tensor according to

$$\begin{aligned} T'_{\alpha \gamma}^{\beta} &= \frac{\partial T'_{\gamma}^{\beta}}{\partial x'^{\alpha}} \\ &= \Lambda_{\alpha}^k \frac{\partial}{\partial x^k} \left( \Lambda_{\xi}^{\beta} \Lambda_{\gamma}^{\mu} T^{\xi}_{\mu} \right) \\ &= \Lambda_{\alpha}^k \Lambda_{\lambda}^{\beta} \Lambda_{\gamma}^{\mu} \frac{\partial T^{\lambda}_{\mu}}{\partial x^k}. \end{aligned}$$

Note that the order of indices matters, even as between upper and lower indices. For instance,  $T_{\gamma}^{\alpha\beta}$  may or may not be the same as  $T_{\gamma}^{\alpha \beta}$ .

Finally we give some special tensors

## CHAPTER 2. THE RELATIVISTIC EULER EQUATIONS

---

- zero tensor, whose components are zero in any reference frame for an arbitrary but fixed combination of upper and lower indices.
- metric tensor, which transforms according to ( $G = \Lambda G \Lambda^T$ )

$$g_{\mu\nu} \rightarrow g'_{\mu\nu} = \Lambda_{\mu}^k \Lambda_{\nu}^{\lambda} g_{k\lambda} = g_{\mu\nu}. \quad (2.20)$$

- Kronecker tensor

$$\delta^{\alpha}_{\beta} = \Lambda^{\alpha}_k \Lambda_{\beta}^{\lambda} \delta^k_{\lambda} = \Lambda^{\alpha}_k \Lambda_{\beta}^k = \delta^{\alpha}_{\beta} = \begin{cases} +1, & \alpha = \beta = 0, 1, 2, 3, \\ 0, & \alpha \neq \beta. \end{cases}$$

- Levi-Civita tensor given in (2.5).

In the next remark we give an important feature of the tensors, which play important role in order to study the invariant property of ultra-relativistic Euler equations. For more information about this invariant property see Appendix A.

**Remark 2.2.1.** *The fundamental result for any Lorentz invariant theory is that if two tensors with the same upper and lower indices are equal in one coordinate frame, then they are equal in any other coordinate system related to the first by a Lorentz-transformation, for instance, if  $T_{\beta}^{\alpha} = S_{\beta}^{\alpha}$  then*

$$T'^{\alpha}_{\beta} = \Lambda^{\alpha}_k \Lambda_{\beta}^{\mu} T_{\mu}^k = \Lambda^{\alpha}_k \Lambda_{\beta}^{\mu} S_{\mu}^k = S'^{\alpha}_{\beta}.$$

*In particular, the statement that a tensor vanishes is Lorentz-invariant.*

### 2.3 Light cone

**Definition**[68]: Space-time is the set of all (possible) events in a universe, it represents the history of an entire universe. An event is a point in the space-time. Worldlines represent the histories of objects in space-time. Hence a worldline is a continuous sequence of events.

It has become usual to use plots such as that shown in the Figure 2.1 to represent space-time events, which called Minkowski or space-time diagrams. Since we cannot plot four dimensions, space-time is reduced to three dimensions with two spatial components and one time component.

Each event in space-time has a double-cone attached to it. The present is represented by the point where the two cones meet, i.e. the tip of the cone (origin). By the conventional choice of units used in relativity, the sides of cone are sloped at 45 degrees. This corresponds to choosing where time is measured in seconds and distance in light-seconds. A light-second is the distance light travels in one seconds.



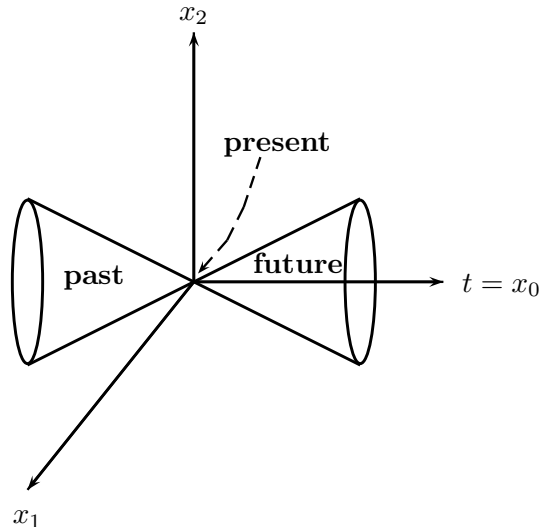


Figure 2.1: Light cone.

- The right-cone (the future light-cone) represents the events, which lie to the future of the event at the origin (present).
- The left-cone (the past light-cone) represents the events, which preceded the event at the origin (present).

The light cone explains the idea that the direction of the light-flash does not depend on the motion of source, but just on the event at which the light-flash is released. In addition, by the “Einstein Principle of Relativity”, all observers, regardless of their motions, must measure the speed of light to be the same constant, in all directions. This fact due to the Maxwell’s Laws. That is to say, all observers will universally agree on the light cones at each event. This means that each observer drawing a space-time diagram in which he is at rest must have the worldlines of light-flashes at the same angle of 45 degrees from his worldline (in time axis), and 45 degrees from his plane of simultaneity (his space axis).

### 2.3.1 Einstein velocity addition

The velocity transformation law can be given as follows see [79]: If in a Lorentz transformation, the barred frame  $(\tilde{t}, \tilde{x})$  moves with velocity  $\nu$  as a measured in the unbarred frame  $(t, x)$ , and if  $v$  denotes the velocity of a particle as measured in the unbarred frame, and  $\tilde{v}$  the velocity of the same particle as measured in the barred frame, then.

$$v = \frac{\nu + \tilde{v}}{1 + \nu\tilde{v}}. \quad (2.21)$$

## 2.4 Notions on conservation laws

In this section we will of course not seek to cover all aspects of the theory of conservation laws. Actually, we present a brief review for the basic concepts and facts related to the work in this thesis. We present a short summary to the main concepts of hyperbolic conservation laws theory. For a comprehensive overview for the theory of the hyperbolic conservation laws, we refer to Dafermos [24], Godlewski and Raviart [37], LeVeque [52, 53], Serre [73], Toro [77], Evans [34] and Smoller [74].

### 2.4.1 Hyperbolic systems of conservation laws

Consider the Cauchy problem for a system of conservation laws in one space dimension

$$\mathbf{u}_t + F(\mathbf{u})_x = 0, \quad (2.22)$$

with the initial data

$$\mathbf{u}(0, x) = \mathbf{u}_0(x). \quad (2.23)$$

Define the half plane  $H = \{(t, x) : t > 0, x \in \mathbb{R}\}$ . Here  $\mathbf{u} : \bar{H} \rightarrow \mathbb{R}^n$ ,  $x \in \mathbb{R}$ ,  $t > 0$  and  $F : \mathbb{R}^n \rightarrow \mathbb{R}^n$  is a smooth function.

When the differentiation in (2.23) is carried out, a quasilinear system of first order results:

$$\mathbf{u}_t + A(\mathbf{u})\mathbf{u}_x = 0, \quad A(\mathbf{u}) = F'(\mathbf{u}). \quad (2.24)$$

**Definition 2.4.1.** *The system (2.22) is called strictly hyperbolic if the matrix  $A(\mathbf{u})$  has  $n$  distinct real eigenvalues*

$$\lambda_1(\mathbf{u}) < \lambda_2(\mathbf{u}) < \dots < \lambda_n(\mathbf{u}), \quad (2.25)$$

*and a complete set of eigenvectors, i.e.  $n$  linearly independent corresponding right eigenvectors*

$$r_1(\mathbf{u}), r_2(\mathbf{u}), \dots, r_n(\mathbf{u}). \quad (2.26)$$

If the eigenvalues are not distinct, i.e.

$$\lambda_1(\mathbf{u}) \leq \lambda_2(\mathbf{u}) \leq \dots \leq \lambda_n(\mathbf{u}), \quad (2.27)$$

but there is still a complete set of eigenvectors, then the system (2.22) is called non-strictly hyperbolic. On the other hand, if some eigenvectors become linearly dependent, then the system (2.22) is called parabolic degenerate.

The conservation laws pose a special challenge for theoretical and numerical analysis, since they may have discontinuous solutions. So that a classical approach, with smooth

## 2.4. NOTIONS ON CONSERVATION LAWS

---

solutions, is not suitable to treat this phenomenon. To treat this difficulty, we will introduce a generalized or weak solution.

An essential issue for the Cauchy problem (2.22), (2.23) is that, its solution may become discontinuous beyond some finite time interval, even if the initial data  $u_0$  is smooth, see e.g. Smoller [74, Chapter 15, pg. 243-244] for an example.

It is well known that smooth solutions for the problem (2.22), (2.23) may do not exist beyond some finite time interval, even if the initial data  $\mathbf{u}_0$  are smooth, see e.g. LeVeque [52, Section 3.3, pg. 25], and Smoller [74, Chapter 15, pg. 243-244]. Thus, solutions globally in time are defined in a generalized sense. This leads us to introduce the following definition for the generalized (weak) solution which is called weak solution or integral solution.

**Definition 2.4.2.** *A bounded measurable function  $\mathbf{u}(t, x)$  for  $t \geq 0$  and  $x \in \mathbb{R}$  is a weak solution of (2.22), (2.23) if*

$$\int_0^\infty \int_{-\infty}^\infty [\varphi_t \mathbf{u} + \varphi_x F(\mathbf{u})] dx dt + \int_{-\infty}^\infty \varphi(0, x) \mathbf{u}(0, x) dx = 0 \quad (2.28)$$

*holds for all  $C^1$ -test function  $\varphi: \mathbb{R}^2 \rightarrow \mathbb{R}$  with compact support.*

The integral formulation (2.28) allows for discontinuous solutions. These solutions often consist of piecewise smooth parts connected by discontinuities. However, not every discontinuity is permissible, where some jump conditions across the curve of discontinuity should be satisfied. These conditions are called the Rankine-Hugoniot conditions, and given as

$$s[\mathbf{u}] = [F(\mathbf{u})], \quad (2.29)$$

where  $s$  is the speed of the discontinuity. The conditions (2.29) are a direct result of the integral form (2.28) across the discontinuity curve, see e.g. Kröner [44] and Smoller [74]. Discontinuities which satisfy (2.29) are called shocks. This expression comes from gas dynamics; there, the shocks are necessarily compressive, i.e. pressure and density of a gas particle increase on crossing the shock, see e.g. Courant and Friedrichs [21].

It is well known that in general, a weak solution of (2.22), (2.23) is not unique, see again LeVeque [52, Section 3.3] and Smoller [74, Chapter 15, § B] for several examples. Hence we need some criterion that enables us to choose the (physically relevant) solutions among all weak solutions of (2.22), (2.23). A simple criterion is proposed that is called entropy condition to determine the physical relevant solution.

One says that a strictly concave function  $H(\mathbf{u})$  is a mathematical entropy of the system (2.22), if there exists a function  $G(u)$ , called entropy flux, such that

$$H'(\mathbf{u})F'(\mathbf{u}) = G'(\mathbf{u}). \quad (2.30)$$

## CHAPTER 2. THE RELATIVISTIC EULER EQUATIONS

---

Then  $(H, G)$  is called an entropy pair for the system (2.22). A weak solution  $\mathbf{u}$  is an entropy solution if  $\mathbf{u}$  satisfies, for all entropy function  $H$ , the entropy condition

$$\frac{\partial H(\mathbf{u})}{\partial t} + \frac{\partial G(\mathbf{u})}{\partial x} \geq 0 \quad (2.31)$$

in the sense of distributions, that is

$$\int_0^\infty \int_{-\infty}^\infty [\varphi_t H(\mathbf{u}) + \varphi_x G(\mathbf{u})] dx dt + \int_{-\infty}^\infty \varphi(0, x) H(\mathbf{u}(0, x)) dx \leq 0 \quad (2.32)$$

for all  $\varphi \in C_0^1(\mathbb{R}^2)$ , with  $\varphi \geq 0$  for  $t \geq 0$  and  $x \in \mathbb{R}$ .

Across a discontinuity, propagation with the speed  $s$ , the condition (2.32) implies to

$$s \cdot (H(\mathbf{u}_r) - H(\mathbf{u}_l)) \leq G(\mathbf{u}_r) - G(\mathbf{u}_l). \quad (2.33)$$

The condition (2.33) is used to pick out a physically relevant, or admissible shock among all others. There are several admissibility criteria, like the conditions of Dafermos [23], Liu [58, 59], and Lax [51], see a review in Dafermos [24]. We mention here only the classical criterion due to Lax [51]: An  $i$ -shock of speed  $s$  is called admissible, if the inequalities

$$\lambda_i(\mathbf{u}_-) \geq s \geq \lambda_i(\mathbf{u}_+) \quad (2.34)$$

hold. Where  $\lambda_i$  is an eigenvalue of the Jacobian matrix  $A(\mathbf{u}) = F'(\mathbf{u})$ , and  $\mathbf{u}_\mp$  are the states to the left on the right of the shock, respectively. In particular, when both parts of (2.34) hold as equalities, the shock is called an  $i$ -contact discontinuity.

### 2.4.2 The Riemann problem

The initial value problem for the system (2.22) with the piecewise constant initial condition

$$\mathbf{u}_0(x) = \begin{cases} \mathbf{u}_-, & x \leq 0 \\ \mathbf{u}_+, & x > 0 \end{cases}. \quad (2.35)$$

is known as the Riemann problem. This problem plays an important role in the study of hyperbolic conservation laws. It is used, as a basic problem, to study the main features of the hyperbolic problems. In addition, it is the basic building block for an important class of numerical as well as the analytical methods as we will see in this thesis, namely for the cone grid and the front tracking schemes. Moreover, due to their simplicity they are also used as test cases for numerical schemes.

An essential issue on the Riemann problem (2.22), (2.35) is that its solution is invariant under the self-similar transformation  $(t, x) \rightarrow (kt, kx)$ ,  $k > 0$ . This means that if  $\mathbf{u}(t, x)$  is a solution of (2.22), (2.35), then for all  $k > 0$ , the function  $\mathbf{u}(kt, kx)$  is also a solution. Since presumably there is a unique solution to the Riemann problem, it is natural to

## 2.4. NOTIONS ON CONSERVATION LAWS

---

consider only self-similar solutions, i.e. the ones depending only on the ratio  $x/t$ . Important work on the topic of the Riemann solution to conservation laws can also be found in Glimm [36], Dafermos [23, 24], Smoller [74] Liu [55, 56, 57, 58] and many references therein.

In Section 3.4 we use the ultra-relativistic Euler equations as an example to show how to construct the exact Riemann solution to strictly hyperbolic conservation laws, which also play a fundamental role for studying the ultra-relativistic Euler equations.

In Section 2.4.1 we have introduced the discontinuous solutions to a general initial-value problem (2.22), (2.23), the shocks and contact discontinuities. In addition to them, the solution to the Riemann problem (2.22), (2.35) has continuous self-similar solutions, the centered simple waves. In the special case when the conservation law (2.22) is given by the system of the Euler equations for gas dynamics, the gas is expanded in such a wave, see e.g. Courant and Friedrichs [21]. Therefore, a centered simple wave for a general conservation law (2.22) is referred to as a rarefaction wave.

According to the difficulties with a general solution for the Riemann problem, we consider only the structure of wave solutions corresponding to an eigenvalue. Indeed, the  $i$ -th eigenvalue  $\lambda_i$  determines a characteristic field, called the  $i$ -field and the corresponding solution is referred to as the  $i$ -wave. The characteristic fields are assorted in two types, they are given in the following definition

**Definition 2.4.3.** *An  $i$ -characteristic field at the state  $u \in \mathbb{R}^p$  is said to be genuinely nonlinear if*

$$\nabla_u \lambda_i(\mathbf{u}) \cdot r_i(\mathbf{u}) \neq 0, \quad (2.36)$$

*and linearly degenerate if*

$$\nabla_u \lambda_i(\mathbf{u}) \cdot r_i(\mathbf{u}) = 0, \quad (2.37)$$

*holds.*

The elementary  $i$ -wave solutions include the shock wave, contact discontinuity and the rarefaction wave. The shocks and contact discontinuities satisfy the jump conditions (2.29). While, the rarefaction waves are continuous solutions, also called expansion waves. Moreover, if the  $i$ -characteristic field is genuinely nonlinear then the  $i$ -wave is either a shock or a rarefaction, while the linearly degenerate  $i$ -characteristic field results in a contact discontinuity, see Smoller [74].

For the large initial Riemann data (2.35), the corresponding Riemann problem can have no solution, see Keyfitz and Kranzer [43] for an example. If the system (2.22) is non-strictly hyperbolic, then the Riemann solution might be non-unique, see e.g. Isaacson and Temple [40] and the references therein.

## CHAPTER 2. THE RELATIVISTIC EULER EQUATIONS

---

In this thesis, we are interested only in the case when each characteristic field is either genuinely nonlinear or linearly degenerate. To construct the solution of the Riemann problem, it is useful to define the concept of the Riemann invariant, which will be studied for our ultra-relativistic Euler equations in Section 3.5.

**Definition 2.4.4.** *A smooth function  $\psi: \mathbb{R}^p \rightarrow \mathbb{R}^p$  is called an  $i$ -Riemann invariant if*

$$\nabla_{\mathbf{u}}\psi(\mathbf{u}) \cdot r_i(\mathbf{u}) = 0, \quad (2.38)$$

for all  $\mathbf{u} \in \mathbb{R}^p$

**Theorem 2.4.5.** *On an  $i$ -rarefaction wave, all  $i$ -Riemann invariants are constant.*

*Proof.* See [37, Chapter I, section 3, pg. 57]. □

## 2.5 Relativistic Euler equations

Relativity plays an important role in areas of astrophysics, gravitational collapse, high energy nuclear collisions, high energy particle beams and free-electron laser technology. In order to derive the relativistic Euler equations using the Einstein's summation convention in Section 2.1, see [45, Section 4.3]. For instance tensor calculus, which enables us to construct new tensors from the old ones, see 2.20. We briefly give a short introductory of the relativistic Euler equations.

### Tensor algebraic combinations

(i) The proper pressure

$$p = \frac{1}{3}(u_\mu u_\nu - g_{\mu\nu})T^{\mu\nu}, \quad (2.39)$$

where  $T^{\mu\nu} = T^{\mu\nu}(t, x)$  is energy-momentum tensor,

(ii) the dimensionless velocity four-vector

$$u^\mu = \frac{1}{n}N^\mu, \quad (2.40)$$

where  $N^\mu = N^\mu(t, x)$  is the particle-density four-vector,

(iii) the proper energy density

$$e = u_\mu u_\nu T^{\mu\nu}, \quad (2.41)$$

(iv) the proper particle density

$$n = \sqrt{N^\mu N_\mu}. \quad (2.42)$$

## 2.5. RELATIVISTIC EULER EQUATIONS

---

The attribute proper for  $p$ ,  $e$  and  $n$  denotes quantities, which are invariant with respect to proper Lorentz-transformations. They take their simplest form in the Lorentz rest frame. Since all quantities under consideration are written down in Lorentz-invariant form, we may omit the word proper in the following. The motion of the gas will be governed by the equations of conservation of energy, momentum and the particle number, which can be written in the following form by using Einstein's summation convention in [79]:

$$\frac{\partial T^{\alpha\beta}}{\partial x^\beta} = 0, \quad \frac{\partial N^\alpha}{\partial x^\alpha} = 0,$$

where

$$T^{\alpha\beta} = -pg^{\alpha\beta} + (p + e)u^\alpha u^\beta$$

denotes the energy-momentum tensor for the ideal relativistic gas. Here  $p$  represents the pressure,  $\mathbf{u} \in \mathbb{R}^3$  is the spatial part of the four-velocity  $(u^0, u^1, u^2, u^3) = (\sqrt{1 + |\mathbf{u}|^2}, \mathbf{u})$  and  $g^{\alpha\beta}$  denotes the flat Minkowski metric, which is

$$g^{\alpha\beta} = \begin{cases} +1, & \alpha = \beta = 0, \\ -1, & \alpha = \beta = 1, 2, 3, \\ 0, & \alpha \neq \beta, \end{cases} \quad (2.43)$$

and

$$N^\alpha = nu^\alpha, \quad (2.44)$$

denotes particle-density four-vector, where  $n$  is the proper particle density. For more details see [79, Part one, pg. 47-52]. In this thesis we study the spatially one dimensional case.

Now we are looking for special solutions of the three-dimensional relativistic Euler equations, which will not depend on  $x^2$ ,  $x^3$  but only on  $x = x^1$ . Moreover we restrict to a one-dimensional flow field  $\mathbf{u} = (u(t, x), 0, 0)^T$ . We put the relativistic Euler equations in the context of the general theory of conservation laws, and discuss the Lorentz invariant properties of the system.

$$\begin{aligned} ((p + ec^2)(1 + u^2) - p)_t + ((p + ec^2)u\sqrt{1 + u^2})_x &= 0, \\ ((p + ec^2)u\sqrt{1 + u^2})_t + ((p + ec^2)u^2 + p)_x &= 0, \\ (n\sqrt{1 + u^2})_t + (nu)_x &= 0. \end{aligned} \quad (2.45)$$

Here  $p > 0$ ,  $v = \frac{u}{\sqrt{1+u^2}}$ ,  $e$ ,  $c$  and  $n > 0$  represent the pressure, the velocity field, the proper energy density, the speed of light and the proper particle density respectively, whereas  $|v| < 1$ ,  $u \in \mathbb{R}$ . In [75] the authors studied the first two equation. Using Glimm's method they proved a large data existence result, for the Cauchy problem when the equation of state has the form  $p(e) = \sigma^2 e$ , where  $\sigma$ , the sound speed, is constant with  $\sigma^2 < 1$ . The equation of state  $p(e) = \sigma^2 e$  corresponds to extremely relativistic gases, when the temperature is very high and particles move near the speed of light. For the

## CHAPTER 2. THE RELATIVISTIC EULER EQUATIONS

---

general isentropic gases, the equation of state is given by  $p = p(e)$ , see [79, Part one, pg. 47-52]. As a special example of barotropic flow, the equation of state  $p = (c^2/3)e$  arises in several important relativistic settings. In particular, this equation of state follows directly from the Stefan-Boltzmann law when a gas is in thermodynamical equilibrium with radiation and the radiation energy density greatly exceeds the total gas energy density. The equation of state  $p = (c^2/3)e$  has also been an important role in order to study the gravitational collapse because it can be derived as a model for the equation of state in a dense Neutron star, for full details, see [79, Part one, pg. 320]. In this thesis, we restrict with the case  $p(e) = \frac{1}{3}e$  and normalized the speed of light to be 1. Then (2.45) reduces to the ultra relativistic equations, which we will study fully in the next chapter.



---

# Chapter 3

## Ultra-Relativistic Euler Equations

### 3.1 Introduction

In this chapter we consider the ultra-relativistic Euler equations, which is a system of nonlinear hyperbolic conservation laws. We derive single shock parametrizations, using the Rankine-Hugoniot jump conditions and parametrizations of rarefaction waves for the one dimensional ultra-relativistic Euler equations. We use these parametrizations in order to develop an exact Riemann solution of the ultra-relativistic Euler equations as we will clarify in this chapter. We derive an unconditionally stable scheme so called cone-grid scheme in order to solve the ultra-relativistic Euler equations. The ultra-relativistic Euler system of conservation laws is given by

$$\begin{aligned}(p(3 + 4u^2))_t + (4pu\sqrt{1 + u^2})_x &= 0, \\ (4pu\sqrt{1 + u^2})_t + (p(1 + 4u^2))_x &= 0, \\ (n\sqrt{1 + u^2})_t + (nu)_x &= 0,\end{aligned}\tag{3.1}$$

where  $p > 0$ ,  $v = \frac{u}{\sqrt{1+u^2}}$  and  $n > 0$ , represent the pressure, the velocity field and the proper particle density respectively, where  $|v| < 1$ ,  $u \in \mathbb{R}$ . A very characteristic feature of these equations is that the first and second equations respectively, for the conservation of energy and momentum form a subsystem for  $p$  and  $u$ , the  $(p, u)$ -(sub)system, where the last equation is the relativistic continuity for  $n$  decouples from this subsystem. This is an important feature of the ultra-relativistic Euler equations, which will be studied in the sequel.

In one space dimension the  $(p, u)$ -(sub)system admits an extensive study and especially a complete solution of the Riemannian initial value problem, which will be studied in this chapter.

These differential equations constitute a strictly hyperbolic system with the characteristic

## CHAPTER 3. ULTRA-RELATIVISTIC EULER EQUATIONS

---

velocities

$$\lambda_1 = \frac{2u\sqrt{1+u^2} - \sqrt{3}}{3+2u^2} < \lambda_2 = \frac{u}{\sqrt{1+u^2}} < \lambda_3 = \frac{2u\sqrt{1+u^2} + \sqrt{3}}{3+2u^2}. \quad (3.2)$$

These eigenvalues may first be obtained in the Lorentz rest frame where  $u = 0$ . Then using the relativistic additivity law for the velocities (2.21), we can easily obtain the eigenvalues (3.2) in the general Lorentz frame see Appendix B. In the Lorentz rest frame we obtain the positive speed of sound  $\lambda = \frac{1}{\sqrt{3}}$ , which is independent of the spatial direction.

The differential equations (3.1) are not sufficient if we take shock discontinuities into account. Therefore we use a weak integral formulation with a piecewise  $C^1$ -solution  $p, u, n : (0, \infty) \times \mathbb{R} \mapsto \mathbb{R}$ ,  $p, n > 0$ , which is given according to Oleinik [66] by

$$\begin{aligned} \oint_{\partial\Omega} p(3+4u^2) dx - 4pu\sqrt{1+u^2} dt &= 0, \\ \oint_{\partial\Omega} 4pu\sqrt{1+u^2} dx - p(1+4u^2) dt &= 0, \\ \oint_{\partial\Omega} n\sqrt{1+u^2} dx - nu dt &= 0. \end{aligned} \quad (3.3)$$

Here  $\Omega \subset \mathbb{R}_0^+ \times \mathbb{R}$  is a bounded and convex region in space-time and with a piecewise smooth, positively oriented boundary. If we apply the Gaussian divergence theorem to the weak formulation (3.3) in time-space regions where the solution is regular we come back to the differential equation form of the Euler equations (3.1).

Furthermore we require that the weak solution (3.3) must also satisfy the entropy-inequality

$$\oint_{\partial\Omega} S^0 dx - S^1 dt \geq 0, \quad (3.4)$$

where

$$S^0(p, u, n) = -n\sqrt{1+u^2} \ln \frac{n^4}{p^3}, \quad S^1(p, u, n) = -nu \ln \frac{n^4}{p^3}. \quad (3.5)$$

This chapter is organized as follows. In Section 3.2 we briefly review the fundamental concepts and notions for the  $(p, u)$ -subsystem. We also prove Lemma 3.2.6, which gives a very simple characterization for the Lax entropy conditions of single shock waves (c.f. [50]). This lemma is needed to develop a new parametrization for single shocks of our system (3.1), namely Proposition 3.3.6 in Section 3.3, which turns out to be very useful in order to describe shock interaction in Chapters 4 and 5. In Section 3.3 we extend the results obtained in [45, Section 4.4, pg. 81-84] about the parametrizations of shocks and

rarefaction waves. For later purposes we also need some other known parametrizations for single shocks and rarefaction waves, which are also given in this section. In Section 3.4 we use the parametrizations for single shocks and rarefaction waves in order to give the exact Riemann solution. In Section 3.5 we introduce a famous topic in hyperbolic systems of conservation law, the so called Riemann invariants. In fact we show that shock curves have good geometry properties in Riemann invariants coordinates. In Section 3.6 we present a new scheme so called a cone-grid scheme in order to solve the one dimensional ultra-relativistic Euler equations. We prove that this scheme is strictly preserves the positivity of the pressure and particle density. In Section 3.7 we introduce a system of hyperbolic conservation law, which is equivalent to the  $(p, u)$ -(sub)system. This equivalent system describes a phonon-Bose gas in terms of the energy density  $e$  and the heat flux  $Q$ . Then we present numerical test cases for the solution of the phonon-Bose equations, using the cone-grid scheme.

## 3.2 The $(p, u)$ system

In this section we consider the ultra-relativistic Euler system of conservation laws of energy and momentum, which called  $(p, u)$  system:

$$\begin{aligned} (p(3 + 4u^2))_t + (4pu\sqrt{1 + u^2})_x &= 0, \\ (4pu\sqrt{1 + u^2})_t + (p(1 + 4u^2))_x &= 0, \end{aligned} \tag{3.6}$$

(e.g. [1, 2, 3, 19, 45, 47, 48, 67, 75]), where  $p > 0$  and  $u \in \mathbb{R}$ . First we fit system (3.6) into a general form of conservation laws

$$W_t + F(W)_x = 0, \tag{3.7}$$

where

$$W = \begin{bmatrix} W_1 \\ W_2 \end{bmatrix} = \begin{bmatrix} p(3 + 4u^2) \\ 4pu\sqrt{1 + u^2} \end{bmatrix}, \quad F(W) = \begin{bmatrix} 4pu\sqrt{1 + u^2} \\ p(1 + 4u^2) \end{bmatrix}. \tag{3.8}$$

The natural domains  $\Omega$  and  $\Omega'$  for the  $(p, u)$  and the  $(W_1, W_2)$  state space are given by

$$\begin{aligned} \Omega &= \{(p, u) \in \mathbb{R} \times \mathbb{R} : p > 0\}, \\ \Omega' &= \{(W_1, W_2) \in \mathbb{R} \times \mathbb{R} : |W_2| < W_1\}, \end{aligned} \tag{3.9}$$

respectively.

**Proposition 3.2.1.** *The mapping  $\Gamma : \Omega \mapsto \Omega'$  with*

$$\Gamma(p, u) = \begin{bmatrix} p(3 + 4u^2) \\ 4pu\sqrt{1 + u^2} \end{bmatrix} \tag{3.10}$$

*is one-to-one, and the Jacobian determinant of this mapping is both continuous and positive in the region  $\Omega$ .*

### CHAPTER 3. ULTRA-RELATIVISTIC EULER EQUATIONS

---

*Proof.* We first show that the mapping is injective: Consider two states  $(p_1, u_1)$  and  $(p_2, u_2) \in \Omega$  such that  $W_1(p_1, u_1) = W_1(p_2, u_2)$  and  $W_2(p_1, u_1) = W_2(p_2, u_2)$ . First, we show that if  $u_1 = u_2 = u$  then  $p_1 = p_2$ . From the equality  $W_1(p_1, u) = W_1(p_2, u)$  we have

$$p_1(3 + 4u^2) = p_2(3 + 4u^2).$$

Since the term  $3 + 4u^2 \neq 0$  for any  $u \in \mathbb{R}$  we must have  $p_1 = p_2$ . We now show that if the images of  $W_1$  and  $W_2$  are equal, then we must have  $u_1 = u_2$  and, by the previous argument,  $p_1 = p_2$ . From  $W_1(p_1, u_1) = W_1(p_2, u_2)$  and  $W_2(p_1, u_1) = W_2(p_2, u_2)$  we have

$$\frac{p_1}{p_2}(3 + 4u_1^2) = (3 + 4u_2^2),$$

and

$$\frac{p_1}{p_2}(u_1\sqrt{1 + u_1^2}) = u_2\sqrt{1 + u_2^2}.$$

Eliminating  $\frac{p_1}{p_2}$  we get

$$u_1\sqrt{1 + u_1^2}(3 + 4u_2^2) = u_2\sqrt{1 + u_2^2}(3 + 4u_1^2), \quad (3.11)$$

which further reduces to

$$(u_1^2 - u_2^2)(9(1 + u_1^2 + u_2^2) + 8u_1^2u_2^2) = 0.$$

Since  $9(1 + u_1^2 + u_2^2) + 8u_1^2u_2^2 \neq 0$ , we get from (3.11)  $u_1 = u_2$ . Thus the mapping  $\Gamma : \Omega \rightarrow \Omega'$  is injective.

Secondly, we show that the mapping is surjective: For all  $(W_1, W_2) \in \Omega'$  there exists

$$(p_1, u_1) = \left( \frac{1}{3} \left[ \sqrt{4W_1^2 - 3W_2^2} - W_1 \right], \frac{W_2}{\sqrt{4p_1(p_1 + W_1)}} \right) \in \Omega, \quad (3.12)$$

such that

$$\Gamma(p_1, u_1) = \begin{bmatrix} W_1 \\ W_2 \end{bmatrix}. \quad (3.13)$$

Then we conclude that the mapping is one-to-one. A straightforward calculation shows that

$$\det \left( \frac{\partial(W_1, W_2)}{\partial(p, u)} \right) = \frac{4p(2u^2 + 3)}{\sqrt{1 + u^2}} > 0,$$

which is continuous on  $\Omega$ . □

There is a useful derivation for the eigenvalues. For this purpose we rewrite the  $2 \times 2$  subsystem for  $p$  and  $u$  in (3.6) in the quasilinear form

$$\begin{pmatrix} p_t \\ u_t \end{pmatrix} + \begin{pmatrix} \frac{2u\sqrt{1+u^2}}{3+2u^2} & \frac{4p}{\sqrt{1+u^2}(3+2u^2)} \\ \frac{3\sqrt{1+u^2}}{4p(3+2u^2)} & \frac{2u\sqrt{1+u^2}}{3+2u^2} \end{pmatrix} \begin{pmatrix} p_x \\ u_x \end{pmatrix} = 0. \quad (3.14)$$

A simple calculation shows that system (3.6) has characteristic velocities (eigenvalues)

$$\lambda_1 = \frac{2u\sqrt{1+u^2} - \sqrt{3}}{3+2u^2} < \lambda_3 = \frac{2u\sqrt{1+u^2} + \sqrt{3}}{3+2u^2}. \quad (3.15)$$

The corresponding right eigenvectors for system (3.14) are

$$r_1 = \left( \frac{-4p}{\sqrt{3}\sqrt{1+u^2}}, 1 \right)^T, \quad r_3 = \left( \frac{4p}{\sqrt{3}\sqrt{1+u^2}}, 1 \right)^T. \quad (3.16)$$

**Proposition 3.2.2.** *System (3.6) is strictly hyperbolic and genuinely nonlinear at each point  $(p, u)$  where  $p > 0$  and  $u \in \mathbb{R}$ .*

*Proof.* The strict hyperbolicity is clear from the eigenvalues. It is easy to check that

$$\begin{aligned} \nabla \lambda_1 \cdot r_1 &= \frac{2((\sqrt{1+u^2} + \sqrt{3}u)^2 + 2)}{\sqrt{1+u^2}(3+2u^2)^2} > 0, \\ \nabla \lambda_3 \cdot r_3 &= \frac{2((\sqrt{1+u^2} - \sqrt{3}u)^2 + 2)}{\sqrt{1+u^2}(3+2u^2)^2} > 0, \end{aligned} \quad (3.17)$$

and this proves the genuine nonlinearity.  $\square$

The differential equations (3.6) are not sufficient if we take shock discontinuities into account. Therefore we use a weak integral formulation with a piecewise  $C^1$ -solution  $p, u : (0, \infty) \times \mathbb{R} \mapsto \mathbb{R}$ ,  $p > 0$  given in the first two equations of (3.3), which we recall

$$\begin{aligned} \oint_{\partial\Omega} p(3+4u^2)dx - 4pu\sqrt{1+u^2}dt &= 0, \\ \oint_{\partial\Omega} 4pu\sqrt{1+u^2}dx - p(1+4u^2)dt &= 0. \end{aligned} \quad (3.18)$$

Here  $\Omega \subset \mathbb{R}_0^+ \times \mathbb{R}$  is a bounded and convex region in space-time and with a piecewise smooth, positively oriented boundary.

The system (3.6) has an own entropy inequality, which reads in one space dimension

$$\oint_{\partial\Omega} h dx - \varphi dt \geq 0, \quad (3.19)$$

where

$$h(p, u) = p^{\frac{3}{4}}\sqrt{1+u^2}, \quad \varphi(p, u) = p^{\frac{3}{4}}u. \quad (3.20)$$

This entropy satisfies an additional conservation law in the points  $(t, x)$  of smoothness, namely

$$\frac{\partial h}{\partial t} + \frac{\partial \varphi}{\partial x} = 0, \quad (3.21)$$

## CHAPTER 3. ULTRA-RELATIVISTIC EULER EQUATIONS

---

which can be obtained with the help of (3.14).

Finally we prove that the relativistic entropy  $h$  is indeed concave for the above system (3.6). To show that  $h$  is strictly concave, i.e. that  $\nabla_U^2 h < 0$ , where  $\nabla_U^2$  denotes the Hessian with respect to the state space  $U = (p, u)$  in the region  $\Omega$

$$h_{pp} = \frac{-3}{16} p^{-\frac{5}{4}} \sqrt{1+u^2},$$

$$h_{pu} = \frac{3}{4} p^{-\frac{1}{4}} \frac{u}{\sqrt{1+u^2}},$$

$$h_{uu} = p^{\frac{3}{4}} \frac{1}{(1+u^2)^{\frac{3}{2}}}.$$

Using these we obtain that

$$h_{pp}h_{uu} - h_{pu}^2 = \frac{-3}{16} p^{-\frac{1}{2}} \frac{1+3u^2}{1+u^2} < 0,$$

which implies that  $h$  is strictly concave.

The weak solutions are invariant with respect to the following homogeneous Lorentz transformations in dimensionless form

$$t' = at + bx, \quad x' = bt + ax, \tag{3.22}$$

where  $a > 1$  and  $b$  are real parameters, which satisfy the condition  $a^2 - b^2 = 1$ . Introducing

$$p'(t', x') := p(t, x), \quad u'(t', x') := b\sqrt{1+u(t, x)^2} + u\sqrt{1+b^2},$$

the Lorentz invariance means that in the new coordinates  $t'$  and  $x'$  we obtain again solutions  $p'$  and  $u'$  of the ultra-relativistic Euler equations.

In the following lemma we give an Einstein's law for relativistic velocities, which turns out to be very useful in order to present a new parametrization for single shock for the ultra-relativistic Euler equations.

**Lemma 3.2.3. *Einstein's law for relativistic velocities***

Given are two velocities  $v_1, v_2$  with  $|v_1| < 1$ ,  $|v_2| < 1$ . Put  $v := \frac{v_1+v_2}{1+v_1v_2}$  and put  $w_1 := \sqrt{\frac{1-v_1}{1+v_1}}$ ,  $w_2 := \sqrt{\frac{1-v_2}{1+v_2}}$ . Then also  $|v| < 1$ , and for  $w := \sqrt{\frac{1-v}{1+v}}$  we have  $w = w_1 \cdot w_2$ .

*Proof.*

$$\begin{aligned}
 1 - v^2 &= (1 - v)(1 + v) \\
 &= \frac{1 + v_1 v_2 - v_1 - v_2}{1 + v_1 v_2} \cdot \frac{1 + v_1 v_2 + v_1 + v_2}{1 + v_1 v_2} \\
 &= \frac{(1 - v_1)(1 - v_2)(1 + v_1)(1 + v_2)}{(1 + v_1 v_2)^2} > 0,
 \end{aligned}$$

hence  $|v| < 1$ . Now

$$\frac{1 - v}{1 + v} = \frac{1 + v_1 v_2 - v_1 - v_2}{1 + v_1 v_2 + v_1 + v_2} = \frac{(1 - v_1)(1 - v_2)}{(1 + v_1)(1 + v_2)}.$$

Taking the square root, we have shown the lemma. □

**Remark 3.2.4.** Often we are using  $u_{1,2} := \frac{v_{1,2}}{\sqrt{1-v_{1,2}^2}}$  and  $u = \frac{v}{\sqrt{1-v^2}}$ . Then we have

$$u = \sqrt{1 + u_1^2} \cdot u_2 + \sqrt{1 + u_2^2} \cdot u_1.$$

### 3.2.1 Jump conditions

For systems of conservation laws, the relations defining the shock waves are the Rankine-Hugoniot jump conditions. These relations state for a shock wave traveling with speed  $v_s = s$ , the change in the conserved quantities  $U$  across the shock and the change in the flux  $F(U)$  across the shock, denoted  $[U]$  and  $[F(U)]$  respectively, satisfy

$$v_s [U] = [F(U)].$$

We consider a straight line shock  $x = x(t)$  with constant speed  $s = v_s = \dot{x}$ ,  $U_- = (p_-, u_-)$  is the constant left state to the shock and  $U_+ = (p_+, u_+)$  is the constant right state to the shock with  $p_{\pm} > 0$ . Then (3.18) leads to the Rankine-Hugoniot jump conditions:

$$\begin{aligned}
 v_s [p_+(3 + 4u_+^2) - p_-(3 + 4u_-^2)] &= 4p_+u_+\sqrt{1 + u_+^2} - 4p_-u_-\sqrt{1 + u_-^2}, \\
 v_s [4p_+u_+\sqrt{1 + u_+^2} - 4p_-u_-\sqrt{1 + u_-^2}] &= p_+(1 + 4u_+^2) - p_-(1 + 4u_-^2).
 \end{aligned} \tag{3.23}$$

In singular points the local form of the entropy inequality (3.19) reads

$$-v_s(h_+ - h_-) + (\varphi_+ - \varphi_-) > 0. \tag{3.24}$$

## CHAPTER 3. ULTRA-RELATIVISTIC EULER EQUATIONS

---

**Remark 3.2.5.** *By using a Lorentz transformation (3.22) and applying a homogeneous scaling of the pressure with a positive scaling factor, we put*

$$\begin{aligned} p_+ &= p, & u_+ &= u, \\ p_- &= 1, & u_- &= 0. \end{aligned} \tag{3.25}$$

*Then the Rankine-Hugoniot conditions (3.23) and the entropy inequality (3.24) become*

$$v_s [p(3 + 4u^2) - 3] = 4pu\sqrt{1 + u^2}, \tag{3.26}$$

$$v_s \cdot 4pu\sqrt{1 + u^2} = p(1 + 4u^2) - 1, \tag{3.27}$$

$$-v_s \left[ p^{\frac{3}{4}}\sqrt{1 + u^2} - 1 \right] + p^{\frac{3}{4}}u > 0. \tag{3.28}$$

*In the sequel we can assume that  $u \neq 0$ , because  $u = 0$  and equation (3.27) imply  $p = 1$ , such that*

$$p_+ = p = 1 = p_-, \quad u_+ = 0 = u_-. \tag{3.29}$$

*In this case there is no shock. Since  $p > 0$ , we conclude from equation (3.26) that also  $p(3 + 4u^2) - 3 \neq 0$ .*

**Lemma 3.2.6.** *Given  $(p_{\pm}, u_{\pm}) \in \mathbb{R}^+ \times \mathbb{R}$ . Assume that the Rankine-Hugoniot jump conditions (3.23) are satisfied. Recall the two characteristic speeds  $\lambda_{1,3}$  in (3.15). Then the following conditions are equivalent:*

1. *The Lax shock condition, which states the following:*

$$p_+ > p_- \text{ implies that } \lambda_1(u_+) < v_s < \lambda_1(u_-) \quad \text{and} \quad p_+ < p_- \text{ implies that } \lambda_3(u_+) < v_s < \lambda_3(u_-).$$

2.  $u_- > u_+$ .

3. *The entropy condition  $-v_s(h_+ - h_-) + (\varphi_+ - \varphi_-) > 0$ , where  $h_{\pm} = h(p_{\pm}, u_{\pm})$  and  $\varphi_{\pm} = \varphi(p_{\pm}, u_{\pm})$  are given by (3.20).*

*Proof.* Due to Remark 3.2.5 it is sufficient to prove this lemma for the special case given in (3.25). For this purpose we first solve the algebraic equations (3.26) and (3.27). Then we obtain

$$\left( 4pu\sqrt{1 + u^2} \right)^2 = (p(3 + 4u^2) - 3) (p(1 + 4u^2) - 1),$$

that is,  $16pu^2 + 6p - 3p^2 - 3 = 0$ . Then

$$u = \pm \frac{\sqrt{3}(p - 1)}{4\sqrt{p}}.$$



Hence, we have two cases for the dependence of  $u$  on the pressure  $p$ , namely:

**Case 1:**  $u = -\frac{\sqrt{3}(p-1)}{4\sqrt{p}}$ , which gives

$$v_s = -\frac{1}{\sqrt{3}}\sqrt{\frac{3p+1}{p+3}}, \quad \lambda_1(u) = -\frac{\sqrt{3}(p-1)\sqrt{3p+1}\sqrt{p+3} + 8\sqrt{3}p}{3(p^2+6p+1)}, \quad \lambda_1(0) = -\frac{1}{\sqrt{3}}. \quad (3.30)$$

**Case 2:**  $u = \frac{\sqrt{3}(p-1)}{4\sqrt{p}}$ , which gives

$$v_s = \frac{1}{\sqrt{3}}\sqrt{\frac{3p+1}{p+3}}, \quad \lambda_3(u) = \frac{\sqrt{3}(p-1)\sqrt{3p+1}\sqrt{p+3} + 8\sqrt{3}p}{3(p^2+6p+1)}, \quad \lambda_3(0) = \frac{1}{\sqrt{3}}. \quad (3.31)$$

First we prove that condition 1 implies condition 2: The eigenvalues  $\lambda_{1,3}$  in (3.15) are strictly monotonically increasing in  $u \in \mathbb{R}$ , hence  $\lambda_{1,3}(u) < \lambda_{1,3}(0)$  is equivalent to  $u < 0$ . Then condition 2 is satisfied.

Next we show that from the second condition, namely  $u < 0$  in our special situation, we obtain the first one: In case 1 the assumption  $u < 0$  gives  $p > 1$ . Then the following equivalences show that  $v_s < \lambda_1(0)$ .

$$\begin{aligned} v_s < -\frac{1}{\sqrt{3}} &\iff \\ -\frac{1}{\sqrt{3}}\sqrt{\frac{3p+1}{p+3}} < -\frac{1}{\sqrt{3}} &\iff \\ 3p+1 > p+3 &\iff \\ p > 1. & \end{aligned}$$

This is one part of condition 1 in the first case. Now we prove the other part of the inequality in case 1:

$$\lambda_1(u) = \frac{2u\sqrt{1+u^2} - \sqrt{3}}{3+2u^2} < v_s. \quad (3.32)$$

By using (3.30) we have the equivalences with (3.32)

$$\begin{aligned} -\frac{\sqrt{3}(p-1)\sqrt{3p+1}\sqrt{p+3} + 8\sqrt{3}p}{3(p^2+6p+1)} < -\frac{1}{\sqrt{3}}\sqrt{\frac{3p+1}{p+3}} &\iff \\ 3(p-1)\sqrt{3p+1}(p+3) + 24p\sqrt{p+3} > 3(p^2+6p+1)\sqrt{3p+1} &\iff \\ 24p\sqrt{p+3} > (12p+12)\sqrt{3p+1} &\iff \\ \frac{2p}{p+1} > \sqrt{\frac{3p+1}{p+3}} &\iff \\ (p-1)(p^2+6p+1) > 0 &\iff \\ p > 1. & \end{aligned}$$

Hence we have shown the equivalence between the first two conditions in the first case. This also remains true for the second case, where  $u < 0$  is equivalent to  $p < 1$ , because the quantities (3.30) and (3.31) differ only by a minus sign.

Finally the equivalence between conditions two and three follows directly from the following equivalences in case 1, where we start from (3.28) and make use of (3.30). Recall that in the first case the condition 2, namely  $u < 0$ , is equivalent to  $p > 1$ .

$$\begin{aligned}
 -v_s \left[ p^{\frac{3}{4}} \sqrt{1+u^2} - 1 \right] + p^{\frac{3}{4}} u &> 0 \iff \\
 \frac{1}{\sqrt{3}} \sqrt{\frac{3p+1}{p+3}} \left( p^{\frac{3}{4}} \frac{\sqrt{3p+1}\sqrt{p+3}}{4\sqrt{p}} - 1 \right) - p^{\frac{3}{4}} \frac{\sqrt{3}(p-1)}{4\sqrt{p}} &> 0 \iff \\
 (3p+1)p^{1/4} - 4\sqrt{\frac{3p+1}{p+3}} - 3p^{1/4}(p-1) &> 0 \iff \\
 3p^{5/4} + p^{1/4} - 4\sqrt{\frac{3p+1}{p+3}} - 3p^{5/4} + 3p^{1/4} &> 0 \iff \\
 p^{1/4} &> \sqrt{\frac{3p+1}{p+3}} \iff \\
 p(p+3)^2 &> (3p+1)^2 \iff \\
 p^3 - 3p^2 + 3p - 1 &> 0 \iff \\
 (p-1)(p-1)^2 &> 0 \iff \\
 p &> 1.
 \end{aligned}$$

Hence we have shown the equivalence between the last two conditions in the first case. This also remains true for the second case, where  $u < 0$  is equivalent to  $p < 1$ , because the quantities  $u$  and  $v_s$  differ only by a minus sign in the two cases. This complete the proof of this lemma.  $\square$

### 3.3 Parametrizations of single shocks and rarefaction waves

In this section we extend the results obtained in [45, Section 4.4, pg. 81-84], about the parametrizations of shocks and rarefaction waves for the ultra-relativistic Euler equations (3.1). We also present a new parametrization for single shocks, which plays an important role in order to describe shock interaction in Section 4.3 as well as to present a new front tracking scheme in Chapter 6.

#### 3.3.1 Single shocks

We consider a straight line shock  $x = x(t)$  with constant speed  $s = v_s = \dot{x}$ ,  $W_- = (p_-, u_-, n_-)$  is the constant left state to the shock and  $W_+ = (p_+, u_+, n_+)$  is the constant

### 3.3. PARAMETRIZATIONS OF SINGLE SHOCKS AND RAREFACTION WAVES

right state to the shock with  $p_{\pm} > 0$ . Then (3.3) leads to the Rankine-Hugoniot jump conditions:

$$\begin{aligned} v_s [p_+(3 + 4u_+^2) - p_-(3 + 4u_-^2)] &= 4p_+u_+\sqrt{1 + u_+^2} - 4p_-u_-\sqrt{1 + u_-^2}, \\ v_s \left[ 4p_+u_+\sqrt{1 + u_+^2} - 4p_-u_-\sqrt{1 + u_-^2} \right] &= p_+(1 + 4u_+^2) - p_-(1 + 4u_-^2), \\ v_s \left[ n_+\sqrt{1 + u_+^2} - n_-\sqrt{1 + u_-^2} \right] &= n_+u_+ - n_-u_-. \end{aligned} \quad (3.33)$$

In singular points the local form of the entropy inequality (3.4) reads

$$-v_s(S_+^0 - S_-^0) + (S_+^1 - S_-^1) > 0. \quad (3.34)$$

**Definition 3.3.1.** *Given are two states  $(p_{\pm}, u_{\pm}, n_{\pm}) \in \mathbb{R}^+ \times \mathbb{R} \times \mathbb{R}^+$ . Assume that the Rankine-Hugoniot jump conditions (3.33) are satisfied.*

1. *Assume that  $0 < p_- < p_+$ . Then we say that the left state  $(p_-, u_-, n_-)$  can be connected with the right state  $(p_+, u_+, n_+)$  by a single 1-shock provided it satisfies the entropy condition  $u_- > u_+$ .*
2. *Assume that  $0 < p_+ < p_-$ . Then we say that the left state  $(p_-, u_-, n_-)$  can be connected with the right state  $(p_+, u_+, n_+)$  by a single 3-shock provided it satisfies the entropy condition  $u_- > u_+$ .*

**Lemma 3.3.2.** *Assume that  $(p_-, u_-, n_-) \equiv (p_-, 0, n_-)$  and  $(p_+, u_+, n_+) \equiv (p, u(p), n_+)$  satisfy the jump condition (3.33). Then the shock curves satisfy*

$$u(p) = \pm \frac{\sqrt{3}(p - p_-)}{4\sqrt{pp_-}}. \quad (3.35)$$

*The positive sign in (3.35) and  $p < p_-$  gives a 3-shock. These 3-shocks satisfy both the Rankine-Hugoniot jump conditions (3.33) as well as the entropy condition (3.34), or likewise  $u_- > u_+$ .*

*The minus sign in (3.35) and  $p_- < p$  gives a 1-shock. These 1-shocks satisfy both the Rankine-Hugoniot jump conditions (3.33) as well as the entropy condition (3.34), or likewise  $u_- > u_+$ . Furthermore  $\frac{du}{dp} < 0$  on  $S_1$  and  $\frac{du}{dp} > 0$  on  $S_3$ .*

*Proof.* The first part of this lemma is clear. From the two solutions (3.30) and (3.31), we see there are two types of shock curves, the positive sign with  $p < p_-$  gives a 3-shock, the minus sign with  $p_- < p$  gives a 1-shock.

We have

$$\frac{du}{dp} = -\frac{\sqrt{3}p_-(p + p_-)}{8(pp_-)^{\frac{3}{2}}} < 0, \quad (3.36)$$

### CHAPTER 3. ULTRA-RELATIVISTIC EULER EQUATIONS

---

on the shock curve  $S_1 = \{(p, u(p), n(p)) \in \mathbb{R}^+ \times \mathbb{R} \times \mathbb{R}^+ : p > p_-\}$  in the state space, and

$$\frac{du}{dp} = \frac{\sqrt{3}p_-(p + p_-)}{8(pp_-)^{\frac{3}{2}}} > 0, \quad (3.37)$$

on the shock curve  $S_3 = \{(p, u(p), n(p)) \in \mathbb{R}^+ \times \mathbb{R} \times \mathbb{R}^+ : p < p_-\}$  in the state space.  $\square$

Now we give parameter representation for single entropy shocks. For this purpose we construct the initial data as follows:

Let  $(p_*, u_*, n_*) \in \mathbb{R}^+ \times \mathbb{R} \times \mathbb{R}^+$ . Equations (3.33) and (3.34) are solved by

$$u(p) = \frac{u_*\sqrt{p_* + 3p}\sqrt{p + 3p_*} \pm \sqrt{3}(p - p_*)\sqrt{1 + u_*^2}}{4\sqrt{pp_*}}, \quad (3.38)$$

$$n(p) = n_*\sqrt{\frac{p}{p_*} \left( \frac{3p + p_*}{p + 3p_*} \right)}, \quad (3.39)$$

$$u_s(p) = \frac{u_*\sqrt{3(p + 3p_*)} \pm \sqrt{p_* + 3p}\sqrt{1 + u_*^2}}{\sqrt{8p_*}}, \quad (3.40)$$

$$v_s = \frac{u_s}{\sqrt{1 + u_s^2}}, \quad v = \frac{u}{\sqrt{1 + u^2}}, \quad v_* = \frac{u_*}{\sqrt{1 + u_*^2}} \quad (3.41)$$

in the following way:

- The ( + ) sign in (3.38), (3.40) and  $p < p_*$  gives a 3-shock with the constant state  $(p_*, u_*, n_*)$  on the left

$$(p_-, u_-, n_-) = (p_*, u_*, n_*), \quad (p_+, u_+, n_+) = (p, u(p), n(p)).$$

These 3-shocks satisfy both the Rankine-Hugoniot conditions (3.33) as well as the entropy condition (3.24).

- The ( - ) sign in (3.38), (3.40) and  $p < p_*$  gives a 1-shock with the constant state  $(p_*, u_*, n_*)$  on the right

$$(p_-, u_-, n_-) = (p, u(p), n(p)), \quad (p_+, u_+, n_+) = (p_*, u_*, n_*).$$

These 1-shocks satisfy both the Rankine-Hugoniot conditions (3.33) as well as the entropy condition (3.24).

Now we define the 2-shocks, that turn out to be contact-discontinuities without entropy production.

Only for these we choose  $n > 0$  instead of  $p$  as a parameter and set

$$(p_-, u_-, n_-) = (p_*, u_*, n_*), \quad (p_+, u_+, n_+) = (p_*, u_*, n). \quad (3.42)$$

These shocks satisfy the Rankine-Hugoniot- and entropy conditions. Note that velocity and pressure are constant across a 2-shock. Here the shock-speed is  $v_s = v_* = \frac{u_*}{\sqrt{1 + u_*^2}}$ .

### 3.3. PARAMETRIZATIONS OF SINGLE SHOCKS AND RAREFACTION WAVES

---

**Remark 3.3.3.** *From the Rankine-Hugoniot jump conditions one can derive by simple algebraic calculations that the only shocks are 1-, 2- and 3-shocks analogously as in the non-relativistic case, see Courant and Friedrichs [21].*

The structure of these shock solutions is quite similar to the classical Euler equations. It is important to notice that both entropies, the original one given by (3.5) and the reduced entropy for the  $(p, u)$ -subsystem given by (3.20), lead to the same entropy shocks, i.e. they lead to equivalent shock selection criteria. The equivalence of the local entropy inequalities (3.34) and (3.24) across a single shock front can be checked without big effort by applying a proper Lorentz-transformation which transforms  $u_*$  to 0 in the shock parameter representations above. The inverse Lorentz-transformation will then preserve these inequalities. We will make essential use of this trick when we construct the general Riemann solution for the  $(p, u)$ -subsystem.

In view of (3.21) and in view of the equivalence of the local shock conditions (3.34) and (3.24) we conclude that (3.4) and (3.19) are indeed equivalent. This equivalence holds at least for piecewise smooth solutions due to standard arguments for the decomposition of curve integrals.

In the case of the classical Euler equations the so called rarefaction waves play a key role as building blocks for the Riemann solutions beside the shock waves. The same is also true for the ultra-relativistic Euler equations. Before we construct the Riemann solutions we need the parametrizations of rarefaction waves, which given in the sequel.

We are going to present another important parametrizations for single shocks, which we will use in the following sections. In order to prescribe nonlinear elementary waves, the following two positive parameters turns out to be very useful.

$$\alpha := \frac{p_+}{p_-}, \quad \beta := \frac{\sqrt{1+u_+^2} - u_+}{\sqrt{1+u_-^2} - u_-}. \quad (3.43)$$

For this purpose we first define the function which are important in order to perform these parametrizations in a completely unified way. For  $\alpha > 0$ , we define  $L_S: \mathbb{R}^+ \mapsto \mathbb{R}^+$  by

$$L_S(\alpha) = \frac{\sqrt{1+3\alpha} + \sqrt{3}\sqrt{3+\alpha}}{\sqrt{8}}. \quad (3.44)$$

According to the function  $L_S$  we can define the following function  $K_S: \mathbb{R}^+ \mapsto \mathbb{R}^+$  by

$$K_S(\alpha) := \frac{L_S(\alpha)}{L_S(\frac{1}{\alpha})} = \frac{\sqrt{1+3\alpha}\sqrt{3+\alpha} + \sqrt{3}(\alpha-1)}{4\sqrt{\alpha}}, \quad (3.45)$$

which we will need in the next sections.

**Lemma 3.3.4.** *The functions  $L_S$  and  $K_S$  are strictly monotonically increasing.*

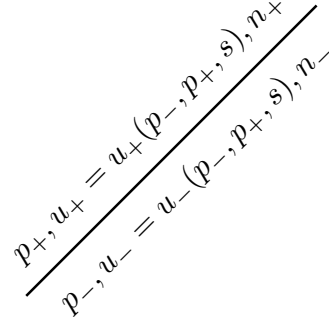


Figure 3.1: Single-shock.

*Proof.* It is easy to check that

$$L'_S(\alpha) = \frac{\sqrt{3}\sqrt{1+3\alpha} + 3\sqrt{3+\alpha}}{4\sqrt{2}\sqrt{1+3\alpha}\sqrt{3+\alpha}} > 0 \quad \text{and} \quad (3.46)$$

$$K'_S(\alpha) = \frac{(1+\alpha)(3(\alpha-1) + \sqrt{3}\sqrt{3+\alpha}\sqrt{1+3\alpha})}{8\alpha^{\frac{3}{2}}\sqrt{3+\alpha}\sqrt{1+3\alpha}} > 0 \quad (3.47)$$

for  $\alpha > 0$ , and this completes the proof of this lemma.  $\square$

**Lemma 3.3.5.** *Given are two states  $\underline{U}_\pm = (p_\pm, u_\pm) \in \mathbb{R}^+ \times \mathbb{R}$  of the subsystem (3.6) such that the lower state  $\underline{U}_-$  can be connected with the upper state  $\underline{U}_+$  by a single shock. Define  $\alpha$  and  $\beta$  according to (3.43), respectively. Let be  $n_- = n(p_-)$  and  $n_+ = n(p_+)$  by using the function  $n(p)$  in (3.39) with  $p_* := p_+$  for a single 1-shock and  $p_* := p_-$  for a single 3-shock.*

1. Assume that  $p_+ > p_-$ , i.e.  $\alpha > 1$ , and further assume that

$$\beta = K_S(\alpha). \quad (3.48)$$

*Then the lower state  $(p_-, u_-, n_-)$  can be connected with the upper state  $(p_+, u_+, n_+)$  by a single 1-shock.*

2. Assume that  $p_- > p_+$ , i.e.  $\alpha < 1$ , and further assume that

$$\beta K_S(\alpha) = 1. \quad (3.49)$$

*Then the lower state  $(p_-, u_-, n_-)$  can be connected with the upper state  $(p_+, u_+, n_+)$  by a single 3-shock.*

*Proof.* See Kunik [45, Section 4.4].  $\square$

In the following lemma we give an alternative characterization for single 1-shocks and single 3-shocks, respectively, in Figure 3.1, which turns out to be very useful in order to describe a new front tracking scheme for the ultra-relativistic Euler equations given in Chapter 6.

### 3.3. PARAMETRIZATIONS OF SINGLE SHOCKS AND RAREFACTION WAVES

---

**Lemma 3.3.6.** *Given are  $p_{\pm} > 0$  and  $s \in \mathbb{R}$  with  $|s| < 1$ . Put  $\alpha := \frac{p_+}{p_-}$  and  $\sigma := \sqrt{\frac{1-s}{1+s}}$ . Define  $u: \mathbb{R}^+ \rightarrow \mathbb{R}$  by  $u(w) = \frac{1}{2}(\frac{1}{w} - w)$ .*

(a) *Assume that  $0 < p_- < p_+$ , i.e.  $\alpha > 1$ , and put*

$$w_- := \frac{\sigma}{L_s(\alpha)}, \quad w_+ := \frac{\sigma}{L_s(\frac{1}{\alpha})}, \quad u_- := u(w_-), \quad u_+ := u(w_+). \quad (3.50)$$

*Let be  $n_- := n(p_-)$  and  $n_+ := n(p_+)$  by using the function  $n(p)$  in (3.39) with  $p_* := p_+$ . Then the lower state  $(p_-, u_-, n_-)$  of the full system (3.1) can be connected with the upper state  $(p_+, u_+, n_+)$  by a single 1-shock with speed  $s$ .*

(b) *Assume that  $0 < p_+ < p_-$ , i.e.  $\alpha < 1$ , and put*

$$w_- := \sigma \cdot L_s(\alpha), \quad w_+ := \sigma \cdot L_s\left(\frac{1}{\alpha}\right), \quad u_- := u(w_-), \quad u_+ := u(w_+). \quad (3.51)$$

*Let be  $n_- := n(p_-)$  and  $n_+ := n(p_+)$  by using the function  $n(p)$  in (3.39) with  $p_* := p_-$ . Then the lower state  $(p_-, u_-, n_-)$  of the full system (3.1) can be connected with the upper state  $(p_+, u_+, n_+)$  by a single 3-shock with speed  $s$ .*

*Proof.* By using Lorentz transformation (3.22), we first start with the special case  $s = v_s = 0$ . In our case the Rankine-Hugoniot jump conditions (3.33) become

$$\begin{aligned} 4p_+u_+\sqrt{1+u_+^2} &= 4p_-u_-\sqrt{1+u_-^2}, \\ p_+(1+4u_+^2) &= p_-(1+4u_-^2), \\ n_+u_+ &= n_-u_-. \end{aligned} \quad (3.52)$$

By solving first two equations in (3.52) and according to Lemma 3.3.5 we have two solutions: case 1 (corresponding to 1-shock), where

$$u_- = \frac{\sqrt{p_- + 3p_+}}{\sqrt{8p_-}}, \quad u_+ = \frac{\sqrt{3p_- + p_+}}{\sqrt{8p_+}}, \quad (3.53)$$

with  $p_+ > p_-$ , and case 2 (corresponding to 3-shock), where

$$u_- = -\frac{\sqrt{p_- + 3p_+}}{\sqrt{8p_-}}, \quad u_+ = -\frac{\sqrt{3p_- + p_+}}{\sqrt{8p_+}}, \quad (3.54)$$

with  $p_+ < p_-$ .

Now we deal with the case of general  $s \in \mathbb{R}$  with  $|s| < 1$ , put  $\sigma := \sqrt{\frac{1-s}{1+s}}$  and recall  $v_{\mp} = \frac{u_{\mp}}{\sqrt{1+u_{\mp}^2}}$ . By using Lemma 3.2.3 and equation (3.53), we have for the first case

$$w_- = \sigma \cdot \sqrt{\frac{1-v_-}{1+v_-}} = \sigma \cdot (\sqrt{1+u_-^2} - u_-) = \sigma \cdot \frac{\sqrt{3}\sqrt{3p_- + p_+} - \sqrt{p_- + 3p_+}}{\sqrt{8p_-}},$$

## CHAPTER 3. ULTRA-RELATIVISTIC EULER EQUATIONS

---

and

$$w_+ = \sigma \cdot \sqrt{\frac{1-v_+}{1+v_+}} = \sigma \cdot (\sqrt{1+u_+^2} - u_+) = \sigma \cdot \frac{\sqrt{3}\sqrt{3p_+ + p_-} - \sqrt{p_+ + 3p_-}}{\sqrt{8p_+}}.$$

According to the definition of the function  $L_S(\alpha)$  we can rewrite these quantities as:

$$\begin{aligned} w_- &:= \frac{\sigma}{L_S(\alpha)}, & w_+ &:= \frac{\sigma}{L_S\left(\frac{1}{\alpha}\right)}, \\ u_- &:= \frac{1}{2}\left(\frac{1}{w_-} - w_-\right), & u_+ &:= \frac{1}{2}\left(\frac{1}{w_+} - w_+\right). \end{aligned}$$

The case of 3-shock follows in the same way:

$$\begin{aligned} w_- &:= \sigma \cdot L_S(\alpha), & w_+ &:= \sigma \cdot L_S\left(\frac{1}{\alpha}\right), \\ u_- &:= \frac{1}{2}\left(\frac{1}{w_-} - w_-\right), & u_+ &:= \frac{1}{2}\left(\frac{1}{w_+} - w_+\right) \end{aligned}$$

using equation (3.54). This complete the proof of this lemma.  $\square$

### 3.3.2 Rarefaction waves

A rarefaction wave with center at the origin  $t = 0$ ,  $x = 0$  is a smooth solution of a system of hyperbolic conservation laws, which depends only on the characteristic speed  $s = \frac{x}{t}$ . If we define the  $2 \times 2$ -matrix in (3.14) by  $A = A(p, u)$  and assume that  $p$  and  $u$  depends only on  $s = \frac{x}{t}$ , then we immediately obtain from these equations with the chain rule

$$A(p, u) \begin{pmatrix} \dot{p} \\ \dot{u} \end{pmatrix} = s \begin{pmatrix} \dot{p} \\ \dot{u} \end{pmatrix}. \quad (3.55)$$

It follows that  $s$  is indeed a characteristic speed of the system, i.e.

$$s = \frac{2u\sqrt{1+u^2} \pm \sqrt{3}}{3+2u^2}, \quad u = \sqrt{\frac{3}{2} \frac{s \mp \frac{1}{\sqrt{3}}}{\sqrt{1-s^2}}}. \quad (3.56)$$

Inserting (3.56) in (3.55) leads to the condition

$$\frac{\dot{p}}{p} = \pm \frac{4}{\sqrt{3}} \frac{\dot{u}}{\sqrt{1+u^2}}, \quad (3.57)$$

and the general primitive with respect to  $s$  on both sides of this equation is with a constant  $C$

$$\ln p = C + \frac{4}{\sqrt{3}} \ln(\sqrt{1+u^2} \pm u). \quad (3.58)$$



### 3.3. PARAMETRIZATIONS OF SINGLE SHOCKS AND RAREFACTION WAVES

---

In the same way we obtain from the continuity equation for  $n$  with (3.56)

$$\ln n = C' + \sqrt{3} \ln(\sqrt{1+u^2} \pm u). \quad (3.59)$$

We finally obtain for positive real numbers  $a, b$  the parametrization of the rarefaction fans with respect to the characteristic speed  $s$

$$u(s) = \sqrt{\frac{3}{2}} \frac{s \mp \frac{1}{\sqrt{3}}}{\sqrt{1-s^2}}, \quad (3.60)$$

$$p(s) = a \left( \sqrt{1+u(s)^2} \pm u(s) \right)^{\frac{4}{\sqrt{3}}} = a \left( (2-\sqrt{3}) \frac{1 \pm s}{1 \mp s} \right)^{\frac{2}{\sqrt{3}}}, \quad (3.61)$$

$$n(s) = b \left( \sqrt{1+u(s)^2} \pm u(s) \right)^{\sqrt{3}} = b \left( (2-\sqrt{3}) \frac{1 \pm s}{1 \mp s} \right)^{\frac{\sqrt{3}}{2}}. \quad (3.62)$$

Sometimes it is also useful to take the pressure  $p$  as a parameter for the rarefaction waves and to rewrite (3.60)-(3.61) in the form

$$u(p) = \pm \frac{\left(\frac{p}{a}\right)^{\frac{\sqrt{3}}{2}} - 1}{2\left(\frac{p}{a}\right)^{\frac{\sqrt{3}}{4}}}, \quad (3.63)$$

$$n(p) = b \left(\frac{p}{a}\right)^{\frac{3}{4}}, \quad (3.64)$$

$$s(p) = \pm \frac{\left(\frac{p}{a}\right)^{\frac{\sqrt{3}}{2}} + \sqrt{3} - 2}{\left(\frac{p}{a}\right)^{\frac{\sqrt{3}}{2}} - \sqrt{3} + 2}. \quad (3.65)$$

In both parametrizations the upper sign represents the 3-waves and the lower sign the 1-waves.

We are going to give parametrization for rarefaction waves. For this purpose we first define the function which are important in order to perform these parametrizations in a completely unified way. For  $\alpha > 0$ , we define  $K_R: \mathbb{R}^+ \rightarrow \mathbb{R}^+$  by

$$K_R(\alpha) = \alpha^{\frac{\sqrt{3}}{4}}. \quad (3.66)$$

In the following lemma, we give a another characterization for the case that the left state  $(p_-, u_-, n_-)$  can be connected with the right state  $(p_+, u_+, n_+)$  by a single 1-rarefaction wave or a single 3-rarefaction wave, respectively.

**Lemma 3.3.7.** *Given are  $(p_{\pm}, u_{\pm}) \in \mathbb{R}^+ \times \mathbb{R}$ . Define  $\alpha$  and  $\beta$  according to (3.43), respectively. Let be  $n_- = n(p_-)$  and  $n_+ = n(p_+)$  by using the function  $n(p)$  in (3.64).*

## CHAPTER 3. ULTRA-RELATIVISTIC EULER EQUATIONS

---

1. Assume that  $p_- > p_+$ , i.e.  $\alpha < 1$  and further assume that

$$\beta = K_R(\alpha). \quad (3.67)$$

Then the lower state  $(p_-, u_-, n_-)$  can be connected with the upper state  $(p_+, u_+, n_+)$  by a single 1-rarefaction wave.

2. Assume that  $p_+ > p_-$ , i.e.  $\alpha > 1$  and further assume that

$$\beta K_R(\alpha) = 1. \quad (3.68)$$

Then the lower state  $(p_-, u_-, n_-)$  can be connected with the upper state  $(p_+, u_+, n_+)$  by a single 3-rarefaction wave.

*Proof.* According to (3.61) with the lower sign, for the case of 1-rarefaction wave, we have

$$p_+ = a(\sqrt{1+u_+^2} - u_+)^{\frac{4}{\sqrt{3}}}, \quad p_- = a(\sqrt{1+u_-^2} - u_-)^{\frac{4}{\sqrt{3}}}.$$

Then

$$\frac{p_+}{p_-} = \alpha = \left( \frac{\sqrt{1+u_+^2} - u_+}{\sqrt{1+u_-^2} - u_-} \right)^{\frac{4}{\sqrt{3}}} = \beta^{\frac{4}{\sqrt{3}}}. \quad (3.69)$$

Hence we obtain for a 1-fan:

$$\beta = \alpha^{\frac{\sqrt{3}}{4}} = K_R(\alpha). \quad (3.70)$$

The proof for a 3-fan follows in the same way.  $\square$

### 3.4 Solution of the Riemann problem

In this section we recall briefly the results obtained in [45, Section 4.4] about the Riemann problem for system (3.6). Now we solve the weak form of the hyperbolic  $2 \times 2$  system (3.6) for given Riemannian initial data of the so called shock tube problem

$$p_0(x) = \begin{cases} p_-, & x \leq 0 \\ p_+, & x > 0 \end{cases}, \quad u_0(x) = \begin{cases} u_-, & x \leq 0 \\ u_+, & x > 0 \end{cases}. \quad (3.71)$$

The basic ingredients for Riemann solutions are the parametrizations of shocks and rarefaction waves studied before. In order to prepare the construction of the Riemann solutions we start with two important simplifications.

1. The first simplification is based on the fact that whenever  $(p, u)$  is a weak solution of (3.6), then also  $(kp, u)$  for a positive constant  $k$ , i.e. we can apply a homogeneous scaling of the pressure with the scaling factor  $k$ .
2. The second simplification is more interesting. It is based on the fact that the weak solutions are invariant with respect to the homogeneous Lorentz-transformations (3.22).

### 3.4. SOLUTION OF THE RIEMANN PROBLEM

---

**Lemma 3.4.1.** [45, Section 4.4] *The expression  $\frac{\sqrt{1+u_+^2}-u_+}{\sqrt{1+u_-^2}-u_-}$  is invariant with respect to the Lorentz-transformation (3.22), if applied to the relativistic Lorentz-vectors  $(\sqrt{1+u_\pm^2}, u_\pm)$  obtained from the initial data  $u_0$  in (6.13).*

We define the equivalence of two Riemann solutions if it is possible to map them on each other by an appropriate scaling of the pressure and by applying an appropriate Lorentz-transformation (3.22). Then we can state that equivalent Riemann solutions depend only on the two positive parameters  $\alpha$  and  $\beta$  which are given in (3.43). For this purpose we use Lemma 3.3.5 and 3.3.7, which are important in order to perform this equivalence in a completely unified way.

This equivalence also allows us to simplify calculations considerably by assuming first the special case

$$p_* = 1, \quad u_* = 0 \tag{3.72}$$

in the single-shock parametrizations (3.38)-(3.41). Afterwards one can easily remove these restrictions by applying an appropriate Lorentz-transformation (3.22) and an appropriate scaling of the pressure. The reason for this simplification is that (3.72) turns out to be an intermediate constant state in the equivalent Riemann solutions.

We give the general Riemann solutions by studying four cases, where the behavior of the solution depends on the corresponding four regions depicted in Figure 3.2. For each case monotonicity arguments as well as the Intermediate Value Theorem can be employed in order to construct an intermediate state  $(p_*, u_*)$  in the so called “star-region”, which can be connected with a single shock or rarefaction wave to the prescribed left and right Riemannian initial data. The boundaries of these four regions characterize the initial data for which the Riemann solution consists only of a single shock or rarefaction wave in the sense of Lemma 3.3.5 and 3.3.7. In this section, we only gave a small abbreviation for each case.

Using the initial data (6.13), we define the following positive parameters  $\alpha = \frac{p_+}{p_-}$ ,  $\beta = \frac{\sqrt{1+u_+^2}-u_+}{\sqrt{1+u_-^2}-u_-}$ , which are important in order to give the following classification of the Riemann solutions in a completely unified way. The parameter  $\alpha$  reflects the homogeneous scaling of the pressure, whereas  $\beta$  reflects the Lorentz invariant due to Lemma 3.4.1.

Each of the following four cases describes a Riemann solution, which is depicted with the corresponding case in Figure 3.2.

**Case 1:**  $\beta < K_S(\alpha)$  and  $\beta K_R(\alpha) > 1$ .

Here the solution is composed of a lower 1-shock and an upper 3-rarefaction wave. The intermediate pressure and velocity are given by the implicit equations

$$K_S\left(\frac{p_*}{p_-}\right) K_R\left(\frac{p_*}{p_+}\right) = \beta, \quad \frac{\sqrt{1+u_*^2}-u_*}{\sqrt{1+u_-^2}-u_-} = K_S\left(\frac{p_*}{p_-}\right). \tag{3.73}$$

## CHAPTER 3. ULTRA-RELATIVISTIC EULER EQUATIONS

---

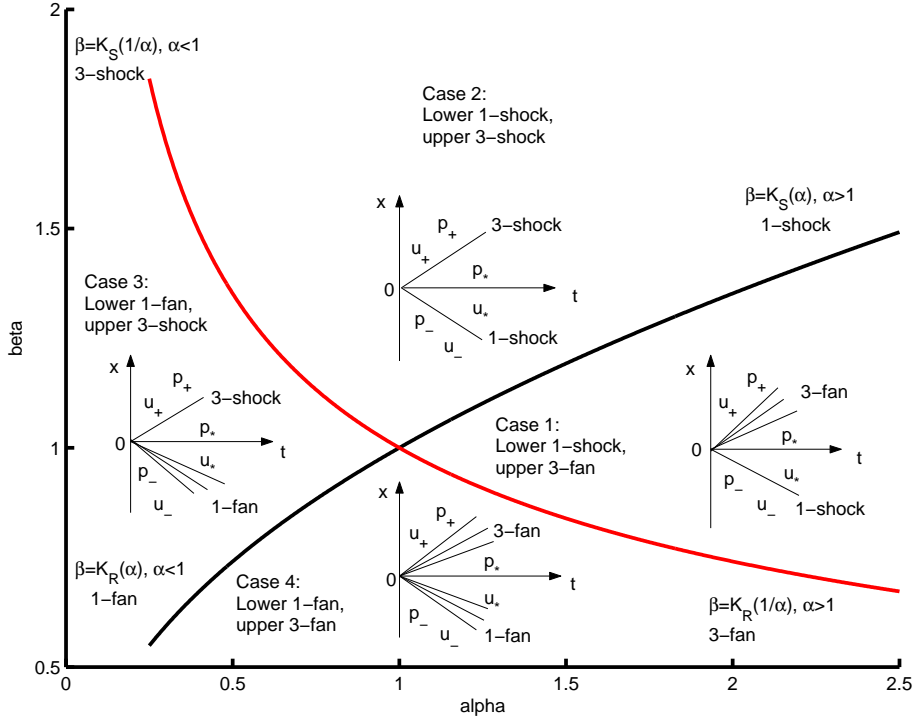


Figure 3.2: Classification of the Riemann solutions.

We obtain in this case the following inequalities:

$$\alpha > 1, \quad p_- < p_* < p_+ \quad \text{and} \quad u_* < \min(u_-, u_+). \quad (3.74)$$

**Case 2:**  $\beta > K_S(\alpha)$  and  $\beta K_S(\alpha) > 1$ .

Here the solution is composed of a lower 1-shock and an upper 3-shock. The intermediate pressure and velocity are given by the implicit equations

$$K_S\left(\frac{p_*}{p_-}\right) K_S\left(\frac{p_*}{p_+}\right) = \beta, \quad \frac{\sqrt{1+u_*^2} - u_*}{\sqrt{1+u_-^2} - u_-} = K_S\left(\frac{p_*}{p_-}\right). \quad (3.75)$$

We obtain in this case the following inequalities:

$$\beta > 1, \quad p_* > \max(p_-, p_+) \quad \text{and} \quad u_- > u_* > u_+. \quad (3.76)$$

Note that especially the condition  $p_* > \max(p_-, p_+)$  describes the compression of the gas in a shock tube from above and below. Furthermore the condition  $u_- > u_* > u_+$  describes the entropy conditions for the solution, which is composed of a lower 1-shock and an upper 3-shock.

**Case 3:**  $\beta > K_R(\alpha)$  and  $\beta K_S(\alpha) < 1$ .

Here the solution is composed of a lower 1-rarefaction wave and an upper 3-shock. The intermediate pressure and velocity are given by the implicit equations

$$K_R\left(\frac{p_*}{p_-}\right) K_S\left(\frac{p_*}{p_+}\right) = \beta, \quad \frac{\sqrt{1+u_*^2} - u_*}{\sqrt{1+u_-^2} - u_-} = K_R\left(\frac{p_*}{p_-}\right). \quad (3.77)$$

We obtain in this case the following inequalities:

$$\alpha < 1, \quad p_- > p_* > p_+ \quad \text{and} \quad u_* > \max(u_-, u_+). \quad (3.78)$$

**Case 4:**  $\beta < K_R(\alpha)$  and  $\beta K_R(\alpha) < 1$ .

Here the solution is composed of a lower 1-rarefaction wave and an upper 3-rarefaction wave. The intermediate pressure and velocity are given by the implicit equations

$$K_R\left(\frac{p_*}{p_-}\right) K_R\left(\frac{p_*}{p_+}\right) = \beta, \quad \frac{\sqrt{1+u_*^2} - u_*}{\sqrt{1+u_-^2} - u_-} = K_R\left(\frac{p_*}{p_-}\right). \quad (3.79)$$

In this case the intermediate fields can be solved explicitly by

$$\frac{p_*}{p_-} = \alpha^{\frac{1}{2}} \beta^{\frac{2}{\sqrt{3}}}, \quad \frac{\sqrt{1+u_*^2} - u_*}{\sqrt{1+u_-^2} - u_-} = \alpha^{\frac{\sqrt{3}}{8}} \beta^{\frac{1}{2}}. \quad (3.80)$$

We obtain in this case the following inequalities:

$$\beta < 1, \quad p_* < \min(p_-, p_+) \quad \text{and} \quad u_- < u_* < u_+. \quad (3.81)$$

Note that especially the condition  $p_* < \min(p_-, p_+)$  describes the rarefaction of the gas in a shock tube from above and below.

## 3.5 Riemann invariants

In this section we introduce the famous topic in hyperbolic systems of conservation laws called Riemann invariants. First we calculate the Riemann invariants for the ultra-relativistic Euler system (3.6). Second we show that shock curves have good geometry properties in Riemann invariants coordinates. We also show that the Riemann invariants have surprising relations with the two functions  $K_S$  and  $K_R$ , which are given in (3.45), (3.66), respectively. The Riemann invariants for system (3.6) can be found from the eigenvectors. An  $i^{\text{th}}$ -Riemann invariants is a function  $\psi$  such that

$$r_i \cdot \nabla \psi = 0.$$

Recall the corresponding right eigenvectors for system (3.6) given in (3.16)

$$r_1 = \left( \frac{-4p}{\sqrt{3}\sqrt{1+u^2}}, 1 \right)^T, \quad r_3 = \left( \frac{4p}{\sqrt{3}\sqrt{1+u^2}}, 1 \right)^T. \quad (3.82)$$

## CHAPTER 3. ULTRA-RELATIVISTIC EULER EQUATIONS

---

Let  $w$  denote a 1-Riemann invariant for system (3.6). Then it must satisfy

$$-\frac{4p}{\sqrt{3}\sqrt{1+u^2}}w_p + w_u = 0. \quad (3.83)$$

It is easy to verify that

$$w = \ln(\sqrt{1+u^2} + u) + \frac{\sqrt{3}}{4} \ln(p) \quad (3.84)$$

satisfies (3.83). Thus  $w$  is a 1-Riemann invariant for system (3.6). Similarly we see that

$$z = \ln(\sqrt{1+u^2} + u) - \frac{\sqrt{3}}{4} \ln(p) \quad (3.85)$$

is a 3-Riemann invariant for system (3.6).

The function  $w = w(p, u)$  is constant across 1-rarefaction waves and  $z = z(p, u)$  is constant across 3-rarefaction waves.

We now study the geometric properties of the shock curves for system (3.6). We know from Proposition 3.2.1 that the conserved quantities are uniquely determined by  $p$  and  $u$ .

**Lemma 3.5.1.** *The mapping  $(p, u) \mapsto (w, z)$  is one-to-one with nonsingular Jacobian in the region  $p > 0, u \in \mathbb{R}$ .*

*Proof.* Let

$$\begin{aligned} h &= w + z = 2 \ln(\sqrt{1+u^2} + u), \\ g &= w - z = \frac{\sqrt{3}}{2} \ln(p), \end{aligned} \quad (3.86)$$

so  $h = h(u)$  is a function of  $u$  and  $g = g(p)$  is a function of  $p$ , with  $h'(u) = \frac{2}{\sqrt{1+u^2}} > 0$ ,  $g'(p) = \frac{\sqrt{3}}{2p} > 0$  when  $p > 0$ . So the mapping  $(p, u) \mapsto (h, g)$  is one-to-one. The determinant of this mapping is

$$\begin{vmatrix} g'(p) & 0 \\ 0 & h'(u) \end{vmatrix} = g'(p)h'(u) > 0.$$

The mapping  $(h, g) \mapsto (w, z)$  is

$$\begin{pmatrix} h \\ g \end{pmatrix} = \begin{pmatrix} 1 & 1 \\ 1 & -1 \end{pmatrix} \begin{pmatrix} w \\ z \end{pmatrix}. \quad (3.87)$$

This is a nonsingular linear mapping and so  $(h, g) \mapsto (w, z)$  is one-to-one. Then  $(p, u) \mapsto (w, z)$  is one-to-one, and the determinant of the Jacobian of this mapping is non zero in the region  $p > 0, u \in \mathbb{R}$ .  $\square$

**Lemma 3.5.2.** *For shock curves of system (3.6) we have*

$$0 < \frac{dw}{dz} < 1 \quad (3.88)$$

along a 1-shock curves  $S_1$  and

$$0 < \frac{dz}{dw} < 1 \quad (3.89)$$

a along a 3-shock curves  $S_3$

*Proof.* Along 1-shock curve, we have

$$\frac{dw}{dz} = \frac{\frac{dw}{dp}}{\frac{dz}{dp}}, \quad (3.90)$$

$$\frac{dw}{dp} = \frac{1}{\sqrt{1+u^2}}u_p + \frac{\sqrt{3}}{4p}, \quad (3.91)$$

$$\frac{dz}{dp} = \frac{1}{\sqrt{1+u^2}}u_p - \frac{\sqrt{3}}{4p}, \quad (3.92)$$

where

$$u(p) = \frac{-\sqrt{3}(p-p_-)}{4\sqrt{pp_-}}, \quad (3.93)$$

and

$$u_p = \frac{-\sqrt{3}p_-(p-p_-)}{8pp_-^{\frac{3}{2}}}. \quad (3.94)$$

From (3.94),  $u_p < 0$  on  $S_1$ , hence from (3.92), we obtain

$$\frac{dz}{dp} < 0. \quad (3.95)$$

Note that two terms in (3.92) are of the same sign and two terms in (3.91) are of different signs, then we have

$$\left| \frac{dz}{dp} \right| > \left| \frac{dw}{dp} \right| \quad (3.96)$$

and thus

$$\left| \frac{dw}{dz} \right| < 1. \quad (3.97)$$

## CHAPTER 3. ULTRA-RELATIVISTIC EULER EQUATIONS

---

In order to show  $0 < \frac{dw}{dz}$ , it is sufficient to prove  $\frac{dw}{dp} < 0$ , since  $\frac{dz}{dp} < 0$  from (3.95).

$$\begin{aligned}
 \frac{dw}{dp} < 0 &\iff \\
 \frac{4\sqrt{pp_-}}{\sqrt{3p_- + p}\sqrt{3p + p_-}} - \frac{\sqrt{3}p_-(p - p_-)}{8(pp_-)^{\frac{3}{2}}} + \frac{\sqrt{3}}{4p} < 0 &\iff \\
 \frac{4(p - p_-) + 2\sqrt{3}\sqrt{3p_- + p}\sqrt{3p + p_-}}{8p\sqrt{3p_- + p}\sqrt{3p + p_-}} < 0 &\iff \\
 \sqrt{3p_- + p}\sqrt{3p + p_-} < 2(p + p_-) &\iff \\
 (p - p_-)^2 > 0 &\iff \\
 p > p_-. &
 \end{aligned}$$

Thus we have  $0 < \frac{dw}{dz} < 1$  along a 1-shock curve. For a 3-shock curve the situation is analogous, and the statement can be proved with the same arguments.  $\square$

We can therefore use either the  $pu$ -plane or the  $zw$ -plane to study our problem. The main result here is that the shock curves are independent of the base point  $(z_-, w_-)$ .

The following lemma gives a new parametrization of the shock curves for system (3.6) in the  $zw$ -plane. In fact this parametrization depends on the function  $K_S, K_R$ , which given in (3.45) and (3.66) respectively, in Section 3.3.

**Lemma 3.5.3.** *Let  $z \equiv z(p_+, u_+)$ ,  $w = w(p_+, u_+)$ . Then the 1-shock curve  $S_1$  for the system (3.6) based at  $(z_-, w_-)$  is given by the following parametrization with respect to the parameter  $\alpha = \frac{p_+}{p_-}$ :*

$$z - z_- = \ln K_S\left(\frac{1}{\alpha}\right) + \ln K_R\left(\frac{1}{\alpha}\right), \quad w - w_- = \ln K_S\left(\frac{1}{\alpha}\right) - \ln K_R\left(\frac{1}{\alpha}\right).$$

While the 3-shock curves  $S_3$  based at  $(z_-, w_-)$  has the parametrization

$$z - z_- = \ln K_S(\alpha) - \ln K_R(\alpha), \quad w - w_- = \ln K_S(\alpha) + \ln K_R(\alpha).$$

*Proof.* We only prove the case for 1-shock curve  $S_1$  using Lemma 3.3.5, the proof for  $S_3$  is similar.

$$\begin{aligned}
 z - z_- &= \ln \frac{u_+ + \sqrt{1 + u_+^2}}{u_- + \sqrt{1 + u_-^2}} - \frac{\sqrt{3}}{4} \ln \frac{p_+}{p_-} \\
 &= \ln \frac{u_- - \sqrt{1 + u_-^2}}{u_+ - \sqrt{1 + u_+^2}} - \frac{\sqrt{3}}{4} \ln \alpha \\
 &= \ln \frac{1}{\beta} + \frac{\sqrt{3}}{4} \ln \frac{1}{\alpha} \\
 &= \ln K_S\left(\frac{1}{\alpha}\right) + \ln K_R\left(\frac{1}{\alpha}\right).
 \end{aligned}$$



### 3.6. CONE-GRID SCHEME FOR THE ONE-DIMENSIONAL ULTRA-RELATIVISTIC EULER EQUATIONS

---

$$\begin{aligned}
w - w_- &= \ln \frac{u_+ + \sqrt{1 + u_+^2}}{u_- + \sqrt{1 + u_-^2}} + \frac{\sqrt{3}}{4} \ln \frac{p_+}{p_-} \\
&= \ln \frac{u_- - \sqrt{1 + u_-^2}}{u_+ - \sqrt{1 + u_+^2}} + \frac{\sqrt{3}}{4} \ln \alpha \\
&= \ln \frac{1}{\beta} - \frac{\sqrt{3}}{4} \ln \frac{1}{\alpha} \\
&= \ln K_S \left( \frac{1}{\alpha} \right) - \ln K_R \left( \frac{1}{\alpha} \right).
\end{aligned}$$

□

The above lemma shows that the differences  $z - z_-$  and  $w - w_-$  along a shock curve depend only on the parameters  $\alpha$ , and thus the geometric shape of the shock curves in the  $zw$ -plane is independent of the base point.

### 3.6 Cone-grid scheme for the one-dimensional ultra-relativistic Euler equations

This scheme was developed by my supervisor Matthias Kunik in his lecture notes [46] and I also do the implementation of this scheme. In the main time a common publication of this scheme in comparison with the front tracking method given in [2].

For numerical purposes the one-dimensional ultra-relativistic Euler equations may be written down in the dimensionless “vector form”,

$$W_t + F(W)_x = 0, \quad (3.98)$$

where

$$W = \begin{pmatrix} T^{00} \\ T^{01} \\ N^0 \end{pmatrix} = \begin{pmatrix} p(3 + 4u^2) \\ 4pu\sqrt{1 + u^2} \\ n\sqrt{1 + u^2} \end{pmatrix}, \quad F(W) = \begin{pmatrix} T^{01} \\ T^{11} \\ N^1 \end{pmatrix} = \begin{pmatrix} 4pu\sqrt{1 + u^2} \\ p(1 + 4u^2) \\ nu \end{pmatrix}. \quad (3.99)$$

The natural domain  $\Omega_W$  for the  $(T^{00}, T^{01}, N^0)$  state space is given by

$$\Omega_W = \{(T^{00}, T^{01}, N^0) \in \mathbb{R} \times \mathbb{R} \times \mathbb{R}^+ : |T^{01}| < T^{00}\}. \quad (3.100)$$

Note that from each quantity  $W = \begin{pmatrix} p(3 + 4u^2) \\ 4pu\sqrt{1 + u^2} \\ n\sqrt{1 + u^2} \end{pmatrix}$  we can easily get back the values of  $p$ ,  $u$  and  $n$  by using the formulas

$$p = \frac{1}{3} \left[ \sqrt{4(T^{00})^2 - 3(T^{01})^2} - T^{00} \right], \quad u = \frac{T^{01}}{\sqrt{4p(p + T^{00})}}, \quad n = \frac{N^0}{\sqrt{1 + u^2}}. \quad (3.101)$$

## CHAPTER 3. ULTRA-RELATIVISTIC EULER EQUATIONS

---

However, this requires that there hold the inequalities  $|T^{01}| < T^{00}$  and  $N^0 > 0$  from (3.100) in order to obtain positive values for  $p$  and  $n$ .

We also prescribe initial data for  $(p, u, n)$  at  $t = 0$  which are restricted by the positivity-conditions  $p > 0$ ,  $n > 0$ . It is sufficient for our numerical purposes to assume that this initial data is piecewise constant on some equidistant spatial grid, which will be fixed later.

In this section we develop a numerical scheme which is discretized in time and space. We will call it cone-grid scheme for the initial value problem. This is rigorously based on the integral conservation laws in terms of curve integrals adapted to the choice of the numerical grid for the discretization of time and space. This scheme is of first order with respect to time and space.

The cone-grid scheme is very simple and can be obtained from the conservation laws on a light cone-grid. We prescribe a fixed time step  $\Delta t > 0$  and calculate the spatial mesh size  $\Delta x$  in terms of the natural Courant-Friedrichs-Lewy (CFL) condition according to

$$\Delta x = 2\Delta t. \quad (3.102)$$

Later on this condition will guarantee that neighboring light cones will not interact within the time step of the numerical scheme. Note that in the theory of the classical Euler equations one has to assume a bound for the characteristic speeds which depend on the choice of the initial data in order to obtain a CFL-condition. This is not necessary in our case, since in the relativistic theory every signal speed is bounded by the velocity of light, which is normalized to one in dimensionless form. In the cone-grid scheme, we consider the Riemann solution of the ultra-relativistic Euler equations inside the light cone depicted in the Figure 3.3. For the formulation of the cone-grid scheme, we use the conservation laws with respect to the domain depicted in Figure 3.3, namely

$$\oint_{\partial\Omega} W(t, x) dx - F(W(t, x)) dt = 0. \quad (3.103)$$

### 3.6.1 The computational domain

The computational domain is the trapezium in Figure 3.4. Given are  $\alpha$  and  $\beta \in \mathbb{R}$ , with  $\alpha < \beta$ ,  $T > 0$  and  $M \in \mathbb{N}$ , which is the number of grid cells for the half of the space interval  $[\alpha, \beta]$ , i.e.

1. The spatial mesh size is

$$\Delta x := \frac{\beta - \alpha}{2M}. \quad (3.104)$$

2. The number

$$N := \left\lceil \frac{T}{\Delta x} \right\rceil = \left\lceil \frac{2TM}{\beta - \alpha} \right\rceil \quad (3.105)$$

is the smallest integer such that  $T \leq N \cdot \Delta x$ , where the ceiling function  $\lceil x \rceil$  is the smallest integer larger than or equal  $x$ .

### 3.6. CONE-GRID SCHEME FOR THE ONE-DIMENSIONAL ULTRA-RELATIVISTIC EULER EQUATIONS

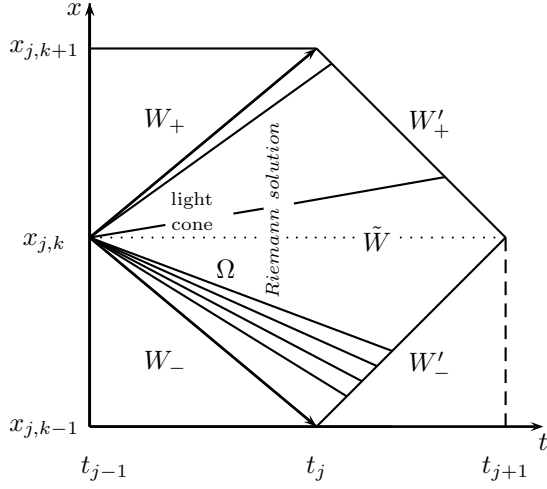


Figure 3.3: Balance regions for the cone-grid scheme (light cone).

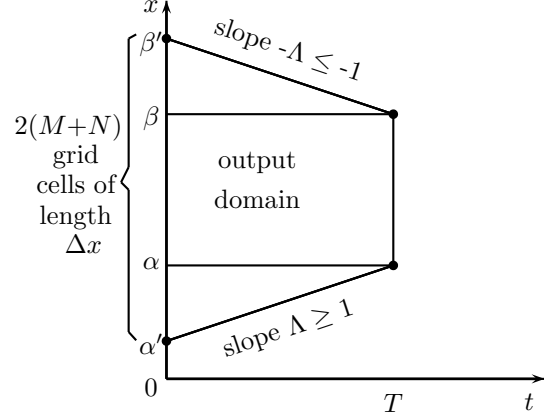


Figure 3.4: Computational domain.

3. Put  $\Delta t := \frac{T}{2N}$ . Then  $T = 2N\Delta t$ . Hence, using 1 and 2 we have

$$\Lambda = \frac{\Delta x}{2\Delta t} = \frac{\Delta x \cdot N}{T} \geq 1, \quad (3.106)$$

such that the CFL-condition is satisfied.  $N$  is the number of grid cells for the half of the time interval  $[0, T]$  and  $\Delta t$  the time step size i.e. the interval  $[0, T]$  splits into  $2N$  sub intervals of length  $\Delta t$ .

4. We have the time discretization  $t_j = j \cdot \Delta t$  for  $j \in \{0, \dots, 2N\}$ .
5. We define the quantities

$$\alpha' = \alpha - T \cdot \Lambda, \quad \beta' = \beta + T \cdot \Lambda, \quad (3.107)$$

which determine the bounds of the trapezium domain on the  $x$ -axis in order to avoid artificial numerical boundary effects, see Figure 3.4. The spatial intervals  $[\alpha', \alpha]$ ,  $[\beta, \beta']$  split into  $N$  sub intervals of length  $\Delta x$ .

6. At time  $t_{j-1}$  we define the grid points

$$x_{j,k} = \alpha' + (j-1)\Lambda \cdot \Delta t + (k-1)\Delta t, \quad j = 1, \dots, 2N+1, \quad k = 1, \dots, 2(M+N) - j + 2.$$

We note that the quantities  $x_{j,k}$  determine all points of each balance cell in Figure 3.3. Especially we can easily check that  $x_{1,1} = \alpha'$  and  $x_{1,2(M+N)+1} = \beta'$  at initial time  $t_0 = 0$  as well as  $x_{2N+1,1} = \alpha$  and  $x_{2N+1,2M+1} = \beta$  at final time  $t_{2N} = T$ , which give the four corner points in the trapezoidal computational domain 3.4.

### 3.6.2 The construction of the solution

Now we consider a restriction to spatial grid points that gives the left corner points of each balance cell in Figure 3.3 as well as in Figure 3.5. In these balance cells we will now solve local Riemann problems. For the left corner-point  $\nu_1$  given by  $\nu_1 = (t_{j-1}, x_{j,k})$  in Figure 3.5 we solve the local Riemann problem

$$\begin{cases} W_t + F(W)_x = 0, \\ W(t_{j-1}, x) = \begin{cases} W_- & \text{if } x \leq x_{j,k} \\ W_+ & \text{if } x > x_{j,k} \end{cases} \end{cases}$$

for  $t > t_{j-1}$  and assume that the numerical solution inside the parallelogram is given by  $W(t, x)$ .

Especially the constant value of  $W(t, x)$  along the cord connecting  $\nu_1$  with  $\nu_3$  will be denoted by  $\tilde{W}$ . Consider the triangular balance regions  $\Omega_{j,k}^+$  and  $\Omega_{j,k}^-$ , spanned by the points  $\nu_1, \nu_3, \nu_4$  and  $\nu_1, \nu_2, \nu_3$ , respectively, see Figure 3.5. On each cord  $\nu_2\nu_3$  and  $\nu_3\nu_4$  we replace the numerical solution by the unknown constant values  $W'_+$  and  $W'_-$ , and require for  $W$  and  $F$  in (3.99) that

$$\int_{\partial\Omega_{j,k}^\mp} W dx - F(W) dt = 0. \quad (3.108)$$

For the balance region  $\partial\Omega_{j,k}^+$ , using 3.106 we obtain:

$$W'_+ - W_+ - \frac{1}{\Lambda} \left[ 2 F(\tilde{W}) - F(W'_+) - F(W_+) \right] = 0, \quad (3.109)$$

i.e. an implicit equation for  $W'_+$ .

For the balance region  $\partial\Omega_{j,k}^-$  we obtain in the same way the following implicit equation for  $W'_-$ :

$$W'_- - W_- + \frac{1}{\Lambda} \left[ 2 F(\tilde{W}) - F(W'_-) - F(W_-) \right] = 0. \quad (3.110)$$

The new states  $W'_\mp$  turn out to be uniquely determined by using (3.109), (3.110) and the CFL-condition  $\Lambda \geq 1$ . Hence the states  $(p'_-, u'_-, n'_-)$  and  $(p'_+, u'_+, n'_+)$  are also determined uniquely.

Note that for fixed values of  $\alpha, \beta$  and  $T$  the quantity  $\Lambda$  in (3.106) depends on  $M$ , such that we can also rewrite it in the form  $\Lambda = \Lambda_M$ . Then we conclude from (3.104), (3.105) that

$$\lim_{M \rightarrow \infty} \Lambda_M = 1.$$

On the other hand, even for a fixed value of  $M$ , not necessary large, we can slightly change the values of  $\alpha, \beta$  and  $T$  such that we have  $\Delta x = 2\Delta t$ . Therefore we will assume in the sequel that  $\Lambda = 1$ .

### 3.6. CONE-GRID SCHEME FOR THE ONE-DIMENSIONAL ULTRA-RELATIVISTIC EULER EQUATIONS

---

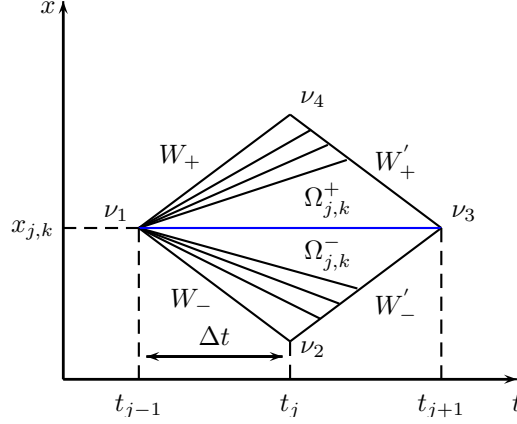


Figure 3.5: Balance cell for the cone-grid scheme.

#### 3.6.3 Formulation of the cone-grid scheme

In order to finish the construction of the cone-grid scheme we have to determine the states  $W'_\pm$  in terms of the states  $W_\pm$  in each balance region  $\Omega_{j,k}^\mp$  of the computational domain, see Figure 3.5. Recall that we assume  $\Lambda = 1$  for the rest of this section, especially in the balance equations (3.109) and (3.110), which we will solve now explicitly. Since the constant value  $\tilde{W}$  along the cord connecting  $\nu_1$  with  $\nu_3$  is determined from Riemann solution given in [3], we can solve (3.109) and (3.110) for the lower and upper part of cell in Figure 3.5. We define

$$r^\pm = \begin{pmatrix} r_1^\pm \\ r_2^\pm \\ r_3^\pm \end{pmatrix} := W'_\pm \pm F(W'_\pm). \quad (3.111)$$

From the balance laws (3.109) and (3.110) we obtain with (3.99) and (3.111)

$$r_1^\pm = p'_\pm(3 + 4u_\pm'^2) \pm 4p'_\pm u'_\pm \sqrt{1 + u_\pm'^2} = \pm 2 \cdot 4\tilde{p}\tilde{u}\sqrt{1 + \tilde{u}^2} + p_\pm(3 + 4u_\pm^2) \mp 4p_\pm u_\pm \sqrt{1 + u_\pm^2}, \quad (3.112)$$

$$r_2^\pm = 4p'_\pm u'_\pm \sqrt{1 + u_\pm'^2} \pm p'_\pm(1 + 4u_\pm'^2) = \pm 2 \cdot \tilde{p}(1 + 4\tilde{u}^2) + 4p_\pm u_\pm \sqrt{1 + u_\pm^2} \mp p_\pm(1 + 4u_\pm^2), \quad (3.113)$$

$$r_3^\pm = n'_\pm \sqrt{1 + u_\pm'^2} \pm n'_\pm u'_\pm = \pm 2\tilde{n}\tilde{u} + n_\pm \sqrt{1 + u_\pm^2} \mp n_\pm u_\pm. \quad (3.114)$$

We can easily solve equations (3.112)-(3.114) explicitly, and obtain that

$$p'_+ = \frac{r_1^+ - r_2^+}{2} \quad \text{and} \quad p'_- = \frac{r_1^- + r_2^-}{2}, \quad (3.115)$$

$$u'_+ = \frac{3r_2^+ - r_1^+}{\sqrt{8(r_1^{+2} - r_2^{+2})}} \quad \text{and} \quad u'_- = \frac{3r_2^- + r_1^-}{\sqrt{8(r_1^{-2} - r_2^{-2})}}, \quad (3.116)$$

$$n'_+ = \sqrt{2} r_3^+ \sqrt{\frac{r_1^+ - r_2^+}{r_1^+ + r_2^+}} \quad \text{and} \quad n'_- = \sqrt{2} r_3^- \sqrt{\frac{r_1^- + r_2^-}{r_1^- - r_2^-}}. \quad (3.117)$$

In order to show that the quantities in (3.116) and (3.117) are well defined, we still have to show that

$$r_1^\pm - r_2^\pm > 0, \quad r_1^\pm + r_2^\pm > 0. \quad (3.118)$$

Then it also follows the positivity of the pressure and of the particle density, which is needed for the cone grid scheme. For this purpose we will use the integral form (3.108), which turns out to be better suited than the implicit equations (3.109) and (3.110).

### 3.6.4 Positivity of pressure and particle density for the cone-grid scheme

Here we show that our cone-grid scheme preserves positivity of the pressure and particle density. In order to prove the positivity properties, let  $p(s)$ ,  $u(s)$ ,  $n(s)$ ,  $s = \frac{x}{t}$  with  $x \in \mathbb{R}$ ,  $t > 0$ , be the solution of the Riemannian initial value problem for the ultra-relativistic Euler equations (3.98) with  $(p_-, u_-, n_-)$  is the constant left state and  $(p_+, u_+, n_+)$  is the constant right state,  $p_\pm > 0$ ,  $n_\pm > 0$ . We rewrite (3.103) for the upper part of the cell  $\Omega_{j,k}^+$  in Figure 3.5 and take without loss of generality

$$\nu_1 = (0, 0), \quad \nu_2 = \left(\Delta t, -\frac{\Delta x}{2}\right), \quad \nu_3 = (2\Delta t, 0) \quad \text{and} \quad \nu_4 = \left(\Delta t, \frac{\Delta x}{2}\right).$$

Then using  $s = \frac{\Delta t - \vartheta}{\Delta t + \vartheta}$ , we have

$$\begin{aligned} -2\Delta t F(\tilde{W}) &= \Delta t W_+ - \Delta t F(W_+) + \int_0^{\Delta t} W \left( \frac{\Delta t - \vartheta}{\Delta t + \vartheta} \right) (-d\vartheta) - F \left( \frac{\Delta t - \vartheta}{\Delta t + \vartheta} \right) d\vartheta \\ &= \Delta t W_+ - \Delta t F(W_+) + \int_1^0 W(s) \frac{2\Delta t}{(1+s)^2} ds + F(s) \frac{2\Delta t}{(1+s)^2} ds. \end{aligned}$$

Thus

$$r^+ = 2F(\tilde{W}) + W_+ - F(W_+) = 2 \int_0^1 \frac{W(s) + F(s)}{(1+s)^2} ds.$$

In the same way, for the lower part of each cell we have

$$r^- = -2F(\tilde{W}) + W_- + F(W_-) = 2 \int_0^1 \frac{W(-s) - F(-s)}{(1+s)^2} ds.$$

### 3.7. THE HYPERBOLIC FOUR-FIELD SYSTEM

Hence we have

$$\begin{aligned}
 r_1^\pm &= 2 \int_0^1 \frac{p(\pm s) \left[ (3 + 4u(\pm s)^2) \pm 4u(\pm s)\sqrt{1 + u(\pm s)^2} \right]}{(1 + s)^2} ds, \\
 r_2^\pm &= 2 \int_0^1 \frac{p(\pm s) \left[ 4u(\pm s)\sqrt{1 + u(\pm s)^2} \pm (1 + 4u(\pm s)^2) \right]}{(1 + s)^2} ds, \\
 r_3^\pm &= 2 \int_0^1 \frac{n(\pm s) \left[ \sqrt{1 + u(\pm s)^2} \pm u(\pm s) \right]}{(1 + s)^2} ds > 0,
 \end{aligned}$$

because the Riemannian initial data  $p_\pm > 0$  and  $n_\pm > 0$  guarantee the positivity of  $n(\pm s)$  for  $|s| < 1$ . We finally conclude that

$$p'_+ = \frac{r_1^+ - r_2^+}{2} = 2 \int_0^1 \frac{p(s)}{(1 + s)^2} ds > 0, \quad p'_- = \frac{r_1^- + r_2^-}{2} = 2 \int_0^1 \frac{p(-s)}{(1 + s)^2} ds > 0 \text{ and } n'_\pm > 0. \tag{3.119}$$

Thus we obtain (3.118), and hence the cone-grid scheme is well defined due to (3.116) and (3.117). Especially the condition (3.118) guarantees a positive pressure and a positive particle density for all later times, provided that these positivity properties are satisfied for the initial data.

## 3.7 The hyperbolic four-field system

The four-field system of hyperbolic heat conduction was studied and solved by Dreyer and Kunik in [28, 29]. They consider this system in one space dimension and solved its pure initial value problem as well as the initial-boundary value problem by using kinetic representations for the unknown fields. This system consists of a conservation law for the energy density  $e$  and of a balance law for the heat flux  $Q$ , and it is derived as a moment system from the Boltzmann-Peierls equation. This hyperbolic system is given as follows

$$\begin{aligned}
 e_t + Q_x &= 0, \\
 Q_t + (e \cdot \chi)_x &= -\frac{1}{\tau_R} Q,
 \end{aligned} \tag{3.120}$$

with  $\chi = \frac{5}{3} - \frac{4}{3}\sqrt{1 - \frac{3}{4}\left(\frac{Q}{e}\right)^2}$  and  $\tau_R > 0$  the relaxation time. In this section we consider the four-field system for  $e$  and  $Q$  in that the relaxation time is infinite, i.e.  $\tau_R \rightarrow \infty$ , which gives the following phonon-Bose hyperbolic system of conservation laws

$$\begin{aligned}
 e_t + Q_x &= 0, \\
 Q_t + (e \cdot \chi)_x &= 0.
 \end{aligned} \tag{3.121}$$

## CHAPTER 3. ULTRA-RELATIVISTIC EULER EQUATIONS

---

We can write down its weak formulation with a bounded convex region  $\Omega$  in space and time as

$$\begin{aligned} \oint_{\partial\Omega} e dx - Q dt &= 0, \\ \oint_{\partial\Omega} Q dx - (e \cdot \chi) dt &= 0. \end{aligned} \tag{3.122}$$

Here  $e : \mathbb{R}_0^+ \times \mathbb{R} \mapsto \mathbb{R}_0^+$  and  $Q : \mathbb{R}_0^+ \times \mathbb{R} \mapsto \mathbb{R}_0^+$  is a piecewise  $C^1$ -solution of the hyperbolic system which may contain a finite number of  $C^1$ -shock curves. We will prescribe appropriate initial data for  $e$  and  $Q$ .

In Subsection 3.7.1 we will explain a correspondence of four-field system with the  $(p, u)$ -(sub)system of the ultra-relativistic Euler equations. In Subsection 3.7.2 we also use the same cone-grid-scheme for the hyperbolic four-field system in order to compute two initial value problems in one space dimension. One of these numerical results will directly be compared with exact solutions.

### 3.7.1 The corresponding with the ultra-relativistic Euler equations

We present a system of hyperbolic system of conservation laws, which is equivalent to the ultra-relativistic Euler equations. This equivalent system describes a phonon-Bose gas in terms of the energy density  $e$  and the heat flux  $Q$ . This system has specific applications in physics, see [26, 27, 28, 29, 30, 42, 45]. Now we explain a correspondence with the  $(p, u)$ -(sub)system (3.6) of the ultra-relativistic Euler equations for the hyperbolic systems.

We first compare the conservation laws of energy and momentum for the ultra-relativistic Euler equations given by (3.6) with the phonon-Bose hyperbolic system (3.121). The natural domains  $\Omega_{rel}$  and  $\Omega_{phon}$  for the  $(p, u)$  and the  $(e, Q)$  state space are given by

$$\begin{aligned} \Omega_{rel} &= \{(p, u) \in \mathbb{R} \times \mathbb{R}^3 : p > 0\}, \\ \Omega_{phon} &= \{(e, Q) \in \mathbb{R} \times \mathbb{R}^3 : |Q| < e\}, \end{aligned} \tag{3.123}$$

respectively. Then we compare the  $(p, u)$ -(sub)system with the four-field system and make the following ansatz for a transformation between the  $(p, u)$ -and the  $(e, Q)$ -state space:

$$e = p(3 + 4\mathbf{u}^2), \quad \mathbf{Q} = 4p\mathbf{u}\sqrt{1 + \mathbf{u}^2}. \tag{3.124}$$

The inverse transformation is given by

$$p = \frac{1}{3} \left[ \sqrt{4e^2 - 3\mathbf{Q}^2} - e \right], \quad \mathbf{u} = \frac{\mathbf{Q}}{\sqrt{4p(p + e)}}. \tag{3.125}$$



### 3.7. THE HYPERBOLIC FOUR-FIELD SYSTEM

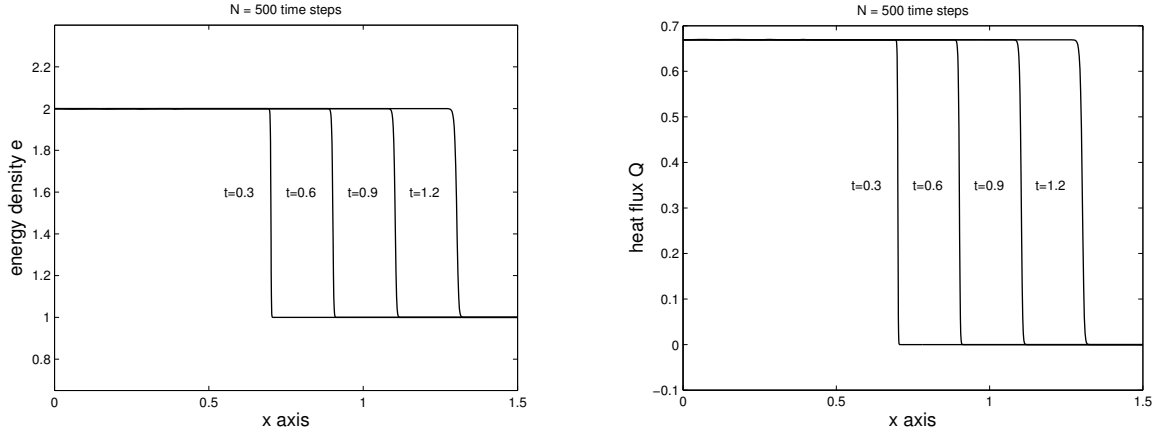


Figure 3.6: Evolution of a single shock at different times.

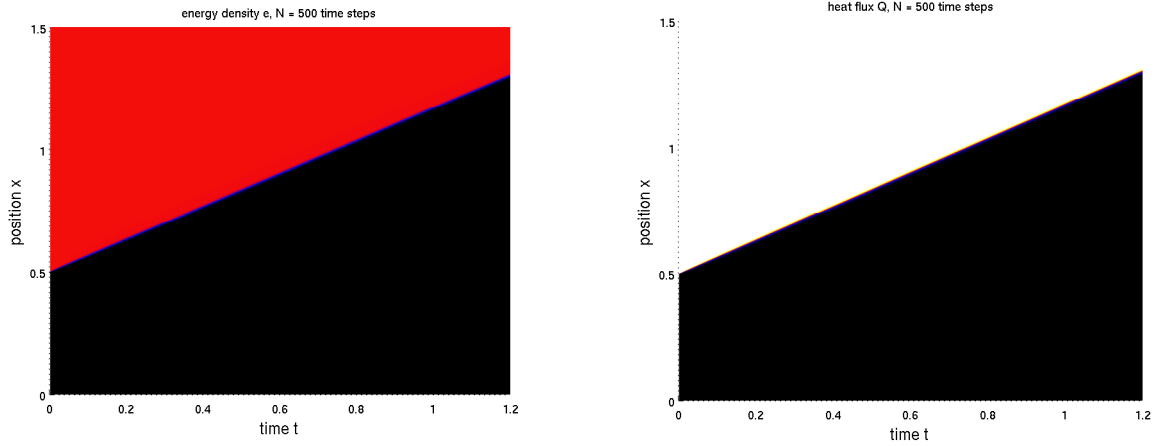


Figure 3.7: a single shock solution using cone grid scheme.

**Remark 3.7.1.** *An algebraic calculation in the state spaces (3.123) shows the equivalence between (3.6) and (3.121).*

We conclude that the mapping:

$$\Gamma(p, u) = \begin{bmatrix} p(3 + 4u^2) \\ 4pu\sqrt{1 + u^2} \end{bmatrix} \quad (3.126)$$

is one-to-one, and the Jacobian determinant of this mapping is both continuous and positive in the region  $\Omega_{rel}$ , see Lemma 3.2.1.

#### 3.7.2 Numerical examples

We present two numerical test cases, where we use the cone-grid-scheme for the hyperbolic phonon-Bose system. One of these numerical results will directly be compared with

## CHAPTER 3. ULTRA-RELATIVISTIC EULER EQUATIONS

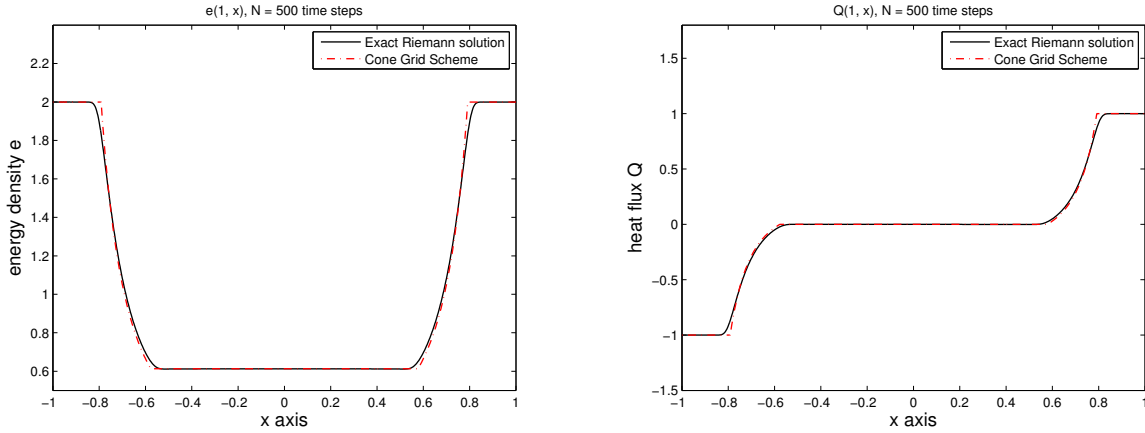


Figure 3.8: Comparison of the results from the test example 3.7.2 at time 1.

explicit solutions.

**Example 3.7.1.** *A single shock solution*

We consider now a single shock solution of the hyperbolic four-field system. The initial data are

$$(e, Q) = \begin{cases} (2.0, \frac{1}{\sqrt{3}} \sqrt{\frac{3\sqrt{2}-1}{\sqrt{2}+1}}), & x < 0.5, \\ (1.0, 0), & x \geq 0.5. \end{cases}$$

**Example 3.7.2.** *The initial data are*

$$(e, Q) = \begin{cases} (2.0, -1.0), & x < 0, \\ (2.0, 1.0), & x \geq 0. \end{cases}$$

This problem has a solution consisting of two strong rarefactions. The spatial domain is taken as  $[-1, 1]$  with 500 mesh elements and the final time is  $t = 1$ . Figure 3.8 show the solution profiles.

---

## Chapter 4

# The Uniqueness Problem for the Ultra-Relativistic Euler Equations

### 4.1 Introduction

This chapter is concerned with the uniqueness problem of the ultra-relativistic Euler equations. Namely we study the uniqueness problem of the Riemann solution given in Section 3.4. We also study the problem of the non-backward uniqueness of the ultra-relativistic Euler equations (3.6).

This chapter is organized as follows. In Section 4.2 we prove the uniqueness for the solution of the Riemann problem, which is given in Section 3.4. The main result in this section is Proposition 4.2.2. In Section 4.3 we give an important formula for the interaction of shock waves from different families by using the results given in Section 3.3. In this formula the states before shock interaction determine explicitly given algebraic expressions for the intermediate state after the interaction. The main result is Proposition 4.3.1. We have not seen a similar result for other hyperbolic systems. This formula has interesting applications, one of this is presented in Section 4.4. In Section 4.4 we present explicit solutions to give an interesting example of the non-backward uniqueness of the ultra-relativistic Euler equations (3.6). This example is one application of the new shock interaction formula given in Section 4.3. The corresponding result for the scalar equation is simple and very well known, but turns out to be much more complicated for our system. In fact this formula also plays an important role in Chapters 5 and 7 to obtain sharp shock interaction estimates.

### 4.2 Uniqueness of the Riemann solutions

**Lemma 4.2.1.** *Parametrizations of single shocks with zero velocity on one side*

*Given are the three states  $(p_j, u_j) \in \mathbb{R}^+ \times \mathbb{R}$ ,  $j = 1, 2, 3$ . For single shocks with velocity*

## CHAPTER 4. THE UNIQUENESS PROBLEM FOR THE ULTRA-RELATIVISTIC EULER EQUATIONS

---

zero on one side there hold the following equalities and inequalities given in Figure 4.1, where  $s_1, s_3$  are the velocities of the lower 1 and 3-shocks, respectively, and  $\tilde{s}_1, \tilde{s}_3$  are the velocities of the upper 1 and 3-shocks, respectively.

*Proof.* This lemma follows directly from the single shock parametrizations in Subsection 3.3.1.  $\square$

To prove the uniqueness of solutions of the Riemann problem for the system (3.6) with initial data (6.13), we exclude the following 12 cases:

- |                                  |                                  |
|----------------------------------|----------------------------------|
| 1. Lower 1-shock, upper 1-shock. | 7. Lower 3-shock, upper 3-shock. |
| 2. Lower 1-fan, upper 1-shock.   | 8. Lower 3-shock, upper 3-fan.   |
| 3. Lower 1-shock, upper 1-fan.   | 9. Lower 3-shock, upper 1-fan.   |
| 4. Lower 1-fan, upper 1-fan.     | 10. Lower 3-fan, upper 1-shock.  |
| 5. Lower 3-fan, upper 3-fan.     | 11. Lower 3-fan, upper 1-fan.    |
| 6. Lower 3-shock, upper 1-shock. | 12. Lower 3-fan, upper 3-shock.  |

We need Lemma 4.2.1 to exclude the preceding 12 cases. We consider an intermediate state  $(p_2, u_2)$  in the region which can be connected with a single shock or rarefaction wave to the prescribed left and right Riemannian initial data  $(p_-, u_-) = (p_1, u_1)$  and  $(p_+, u_+) = (p_3, u_3)$ . We consider the special case  $p_2 = 1, u_2 = 0$ , because under these restrictions it is easy to deduce the necessary inequalities from Lemma 4.2.1, which are depicted in Figure 4.1.

Afterwards, one can easily remove these restrictions by applying an appropriate Lorentz transformation (3.22) and an appropriate scaling of the pressure. One can easily exclude the preceding 12 cases by using the monotonicity of the velocities from lower to upper.

According to the above results about the solution and uniqueness of the solution of the Riemann problem for system (3.6) with initial data (6.13), we have thus proved the following proposition.

**Proposition 4.2.2.** *There exists a solution of the Riemann problem for system (3.6) with initial data (6.13) in the case  $p_{\pm} > 0, u_{\pm} \in \mathbb{R}$ . The solution is given by a 1-wave followed by a 3-wave, satisfies  $p > 0$ , and all speeds are strictly bounded by the speed of light, which is normalized to one. The solution is unique in the class of centered rarefaction waves and centered straight lines admissible shock waves.*

In the Figure 4.1 we give the full information about the classification of single shocks. Given are the three states  $(p_j, u_j) \in \mathbb{R}^+ \times \mathbb{R}, j = 1, 2, 3$ . For each shock we assume that

## 4.2. UNIQUENESS OF THE RIEMANN SOLUTIONS

---

the velocity is zero on one side, using Remark 3.2.5. Also we assume that the pressure is one on the same side (because we can apply a homogeneous scaling of the pressure with a positive scaling factor). Where  $s_1, s_3$  are the velocities of the lower 1 and 3-shocks, respectively and  $\tilde{s}_1, \tilde{s}_3$  are the velocities of the upper 1 and 3-shocks, respectively.

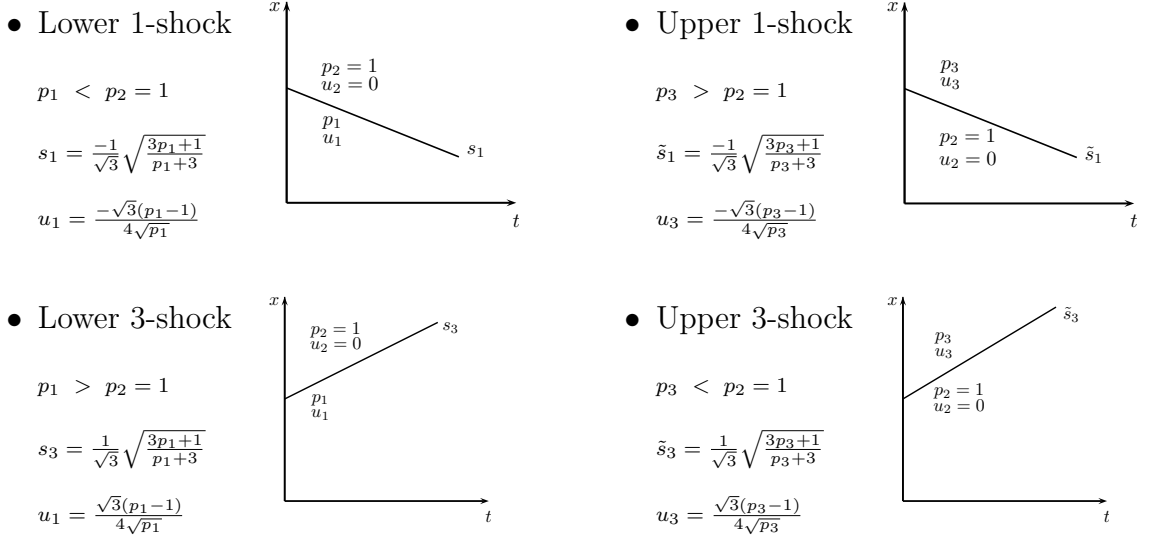


Figure 4.1: Classification of single shocks

Based on this classification of shocks, which are depicted in Figure 4.1, we prove the uniqueness of solutions of the Riemann problem for the system (3.6) with initial data (6.13). Also we use this classification of shocks to show that the system of the ultra-relativistic Euler equations has no backward uniqueness, which is given in the last section of this chapter.

**Lemma 4.2.3.** *The function  $f(p) = \frac{1+3p}{p+3}$  is strictly monotonically increasing for  $p > 0$ .*

Here we will show how we exclude only the first two cases and the other cases follow in the same way.

**Excluding case 1:** Lower 1-shock and upper 1-shock

According to Lemma 4.2.1 we have for lower 1-shock:

$$p_1 < p_2 = 1, \quad s_1 = \frac{-1}{\sqrt{3}} \sqrt{\frac{1+3p_1}{p_1+3}}, \quad (4.1)$$

and for upper 1-shock:

$$1 = p_2 < p_3, \quad \tilde{s}_1 = \frac{-1}{\sqrt{3}} \sqrt{\frac{1+3p_3}{p_3+3}}. \quad (4.2)$$

## CHAPTER 4. THE UNIQUENESS PROBLEM FOR THE ULTRA-RELATIVISTIC EULER EQUATIONS

---

Hence we have

$$p_1 < p_3. \quad (4.3)$$

In such a Riemann solution there should hold

$$s_1 < \tilde{s}_1.$$

Hence

$$\frac{-1}{\sqrt{3}} \sqrt{\frac{1+3p_1}{p_1+3}} < \frac{-1}{\sqrt{3}} \sqrt{\frac{1+3p_3}{p_3+3}}.$$

Thus

$$\frac{1+3p_1}{p_1+3} > \frac{1+3p_3}{p_3+3}.$$

This condition with condition (4.3) give the contradiction with Lemma 4.2.3. Then this case is refused.

**Excluding case 2:** Lower 1-fan and upper 1-shock

For lower 1-fan:

$$\lambda_1(u_2) = \lambda_1(0) = \frac{-1}{\sqrt{3}}.$$

According to Lemma 4.2.1 we have for upper 1-shock:

$$1 = p_2 < p_3, \quad \sigma_1 = \frac{-1}{\sqrt{3}} \sqrt{\frac{1+3p_3}{p_3+3}}. \quad (4.4)$$

In such a Riemann solution there should hold

$$\begin{aligned} \lambda_1(u_2) \leq \sigma_1 &\iff \\ \frac{-1}{\sqrt{3}} < \frac{-1}{\sqrt{3}} \sqrt{\frac{1+3p_3}{p_3+3}} &\iff \\ p_3 \leq 1. & \end{aligned}$$

Which contradicts condition (4.4). Then this case is refused.

### 4.3 Shock interaction

In this section we describe the interaction of two shock waves for the ultra-relativistic Euler equations. We give new explicit shock interaction formulas. Assume that there are two shocks an upper 1-shock  $S_1$  and lower 3-shock  $S_3$  with velocities  $s_1$  and  $s_3$ , respectively, starting at  $t = 0$  on the  $(t, x)$ -plane as shown in Figure 4.2. The two shocks must collide with each other at a finite time  $t = t_1$ , when the middle state disappears and a new Riemann problem is formed. There are two outcoming shocks an upper 3-shock  $S'_3$  and lower 1-shock  $S'_1$  with velocities  $s'_3$  and  $s'_1$ , respectively. In the next proposition we construct the solution of the Riemann problem in the explicit shock interaction formulas.

**Proposition 4.3.1.** *Given are the three states  $(p_j, u_j) \in \mathbb{R}^+ \times \mathbb{R}$ ,  $j = 1, 2, 3$ . Assume that, as depicted in Figure 4.2, the states  $(p_1, u_1)$  and  $(p_2, u_2)$  as well as  $(p_2, u_2)$  and  $(p_3, u_3)$  can be connected by a single lower 3-shock  $S_3$  and a single upper 1-shock  $S_1$ , respectively. The intermediate state  $(p_*, u_*)$  in the so called “star-region”, which is illustrated in Figure 4.2, can be connected with a single shocks to the prescribed left and right Riemannian initial data. The intermediate pressure is given by*

$$p_* = \frac{p_1 p_3}{p_2}. \quad (4.5)$$

*Proof.* To prove this proposition we show that the  $p_*$  stated in the proposition satisfies the statements of case 2 of the Riemann solutions, i.e. we will prove that:

1.  $p_*$  satisfies the first equality of (3.75), i.e. the Rankine-Hugoniot jump conditions in Lemma 3.3.5,
2.  $p_*$  satisfies the inequality  $p_* > \max(p_1, p_3)$ .

According to Lemma 3.3.5 (before interaction) we have:

(i)  $p_1 > p_2$  for incoming single 3-shock and  $p_3 > p_2$  for incoming single 1-shock,

(ii)

$$K_S \left( \frac{p_2}{p_1} \right) = \frac{\sqrt{1 + u_1^2} - u_1}{\sqrt{1 + u_2^2} - u_2}$$

for incoming lower 3-shock, and

(iii)

$$K_S \left( \frac{p_3}{p_2} \right) = \frac{\sqrt{1 + u_3^2} - u_3}{\sqrt{1 + u_2^2} - u_2}$$

for incoming upper 1-shock.

We have for the outgoing shocks  $S'_3, S'_1$  (after interaction):

$$\alpha' = \frac{p_3}{p_*}, \quad \beta' = \frac{\sqrt{1 + u_3^2} - u_3}{\sqrt{1 + u_*^2} - u_*},$$

and

$$\alpha'' = \frac{p_*}{p_1}, \quad \beta'' = \frac{\sqrt{1 + u_*^2} - u_*}{\sqrt{1 + u_1^2} - u_1},$$

respectively. Accordingly

$$\beta' \cdot \beta'' = \frac{\sqrt{1 + u_3^2} - u_3}{\sqrt{1 + u_1^2} - u_1} = \frac{K_S \left( \frac{p_3}{p_2} \right)}{K_S \left( \frac{p_2}{p_1} \right)} = K_S \left( \frac{p_3}{p_2} \right) \cdot K_S \left( \frac{p_1}{p_2} \right).$$

## CHAPTER 4. THE UNIQUENESS PROBLEM FOR THE ULTRA-RELATIVISTIC EULER EQUATIONS

---

Hence we have with  $\alpha = \frac{p_3}{p_1}$ ,  $\beta = \frac{\sqrt{1+u_3^2}-u_3}{\sqrt{1+u_1^2}-u_1}$ :

$$\beta = K_S\left(\frac{p_3}{p_2}\right) \cdot K_S\left(\frac{p_1}{p_2}\right) = K_S\left(\frac{p_1 p_3}{p_2}\right) \cdot K_S\left(\frac{p_1 p_3}{p_2}\right) = K_S\left(\frac{p_*}{p_1}\right) \cdot K_S\left(\frac{p_*}{p_3}\right).$$

This complete the first statement of the proof. For the second statement of this lemma, we have

$$p_* > p_1 \iff \frac{p_1 p_3}{p_2} > p_1 \iff p_3 > p_2.$$

In the same way we can show that  $p_* > p_3$ , so  $p_* > \max(p_1, p_3)$ . In order to guarantee that the outgoing 1-shock  $S'_1$  with velocity  $s'_1$  and the 3-shock wave  $S'_3$  with velocity  $s'_3$  fit together to complete a Riemann solution of (3.6) and (6.13), we only have to check that

$$s'_1 < s'_3. \quad (4.6)$$

To prove this inequality we use the characterization for single 1-shocks and single 3-shocks (3.50), (3.51) with  $\sigma'_1 = \sqrt{\frac{1-s'_1}{1+s'_1}}$  and  $\sigma'_3 = \sqrt{\frac{1-s'_3}{1+s'_3}}$ , where  $s'_1$ ,  $s'_3$  are the shocks velocities for the outgoing single lower 1-shock  $S'_1$  and single upper 3-shock  $S'_3$ , respectively:

$$\sqrt{1+u_*^2} - u_* = \sigma'_1 \cdot \frac{1}{L_S\left(\frac{p_2}{p_3}\right)}. \quad (4.7)$$

Also, we have

$$\sqrt{1+u_*^2} - u_* = \sigma'_3 \cdot L_S\left(\frac{p_2}{p_1}\right). \quad (4.8)$$

From these two equations we have:

$$\sigma'_1 = \sigma'_3 \cdot L_S\left(\frac{p_2}{p_3}\right) \cdot L_S\left(\frac{p_2}{p_1}\right).$$

We have that  $L_S(\alpha) > 1$  for  $\alpha > 0$ , hence  $\sigma'_1 > \sigma'_3$  and this completes the proof of the lemma.  $\square$

**Remark 4.3.2.** According to the parametrizations of single shocks (3.50) and (3.51), one can easily prove that:

$$\sigma'_1 = \sigma_1 K_S\left(\frac{p_2}{p_1}\right) \quad \text{and} \quad \sigma'_3 = \sigma_3 K_S\left(\frac{p_3}{p_2}\right),$$

hence we can calculate  $s'_1$  and  $s'_3$ , respectively.



#### 4.4. NON-BACKWARD UNIQUENESS FOR NONLINEAR HYPERBOLIC CONSERVATION LAWS

---

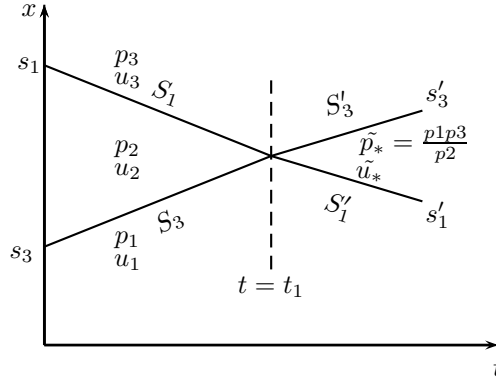


Figure 4.2:  $S_3 S_1 \rightarrow S'_1 S'_3$ .

**Remark 4.3.3.** *We can calculate  $u_*$  from (4.7) as follows*

$$u_* = \frac{(L_S \left( \frac{p_2}{p_3} \right) - \sigma'_1)(L_S \left( \frac{p_2}{p_3} \right) + \sigma'_1)}{2\sigma'_1 L_S \left( \frac{p_2}{p_3} \right)}. \quad (4.9)$$

*One can also use (4.8) to calculate  $u_*$ .*

In fact, these remarks play an important role in the next section, where we show that the system of the ultra-relativistic Euler equations has no backward uniqueness.

## 4.4 Non-backward uniqueness for nonlinear hyperbolic conservation laws

In this section we study the problem of the non-backward uniqueness of the hyperbolic conservation laws. We will give two examples for nonlinear hyperbolic conservation laws, the first one is Burgers equation and the second one is the ultra-relativistic Euler equations. We will show that for these examples that there are no backward uniqueness. Backward uniqueness means the following: If we know the solution at one time, then we can reconstruct the solution in the past. In Smoller [74, Chapter 15, § E] the reader will find a simple example for non-backward uniqueness for the Burgers equation. To show this for the ultra-relativistic Euler equations uses a similar idea, but is much more complicated to realize. In this section we give an example to show that there is no backward uniqueness for the ultra-relativistic Euler equations.

### 4.4.1 Burgers equation

Consider the Burgers equation

$$u_t + \left( \frac{u^2}{2} \right)_x = 0, \quad (4.10)$$

**CHAPTER 4. THE UNIQUENESS PROBLEM FOR THE ULTRA-RELATIVISTIC EULER EQUATIONS**

---

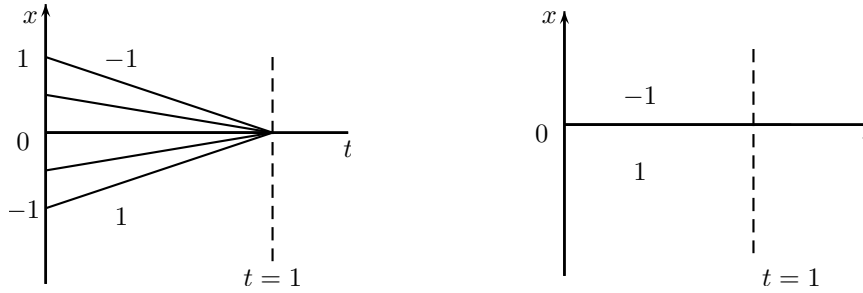


Figure 4.3: Two different initial data give the same solution at  $t = 1$

which we can write in the form

$$u_t + uu_x = 0. \tag{4.11}$$

We define  $u_1(t, x)$  to be a solution of the equation (4.10), which present the compression wave, for  $0 \leq t < 1$  we set

$$u_1(t, x) = \begin{cases} 1, & x \leq t - 1, \\ \frac{x}{t-1}, & t - 1 < x \leq 1 - t, \\ -1, & x > 1 - t. \end{cases} \tag{4.12}$$

We define  $u_2(t, x)$  to be a solution of the equation (4.10), which present the single shock, we set

$$u_2(t, x) = \begin{cases} 1, & x \leq 0, \\ -1, & x > 0. \end{cases} \tag{4.13}$$

The  $u_{1,2}$  are depicted in Figure (4.3). It is easy to check that they are all solutions, moreover, each of  $u_{1,2}$  satisfies the entropy condition.

Thus they are all correct solutions. The point that we wish to emphasize here is that all of these solutions coincide at  $t = 1$ :

$$u(1, x) = \begin{cases} 1, & x \leq 0, \\ -1, & x > 0. \end{cases} \tag{4.14}$$

At  $t = 1$  we know that a shock has formed. We don't know when it was formed, nor can we even say how it was formed.

We emphasize again that all of these solutions are the right ones, in that they belong to the class of solutions, which are uniquely determined by their initial values. But this uniqueness is only in the direction of increasing  $t$ . Two solutions in this class which agree at  $t = 1$  must be equal for all  $t > 1$ , but need not be equal for  $t < 1$ . It is in this strong sense that solutions of conservation laws do not have backward uniqueness.

The numerical simulation in Figure 4.4 carried out with MATLAB serve for illustration the non-backward uniqueness using cone-grid scheme.

#### 4.4. NON-BACKWARD UNIQUENESS FOR NONLINEAR HYPERBOLIC CONSERVATION LAWS

---

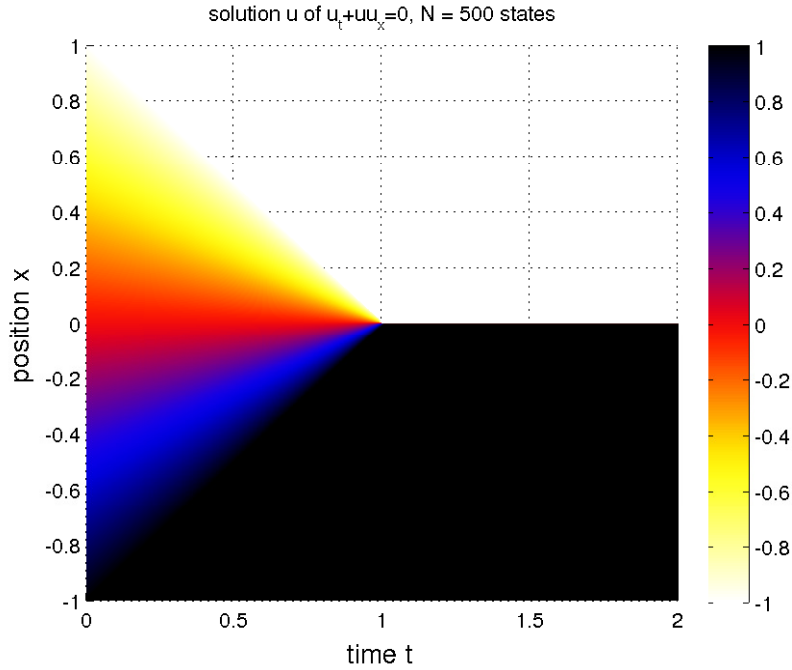


Figure 4.4: Burgers solution for  $0 < t < 2$ .

#### 4.4.2 Ultra-relativistic Euler equations

To show this for the ultra-relativistic Euler equations uses a similar idea, but is much more complicated to realize. In this section we give an example to show that there is no backward uniqueness for the ultra-relativistic Euler equations. In this example we will give two different solutions of the ultra-relativistic Euler equations, which give the same solution at  $t = 1$ . We first give a parametrizations of the compression waves, which we need to give one of these two solutions.

##### Parametrizations of the compression waves

We can obtain the parametrization of the compression waves from the parametrization of the rarefaction waves (3.60) and (3.61) by replacing  $s$  by  $-s$ , where  $s$  is the characteristic speed, i.e. we have

$$u(s) = \sqrt{\frac{3-s \mp \frac{1}{\sqrt{3}}}{2\sqrt{1-s^2}}}, \quad (4.15)$$

$$p(s) = a \left( \sqrt{1+u(s)^2} \pm u(s) \right)^{\frac{4}{\sqrt{3}}} = a \left( (2-\sqrt{3}) \frac{1 \mp s}{1 \pm s} \right)^{\frac{2}{\sqrt{3}}}. \quad (4.16)$$

The upper sign represents the 3-compression waves and the lower sign the 1-compression waves.

## CHAPTER 4. THE UNIQUENESS PROBLEM FOR THE ULTRA-RELATIVISTIC EULER EQUATIONS

---

We are going to present another important parametrization for the compression waves. For this purpose we first recall the function  $K_R$  given in 3.66, which are important in order to perform these parametrizations in a completely unified way. Namely, as in Lemma 3.3.7 we can give another parametrization for the compression waves.

In the following lemma, we give another characterization for the case that the left state  $(p_-, u_-)$  can be connected with the right state  $(p_+, u_+)$  by a single 1-compression wave or a single 3-compression wave, respectively.

**Lemma 4.4.1.** *Given are  $(p_{\pm}, u_{\pm}) \in \mathbb{R}^+ \times \mathbb{R}$ . Define  $\alpha$  and  $\beta$  according to (3.43), respectively.*

1. *Assume that  $p_- < p_+$ , i.e.  $\alpha > 1$  and further assume that*

$$\beta = K_R(\alpha). \quad (4.17)$$

*Then the left state  $(p_-, u_-)$  can be connected with the right state  $(p_+, u_+)$  by a single 1-compression wave.*

2. *Assume that  $p_+ < p_-$ , i.e.  $\alpha < 1$  and further assume that*

$$\beta K_R(\alpha) = 1. \quad (4.18)$$

*Then the left state  $(p_-, u_-)$  can be connected with the right state  $(p_+, u_+)$  by a single 3-compression wave.*

*Proof.* The proof follows in the same way as in Lemma 3.3.7. □

We shall illustrate the non-backward uniqueness in the following example.

### An example of non-backward uniqueness for the ultra-relativistic Euler system

We present two weak solutions  $U_1(t, x) = (p_1(t, x), u_1(t, x))$  and  $U_2(t, x) = (p_2(t, x), u_2(t, x))$  of the system (3.6) for a given pressure  $p_0 > 1$ .

**The first solution** corresponding to two interacting compression waves for  $0 \leq t < 1$  is

$$p_1(t, x) = \begin{cases} p_0, & x \leq s_1(t-1) \\ \delta \left( \frac{1+\frac{x}{t-1}}{1-\frac{x}{t-1}} \right)^{\frac{2}{\sqrt{3}}}, & s_1(t-1) < x \leq s_2(t-1) \\ p_c, & s_2(t-1) < x \leq s_2(1-t) \\ \delta \left( \frac{1-\frac{x}{t-1}}{1+\frac{x}{t-1}} \right)^{\frac{2}{\sqrt{3}}}, & s_2(1-t) < x \leq s_1(1-t) \\ p_0, & x > s_1(1-t) \end{cases}, \quad u_1(t, x) = \begin{cases} u_0, & x \leq s_1(t-1) \\ \sqrt{\frac{3}{2}} \frac{\frac{x}{t-1} - \frac{1}{\sqrt{3}}}{\sqrt{1 - \left(\frac{x}{t-1}\right)^2}}, & s_1(t-1) < x \leq s_2(t-1) \\ u_c, & s_2(t-1) < x \leq s_2(1-t) \\ \sqrt{\frac{3}{2}} \frac{\frac{x}{t-1} + \frac{1}{\sqrt{3}}}{\sqrt{1 - \left(\frac{x}{t-1}\right)^2}}, & s_2(1-t) < x \leq s_1(1-t) \\ -u_0, & x > s_1(1-t) \end{cases}, \quad (4.19)$$

#### 4.4. NON-BACKWARD UNIQUENESS FOR NONLINEAR HYPERBOLIC CONSERVATION LAWS

---

where

$$u_0 = \frac{\sqrt{3}(p_0 - 1)}{4\sqrt{p_0}}, \quad u_c = 0. \quad (4.20)$$

According to equation (3.80), we have

$$p_c = p_0 \alpha^{\frac{1}{2}} \beta^{\frac{2}{\sqrt{3}}} = p_0 \left( \frac{\sqrt{3}p_0 + 1 \sqrt{p_0 + 3} - \sqrt{3}(p_0 - 1)}{4\sqrt{p_0}} \right)^{\frac{4}{\sqrt{3}}}, \quad (4.21)$$

hence from equations (4.16) and (4.21) we have that

$$\delta = (2 - \sqrt{3})^{\frac{2}{\sqrt{3}}} p_c = (2 - \sqrt{3})^{\frac{2}{\sqrt{3}}} p_0 \left( \frac{\sqrt{3}p_0 + 1 \sqrt{p_0 + 3} - \sqrt{3}(p_0 - 1)}{4\sqrt{p_0}} \right)^{\frac{4}{\sqrt{3}}}. \quad (4.22)$$

The slopes

$$s_1 = \lambda_3(u_0) = \frac{\sqrt{3}(p_0 - 1)\sqrt{3}p_0 + 1\sqrt{p_0 + 3} + 8\sqrt{3}p_0}{3(p_0^2 + 6p_0 + 1)}, \quad s_2 = \lambda_3(u_c) = \frac{1}{\sqrt{3}}, \quad (4.23)$$

are the bounds for the lower 3-compression fan and the slopes  $-s_2, -s_1$  are the bounds for the upper 1-compression fan. To show that the compression fans give a classical solution of the Euler system (3.6) follows the same line as for the rarefaction waves.

**The second solution** corresponding to two interacting shock waves for  $0 \leq t < 1$  is with  $p_* = 1, u_* = 0$ :

$$p_2(t, x) = \begin{cases} p_0, & x \leq s(t-1) \\ p_*, & s(t-1) < x \leq s(1-t) \\ p_0, & x > s(1-t) \end{cases}, \quad u_2(t, x) = \begin{cases} u_0, & x \leq s(t-1) \\ u_*, & s(t-1) < x \leq s(1-t) \\ -u_0, & x > s(1-t) \end{cases}. \quad (4.24)$$

By using Lemma 4.2.1 and the formulas for the 3-shock in Figure 4.1 we obtain that

$$s = \frac{1}{\sqrt{3}} \sqrt{\frac{3p_0 + 1}{p_0 + 3}} \quad (4.25)$$

is the slope of the incoming lower 3-shock. Recall that  $u_0$  is given in (4.20).

For both solutions and  $t > 1$  we have the same slope  $s'$  of the outgoing upper 3-shock and  $-s'$  of the outgoing lower 1-shock. Note that  $u'_* = 0$  in Figure 4.5 is clear from symmetry reasons, but can be checked easily by using Lemma 4.2.1 and the formulas for the 3-shock in Figure 4.1. In the same way we can directly obtain  $s'$  from Lemma 4.2.1. Regarding that  $p_0 > 1$  and  $s$  in (4.25) we obtain the following relations for  $s'$ :

$$s' = \frac{1}{\sqrt{3}} \sqrt{\frac{p_0 + 3}{3p_0 + 1}} < s. \quad (4.26)$$

# CHAPTER 4. THE UNIQUENESS PROBLEM FOR THE ULTRA-RELATIVISTIC EULER EQUATIONS

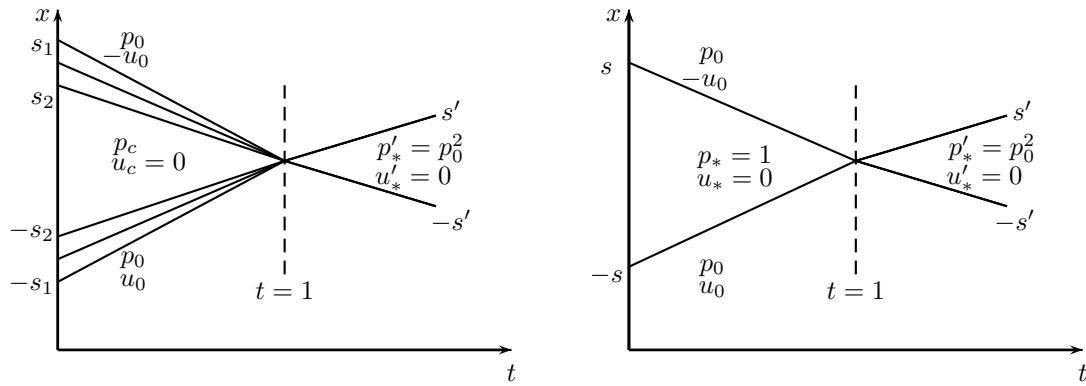


Figure 4.5: Two different solutions for  $0 \leq t < 1$  give the same solution for  $t \geq 1$ .

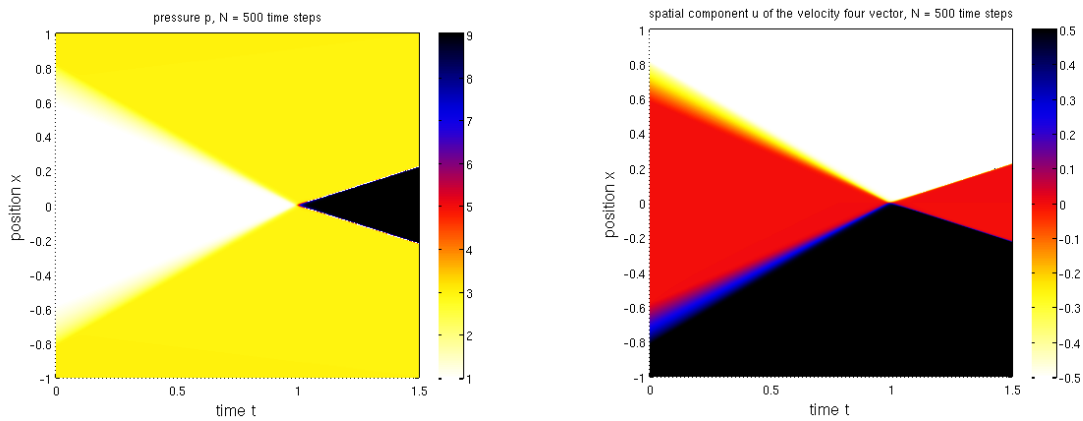


Figure 4.6: The first solution corresponding to two interacting compression waves.

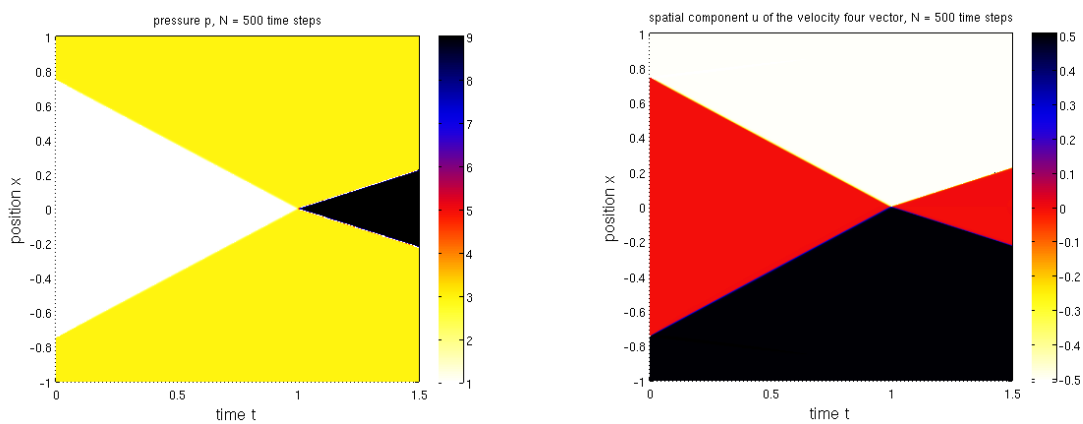


Figure 4.7: The second solution corresponding to two interacting shock waves.

#### 4.4. NON-BACKWARD UNIQUENESS FOR NONLINEAR HYPERBOLIC CONSERVATION LAWS

---

Now we have that  $U_1(t, x)$  and  $U_2(t, x)$  are both weak solutions satisfying the entropy condition  $u_- > u_+$  at each shock. Thus they are correct solutions. It is easy to show that both solutions coincide at  $t = 1$ . At  $t = 1$  the two outgoing shocks are created, and the solution at  $t = 1$  is given by the following Riemannian initial data

$$p(1, x) = \begin{cases} p_0, & x \leq 0 \\ p_0, & x > 0 \end{cases}, \quad u(1, x) = \begin{cases} u_0, & x \leq 0 \\ -u_0, & x > 0 \end{cases}. \quad (4.27)$$

Two Riemann solutions, which agree at  $t = 1$ , must be equal for all  $t > 1$  due to the Proposition 4.3.1, but need not be equal for  $t < 1$ . It is in this strong sense that solutions of conservation laws do not have backward uniqueness.

The numerical simulations in Figures 4.6 and 4.7 carried out with MATLAB serve for illustration the non-backward uniqueness for the ultra-relativistic Euler equations using cone-grid scheme.





---

## Chapter 5

# The Interaction of Waves for the Ultra-Relativistic Euler Equations

### 5.1 Introduction

In this chapter we are interested in the interaction estimates of nonlinear waves for the ultra-relativistic Euler system (3.6). More precisely, we consider the interaction of two shocks, of a shock and a centered rarefaction wave and of two centered rarefaction waves producing transmitted waves.

The two waves are assumed to collide with each other, where the middle state in general only disappears asymptotic in time such that a new Riemann problem is formed. Especially when rarefaction waves are involved, the interaction causes complicated transient phenomena, which are not covered by the asymptotic behavior of the interacting waves.

Before wave interaction we consider three states  $(p_j, u_j) \in \mathbb{R}^+ \times \mathbb{R}$ ,  $j = 1, 2, 3$ . Assume that, as depicted in Figures 5.5 and 5.6, the states  $(p_1, u_1)$  and  $(p_2, u_2)$  as well as  $(p_2, u_2)$  and  $(p_3, u_3)$  can be connected by a single lower wave and a single upper wave, respectively. There is an intermediate state  $(p_2, u_2)$  before interaction, which disappears asymptotic in time. Then, after interaction, the resulting asymptotic Riemann solution shows a new intermediate state  $(p_*, u_*)$ .

One basic feature presented in this chapter is based on the fact that the resulting intermediate state  $(p_*, u_*)$  is given in the explicit form

$$p_* = \frac{p_1 p_3}{p_2} \tag{5.1}$$

in the case that the incoming two waves are from different families. This is a generalization of a former result in Proposition 4.3.1, where the result was only stated for two colliding shocks from different families. However, in the remaining cases concerning the interaction of two shocks from the same family and of a shock and a centered rarefaction

## CHAPTER 5. THE INTERACTION OF WAVES FOR THE ULTRA-RELATIVISTIC EULER EQUATIONS

---

wave from the same family, we find that (5.1) is violated, and instead of (5.1) we give algebraic inequalities for the intermediate pressure  $p_*$  in terms of the known incoming waves. Finally we show that all possible interactions are completely covered by the Figures 5.5 and 5.6 and determine the outgoing Riemann solution in each case.

The resulting new approach will be used to introduce a special strength function which enables us to show that the strength after interactions of single waves is non increasing. This turns out to be the main result of this chapter. We do not know a similar strength function for a general  $2 \times 2$  hyperbolic systems of conservation laws. In the most papers about hyperbolic systems of conservation laws a more classical approach is familiar, which uses the change of Riemann invariants as a measure of wave strength, see [25, 60, 67, 76, 81] and references therein.

The fundamental concepts of single shock and rarefaction wave parametrizations and the solution of the Riemann problem given in Sections 3.3 and 3.4, respectively, are the basic tools for our analysis in this chapter.

This chapter is organized as follows. In Section 5.2 we introduce the new strength function, which measures the strengths of the waves of the ultra-relativistic Euler equations (3.6) in a natural way, and derive sharp estimates for these strengths in Proposition 5.2.7. The strength of the waves is given in explicit algebraic expressions. We also give the interpretation of the strength for the Riemann solution for system (3.6). In Section 5.3 we derive the formula (5.1) for the interaction of waves from different families in Propositions 4.3.1 and 5.3.3. We study the interactions between shocks and rarefaction waves in terms of the new strength function and obtain that the strength after interactions is non increasing. The cases where the strength is conserved after interaction is given in Proposition 5.3.4, and the other cases of strictly decreasing strength are considered in Proposition 5.3.5.

### 5.2 Strength of the waves

In this section we give a new function, which measures the strengths of the waves in the Riemann solution in a natural way, and derive sharp estimates for these strengths. In Lemmas 5.2.1 and 5.2.3 we present some properties of the functions  $K_S$  and  $K_R$ , which are given in 3.45, 3.66, respectively. These results turn out to be very useful in order to perform the estimates of the strengths for the waves of system (3.6) in a completely unified way.

**Lemma 5.2.1.** *The functions  $K_S(\alpha)$  and  $K_R(\alpha)$  are strictly monotonically increasing for  $\alpha > 0$  and satisfy*

$$K_S\left(\frac{1}{\alpha}\right) = \frac{1}{K_S(\alpha)}, \quad K_R\left(\frac{1}{\alpha}\right) = \frac{1}{K_R(\alpha)}. \quad (5.2)$$

## 5.2. STRENGTH OF THE WAVES

Moreover,  $\alpha = 1$  is a tangent point for both curves with

$$K_S(1) = K_R(1) = 1, \quad K'_S(1) = K'_R(1) = \frac{\sqrt{3}}{4}, \quad K''_S(1) = K''_R(1) = \frac{3 - 4\sqrt{3}}{16}.$$

*Proof.* See Kunik [45, Section 4.4]. □

**Remark 5.2.2.** We have for  $\alpha, \beta > 0$

- (i)  $K'_S(\alpha) > 0, K'_R(\alpha) > 0,$
- (ii)  $K_R^{-1}(\beta) = \beta^{4/\sqrt{3}},$
- (iii)  $K_S^{-1}(\beta) = 1 + \frac{2}{3}(\beta - \frac{1}{\beta})^2 + \frac{2}{3}(\beta - \frac{1}{\beta})\sqrt{3 + (\beta - \frac{1}{\beta})^2},$
- (iv)  $\alpha \frac{K'_S(\alpha)}{K_S(\alpha)} = \frac{\sqrt{3}(\alpha + 1)}{2\sqrt{3 + \alpha}\sqrt{1 + 3\alpha}},$
- (v)  $\frac{d}{d\alpha} \left[ \alpha \frac{K'_S(\alpha)}{K_S(\alpha)} \right] = \frac{\sqrt{3}(\alpha - 1)}{(3 + \alpha)^{\frac{3}{2}}(1 + 3\alpha)^{\frac{3}{2}}},$
- (vi)  $\alpha \frac{K'_R(\alpha)}{K_R(\alpha)} = \frac{\sqrt{3}}{4},$
- (vii)  $\frac{d}{d\alpha} \left[ \alpha \frac{K'_R(\alpha)}{K_R(\alpha)} \right] = 0.$

**Lemma 5.2.3.** For  $\alpha, \beta > 0$  we have

- (a)  $\alpha \geq 1 \implies K_S(\alpha) \geq K_R(\alpha) > 0,$
- (b)  $0 < \alpha \leq 1 \implies 0 < K_S(\alpha) \leq K_R(\alpha),$
- (c)  $\beta \geq 1 \implies K_S^{-1}(\beta) \leq K_R^{-1}(\beta),$
- (d)  $0 < \beta \leq 1 \implies K_S^{-1}(\beta) \geq K_R^{-1}(\beta).$  For  $\alpha \neq 1$  and  $\beta \neq 1$ , respectively, these inequalities are strict.

*Proof.* Due to Remark 5.2.2 (v) the function  $\alpha \mapsto \alpha \frac{K'_S(\alpha)}{K_S(\alpha)}$  is strictly monotonically increasing for  $\alpha \geq 1$ , and has value  $\frac{\sqrt{3}}{4}$  at  $\alpha = 1$ . We obtain for  $\alpha > 1$ :

$$\begin{aligned} \alpha \frac{K'_S(\alpha)}{K_S(\alpha)} &> \frac{\sqrt{3}}{4} \implies \\ \frac{K'_S(\alpha)}{K_S(\alpha)} &> \frac{\sqrt{3}}{4\alpha} = \frac{K'_R(\alpha)}{K_R(\alpha)} \implies \\ \log K_S(\alpha) &= \int_1^\alpha \frac{K'_S(t)}{K_S(t)} dt > \int_1^\alpha \frac{K'_R(t)}{K_R(t)} dt = \log K_R(\alpha) \implies \\ &K_S(\alpha) > K_R(\alpha), \end{aligned}$$

## CHAPTER 5. THE INTERACTION OF WAVES FOR THE ULTRA-RELATIVISTIC EULER EQUATIONS

---

and it follows (a). For  $0 < \alpha \leq 1$  we have from (5.2) and part (a):

$$K_S(\alpha) = \frac{1}{K_S(\frac{1}{\alpha})} \leq \frac{1}{K_R(\frac{1}{\alpha})} = K_R(\alpha),$$

and hence (b) is follows.

(c) For  $\beta \geq 1$  we have  $K_S^{-1}(\beta) \geq 1$  as well as  $\beta = K_S(K_S^{-1}(\beta)) \geq K_R(K_S^{-1}(\beta))$  from (a). It follows that

$$K_R^{-1}(\beta) \geq K_R^{-1}(K_R(K_S^{-1}(\beta))) = K_S^{-1}(\beta).$$

(d) For  $0 < \beta \leq 1$  we have  $K_S^{-1}(\beta) \leq 1$  as well as  $\beta = K_S(K_S^{-1}(\beta)) \leq K_R(K_S^{-1}(\beta))$  from (b). It follows that

$$K_R^{-1}(\beta) \leq K_R^{-1}(K_R(K_S^{-1}(\beta))) = K_S^{-1}(\beta).$$

□

In the following lemma we show that the pressure changes for shock and rarefaction wave actually do differ in the terms of third order.

**Lemma 5.2.4.** *For each  $\tilde{\alpha} > 1$  there is a constant  $c > 0$ , such that for all  $\alpha \in [\frac{1}{\tilde{\alpha}}, \tilde{\alpha}]$  we have*

$$|K_S(\alpha) - K_R(\alpha)| \leq c |\alpha - 1|^3.$$

*Proof.* Due to Taylor's formula there are two parameters  $\xi, \eta > 0$  between  $\alpha > 0$  and 1 such that

$$K_S(\alpha) = 1 + \frac{\sqrt{3}}{4}(\alpha - 1) + \frac{3 - 4\sqrt{3}}{32}(\alpha - 1)^2 + \frac{1}{6}K_S'''(\xi)(\alpha - 1)^3,$$

$$K_R(\alpha) = 1 + \frac{\sqrt{3}}{4}(\alpha - 1) + \frac{3 - 4\sqrt{3}}{32}(\alpha - 1)^2 + \frac{1}{6}K_R'''(\eta)(\alpha - 1)^3,$$

using Lemma 5.2.1, where  $c = \max_{\frac{1}{\tilde{\alpha}} \leq \xi \leq \tilde{\alpha}} \frac{|K_S'''(\xi)|}{6} + \max_{\frac{1}{\tilde{\alpha}} \leq \eta \leq \tilde{\alpha}} \frac{|K_R'''(\eta)|}{6}$ , which completes the proof of this lemma. □

### 5.2.1 Strength function $S(\alpha, \beta)$

Here we will present a new function  $S(\alpha, \beta)$ , which measures the strength of the waves of the Riemann solution, where  $\alpha$  and  $\beta$  are given in (3.43). Define the following four regions for the points  $(\alpha, \beta)$  of the quarter plane  $\mathbb{R}^+ \times \mathbb{R}^+$  as depicted in Figure 3.2. According to the structure of the four regions in the solution of the Riemann problem, we construct a continuous function  $\alpha_* : \mathbb{R}^+ \times \mathbb{R}^+ \mapsto \mathbb{R}^+$ . In fact this function is corresponding to the intermediate states in the Riemann solution, which are given in Section 3.4. Later on we use this function in order to present the strength function  $S : \mathbb{R}^+ \times \mathbb{R}^+ \mapsto \mathbb{R}_0^+$ , namely in Definition 5.2.6.

**Region 1:**

Suppose that  $K_R(\frac{1}{\alpha}) < \beta < K_S(\alpha)$  with  $\alpha > 1$ . Since  $K_S(\xi)K_R(\frac{\xi}{\alpha})$  is strictly monotonically increasing with respect to  $\xi > 0$  with

$$\lim_{\xi \downarrow 0} K_S(\xi)K_R\left(\frac{\xi}{\alpha}\right) = 0, \quad \lim_{\xi \rightarrow \infty} K_S(\xi)K_R\left(\frac{\xi}{\alpha}\right) = \infty,$$

we conclude from the Intermediate Value Theorem that the implicit equation

$$K_S(\alpha_*)K_R\left(\frac{\alpha_*}{\alpha}\right) = \beta \tag{5.3}$$

has a unique solution  $\alpha_* = \alpha_*(\alpha, \beta) > 0$ . From  $K_R(\frac{1}{\alpha}) < \beta < K_S(\alpha)$  we conclude

$$1 < \alpha_* < \alpha. \tag{5.4}$$

Note that in region 1 we have in accordance with (5.3)

$$\lim_{\beta \downarrow K_R(\frac{1}{\alpha})} \alpha_*(\alpha, \beta) = 1, \quad \lim_{\beta \uparrow K_S(\alpha)} \alpha_*(\alpha, \beta) = \alpha. \tag{5.5}$$

**Region 2:**

Suppose that  $\beta \geq \max(K_S(\alpha), K_S(\frac{1}{\alpha}))$  with  $\alpha > 0$ . Since  $K_S(\xi)K_S(\frac{\xi}{\alpha})$  is strictly monotonically increasing with respect to  $\xi > 0$  with

$$\lim_{\xi \downarrow 0} K_S(\xi)K_S\left(\frac{\xi}{\alpha}\right) = 0, \quad \lim_{\xi \rightarrow \infty} K_S(\xi)K_S\left(\frac{\xi}{\alpha}\right) = \infty,$$

we conclude from the Intermediate Value Theorem that the implicit equation

$$K_S(\alpha_*)K_S\left(\frac{\alpha_*}{\alpha}\right) = \beta \tag{5.6}$$

has a unique solution  $\alpha_* = \alpha_*(\alpha, \beta) > 0$ . From  $\beta \geq \max(K_S(\alpha), K_S(\frac{1}{\alpha}))$  we conclude

$$\alpha_* \geq \max(1, \alpha). \tag{5.7}$$

Note that in region 2 we have in accordance with (5.6)

$$\begin{cases} \lim_{\beta \downarrow K_S(\alpha)} \alpha_*(\alpha, \beta) = \alpha_*(\alpha, K_S(\alpha)) = \alpha, & \text{if } \alpha > 1, \\ \lim_{\beta \downarrow K_S(\frac{1}{\alpha})} \alpha_*(\alpha, \beta) = \alpha_*(\alpha, K_S(\frac{1}{\alpha})) = 1, & \text{if } \alpha < 1. \end{cases} \tag{5.8}$$

**Region 3:**

Suppose that  $K_R(\alpha) < \beta < K_S(\frac{1}{\alpha})$  with  $\alpha < 1$ . Since  $K_R(\xi)K_S(\frac{\xi}{\alpha})$  is strictly monotonically increasing with respect to  $\xi > 0$  with

$$\lim_{\xi \downarrow 0} K_R(\xi)K_S\left(\frac{\xi}{\alpha}\right) = 0, \quad \lim_{\xi \rightarrow \infty} K_R(\xi)K_S\left(\frac{\xi}{\alpha}\right) = \infty,$$

## CHAPTER 5. THE INTERACTION OF WAVES FOR THE ULTRA-RELATIVISTIC EULER EQUATIONS

---

we conclude from the Intermediate Value Theorem that the implicit equation

$$K_R(\alpha_*)K_S\left(\frac{\alpha_*}{\alpha}\right) = \beta \quad (5.9)$$

has a unique solution  $\alpha_* = \alpha_*(\alpha, \beta) > 0$ . From  $K_R(\alpha) < \beta < K_S(\frac{1}{\alpha})$  we conclude

$$\alpha < \alpha_* < 1. \quad (5.10)$$

Note that in region 3 we have in accordance with (5.9)

$$\lim_{\beta \downarrow K_R(\alpha)} \alpha_*(\alpha, \beta) = \alpha, \quad \lim_{\beta \uparrow K_S(\frac{1}{\alpha})} \alpha_*(\alpha, \beta) = 1. \quad (5.11)$$

### Region 4:

Suppose that  $\beta \leq \min(K_R(\alpha), K_R(\frac{1}{\alpha}))$  with  $\alpha > 0$ . Since  $K_R(\xi)K_R(\frac{\xi}{\alpha})$  is strictly monotonically increasing with respect to  $\xi > 0$  with

$$\lim_{\xi \downarrow 0} K_R(\xi)K_R\left(\frac{\xi}{\alpha}\right) = 0, \quad \lim_{\xi \rightarrow \infty} K_R(\xi)K_R\left(\frac{\xi}{\alpha}\right) = \infty,$$

we conclude from the Intermediate Value Theorem that the implicit equation

$$K_R(\alpha_*)K_R\left(\frac{\alpha_*}{\alpha}\right) = \beta \quad (5.12)$$

has a unique solution  $\alpha_* = \alpha_*(\alpha, \beta) > 0$ . From  $\beta \leq \min(K_R(\alpha), K_R(\frac{1}{\alpha}))$  we conclude

$$\alpha_* \leq \min(1, \alpha). \quad (5.13)$$

Note that in region 4 we have in accordance with (5.12)

$$\begin{cases} \lim_{\beta \uparrow K_R(\alpha)} \alpha_*(\alpha, \beta) = \alpha_*(\alpha, K_R(\alpha)) = \alpha, & \text{if } \alpha < 1, \\ \lim_{\beta \uparrow K_R(\frac{1}{\alpha})} \alpha_*(\alpha, \beta) = \alpha_*(\alpha, K_R(\frac{1}{\alpha})) = 1, & \text{if } \alpha \geq 1. \end{cases} \quad (5.14)$$

**Remark 5.2.5.** *Thus we have concluded the construction of the function  $\alpha_*$  in each region, see Figure 3.2. We also obtain the continuity of  $\alpha_*$ , namely through the boundary curves between each two neighboring regions, resulting from equations (5.5), (5.8), (5.11), (5.14).*

Now we are able to give the function  $S(\alpha, \beta)$ , which measures the strength of the waves.

**Definition 5.2.6.** *Let  $\alpha, \beta > 0$ . The solution  $\alpha_* = \alpha_*(\alpha, \beta)$  of (5.3), (5.6), (5.9), (5.12) with respect to the preceding four regions defines a continuous function  $\alpha_* : \mathbb{R}^+ \times \mathbb{R}^+ \mapsto \mathbb{R}^+$ . Using this function, we define  $S : \mathbb{R}^+ \times \mathbb{R}^+ \mapsto \mathbb{R}_0^+$  with*

$$S(\alpha, \beta) := |\ln \alpha_*(\alpha, \beta)| + \left| \ln \frac{\alpha_*(\alpha, \beta)}{\alpha} \right|. \quad (5.15)$$

## 5.2. STRENGTH OF THE WAVES

In the following proposition we prove fundamental properties and estimates for the strength function. The function  $S(\alpha, \beta)$  will be used to calculate the strength of the single shocks and rarefaction waves as well as of a complete Riemann solution.

**Proposition 5.2.7.** *Using the same notations as in the Definition 5.2.6, we have*

- (1)  $S(\alpha, \beta) \geq 0$  and  $S(\alpha, \beta) = 0$  if and only if  $\alpha = \beta = 1$ . The function  $S$  is continuous.
- (2) If  $(\alpha, \beta)$  is in region 1 or in region 3, then  $S(\alpha, \beta) = |\ln \alpha|$ .
- (3) If  $(\alpha, \beta)$  is in region 4, then  $\beta \leq 1$  and  $S(\alpha, \beta) = \frac{4}{\sqrt{3}} \ln \frac{1}{\beta}$ .
- (4) We have for all  $(\alpha, \beta) \in \mathbb{R}^+ \times \mathbb{R}^+ : S(\alpha, \beta) = S(\frac{1}{\alpha}, \beta)$ .
- (5) We have for all  $(\alpha, \beta) \in \mathbb{R}^+ \times \mathbb{R}^+ : \max(|\ln \alpha|, 2|\ln \beta|) \leq S(\alpha, \beta) \leq \max(|\ln \alpha|, \frac{4}{\sqrt{3}}|\ln \beta|)$ .

*Proof.* (1)  $S \geq 0$  is continuous by its definition, using the continuity of  $\alpha_*$ .  $S(\alpha, \beta) = 0$  implies  $\alpha = \alpha_* = 1$ . By (5.4) and (5.10), this is only possible if  $(\alpha, \beta)$  lies in region 2 or region 4. This implies  $\beta = K_S(\frac{1}{\alpha}) = 1$  in region 2 and  $\beta = K_R(\frac{1}{\alpha}) = 1$  in region 4.

We prove part (2). In region 1 we have from (5.4):

$$S(\alpha, \beta) = |\ln \alpha_*| + \left| \ln \frac{\alpha_*}{\alpha} \right| = \ln \alpha_* + \ln \frac{\alpha}{\alpha_*} = \ln \alpha = |\ln \alpha|.$$

In region 3 we obtain from (5.10):

$$S(\alpha, \beta) = |\ln \alpha_*| + \left| \ln \frac{\alpha_*}{\alpha} \right| = \ln \frac{1}{\alpha_*} + \ln \frac{\alpha_*}{\alpha} = \ln \frac{1}{\alpha} = |\ln \alpha|.$$

We prove part (3). In region 4 we obtain from (5.12):

$$\left( \frac{\alpha_*^2}{\alpha} \right)^{\frac{\sqrt{3}}{4}} = \beta, \quad \text{i.e.} \quad \alpha_* = \alpha^{\frac{1}{2}} \beta^{\frac{2}{\sqrt{3}}} \leq 1,$$

and with (5.13):

$$S(\alpha, \beta) = \ln \frac{1}{\alpha_*} + \ln \frac{\alpha}{\alpha_*} = \ln \frac{\alpha}{\alpha_*^2} = \ln \left( \left( \frac{1}{\beta} \right)^{\frac{4}{\sqrt{3}}} \right) = \frac{4}{\sqrt{3}} \ln \frac{1}{\beta}.$$

We prove part (4). Here  $(\alpha, \beta)$  lies in region 1  $\iff (\frac{1}{\alpha}, \beta)$  lies in region 3 is clear. For region 1 and region 3 we obtain  $S(\alpha, \beta) = S(\frac{1}{\alpha}, \beta) = |\ln \alpha|$ . In region 2 and region 4 we have  $K(\alpha_*)K(\frac{\alpha_*}{\alpha}) = \beta$ , where either  $K = K_S$  or  $K = K_R$ . We replace  $\alpha$  and  $\alpha_*$  by  $\tilde{\alpha} := \frac{1}{\alpha}$ ,  $\tilde{\alpha}_* := \frac{\alpha_*}{\alpha}$ , respectively, and regard that  $K(\tilde{\alpha}_*)K(\frac{\tilde{\alpha}_*}{\tilde{\alpha}}) = \beta$ , which implies

$$S(\tilde{\alpha}, \beta) = |\ln \tilde{\alpha}_*| + \left| \ln \frac{\tilde{\alpha}_*}{\tilde{\alpha}} \right| = \left| \ln \frac{\alpha_*}{\alpha} \right| + |\ln \alpha_*| = S(\alpha, \beta)$$

## CHAPTER 5. THE INTERACTION OF WAVES FOR THE ULTRA-RELATIVISTIC EULER EQUATIONS

---

also in region 2 and region 4.

We prove part (5). Due to part (4) we assume  $(\alpha, \beta) \in \mathbb{R}^+ \times \mathbb{R}^+$  and  $\alpha \geq 1$ . We first note that  $(\alpha, \beta)$  is not in region 3. So we prove part (5) in the other three regions.

**Case 1.** Suppose that  $(\alpha, \beta)$  is in region 1, such that  $S(\alpha, \beta) = |\ln \alpha|$  from part (2). We obtain

$$S(\alpha, \beta) \leq \max(|\ln \alpha|, \frac{4}{\sqrt{3}}|\ln \beta|).$$

Now to proceed, we need the following lemma.

**Lemma 5.2.8.** *For  $\alpha \geq 1$  we have  $K_S(\alpha) \leq \sqrt{\alpha}$ .*

*Proof.* We show for all  $t \geq 1$  that

$$\ln K_S(\alpha) = \int_1^\alpha \frac{K'_S(t)}{K_S(t)} dt \leq \frac{1}{2} \ln \alpha$$

by proving  $t \frac{K'_S(t)}{K_S(t)} \leq \frac{1}{2}$ . For  $t = 1$  we have  $\frac{K'_S(1)}{K_S(1)} = \frac{\sqrt{3}}{4} < \frac{1}{2}$ . Using Remark 5.2.2 (v) we conclude that  $t \frac{K'_S(t)}{K_S(t)}$  is strictly increasing for  $t > 1$  with  $\lim_{t \rightarrow \infty} \left[ t \frac{K'_S(t)}{K_S(t)} \right] = \frac{1}{2}$ . This completes the proof of the lemma.  $\square$

Now we obtain in case 1, regarding  $\alpha \geq 1$ :

$$\begin{aligned} \beta < K_S(\alpha) \leq \alpha^{\frac{1}{2}} \quad \text{implies} \quad 2 \ln \beta \leq \ln \alpha = S(\alpha, \beta), \\ \frac{1}{\beta} < K_R(\alpha) = \alpha^{\frac{\sqrt{3}}{4}} \leq \alpha^{\frac{1}{2}} \quad \text{implies} \quad 2 \ln \frac{1}{\beta} \leq \ln \alpha = S(\alpha, \beta). \end{aligned}$$

Both implies  $\max(|\ln \alpha|, 2|\ln \beta|) \leq S(\alpha, \beta)$ .

**Case 2:** Suppose that  $(\alpha, \beta)$  with  $\alpha \geq 1$  is in region 2. In this region we have

$$S(\alpha, \beta) = |\ln \alpha_*| + \left| \ln \frac{\alpha_*}{\alpha} \right| = \ln \frac{\alpha_*^2}{\alpha}, \tag{5.16}$$

using equation (5.7). We obtain from equation (5.6) and Lemma 5.2.3 part (a) that

$$\beta = K_S(\alpha_*) K_S\left(\frac{\alpha_*}{\alpha}\right) \geq \left(\frac{\alpha_*^2}{\alpha}\right)^{\frac{\sqrt{3}}{4}}.$$

Using (5.16) with  $\beta \geq 1$  we have

$$\begin{aligned} S(\alpha, \beta) &= \frac{4}{\sqrt{3}} \ln \left( \left( \frac{\alpha_*^2}{\alpha} \right)^{\frac{\sqrt{3}}{4}} \right) \\ &\leq \frac{4}{\sqrt{3}} \ln \beta \leq \max(|\ln \alpha|, \frac{4}{\sqrt{3}}|\ln \beta|). \end{aligned}$$



Lemma 5.2.8 and equation (5.7) imply in case 2 that

$$\beta = K_S(\alpha_*)K_S\left(\frac{\alpha_*}{\alpha}\right) \leq \left(\frac{\alpha_*^2}{\alpha}\right)^{\frac{1}{2}}.$$

Hence we have

$$S(\alpha, \beta) = \ln \frac{\alpha_*^2}{\alpha} \geq 2 \ln \beta,$$

using (5.16). But  $\alpha_* \geq \alpha \geq 1$ , and therefore

$$S(\alpha, \beta) \geq |\ln \alpha_*| \geq |\ln \alpha|.$$

This implies  $\max(|\ln \alpha|, 2|\ln \beta|) \leq S(\alpha, \beta)$  and concludes the proof of (5) in case 2.

**Case 3.** Suppose that  $(\alpha, \beta)$  with  $\alpha \geq 1$  and  $\beta < 1$  is in region 4. From part (3) we have

$$S(\alpha, \beta) = \frac{4}{\sqrt{3}} \ln \frac{1}{\beta} \leq \max(|\ln \alpha|, \frac{4}{\sqrt{3}}|\ln \beta|). \quad (5.17)$$

Hence

$$S(\alpha, \beta) \geq 2 \ln \frac{1}{\beta} = 2|\ln \beta|.$$

In region 4 we also have  $\frac{1}{\beta} \geq K_R(\alpha)$ , and hence

$$S(\alpha, \beta) = \frac{4}{\sqrt{3}} \ln \frac{1}{\beta} = \ln K_R^{-1}\left(\frac{1}{\beta}\right) \geq \ln K_R^{-1}(K_R(\alpha)) = \ln \alpha = |\ln \alpha|.$$

We finally conclude in region 4 that

$$S(\alpha, \beta) \geq \max(|\ln \alpha|, 2|\ln \beta|).$$

□

Using Remark 5.2.5, which implies the continuity of the function  $\alpha_*$  through the boundary curves between each two neighbored regions, and Proposition 5.2.7 we obtain the following result.

**Lemma 5.2.9.**

- (1) For  $\alpha \geq 1$  we have  $S(\alpha, K_R(\frac{1}{\alpha})) = \ln \alpha$  as well as  $S(\alpha, K_S(\alpha)) = \ln \alpha$ .
- (2) For  $\alpha \leq 1$  we have  $S(\alpha, K_S(\frac{1}{\alpha})) = \ln \frac{1}{\alpha}$  as well as  $S(\alpha, K_R(\alpha)) = \ln \frac{1}{\alpha}$ .

In the following definition we summarize the strengths of shock waves and rarefaction waves in explicitly algebraic expressions, more precisely through the boundary of the curves, which are depicted in Figure 3.2.

**CHAPTER 5. THE INTERACTION OF WAVES FOR THE ULTRA-RELATIVISTIC EULER EQUATIONS**

---

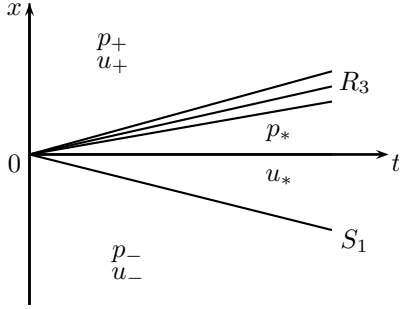


Figure 5.1: case 1.

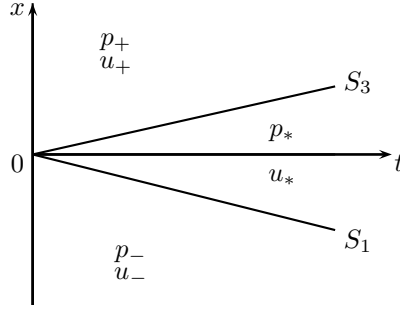


Figure 5.2: case 2.

**Definition 5.2.10.** Let  $\Omega := \{(p, u) : p > 0, u \in \mathbb{R}\}$  be the state space for the ultra relativistic Euler equations (3.6) where,  $p = p(t, x)$ ,  $u = u(t, x)$ ,  $t \geq 0, x \in \mathbb{R}$ . We put  $W_{\pm} := (p_{\pm}, u_{\pm}) \in \Omega$  and consider the Riemann problem with initial data (6.13). Recall  $\alpha = \frac{p_+}{p_-}$  and  $\beta = \frac{\sqrt{1+u_+^2}-u_+}{\sqrt{1+u_-^2}-u_-}$ .

1. For  $\beta K_R(\alpha) = 1$  the two conditions  $\alpha > 1$  and  $\beta < K_S(\alpha)$  are equivalent. If all these conditions are satisfied, then the initial data (6.13) can be connected by a single 3-rarefaction wave  $R_3$ . In this case we have  $S(\alpha, \beta) = S(\alpha, K_R(\frac{1}{\alpha})) = \ln \alpha$ , and we call  $Str(R_3) = \ln \alpha$  the strength of the 3-rarefaction wave.
2. For  $\beta K_S(\alpha) = 1$  the two conditions  $\alpha < 1$  and  $\beta > K_R(\alpha)$  are equivalent. If all these conditions are satisfied, then the initial data (6.13) can be connected by a single 3-shock  $S_3$ . In this case we have  $S(\alpha, \beta) = S(\alpha, K_S(\frac{1}{\alpha})) = \ln \frac{1}{\alpha}$ , and we call  $Str(S_3) = \ln \frac{1}{\alpha}$  the strength of the 3-shock.
3. For  $\beta = K_R(\alpha)$  the two conditions  $\alpha < 1$  and  $\beta K_S(\alpha) < 1$  are equivalent. If all these conditions are satisfied, then the initial data (6.13) can be connected by a single 1-rarefaction wave  $R_1$ . In this case we have  $S(\alpha, \beta) = S(\alpha, K_R(\alpha)) = \ln \frac{1}{\alpha}$ , and we call  $Str(R_1) = \ln \frac{1}{\alpha}$  the strength of the 1-rarefaction wave.
4. For  $\beta = K_S(\alpha)$  the two conditions  $\alpha > 1$  and  $\beta K_R(\alpha) > 1$  are equivalent. If all these conditions are satisfied, then the initial data (6.13) can be connected by a single 1-shock  $S_1$ . In this case we have  $S(\alpha, \beta) = S(\alpha, K_S(\alpha)) = \ln \alpha$ , and we call  $Str(S_1) = \ln \alpha$  the strength of the 1-shock.

**5.2.2 Interpretation of  $S(\alpha, \beta)$  for general Riemannian initial data:**

Here we give the interpretation of the strength for the classical Riemann solution from Section 3.4. Recall  $\alpha = \frac{p_+}{p_-}$  and  $\beta = \frac{\sqrt{1+u_+^2}-u_+}{\sqrt{1+u_-^2}-u_-}$  with the initial data (6.13).

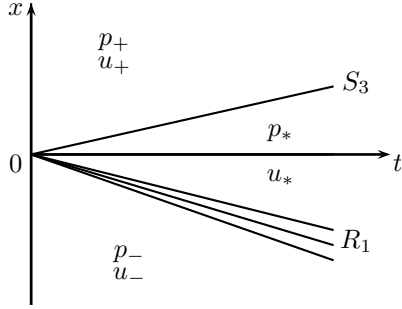


Figure 5.3: case 3.

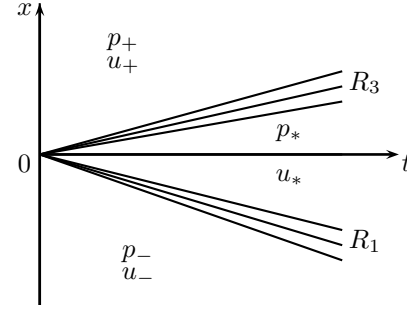


Figure 5.4: case 4.

- 1. Riemann solution for  $(\alpha, \beta)$  in region 1:** Here the intermediate state  $(p_*, u_*)$  satisfies

$$\alpha_* = \frac{p_*}{p_-} > 1, \quad K_S(\alpha_*) = \frac{\sqrt{1 + u_*^2} - u_*}{\sqrt{1 + u_-^2} - u_-} > 1. \quad (5.18)$$

For  $(\alpha, \beta)$  in region 1, the Riemann solution consists of a lower 1-shock  $S_1$  and an upper 3-fan  $R_3$ , see Figure 5.1, and  $S(\alpha, \beta)$  is the sum of the strength of  $S_1$  and the strength of  $R_3$ , i.e.

$$S(\alpha, \beta) = \ln \frac{p_*}{p_-} + \ln \frac{p_+}{p_*}. \quad (5.19)$$

- 2. Riemann solution for  $(\alpha, \beta)$  in region 2:** Here the intermediate state  $(p_*, u_*)$  satisfies

$$\alpha_* = \frac{p_*}{p_-} > 1, \quad K_S(\alpha_*) = \frac{\sqrt{1 + u_*^2} - u_*}{\sqrt{1 + u_-^2} - u_-} > 1. \quad (5.20)$$

For  $(\alpha, \beta)$  in region 2, the Riemann solution consists of a lower 1-shock  $S_1$  and an upper 3-shock  $S_3$ , see Figure 5.2, and  $S(\alpha, \beta)$  is the sum of the strength of  $S_1$  and the strength of  $S_3$ , i.e.

$$S(\alpha, \beta) = \ln \frac{p_*}{p_-} + \ln \frac{p_*}{p_+}. \quad (5.21)$$

- 3. Riemann solution for  $(\alpha, \beta)$  in region 3:** Here the intermediate state  $(p_*, u_*)$  satisfies

$$\alpha_* = \frac{p_*}{p_-} < 1, \quad K_R(\alpha_*) = \frac{\sqrt{1 + u_*^2} - u_*}{\sqrt{1 + u_-^2} - u_-} < 1.$$

For  $(\alpha, \beta)$  in region 3, the Riemann solution consists of a lower 1-fan  $R_1$  and an upper 3-shock  $S_3$ , see Figure 5.3, and  $S(\alpha, \beta)$  is the sum of the strength of  $R_1$  and the strength of  $S_3$ , i.e.

$$S(\alpha, \beta) = \ln \frac{p_-}{p_*} + \ln \frac{p_*}{p_+}. \quad (5.22)$$

## CHAPTER 5. THE INTERACTION OF WAVES FOR THE ULTRA-RELATIVISTIC EULER EQUATIONS

---

**4. Riemann solution for  $(\alpha, \beta)$  in region 4:** Here the intermediate state  $(p_*, u_*)$  satisfies

$$\alpha_* = \frac{p_*}{p_-} < 1, \quad K_R(\alpha_*) = \frac{\sqrt{1+u_*^2} - u_*}{\sqrt{1+u_-^2} - u_-} < 1.$$

For  $(\alpha, \beta)$  in region 4, the Riemann solution consists of a lower 1-fan  $R_1$  and an upper 3-fan  $R_3$ , see Figure 5.4, and  $S(\alpha, \beta)$  is the sum of the strength of  $R_1$  and the strength of  $R_3$ , i.e.

$$S(\alpha, \beta) = \ln \frac{p_-}{p_*} + \ln \frac{p_+}{p_*}. \quad (5.23)$$

### 5.3 Wave interactions with non increasing strength

In this section we give asymptotic interaction estimates of the waves satisfying the weak formulation (3.18), (3.19) of the ultra-relativistic Euler equations. First we consider the interacting waves and the outgoing asymptotic Riemann solution. Namely the interaction of two shocks, of a shock and a rarefaction wave and of two centered rarefaction waves producing transmitted waves is considered here. The interaction of waves for general systems of hyperbolic conservation laws can be found in [18, 64] and Smoller [74, Chapter 20, §C]. Using our parametrizations of single shocks and rarefaction waves, we first study the interacting waves. More precisely we give asymptotic interaction estimates of the waves, using the function  $S(\alpha, \beta)$  in Subsection 5.2.1. Especially for six cases of interaction of incoming waves we have the conservative strength. For other eight cases we obtain that the strength is strictly decreasing.

In the following two lemmas we give new features for the functions  $K_S$  and  $K_R$  in (3.45) and (3.66). In fact these features play an important role in order to perform the interaction estimates in a completely unified way.

**Lemma 5.3.1.** *For  $x, y > 1$  we have  $K_S(x)K_S(y) < K_S(xy)$ .*

*Proof.* From  $xy > x$  and Remark 5.2.2 part (v) we conclude that

$$x \frac{K'_S(x)}{K_S(x)} < xy \frac{K'_S(xy)}{K_S(xy)},$$

hence

$$\frac{\partial}{\partial x} \ln(K_S(x)K_S(y)) < \frac{\partial}{\partial x} \ln(K_S(xy)).$$

Integration with respect to  $x$  for fixed  $y > 1$  gives

$$\int_1^x \frac{\partial}{\partial \xi} \ln(K_S(\xi)K_S(y)) d\xi < \int_1^x \frac{\partial}{\partial \xi} \ln(K_S(\xi y)) d\xi.$$

Hence we have

$$\ln(K_S(x)K_S(y)) - \ln K_S(y) < \ln(K_S(xy)) - \ln K_S(y).$$

This completes the proof of the lemma. □

### 5.3. WAVE INTERACTIONS WITH NON INCREASING STRENGTH

---

**Lemma 5.3.2.** *Let be  $x > y > 1$ . Then*

(a)  $K_S(x)K_S(y) > K_R\left(\frac{x}{y}\right)$  and

(b)  $K_R(x)K_R(y) > K_S\left(\frac{x}{y}\right)$ .

*Proof.* (a) We have  $1 < \frac{x}{y} < x$ , hence we have from the monotonicity of  $K_S$  and from Lemma 5.2.3

$$K_S(x)K_S(y) > K_S(x) > K_S\left(\frac{x}{y}\right) > K_R\left(\frac{x}{y}\right). \quad (5.24)$$

(b) We take the logarithmic derivative of  $K_S\left(\frac{x}{y}\right)$  with respect to  $x$ , and obtain the inequality

$$\begin{aligned} \frac{\partial}{\partial x} \ln K_S\left(\frac{x}{y}\right) &= \frac{1}{y} \frac{K'_S\left(\frac{x}{y}\right)}{K_S\left(\frac{x}{y}\right)} = \frac{\frac{1}{x} + \frac{1}{y}}{2} \frac{\sqrt{3}}{\sqrt{3 + \frac{x}{y}} \sqrt{1 + 3\frac{x}{y}}} \\ &< \frac{\sqrt{3}}{\sqrt{4}\sqrt{4}} = \frac{\sqrt{3}}{4} = \frac{\partial}{\partial x} \ln(K_R(x)K_R(y)). \end{aligned}$$

We obtain

$$\begin{aligned} \ln K_S\left(\frac{x}{y}\right) &= \int_y^x \frac{\partial}{\partial \xi} \ln K_S\left(\frac{\xi}{y}\right) d\xi \\ &< \int_y^x \frac{\partial}{\partial \xi} \ln(K_R(\xi)K_R(y)) d\xi \\ &= \ln(K_R(x)K_R(y)) - \ln(K_R(y)^2) \\ &< \ln(K_R(x)K_R(y)), \end{aligned}$$

and hence the statement of (b). □

We want to show that the strength of the outgoing asymptotic Riemann solution is non increasing after interactions of shocks and rarefaction waves. So we deal with the cases of conservative strength in Subsection 5.3.1, and the other cases of strictly decreasing strength is considered in Subsection 5.3.2 .

#### 5.3.1 The cases with conservation of strength

In this section we show that the strength is conserved for the interactions of waves of the different families, and also for the interactions of shocks of the same family. This means we prove that the strength of the incoming two waves is equal to strength of the outgoing asymptotic Riemann solution, using the function  $S(\alpha, \beta)$  given in (5.15). Here we cover all cases, which gives the conservation of strength.

## CHAPTER 5. THE INTERACTION OF WAVES FOR THE ULTRA-RELATIVISTIC EULER EQUATIONS

---

Our study dealing with the cases of conservation of strength also allows us to determine the type of the outgoing Riemann solutions. In Propositions 4.3.1 and 5.3.3 we present the explicit form of the transmitted Riemann solutions in the case of incoming waves with different families. Especially the pressure in the outgoing star region is given in simple algebraic terms of the pressures before interaction, which generalizes a result given in Proposition 4.3.1. This is important for the study of shock interactions, because in the general Riemann solution for the ultra relativistic Euler equations the intermediate pressure is only given in implicit form.

We start with the following three interactions of the different families. The first wave is the lower one and the second wave is the upper one, respectively:

- (i)  $S_3$  interacts with  $S_1$ ,
- (ii)  $R_3$  interacts with  $S_1$  and  $S_3$  interacts with  $R_1$ ,
- (iii)  $R_3$  interacts with  $R_1$ .

In Chapter 4, namely Proposition 4.3.1 we described the interaction of two shock waves for the ultra-relativistic Euler equations. We gave new explicit shock interaction formulas. We assumed that there are two shocks, an upper 1-shock  $S_1$  and a lower 3-shock  $S_3$  with velocities  $s_1$  and  $s_3$ , respectively, starting at  $t = 0$  on the  $(t, x)$ -plane as shown in Figure 5.5<sub>(I)</sub>. The two shocks must collide with each other at a finite time  $t = t_1$ , when the middle state disappears and a new Riemann problem is formed. We constructed the solution of the Riemann problem in the explicit formulas. Here we can generalize Proposition 4.3.1 to the other incoming waves from different families.

**Proposition 5.3.3.** *Given are the three states  $(p_j, u_j) \in \mathbb{R}^+ \times \mathbb{R}$ ,  $j = 1, 2, 3$ . Assume that, as depicted in Figures 5.5<sub>(II),(III),(IV)</sub>, the states  $(p_1, u_1)$  and  $(p_2, u_2)$  as well as  $(p_2, u_2)$  and  $(p_3, u_3)$  can be connected by a lower 3-wave and an upper 1-wave, respectively. The intermediate state  $(p_*, u_*)$  in the so called “star-region”, which is illustrated in Figure 5.5<sub>(II),(III),(IV)</sub>, can be connected with two single waves to the prescribed left and right Riemannian initial data, namely*

- (i)  $R_3 S_1 \rightarrow S'_1 R'_3$ ,
- (ii)  $S_3 R_1 \rightarrow R'_1 S'_3$ ,
- (iii)  $R_3 R_1 \rightarrow R'_1 R'_3$ .

The intermediate pressure is given by

$$p_* = \frac{p_1 p_3}{p_2}. \quad (5.25)$$

*Proof.* The proof follows in the same way like in Proposition 4.3.1. □

### 5.3. WAVE INTERACTIONS WITH NON INCREASING STRENGTH

We study the interaction of waves of the different families and of the same family. In the following proposition make essentially use of the strength function  $S(\alpha, \beta)$  in (5.15). We show that the strength is conserved for the above interactions of waves of the different families, and also for the interactions of shocks of the same family. We also determine the type of the outgoing Riemann solutions. Recall that the first wave is the lower one and the second wave is the upper one, respectively.

**Proposition 5.3.4.** *Given are the three states  $(p_j, u_j) \in \mathbb{R}^+ \times \mathbb{R}$ ,  $j = 1, 2, 3$ . Assume that, as depicted in Figure 5.5, the states  $(p_1, u_1)$  and  $(p_2, u_2)$  as well as  $(p_2, u_2)$  and  $(p_3, u_3)$  can be connected by a lower wave and an upper wave, respectively. Then we have*

- (i)  $S_3 S_1 \rightarrow S'_1 S'_3$  with  $Str(S_3) + Str(S_1) = Str(S'_1) + Str(S'_3)$ .
- (ii)  $S_3 R_1 \rightarrow R'_1 S'_3$  with  $Str(S_3) + Str(R_1) = Str(R'_1) + Str(S'_3)$ .
- (iii)  $R_3 S_1 \rightarrow S'_1 R'_3$  with  $Str(R_3) + Str(S_1) = Str(S'_1) + Str(R'_3)$ .
- (iv)  $R_3 R_1 \rightarrow R'_1 R'_3$  with  $Str(R_3) + Str(R_1) = Str(R'_1) + Str(R'_3)$ .
- (v)  $S_1 \tilde{S}_1 \rightarrow S'_1 R'_3$  with  $Str(S_1) + Str(\tilde{S}_1) = Str(S'_1) + Str(R'_3)$ .
- (vi)  $S_3 \tilde{S}_3 \rightarrow R'_1 S'_3$  with  $Str(S_3) + Str(\tilde{S}_3) = Str(R'_1) + Str(S'_3)$ .

*Proof.* We prove first part of (i).  $S_3$  interacts with  $S_1$ , the interaction is depicted in Figure 5.5(I). Put  $p_- = p_1$ ,  $p_+ = p_3$ ,  $u_- = u_1$ ,  $u_+ = u_3$  and recall  $\alpha = \frac{p_3}{p_1}$  and  $\beta = \frac{\sqrt{1+u_3^2}-u_3}{\sqrt{1+u_1^2}-u_1}$ . According to Lemma 3.3.5 we have

$$\text{for } S_3 : \alpha_1 = \frac{p_2}{p_1} < 1, \text{ i.e. } p_2 < p_1, \quad \beta_1 = \frac{\sqrt{1+u_2^2}-u_2}{\sqrt{1+u_1^2}-u_1} = K_S\left(\frac{1}{\alpha_1}\right), \quad (5.26)$$

$$\text{for } S_1 : \alpha_2 = \frac{p_3}{p_2} > 1, \text{ i.e. } p_2 < p_3, \quad \beta_2 = \frac{\sqrt{1+u_3^2}-u_3}{\sqrt{1+u_2^2}-u_2} = K_S(\alpha_2).$$

To prove this part we show that the initial data (6.13) satisfies the statements of case 2 of the Riemann solutions for  $\alpha > 1$  or  $\alpha < 1$ , where  $\alpha = \frac{p_3}{p_1}$ . So we only have to check that

$$\beta > K_S(\alpha), \quad \beta K_S(\alpha) > 1. \quad (5.27)$$

First for  $\alpha > 1$ , i.e.  $p_3 > p_1$ . Regarding  $p_1 > p_2$ ,  $p_3 > p_2$  and  $p_3 > p_1$  we obtain from (5.26) and Lemma 5.3.2 (a)

$$\beta = \beta_2 \beta_1 = K_S\left(\frac{p_1}{p_2}\right) K_S\left(\frac{p_3}{p_2}\right) > K_S\left(\frac{p_3}{p_1}\right).$$

$$\beta K_S(\alpha) = K_S\left(\frac{p_1}{p_2}\right) K_S\left(\frac{p_3}{p_2}\right) K_S\left(\frac{p_3}{p_1}\right) > 1.$$

## CHAPTER 5. THE INTERACTION OF WAVES FOR THE ULTRA-RELATIVISTIC EULER EQUATIONS

---

Second for  $\alpha < 1$ , i.e.  $p_3 < p_1$ . Regarding  $p_1 > p_2$ ,  $p_3 > p_2$  and  $p_3 < p_1$  we obtain from (5.26)

$$\beta = \beta_2\beta_1 = K_S\left(\frac{p_1}{p_2}\right) K_S\left(\frac{p_3}{p_2}\right) > K_S\left(\frac{p_3}{p_1}\right),$$

and from Lemma 5.3.2 (a)

$$\begin{aligned} \beta K_S(\alpha) &= K_S\left(\frac{p_1}{p_2}\right) K_S\left(\frac{p_3}{p_2}\right) K_S\left(\frac{p_3}{p_1}\right) \\ &> K_S\left(\frac{p_1}{p_2}\right) K_S\left(\frac{p_3}{p_2}\right) K_S\left(\frac{p_2}{p_1}\right) K_S\left(\frac{p_2}{p_3}\right) = 1. \end{aligned}$$

We prove second part of (i). Recall that  $Str(S_3) = \ln \frac{p_1}{p_2}$  along  $S_3$  and  $Str(S_1) = \ln \frac{p_3}{p_2}$  along  $S_1$ . Hence we have before interaction:

$$Str(S_3) + Str(S_1) = \ln \frac{p_1}{p_2} + \ln \frac{p_3}{p_2} = \ln \frac{p_1 p_3}{p_2^2}. \quad (5.28)$$

According to equation (5.21), we have after interaction:

$$Str(S'_1) + Str(S'_3) = \ln \frac{p_*}{p_1} + \ln \frac{p_*}{p_3} = \ln \frac{p_*^2}{p_1 p_3} = \ln \frac{p_1 p_3}{p_2^2}, \quad (5.29)$$

using Proposition 4.3.1. Then we get the conservativity in this case.

We prove first part of (ii). Consider the case where  $S_3$  interacts with  $R_1$ , the interaction is depicted in Figure 5.5<sub>(II)</sub>. According to Lemma 3.3.5 (2) and Lemma 3.3.7 (1) we have

$$\text{for } S_3 : \alpha_1 = \frac{p_2}{p_1} < 1, \text{ i.e. } p_2 < p_1, \quad \beta_1 = \frac{\sqrt{1+u_2^2} - u_2}{\sqrt{1+u_1^2} - u_1} = K_S\left(\frac{1}{\alpha_1}\right), \quad (5.30)$$

$$\text{for } R_1 : \alpha_2 = \frac{p_3}{p_2} < 1, \text{ i.e. } p_3 < p_2, \quad \beta_2 = \frac{\sqrt{1+u_3^2} - u_3}{\sqrt{1+u_2^2} - u_2} = K_R(\alpha_2).$$

Hence  $p_1 > p_3$ , i.e.  $\alpha < 1$ .

To prove this part we show that the initial data (6.13) satisfies the statements of case 3 of the Riemann solutions. So we only have to check that

$$\beta > K_R(\alpha), \quad \beta K_S(\alpha) < 1. \quad (5.31)$$

Regarding  $p_1 > p_2 > p_3$ , we obtain from (5.30) and Lemma 5.2.3 (a)

$$\begin{aligned} \beta = \beta_2\beta_1 &= K_S\left(\frac{p_1}{p_2}\right) K_R\left(\frac{p_3}{p_2}\right) > K_R\left(\frac{p_1}{p_2}\right) K_R\left(\frac{p_3}{p_2}\right) \\ &= K_R\left(\frac{p_1 p_3}{p_2^2}\right) > K_R\left(\frac{p_3}{p_1}\right) = K_R(\alpha), \end{aligned}$$



### 5.3. WAVE INTERACTIONS WITH NON INCREASING STRENGTH

and from Lemma 5.2.3 (b) and Lemma 5.3.2 (b)

$$\begin{aligned}\beta K_S(\alpha) &= K_S\left(\frac{p_1}{p_2}\right) K_R\left(\frac{p_3}{p_2}\right) K_S\left(\frac{p_3}{p_1}\right) \\ &< K_S\left(\frac{p_1}{p_2}\right) K_R\left(\frac{p_3}{p_2}\right) K_R\left(\frac{p_3}{p_1}\right) \\ &< K_S\left(\frac{p_1}{p_2}\right) K_S\left(\frac{p_2}{p_1}\right) = 1.\end{aligned}$$

We prove second part of (ii). Recall that  $Str(S_3) = \ln \frac{p_1}{p_2}$  along  $S_3$  and  $Str(R_1) = \ln \frac{p_2}{p_3}$  along  $R_1$ . Hence we have before interaction:

$$Str(S_3) + Str(R_1) = \ln \frac{p_1}{p_2} + \ln \frac{p_2}{p_3} = \ln \frac{p_1}{p_3}. \quad (5.32)$$

According to equation (5.22), we have after interaction:

$$Str(R'_1) + Str(S'_3) = \ln \frac{p_1}{p_*} + \ln \frac{p_*}{p_3} = \ln \frac{p_1}{p_3}. \quad (5.33)$$

Then we get the statement in this case.

We prove part (iii). Consider the case where  $R_3$  interacts with  $S_1$ , the interaction is depicted in Figure 5.5(III). According to Lemma 3.3.5 (1) and Lemma 3.3.7 (2) we have

$$\text{for } R_3 : \alpha_1 = \frac{p_2}{p_1} > 1, \text{ i.e. } p_2 > p_1, \quad \beta_1 = \frac{\sqrt{1+u_2^2} - u_2}{\sqrt{1+u_1^2} - u_1} = K_R\left(\frac{1}{\alpha_1}\right), \quad (5.34)$$

$$\text{for } S_1 : \alpha_2 = \frac{p_3}{p_2} > 1, \text{ i.e. } p_3 > p_2, \quad \beta_2 = \frac{\sqrt{1+u_3^2} - u_3}{\sqrt{1+u_2^2} - u_2} = K_S(\alpha_2).$$

To prove this part we show that the initial data (6.13) satisfies the statements of case 1 of the Riemann solutions. So we only have to check that

$$\beta < K_S(\alpha), \quad \beta K_R(\alpha) > 1. \quad (5.35)$$

Regarding  $p_3 > p_2 > p_1$ , we obtain from (5.34) and Lemma 5.3.2 (b) and Lemma 5.2.3 (a)

$$\begin{aligned}\beta = \beta_2 \beta_1 &= K_R\left(\frac{p_1}{p_2}\right) K_S\left(\frac{p_3}{p_2}\right) < K_R\left(\frac{p_1}{p_2}\right) K_R\left(\frac{p_3}{p_1}\right) K_R\left(\frac{p_2}{p_1}\right) \\ &= K_R\left(\frac{p_3}{p_1}\right) < K_S\left(\frac{p_3}{p_1}\right) = K_S(\alpha),\end{aligned}$$

**CHAPTER 5. THE INTERACTION OF WAVES FOR THE  
ULTRA-RELATIVISTIC EULER EQUATIONS**

---

$$\begin{aligned}\beta K_R(\alpha) &= K_R\left(\frac{p_1}{p_2}\right) K_S\left(\frac{p_3}{p_2}\right) K_R\left(\frac{p_3}{p_1}\right) \\ &= K_S\left(\frac{p_3}{p_2}\right) K_R\left(\frac{p_3}{p_2}\right) > 1.\end{aligned}$$

We prove second part of (iii). Recall that  $Str(R_3) = \ln \frac{p_2}{p_1}$  along  $R_3$  and  $Str(S_1) = \ln \frac{p_3}{p_2}$  along  $S_1$ . Hence we have before interaction:

$$Str(R_3) + Str(S_1) = \ln \frac{p_2}{p_1} + \ln \frac{p_3}{p_2} = \ln \frac{p_3}{p_1}. \quad (5.36)$$

According to equation (5.19), we have after interaction:

$$Str(S'_1) + Str(R'_3) = \ln \frac{p_*}{p_1} + \ln \frac{p_3}{p_*} = \ln \frac{p_3}{p_1}. \quad (5.37)$$

Then we get the statement in this case.

We prove first part of (iv).  $R_3$  interacts with  $R_1$ , the interaction is depicted in Figure 5.5<sub>(IV)</sub>. According to Lemma 3.3.7 we have

$$\text{for } R_3 : \alpha_1 = \frac{p_2}{p_1} > 1, \text{ i.e. } p_2 > p_1, \quad \beta_1 = \frac{\sqrt{1+u_2^2} - u_2}{\sqrt{1+u_1^2} - u_1} = K_R\left(\frac{1}{\alpha_1}\right), \quad (5.38)$$

$$\text{for } R_1 : \alpha_2 = \frac{p_3}{p_2} < 1, \text{ i.e. } p_2 > p_3, \quad \beta_2 = \frac{\sqrt{1+u_3^2} - u_3}{\sqrt{1+u_2^2} - u_2} = K_R(\alpha_2).$$

To prove this part we show that the initial data (6.13) satisfies the statements of case 4 of the Riemann solutions for  $\alpha > 1$  or  $\alpha < 1$ , where  $\alpha = \frac{p_3}{p_1}$ . So we only have to check that

$$\beta < K_R(\alpha), \quad \beta K_R(\alpha) < 1. \quad (5.39)$$

First for  $\alpha > 1$ , i.e.  $p_3 > p_1$ . Regarding  $p_2 > p_1$ ,  $p_2 > p_3$  and  $p_3 > p_1$  we obtain from (5.38)

$$\begin{aligned}\beta &= \beta_2 \beta_1 = K_R\left(\frac{p_1}{p_2}\right) K_R\left(\frac{p_3}{p_2}\right) < K_R\left(\frac{p_3}{p_1}\right), \\ \beta K_R(\alpha) &= K_R\left(\frac{p_1}{p_2}\right) K_R\left(\frac{p_3}{p_2}\right) K_R\left(\frac{p_3}{p_1}\right) = K_R\left(\frac{p_3^2}{p_2^2}\right) < 1.\end{aligned}$$

Second for  $\alpha < 1$ , i.e.  $p_3 < p_1$ . Regarding  $p_2 > p_1$ ,  $p_2 > p_3$  and  $p_3 < p_1$  we obtain from (5.38), Lemma 5.3.2 (b) and Lemma 5.2.3 (b)

$$\beta = \beta_2 \beta_1 = K_R\left(\frac{p_1}{p_2}\right) K_R\left(\frac{p_3}{p_2}\right) < K_S\left(\frac{p_3}{p_1}\right) < K_R\left(\frac{p_3}{p_1}\right) = K_R(\alpha),$$

$$\beta K_R(\alpha) = K_R\left(\frac{p_1}{p_2}\right) K_R\left(\frac{p_3}{p_2}\right) K_R\left(\frac{p_3}{p_1}\right) = K_R\left(\frac{p_3^2}{p_2^2}\right) < 1.$$

### 5.3. WAVE INTERACTIONS WITH NON INCREASING STRENGTH

We prove second part of (iv). Recall that  $Str(R_3) = \ln \frac{p_2}{p_1}$  along  $R_3$  and  $Str(R_1) = \ln \frac{p_2}{p_3}$  along  $R_1$ . Hence we have before interaction:

$$Str(R_3) + Str(R_1) = \ln \frac{p_2}{p_1} + \ln \frac{p_2}{p_3} = \ln \frac{p_2^2}{p_1 p_3}. \quad (5.40)$$

According to equation (5.23), we have after interaction:

$$Str(R'_1) + str(R'_3) = \ln \frac{p_1}{p_*} + \ln \frac{p_3}{p_*} = \ln \frac{p_1 p_3}{p_*^2} = \ln \frac{p_1 p_3}{p_2^2}, \quad (5.41)$$

using Proposition 5.3.3. Then we get the conservativity in this case.

We prove first part of (v).  $S_1$  interacts with  $\tilde{S}_1$ , the interaction is depicted in Figure 5.5<sub>(v)</sub>. According to Lemma 3.3.5 (1) we have

$$\text{for } S_1 : \alpha_1 = \frac{p_2}{p_1} > 1, \text{ i.e. } p_2 > p_1, \quad \beta_1 = \frac{\sqrt{1+u_2^2} - u_2}{\sqrt{1+u_1^2} - u_1} = K_S(\alpha_1), \quad (5.42)$$

$$\text{for } \tilde{S}_1 : \alpha_2 = \frac{p_3}{p_2} > 1, \text{ i.e. } p_3 > p_2, \quad \beta_2 = \frac{\sqrt{1+u_3^2} - u_3}{\sqrt{1+u_2^2} - u_2} = K_S(\alpha_2).$$

Hence  $p_3 > p_1$ , i.e.  $\alpha > 1$ .

To prove this proposition we show that the initial data (6.13) satisfies the statements of case 1 of the Riemann solutions. So we only have to check that

$$\beta < K_S(\alpha), \quad \beta K_R(\alpha) > 1. \quad (5.43)$$

Regarding  $p_3 > p_2 > p_1$ , we obtain from (5.42) and Lemma 5.3.1

$$\beta = \beta_2 \beta_1 = K_S\left(\frac{p_3}{p_2}\right) K_S\left(\frac{p_2}{p_1}\right) < K_S\left(\frac{p_3}{p_1}\right) = K_S(\alpha), \quad (5.44)$$

$$\beta K_R(\alpha) = K_S\left(\frac{p_3}{p_2}\right) K_S\left(\frac{p_2}{p_1}\right) K_R\left(\frac{p_3}{p_1}\right) > 1.$$

We prove second part of (v). Recall that  $Str(S_1) = \ln \frac{p_2}{p_1}$  along  $S_1$  and  $Str(\tilde{S}_1) = \ln \frac{p_3}{p_2}$  along  $\tilde{S}_1$ . Hence we have before interaction:

$$Str(S_1) + Str(\tilde{S}_1) = \ln \frac{p_2}{p_1} + \ln \frac{p_3}{p_2} = \ln \frac{p_3}{p_1}. \quad (5.45)$$

According to equation (5.19), we have after interaction:

$$Str(S'_1) + Str(R'_3) = \ln \frac{p_*}{p_1} + \ln \frac{p_3}{p_*} = \ln \frac{p_3}{p_1}. \quad (5.46)$$

Then we get the statement in this case.

## CHAPTER 5. THE INTERACTION OF WAVES FOR THE ULTRA-RELATIVISTIC EULER EQUATIONS

---

We prove part (vi).  $S_3$  interacts with  $\tilde{S}_3$ , the interaction is depicted in Figure 5.5<sub>(VI)</sub>. According to Lemma 3.3.5 (2) we have

$$\text{for } S_3 : \alpha_1 = \frac{p_2}{p_1} < 1, \text{ i.e. } p_2 < p_1, \quad \beta_1 = \frac{\sqrt{1+u_2^2} - u_2}{\sqrt{1+u_1^2} - u_1} = K_S \left( \frac{1}{\alpha_1} \right), \quad (5.47)$$

$$\text{for } \tilde{S}_3 : \alpha_2 = \frac{p_3}{p_2} < 1, \text{ i.e. } p_3 < p_2, \quad \beta_2 = \frac{\sqrt{1+u_3^2} - u_3}{\sqrt{1+u_2^2} - u_2} = K_S \left( \frac{1}{\alpha_2} \right).$$

To prove this proposition we show that the initial data (6.13) satisfies the statements of case 3 of the Riemann solutions. So we only have to check that

$$\beta > K_R(\alpha), \quad \beta K_S(\alpha) < 1. \quad (5.48)$$

Regarding  $p_1 > p_2 > p_3$ , we obtain from (5.47) and Lemma 5.2.3 (a)

$$\beta = \beta_2 \beta_1 = K_S \left( \frac{p_1}{p_2} \right) K_S \left( \frac{p_2}{p_3} \right) > K_R \left( \frac{p_1}{p_3} \right) K_R \left( \frac{p_2}{p_3} \right) = K_R \left( \frac{p_1}{p_2} \right) > K_R \left( \frac{p_3}{p_1} \right) = K_R(\alpha), \quad (5.49)$$

and from Lemma 5.3.1

$$\beta K_S(\alpha) = K_S \left( \frac{p_1}{p_2} \right) K_S \left( \frac{p_2}{p_3} \right) K_S \left( \frac{p_3}{p_1} \right) < K_S \left( \frac{p_1}{p_3} \right) K_S \left( \frac{p_3}{p_1} \right) = 1.$$

We prove second part of (vi). Recall that  $Str(S_3) = \ln \frac{p_1}{p_2}$  along  $S_3$  and  $Str(\tilde{S}_3) = \ln \frac{p_2}{p_3}$  along  $\tilde{S}_3$ . Hence we have before interaction:

$$Str(S_3) + Str(\tilde{S}_3) = \ln \frac{p_1}{p_2} + \ln \frac{p_2}{p_3} = \ln \frac{p_1}{p_3}. \quad (5.50)$$

According to equation (5.19), we have after interaction:

$$Str(R'_1) + Str(S'_3) = \ln \frac{p_1}{p_*} + \ln \frac{p_*}{p_3} = \ln \frac{p_1}{p_3}, \quad (5.51)$$

which completes this part. This completes the proof of the proposition.  $\square$

### 5.3.2 The cases with strictly decreasing strength

Here we will study the other cases for the interaction of waves, which give a strictly decreasing strength. More precisely we study the interaction of waves belonging to the same family:  $R_3 S_3$ ,  $S_3 R_3$ ,  $R_1 S_1$  and  $S_1 R_1$ . We show that the strength is strictly decreasing, i.e. the strength after interaction of two waves, namely shocks and rarefaction waves is less than the strength before interaction.

We consider the following cases of incoming waves and study their interactions. Recall that the first incoming wave is the lower one and the second incoming wave is the upper one, respectively:

### 5.3. WAVE INTERACTIONS WITH NON INCREASING STRENGTH

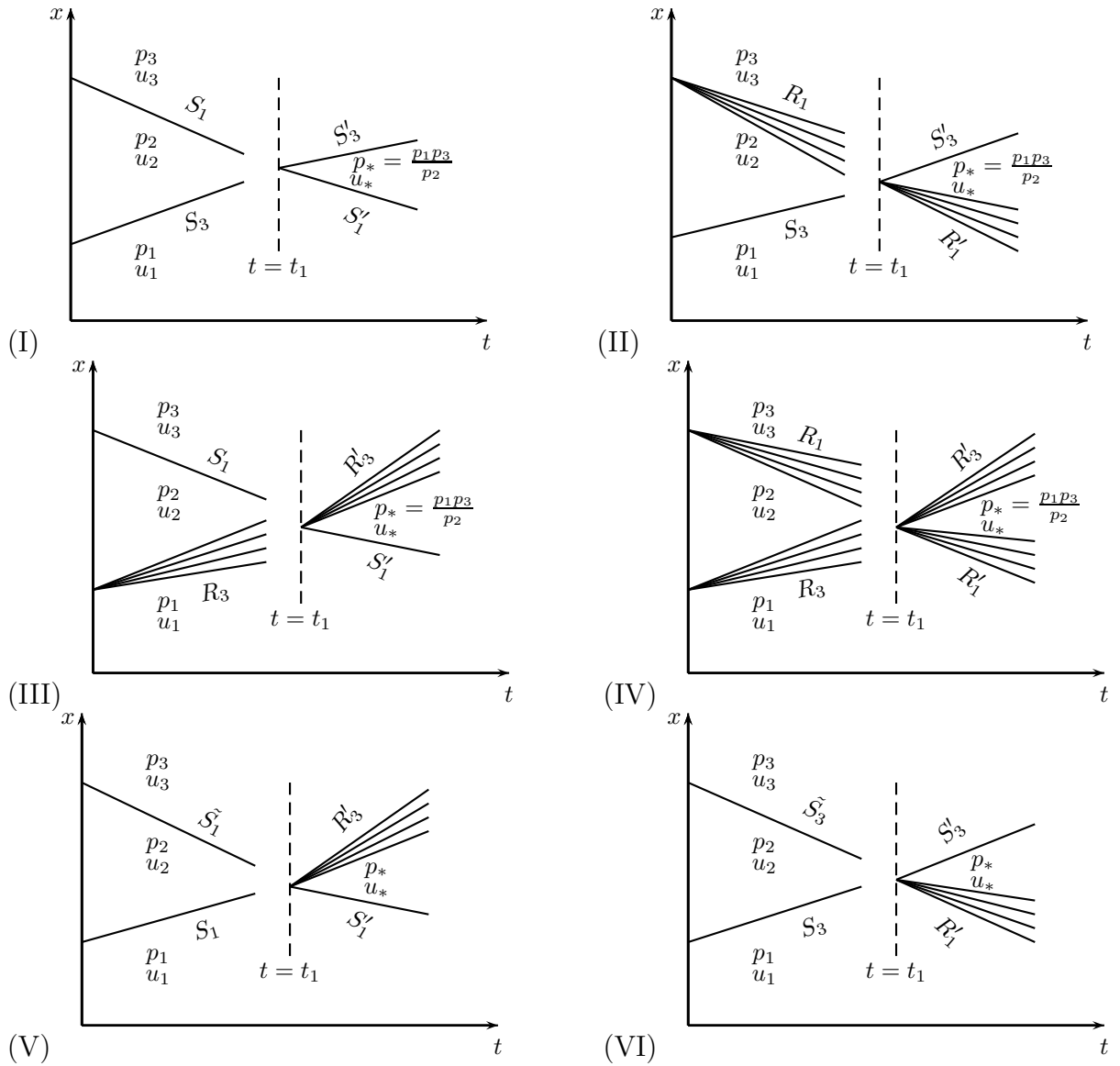


Figure 5.5: Asymptotic interaction of waves with conserved strength.

## CHAPTER 5. THE INTERACTION OF WAVES FOR THE ULTRA-RELATIVISTIC EULER EQUATIONS

---

- (i)  $R_3$  interacts with  $S_3$  and  $S_3$  interacts with  $R_3$ ,
- (ii)  $R_1$  interacts with  $S_1$  and  $S_1$  interacts with  $R_1$ .

We show that the strength is strictly decreasing for the interactions of waves of the same families. Also we determine the type of the outgoing Riemann solutions.

**Proposition 5.3.5.** *Given are the three states  $(p_j, u_j) \in \mathbb{R}^+ \times \mathbb{R}$ ,  $j = 1, 2, 3$ . Assume that, as depicted in Figure 5.6, the states  $(p_1, u_1)$  and  $(p_2, u_2)$  as well as  $(p_2, u_2)$  and  $(p_3, u_3)$  can be connected by a lower wave and an upper wave. Then the following estimates are valid for the corresponding interactions.*

(a)<sub>1</sub>  $R_3 S_3 \rightarrow S'_1 S'_3$  and  $R_3 S_3 \rightarrow S'_1 R'_3$  with

(a)<sub>2</sub>

$Str(R_3) + Str(S_3) < Str(S'_1) + Str(S'_3)$  and  $Str(R_3) + Str(S_3) < Str(S'_1) + Str(R'_3)$ , respectively,

(b)<sub>1</sub>  $S_1 R_1 \rightarrow S'_1 S'_3$  and  $S_1 R_1 \rightarrow R'_1 S'_3$  with

(b)<sub>2</sub>

$Str(S_1) + Str(R_1) < Str(S'_1) + Str(S'_3)$  and  $Str(S_1) + Str(R_1) < Str(R'_1) + Str(S'_3)$ , respectively,

(c)<sub>1</sub>  $S_3 R_3 \rightarrow S'_1 S'_3$  and  $S_3 R_3 \rightarrow S'_1 R'_3$  with

(c)<sub>2</sub>

$Str(S_3) + Str(R_3) < Str(S'_1) + Str(S'_3)$  and  $Str(S_3) + Str(R_3) < Str(S'_1) + Str(R'_3)$ , respectively,

(d)<sub>1</sub>  $R_1 S_1 \rightarrow S'_1 S'_3$  and  $R_1 S_1 \rightarrow R'_1 S'_3$  with

(d)<sub>2</sub>

$Str(R_1) + Str(S_1) < Str(S'_1) + Str(S'_3)$  and  $Str(R_1) + Str(S_1) < Str(R'_1) + Str(S'_3)$ , respectively.

*Proof.* We first consider part (a)<sub>1</sub>,  $R_3$  interacts with  $S_3$ . The interaction is depicted in Figure 5.6(I),(II). Then we have two possibilities for the outgoing waves. They depend on  $\alpha < 1$  or  $\alpha > 1$ , where  $\alpha = \frac{p_3}{p_1}$ . According to Lemma 3.3.7 (2) and Lemma 3.3.5 (2) we have

$$\text{for } R_3 : \alpha_1 = \frac{p_2}{p_1} > 1, \text{ i.e. } p_2 > p_1, \quad \beta_1 = \frac{\sqrt{1+u_2^2} - u_2}{\sqrt{1+u_1^2} - u_1} = K_R \left( \frac{1}{\alpha_1} \right), \quad (5.52)$$

$$\text{for } S_3 : \alpha_2 = \frac{p_3}{p_2} < 1, \text{ i.e. } p_3 < p_2, \quad \beta_2 = \frac{\sqrt{1+u_3^2} - u_3}{\sqrt{1+u_2^2} - u_2} = K_S \left( \frac{1}{\alpha_2} \right).$$

### 5.3. WAVE INTERACTIONS WITH NON INCREASING STRENGTH

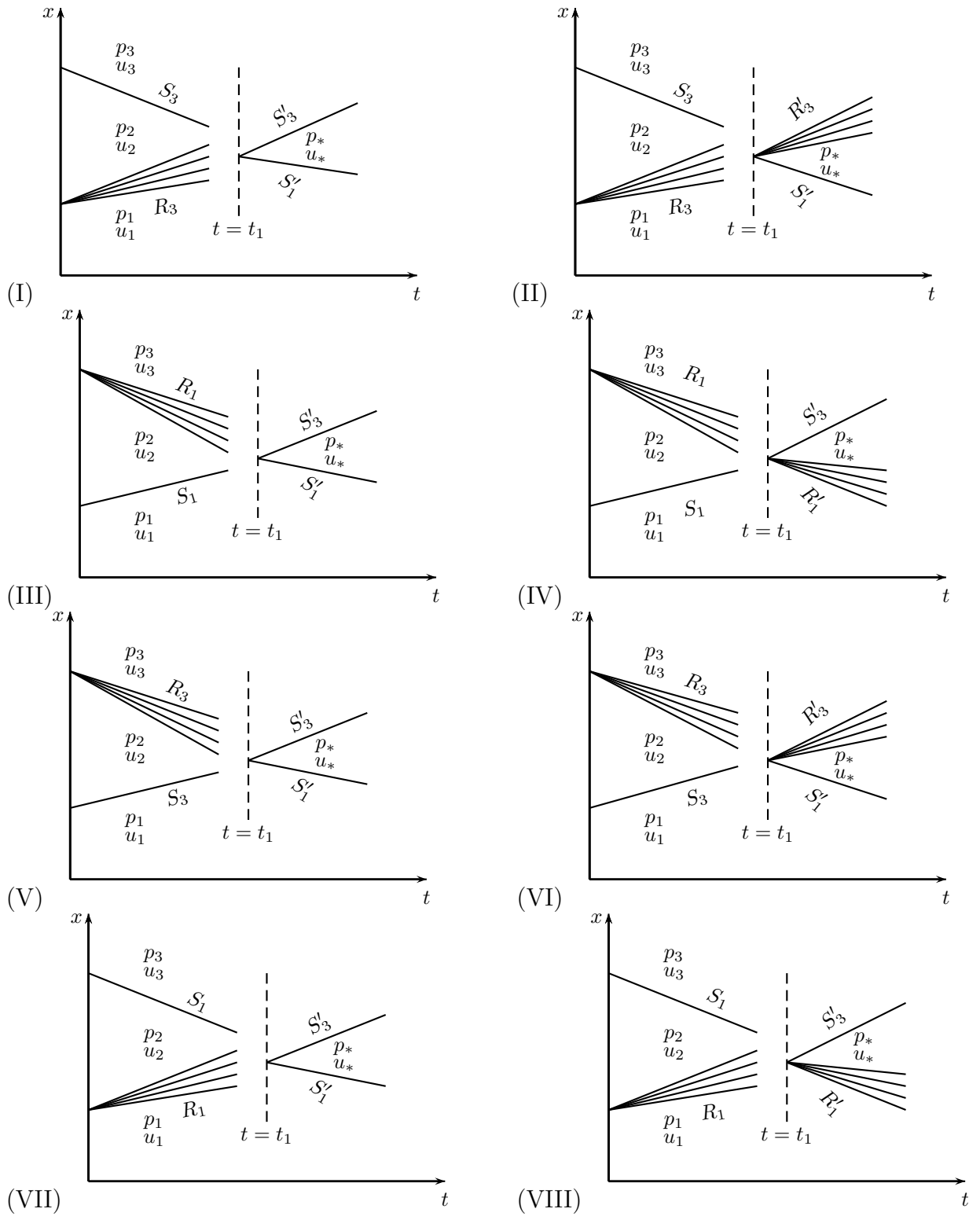


Figure 5.6: Asymptotic interaction of waves with decreasing strength.

## CHAPTER 5. THE INTERACTION OF WAVES FOR THE ULTRA-RELATIVISTIC EULER EQUATIONS

---

First we assume that  $\alpha = \frac{p_3}{p_1} < 1$ . To prove this proposition in this case, namely  $R_3 S_3 \rightarrow S'_1 S'_3$  we show that the initial data (6.13) satisfies the statements of case 2 of the Riemann solutions. So we only have to check that

$$\beta > K_S(\alpha), \quad \beta K_S(\alpha) > 1. \quad (5.53)$$

Regarding  $p_2 > \max(p_1, p_3)$ ,  $p_1 > p_3$  we obtain from (5.52), Lemma 5.3.2 (a)

$$\begin{aligned} \beta = \beta_2 \beta_1 &= K_S\left(\frac{p_2}{p_3}\right) K_R\left(\frac{p_1}{p_2}\right) \\ &> K_S\left(\frac{p_2}{p_3}\right) K_S\left(\frac{p_3}{p_2}\right) K_S\left(\frac{p_3}{p_1}\right) \\ &= K_S\left(\frac{p_3}{p_1}\right) = K_S(\alpha), \end{aligned}$$

and from Lemma 5.3.1 and Lemma 5.2.3 (b)

$$\begin{aligned} \beta K_S(\alpha) &= K_S\left(\frac{p_2}{p_3}\right) K_R\left(\frac{p_1}{p_2}\right) K_S\left(\frac{p_3}{p_1}\right) \\ &> K_S\left(\frac{p_2}{p_1}\right) K_S\left(\frac{p_1}{p_3}\right) K_R\left(\frac{p_1}{p_2}\right) K_S\left(\frac{p_3}{p_1}\right) \\ &= K_S\left(\frac{p_2}{p_1}\right) K_R\left(\frac{p_1}{p_2}\right) \\ &> K_S\left(\frac{p_2}{p_1}\right) K_S\left(\frac{p_1}{p_2}\right) = 1. \end{aligned}$$

Second we assume that  $\alpha = \frac{p_3}{p_1} > 1$ . To prove this proposition in this case, namely  $R_3 S_3 \rightarrow S'_1 R'_3$  we show that the initial data (6.13) satisfies the statements of case 1 of the Riemann solutions. So we only have to check that

$$\beta < K_S(\alpha), \quad \beta K_R(\alpha) > 1. \quad (5.54)$$

Regarding  $p_2 > \max(p_1, p_3)$ ,  $p_3 > p_1$  we obtain from (5.52), Lemma 5.3.2 (b) and Lemma 5.2.3 (a)

$$\begin{aligned} \beta &= K_S\left(\frac{p_2}{p_3}\right) K_R\left(\frac{p_1}{p_2}\right) \\ &< K_R\left(\frac{p_2}{p_1}\right) K_R\left(\frac{p_3}{p_1}\right) K_R\left(\frac{p_1}{p_2}\right) \\ &= K_R\left(\frac{p_3}{p_1}\right) \\ &< K_S\left(\frac{p_3}{p_1}\right) = K_S(\alpha), \end{aligned}$$



### 5.3. WAVE INTERACTIONS WITH NON INCREASING STRENGTH

and from Lemma 5.2.3 (b)

$$\begin{aligned}\beta K_R(\alpha) &= K_S\left(\frac{p_2}{p_3}\right) K_R\left(\frac{p_1}{p_2}\right) K_R\left(\frac{p_3}{p_1}\right) \\ &= K_S\left(\frac{p_2}{p_3}\right) K_R\left(\frac{p_3}{p_2}\right) \\ &> K_S\left(\frac{p_2}{p_3}\right) K_S\left(\frac{p_3}{p_2}\right) = 1.\end{aligned}$$

We prove part (a)<sub>2</sub>. First, consider the interaction  $R_3 S_3 \rightarrow S'_1 S'_3$ . The first case in (a)<sub>1</sub> gives the outgoing Riemann solution in region 2. Hence we use (3.76) and conclude that

$$p_2 > \max(p_1, p_3), \quad p_1 > p_3, \quad p_* > \max(p_1, p_3) \quad \text{and} \quad (5.55)$$

$$K_R\left(\frac{p_1}{p_2}\right) K_S\left(\frac{p_2}{p_3}\right) = K_S\left(\frac{p_*}{p_1}\right) K_S\left(\frac{p_*}{p_3}\right). \quad (5.56)$$

Using monotonicity of functions  $K_S$ ,  $K_R$ , one can easily show

$$p_* < p_2. \quad (5.57)$$

Recall that  $Str(R_3) = \ln \frac{p_2}{p_1}$  along  $R_3$  and  $Str(S_3) = \ln \frac{p_2}{p_3}$  along  $S_3$ . Hence we have before interaction:

$$Str(R_3) + Str(S_3) = \ln \frac{p_2}{p_1} + \ln \frac{p_2}{p_3} = \ln \frac{p_2^2}{p_1 p_3}.$$

According to equation (5.21), we have after interaction:

$$Str(S'_1) + Str(S'_3) = \ln \frac{p_*}{p_1} + \ln \frac{p_*}{p_3} = \ln \frac{p_*^2}{p_1 p_3}.$$

Thus, to show that the strength is decreasing, using (5.57) we have

$$Str(S'_1) + Str(S'_3) = \ln \frac{p_*^2}{p_1 p_3} < \ln \frac{p_2^2}{p_1 p_3} = Str(R_3) + Str(S_3).$$

Second, consider the interaction  $R_3 S_3 \rightarrow S'_1 R'_3$ . The second case in (a)<sub>1</sub> gives the outgoing Riemann solution in region 1. Hence we use (3.74) and conclude that

$$p_2 > \max(p_1, p_3), \quad p_3 > p_1 \quad \text{and} \quad p_1 < p_* < p_3. \quad (5.58)$$

We have before interaction:

$$Str(R_3) + Str(S_3) = \ln \frac{p_2}{p_1} + \ln \frac{p_2}{p_3} = \ln \frac{p_2^2}{p_1 p_3}.$$

According to equation (5.19), we have after interaction:

$$Str(S'_1) + Str(R'_3) = \ln \frac{p_*}{p_1} + \ln \frac{p_3}{p_*} = \ln \frac{p_3}{p_1}. \quad (5.59)$$

## CHAPTER 5. THE INTERACTION OF WAVES FOR THE ULTRA-RELATIVISTIC EULER EQUATIONS

---

Thus, to show that the strength is decreasing, using (5.58) we have

$$\text{Str}(S'_1) + \text{Str}(R'_3) = \ln \frac{p_3}{p_1} < \ln \frac{p_2^2}{p_1 p_3} = \text{Str}(R_3) + \text{Str}(S_3).$$

We prove part (b)<sub>1</sub>,  $S_1$  interacts with  $R_1$ . The interaction is depicted in Figure 5.6<sub>(III),(IV)</sub>. Then we have two possibilities for the outgoing waves. They depend on  $\alpha > 1$  or  $\alpha < 1$ , where  $\alpha = \frac{p_3}{p_1}$ . According to Lemma 3.3.5 (1) and Lemma 3.3.7 (1) we have

$$\text{for } S_1 : \alpha_1 = \frac{p_2}{p_1} > 1, \text{ i.e. } p_2 > p_1, \quad \beta_1 = \frac{\sqrt{1+u_2^2} - u_2}{\sqrt{1+u_1^2} - u_1} = K_S(\alpha_1), \quad (5.60)$$

$$\text{for } R_1 : \alpha_2 = \frac{p_3}{p_2} < 1, \text{ i.e. } p_3 < p_2, \quad \beta_2 = \frac{\sqrt{1+u_3^2} - u_3}{\sqrt{1+u_2^2} - u_2} = K_R(\alpha_2).$$

First we assume that  $\alpha = \frac{p_3}{p_1} > 1$ . To prove this proposition in this case, namely  $S_1 R_1 \rightarrow S'_1 S'_3$  we show that the initial data (6.13) satisfies the statements of case 2 of the Riemann solutions. So we only have to check that

$$\beta > K_S(\alpha), \quad \beta K_S(\alpha) > 1. \quad (5.61)$$

Regarding  $p_2 > \max(p_1, p_3)$ ,  $p_3 > p_1$  we obtain from (5.60), Lemma 5.2.3 (b) and Lemma 5.3.1

$$\begin{aligned} \beta = \beta_2 \beta_1 &= K_S\left(\frac{p_2}{p_1}\right) K_R\left(\frac{p_3}{p_2}\right) \\ &> K_S\left(\frac{p_2}{p_1}\right) K_S\left(\frac{p_3}{p_2}\right) \\ &> K_S\left(\frac{p_2}{p_3}\right) K_S\left(\frac{p_3}{p_1}\right) K_S\left(\frac{p_3}{p_2}\right) \\ &= K_S\left(\frac{p_3}{p_1}\right) = K_S(\alpha), \end{aligned}$$

and from Lemma 5.3.2 (a)

$$\begin{aligned} \beta K_S(\alpha) &= K_S\left(\frac{p_2}{p_1}\right) K_R\left(\frac{p_3}{p_2}\right) K_S\left(\frac{p_3}{p_1}\right) \\ &> K_R\left(\frac{p_2}{p_3}\right) K_R\left(\frac{p_3}{p_2}\right) = 1. \end{aligned}$$

Second we assume that  $\alpha = \frac{p_3}{p_1} < 1$ . To prove this proposition in this case, namely  $S_1 R_1 \rightarrow R'_1 S'_3$  we show that the initial data (6.13) satisfies the statements of case 3 of the Riemann solutions. So we only have to check that

$$\beta > K_R(\alpha), \quad \beta K_S(\alpha) < 1. \quad (5.62)$$

### 5.3. WAVE INTERACTIONS WITH NON INCREASING STRENGTH

Regarding  $p_2 > \max(p_1, p_3)$ ,  $p_1 > p_3$  we obtain from (5.52) and Lemma 5.2.3 (a)

$$\begin{aligned}\beta = \beta_2\beta_1 &= K_S\left(\frac{p_2}{p_1}\right) K_R\left(\frac{p_3}{p_2}\right) \\ &> K_R\left(\frac{p_2}{p_1}\right) K_R\left(\frac{p_3}{p_2}\right) = K_R\left(\frac{p_3}{p_1}\right) = K_R(\alpha),\end{aligned}$$

and from Lemma 5.2.3 (b) and Lemma 5.3.2 (b)

$$\begin{aligned}\beta K_S(\alpha) &= K_S\left(\frac{p_2}{p_1}\right) K_R\left(\frac{p_3}{p_2}\right) K_S\left(\frac{p_3}{p_1}\right) \\ &< K_S\left(\frac{p_2}{p_1}\right) K_R\left(\frac{p_3}{p_2}\right) K_R\left(\frac{p_3}{p_1}\right) \\ &< K_S\left(\frac{p_2}{p_1}\right) K_S\left(\frac{p_1}{p_2}\right) = 1.\end{aligned}$$

We prove part (b)<sub>2</sub>. First, consider the interaction  $S_1 R_1 \rightarrow S'_1 S'_3$ . The first case in (b)<sub>1</sub> gives the outgoing Riemann solution in region 2. Hence we use (3.76) and conclude that

$$p_2 > \max(p_1, p_3), \quad p_3 > p_1, \quad p_* > \max(p_1, p_3) \quad \text{and} \quad (5.63)$$

$$K_S\left(\frac{p_2}{p_1}\right) K_R\left(\frac{p_3}{p_2}\right) = K_S\left(\frac{p_*}{p_1}\right) K_S\left(\frac{p_*}{p_3}\right). \quad (5.64)$$

Using monotonicity of functions  $K_S, K_R$ , one can easily show

$$p_* < p_2. \quad (5.65)$$

Recall that  $Str(S_1) = \ln \frac{p_2}{p_1}$  along  $S_1$  and  $Str(R_1) = \ln \frac{p_2}{p_3}$  along  $R_1$ . Hence we have before interaction:

$$Str(S_1) + Str(R_1) = \ln \frac{p_2}{p_1} + \ln \frac{p_2}{p_3} = \ln \frac{p_2^2}{p_1 p_3}.$$

According to equation (5.21), we have after interaction:

$$Str(S'_1) + Str(S'_3) = \ln \frac{p_*}{p_1} + \ln \frac{p_*}{p_3} = \ln \frac{p_*^2}{p_1 p_3}.$$

Thus, to show that the strength is decreasing, using (5.65) we have

$$Str(S'_1) + Str(S'_3) = \ln \frac{p_*^2}{p_1 p_3} < \ln \frac{p_2^2}{p_1 p_3} = Str(R_3) + Str(S_3).$$

Second, consider the interaction  $S_1 R_1 \rightarrow R'_1 S'_3$ . The second case in (b)<sub>1</sub> gives the outgoing Riemann solution in region 1. Hence we use (3.78) and conclude that

**CHAPTER 5. THE INTERACTION OF WAVES FOR THE  
ULTRA-RELATIVISTIC EULER EQUATIONS**

---

$$p_2 > \max(p_1, p_3), \quad p_1 > p_3 \quad \text{and} \quad p_1 > p_* > p_3. \quad (5.66)$$

We have before interaction:

$$\text{Str}(S_1) + \text{Str}(R_1) = \ln \frac{p_2}{p_1} + \ln \frac{p_2}{p_3} = \ln \frac{p_2^2}{p_1 p_3}.$$

According to equation (5.22), we have after interaction:

$$\text{Str}(R'_1) + \text{Str}(S'_3) = \ln \frac{p_1}{p_*} + \ln \frac{p_*}{p_3} = \ln \frac{p_1}{p_3}. \quad (5.67)$$

Thus, to show that the strength is decreasing, using (5.66) we have

$$\text{Str}(R'_1) + \text{Str}(S'_3) = \ln \frac{p_1}{p_3} < \ln \frac{p_2^2}{p_1 p_3} = \text{Str}(S_1) + \text{Str}(R_1).$$

We prove part (c)<sub>1</sub>,  $S_3$  interacts with  $R_3$ . The interaction is depicted in Figure 5.6<sub>(V),(VI)</sub>. Then we have two possibilities for the outgoing waves. They depend on  $\alpha > 1$  or  $\alpha < 1$ , where  $\alpha = \frac{p_3}{p_1}$ . According to Lemma 3.3.5 (2) and Lemma 3.3.7 (2) we have

$$\text{for } S_3 : \alpha_1 = \frac{p_2}{p_1} < 1, \text{ i.e. } p_2 < p_1, \quad \beta_1 = \frac{\sqrt{1+u_2^2} - u_2}{\sqrt{1+u_1^2} - u_1} = K_R \left( \frac{1}{\alpha_1} \right), \quad (5.68)$$

$$\text{for } R_3 : \alpha_2 = \frac{p_3}{p_2} > 1, \text{ i.e. } p_3 > p_2, \quad \beta_2 = \frac{\sqrt{1+u_3^2} - u_3}{\sqrt{1+u_2^2} - u_2} = K_S \left( \frac{1}{\alpha_2} \right).$$

First we assume that  $\alpha = \frac{p_3}{p_1} < 1$ . To prove this proposition in this case, namely  $S_3 R_3 \rightarrow S'_1 S'_3$  we show that the initial data (6.13) satisfies the statements of case 2 of the Riemann solutions. So we only have to check that

$$\beta > K_S(\alpha), \quad \beta K_S(\alpha) > 1. \quad (5.69)$$

Regarding  $p_2 < \min(p_1, p_3)$ ,  $p_3 < p_1$  we obtain from (5.68) and 5.3.2 (a)

$$\begin{aligned} \beta = \beta_2 \beta_1 &= K_S \left( \frac{p_1}{p_2} \right) K_R \left( \frac{p_2}{p_3} \right) \\ &> K_S \left( \frac{p_1}{p_2} \right) K_S \left( \frac{p_2}{p_1} \right) K_S \left( \frac{p_3}{p_1} \right) \\ &= K_S \left( \frac{p_3}{p_1} \right) = K_S(\alpha), \end{aligned}$$

### 5.3. WAVE INTERACTIONS WITH NON INCREASING STRENGTH

and from Lemma 5.3.1 and Lemma 5.2.3 (b)

$$\begin{aligned}
 \beta K_S(\alpha) &= K_S\left(\frac{p_1}{p_2}\right) K_R\left(\frac{p_2}{p_3}\right) K_S\left(\frac{p_3}{p_1}\right) \\
 &> K_S\left(\frac{p_1}{p_3}\right) K_S\left(\frac{p_3}{p_2}\right) K_R\left(\frac{p_2}{p_3}\right) K_S\left(\frac{p_3}{p_1}\right) \\
 &= K_S\left(\frac{p_3}{p_2}\right) K_R\left(\frac{p_2}{p_3}\right) \\
 &> K_S\left(\frac{p_3}{p_2}\right) K_S\left(\frac{p_2}{p_3}\right) = 1.
 \end{aligned}$$

Second we assume that  $\alpha = \frac{p_3}{p_1} > 1$ . To prove this proposition in this case, namely  $S_3 R_3 \rightarrow S'_1 R'_3$  we show that the initial data (6.13) satisfies the statements of case 1 of the Riemann solutions. So we only have to check that

$$\beta < K_S(\alpha), \quad \beta K_R(\alpha) > 1. \quad (5.70)$$

Regarding  $p_2 < \min(p_1, p_3), p_3 > p_1$  we obtain from (5.68), Lemma 5.3.2 (b) and Lemma 5.2.3 (a)

$$\begin{aligned}
 \beta &= K_S\left(\frac{p_1}{p_2}\right) K_R\left(\frac{p_2}{p_3}\right) \\
 &< K_R\left(\frac{p_3}{p_1}\right) K_R\left(\frac{p_3}{p_2}\right) K_R\left(\frac{p_2}{p_3}\right) \\
 &= K_R\left(\frac{p_3}{p_1}\right) < K_S\left(\frac{p_3}{p_1}\right) = K_S(\alpha),
 \end{aligned}$$

and from Lemma 5.2.3 (b)

$$\begin{aligned}
 \beta K_R(\alpha) &= K_S\left(\frac{p_1}{p_2}\right) K_R\left(\frac{p_2}{p_3}\right) K_R\left(\frac{p_3}{p_1}\right) \\
 &= K_S\left(\frac{p_1}{p_2}\right) K_R\left(\frac{p_2}{p_1}\right) \\
 &> K_S\left(\frac{p_1}{p_2}\right) K_S\left(\frac{p_2}{p_1}\right) = 1.
 \end{aligned}$$

We prove part (c)<sub>2</sub>. First, consider the interaction  $S_3 R_3 \rightarrow S'_1 S'_3$ . The first case in (c)<sub>2</sub> gives the outgoing Riemann solution in region 2. Hence we use (3.76) and conclude that

$$p_2 < \min(p_1, p_3), \quad p_1 > p_3, \quad p_* > \max(p_1, p_3) \quad \text{and} \quad (5.71)$$

$$K_S\left(\frac{p_1}{p_2}\right) K_R\left(\frac{p_2}{p_3}\right) = K_S\left(\frac{p_*}{p_1}\right) K_S\left(\frac{p_*}{p_3}\right). \quad (5.72)$$

## CHAPTER 5. THE INTERACTION OF WAVES FOR THE ULTRA-RELATIVISTIC EULER EQUATIONS

---

Using monotonicity of functions  $K_S, K_R$ , one can easily show

$$p_* < \frac{p_1 p_3}{p_2}. \quad (5.73)$$

Recall that  $Str(S_3) = \ln \frac{p_1}{p_2}$  along  $S_3$  and  $Str(R_3) = \ln \frac{p_3}{p_2}$  along  $R_3$ . Hence we have before interaction:

$$Str(S_3) + Str(R_3) = \ln \frac{p_1}{p_2} + \ln \frac{p_3}{p_2} = \ln \frac{p_1 p_3}{p_2^2}.$$

According to equation (5.21), we have after interaction:

$$Str(S'_1) + Str(S'_3) = \ln \frac{p_*}{p_1} + \ln \frac{p_*}{p_3} = \ln \frac{p_*^2}{p_1 p_3}.$$

Thus, to show that the strength is decreasing, using (5.73) we have

$$Str(S'_1) + Str(S'_3) = \ln \frac{p_*^2}{p_1 p_3} < \ln \frac{p_1 p_3}{p_2^2} = Str(R_3) + Str(S_3).$$

Second, consider the interaction  $S_3 R_3 \rightarrow S'_1 R'_3$ . The second case in  $(c)_2$  gives the outgoing Riemann solution in region 1. Hence we use (3.74) and conclude that

$$p_2 < \min(p_1, p_3), \quad p_3 > p_1 \quad \text{and} \quad p_1 < p_* < p_3. \quad (5.74)$$

We have before interaction:

$$Str(S_3) + Str(R_3) = \ln \frac{p_1}{p_2} + \ln \frac{p_3}{p_2} = \ln \frac{p_1 p_3}{p_2^2}.$$

According to equation (5.19), we have after interaction:

$$Str(S'_1) + Str(R'_3) = \ln \frac{p_*}{p_1} + \ln \frac{p_3}{p_*} = \ln \frac{p_3}{p_1}. \quad (5.75)$$

Thus, to show that the strength is decreasing, using (5.74) we have

$$Str(S'_1) + Str(R'_3) = \ln \frac{p_3}{p_1} < \ln \frac{p_1 p_3}{p_2^2} = Str(R_3) + Str(S_3).$$

We prove part  $(d)_1$ . We consider  $R_1$  interacts with  $S_1$ . The interaction is depicted in Figure 5.6<sub>(VII),(VIII)</sub>. Then we have two possibilities for the outgoing waves. They depend on  $\alpha > 1$  or  $\alpha < 1$ , where  $\alpha = \frac{p_3}{p_1}$ . According to Lemma 3.3.7 (1) and Lemma 3.3.5 (1) we have

$$\text{for } R_1 : \alpha_1 = \frac{p_2}{p_1} < 1, \text{ i.e. } p_2 < p_1, \quad \beta_1 = \frac{\sqrt{1+u_2^2} - u_2}{\sqrt{1+u_1^2} - u_1} = K_R(\alpha_1), \quad (5.76)$$

$$\text{for } S_1 : \alpha_2 = \frac{p_3}{p_2} > 1, \text{ i.e. } p_3 > p_2, \quad \beta_2 = \frac{\sqrt{1+u_3^2} - u_3}{\sqrt{1+u_2^2} - u_2} = K_S(\alpha_2).$$

### 5.3. WAVE INTERACTIONS WITH NON INCREASING STRENGTH

---

First we assume that  $\alpha = \frac{p_3}{p_1} > 1$ . To prove this proposition in this case, namely  $R_1 S_1 \rightarrow S'_1 S'_3$ , we show that the initial data (6.13) satisfies the statements of case 2 of the Riemann solutions. So we only have to check that

$$\beta > K_S(\alpha), \quad \beta K_S(\alpha) > 1. \quad (5.77)$$

Regarding  $p_2 < \min(p_1, p_3)$ ,  $p_3 > p_1$  we obtain from (5.76), Lemma 5.2.3 (b) and Lemma 5.3.1

$$\begin{aligned} \beta = \beta_2 \beta_1 &= K_R\left(\frac{p_2}{p_1}\right) K_S\left(\frac{p_3}{p_2}\right) \\ &> K_S\left(\frac{p_2}{p_1}\right) K_S\left(\frac{p_3}{p_2}\right) \\ &> K_S\left(\frac{p_2}{p_1}\right) K_S\left(\frac{p_3}{p_1}\right) K_S\left(\frac{p_1}{p_2}\right) \\ &= K_S\left(\frac{p_3}{p_1}\right) = K_S(\alpha), \end{aligned}$$

and from Lemma 5.3.2 (a)

$$\begin{aligned} \beta K_S(\alpha) &= K_R\left(\frac{p_2}{p_1}\right) K_S\left(\frac{p_3}{p_2}\right) K_S\left(\frac{p_3}{p_1}\right) \\ &> K_R\left(\frac{p_2}{p_1}\right) K_R\left(\frac{p_1}{p_2}\right) = 1. \end{aligned}$$

Second we assume that  $\alpha = \frac{p_3}{p_1} < 1$ . To prove this proposition in this case, namely  $R_1 S_1 \rightarrow R'_1 S'_3$ , we show that the initial data (6.13) satisfies the statements of case 3 of the Riemann solutions. So we only have to check that

$$\beta > K_R(\alpha), \quad \beta K_S(\alpha) < 1. \quad (5.78)$$

Regarding  $p_2 < \min(p_1, p_3)$ ,  $p_1 > p_3$  we obtain from (5.76) and Lemma 5.2.3 (a)

$$\begin{aligned} \beta &= K_R\left(\frac{p_2}{p_1}\right) K_S\left(\frac{p_3}{p_2}\right) \\ &> K_R\left(\frac{p_2}{p_1}\right) K_R\left(\frac{p_3}{p_2}\right) \\ &= K_R\left(\frac{p_3}{p_1}\right) = K_R(\alpha), \end{aligned}$$

and from Lemma 5.2.3 (b) and Lemma 5.3.2 (b)

$$\begin{aligned} \beta K_S(\alpha) &= K_R\left(\frac{p_2}{p_1}\right) K_S\left(\frac{p_3}{p_2}\right) K_S\left(\frac{p_3}{p_1}\right) \\ &< K_R\left(\frac{p_2}{p_1}\right) K_R\left(\frac{p_1}{p_2}\right) K_R\left(\frac{p_1}{p_3}\right) K_R\left(\frac{p_3}{p_1}\right) = 1. \end{aligned}$$

## CHAPTER 5. THE INTERACTION OF WAVES FOR THE ULTRA-RELATIVISTIC EULER EQUATIONS

---

We prove part  $(d)_2$ . First, consider the interaction  $R_1 S_1 \rightarrow S'_1 S'_3$ . The first case in  $(d)_1$  gives the outgoing Riemann solution in region 2. Hence we use (3.76) and conclude that

$$p_2 < \min(p_1, p_3), \quad p_3 > p_1, \quad p_* > \max(p_1, p_3) \quad \text{and} \quad (5.79)$$

$$K_R \left( \frac{p_2}{p_1} \right) K_S \left( \frac{p_3}{p_2} \right) = K_S \left( \frac{p_*}{p_1} \right) K_S \left( \frac{p_*}{p_3} \right). \quad (5.80)$$

Using monotonicity of functions  $K_S, K_R$ , one can easily show

$$p_* < \frac{p_1 p_3}{p_2}. \quad (5.81)$$

Recall that  $Str(R_1) = \ln \frac{p_1}{p_2}$  along  $R_1$  and  $Str(S_1) = \ln \frac{p_3}{p_2}$  along  $S_1$ . Hence we have before interaction:

$$Str(R_1) + Str(S_1) = \ln \frac{p_1}{p_2} + \ln \frac{p_3}{p_2} = \ln \frac{p_1 p_3}{p_2^2}.$$

According to equation (5.21), we have after interaction:

$$Str(S'_1) + Str(S'_3) = \ln \frac{p_*}{p_1} + \ln \frac{p_*}{p_3} = \ln \frac{p_*^2}{p_1 p_3}.$$

Thus, to show that the strength is decreasing, using (5.81) we have

$$Str(S'_1) + Str(S'_3) = \ln \frac{p_*^2}{p_1 p_3} < \ln \frac{\left( \frac{p_1 p_3}{p_2} \right)^2}{p_1 p_3} = \ln \frac{p_1 p_3}{p_2^2} = Str(R_1) + Str(S_1).$$

Second, consider the interaction  $R_1 S_1 \rightarrow R'_1 S'_3$ . The second case in  $(d)_1$  gives the outgoing Riemann solution in region 3. Hence we use (3.78) and conclude that

$$p_2 < \min(p_1, p_3), \quad p_1 > p_3 \quad \text{and} \quad p_3 < p_* < p_1. \quad (5.82)$$

We have before interaction:

$$Str(R_1) + Str(S_1) = \ln \frac{p_1}{p_2} + \ln \frac{p_3}{p_2} = \ln \frac{p_1 p_3}{p_2^2}.$$

According to equation (5.22), we have after interaction:

$$Str(R'_1) + Str(S'_3) = \ln \frac{p_1}{p_*} + \ln \frac{p_*}{p_3} = \ln \frac{p_1}{p_3}.$$

Thus, to show that the strength is decreasing, using (5.82) we have

$$Str(R'_1) + Str(S'_3) = \ln \frac{p_1}{p_3} < \ln \frac{p_1 p_3}{p_2^2} = Str(R_1) + Str(S_1).$$

This completes the proof of the proposition. □



---

# Chapter 6

## The Front Tracking Scheme

### 6.1 Introduction

Let us consider a Cauchy problem associated with a strictly hyperbolic  $n \times n$  system of conservation laws

$$U_t + f(U)_x = 0, \quad (t, x) \in \mathbb{R} \times [0, \infty), \quad (6.1)$$

and initial data

$$U(0, x) = \bar{U}(x), \quad (6.2)$$

where the flux function  $f$  is smooth, defined on a neighborhood of the origin. Moreover, suppose that each characteristic field is either genuinely nonlinear or linearly degenerate. Given a function  $\bar{U}$  with sufficiently small total variation, one can prove the global existence of weak solutions. In 1965, Glimm proved existence of solutions to (6.1) [36]. Nowadays, one of the most largely used methods to find the same result is front tracking, presented in [14, 39], that consist in constructing a sequence of piecewise constant approximate solutions, a subsequence of which converges to a weak solution of the Cauchy problem (6.1) and (6.2).

The front tracking scheme is an effectual tool for resolving discontinuities in the solution of hyperbolic systems of conservation laws. The basic ideas concerned in the construction of piecewise constant approximate solutions, based on front tracking, were introduced in the papers of Dafermos [22] for scalar equations and DiPerna [25] for  $2 \times 2$  systems, then extended in [10, 12, 70] to general  $N \times N$  systems with genuinely nonlinear or linearly degenerate characteristic fields. In principle the method of front tracking is applicable whenever a solution of the Riemann problem is exist. The front tracking scheme has been used numerically to treat scalar equations and systems of hyperbolic conservations laws [20, 38, 71, 72, 82, 83]. Whereas as an analytical tool it has been used to analyze scalar equations and systems of hyperbolic conservation law in one and more spatial dimensions, see [10, 14, 15, 16, 17, 22, 65, 70].

The front tracking scheme was also studied by Alber [4, 5], Ancona et al. [6, 7, 8], Lin [54] and Wendroff [80], see also Baiti et al. [11], which address the case of a  $2 \times 2$  system

## CHAPTER 6. THE FRONT TRACKING SCHEME

---

arising in the study of granular flows.

The construction of the approximate solutions starts at initial time  $t = 0$  by taking a piecewise constant approximation  $\tilde{U}(x)$  of the initial data  $\bar{U}(x)$ . At each point of jump, we construct a piecewise constant approximate solution of the corresponding Riemann problem is chosen so that it coincides with the exact one if it contains only single shocks or contact discontinuities. Otherwise, if centered rarefaction waves are present, they are approximated by rarefaction fans containing several small jumps. Piecing together the solution of all the Riemann problems, we obtain an approximate solution of (6.1) and (6.2) defined until the first time  $t_1$  where the two lines of discontinuities interact. The approximate solution can be further prolonged in time by solving the new Riemann problem constructed by the interaction. This yields an approximate solution valid up to the next time  $t_2 > t_1$  where two more fronts interact. Once again we solve the corresponding Riemann problem, which extend the solution further in time, and so on.

For  $n \times n$  systems the difficulty arise, because the number of lines of discontinuity (fronts) may be infinite in finite time, in which case the construction would break down. This is due mostly to the fact that at each interaction point there are two incoming fronts, while the number of outgoing ones is  $n$  or even larger if rarefaction waves are involved. In [12, 13, 14] one defines the notion of generation order which tells how many interactions were needed to produce a wavefront. In order to get over this difficulty, one can follow the algorithms in [10, 13, 14, 70] are adopt two different procedures:

1. An accurate Riemann solution which introduces several new fronts and
2. a simplified Riemann solution, which involves at most two physical outgoing fronts and collect the remaining new waves, the so called non-physical front traveling with a speed strictly larger than all characteristic speeds.

In which these algorithms are used to prove the converge of a weak solution of (6.1) and (6.2) at least in the case of small total variation data. Thereafter these results were extended to systems of conservation laws in which the characteristic fields are neither genuinely nonlinear nor linearly degenerate, see [6, 8, 9].

Nevertheless, when we deal with a  $2 \times 2$  system it is possible to avoid non-physical fronts and always use an accurate solution to construct approximate solutions. This was initially proved for the front tracking introduced by DiPerna in [25], in the case of small total variation data. However his construction is quite tricky and less used than the one proposed by Bressan in [14] and refined in [10], a slight modification of which can avoid the introduction of non-physical fronts in the  $2 \times 2$  case, too. In few words, in the case of  $2 \times 2$  system, the only problem comes from the fact that rarefaction waves approximated by several fronts and this is the unique way the total number of waves could increase.

In this chapter we present a new front tracking scheme for the ultra-relativistic Euler equations. The basic ingredient for our new scheme is the front tracking Riemann solution. In this Riemann solution we approximate a continuous rarefaction waves by a

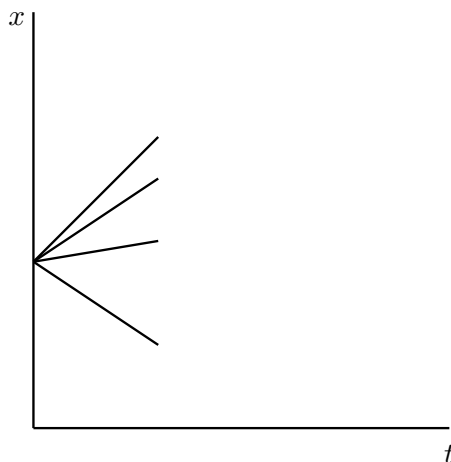


Figure 6.1: A local Riemann solution.

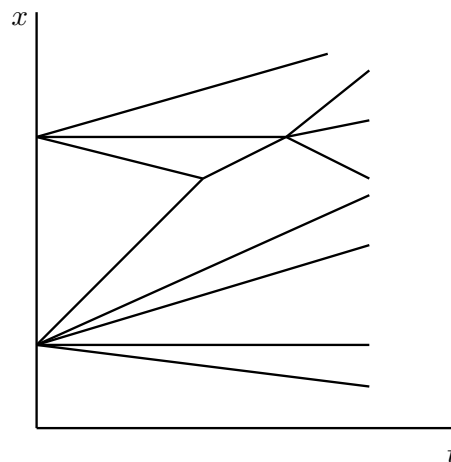


Figure 6.2: Front interactions.

finite collection of discontinuities, so called non-entropy shocks (fronts). So the scheme is based on approximations to the solutions of the local Riemann problems, where the solution is represented by constant states separated by straight line shock segments. The solution procedure for an initial value problem takes care for the interaction of these shock segments of the neighboring local Riemann problems. At each intersection point the discontinuous solution is again equal to the initial conditions of a new local Riemann problem. The straight line shocks can again intersect with each other and so on, see Figures 6.1, 6.2.

A continuous rarefaction wave is approximated by a collection of non-entropy shocks, called fronts, see Figures 6.4 and 6.5. In fact, we introduce a parameter  $\varepsilon$ , which describes the strength of each non-entropy shock. The number of fronts that discretize a rarefaction wave depends on the strength of the non-entropy shocks, and we try to keep the strength of them less than  $\varepsilon$ , i.e. as small as possible, but all of them with the same strength for the approximation of a single rarefaction fan.

In this chapter, the front tracking method is considered as a numerical tool to solve the initial value problem for the ultra-relativistic Euler equations. In fact this method will also serve as an analytical tool as we will see in the next chapter.

This chapter is organized as follows. In Section 6.2 we present the fundamental concepts and notions for our front tracking scheme for the ultra-relativistic Euler equations (3.1), namely the parametrizations of single non-entropy shocks (fronts) and the discretization of rarefaction waves. In Subsection 6.2.3 we give the front tracking Riemann solution, which consider the heart for our new scheme. In Section 6.3 we present numerical test cases for the solution of the ultra-relativistic Euler equations. For the comparison we use exact Riemann solution, cone-grid and front tracking schemes. We also calculate the experimental order of convergence and numerical  $L^1$ -stability of these schemes.

## 6.2 Front tracking scheme

In this section we introduce our new front tracking technique for the ultra-relativistic Euler equations (3.3) in one space dimension. Most standard front tracking methods [10, 12, 13] allow some non-physical waves, i.e. the Rankine-Hugoniot conditions are not satisfied in general. In contrast, our new front tracking technique for the ultra-relativistic Euler equations gives only exact weak solutions.

### 6.2.1 Single non-entropy shocks

We give the parametrizations for the non-entropy shocks, which we need for the formulation of the discretization of rarefaction waves. We obtain these parametrizations by solving the Rankine-Hugoniot jump conditions (3.33). In Subsection 3.3.1 we have only give the parametrizations for the entropy shocks, namely equations (3.38)-(3.41) and Lemmas 3.3.5 and 3.3.6. We formulate analogously parametrizations for non-entropy shocks. Note that the non-entropy 1 and 3 shocks, which we denote by  $ne_1$  and  $ne_3$ , respectively, violate the entropy condition. This means that these non-entropy shocks satisfy  $u_- < u_+$ . First we give the definition of the non-entropy shocks, which is similar to the Definition 3.3.1 of entropy shocks in Subsection 3.3.1, but violate the entropy condition. Second we give the parametrizations for the non-entropy shocks.

**Definition 6.2.1.** *Given are two states  $(p_{\pm}, u_{\pm}, n_{\pm}) \in \mathbb{R}^+ \times \mathbb{R} \times \mathbb{R}^+$ . Assume that the Rankine-Hugoniot jump conditions (3.33) are satisfied.*

1. *Assume that  $0 < p_+ < p_-$ . If in addition  $u_- < u_+$ , then we say that the left state  $(p_-, u_-, n_-)$  can be connected with the right state  $(p_+, u_+, n_+)$  by a single non-entropy 1-shock ( $ne_1$  shock).*
2. *Assume that  $0 < p_- < p_+$ . If in addition  $u_- < u_+$ , then we say that the left state  $(p_-, u_-, n_-)$  can be connected with the right state  $(p_+, u_+, n_+)$  by a single non-entropy 3-shock ( $ne_3$  shock).*

**Remark 6.2.2.** *Since  $u_- > u_+$  is the entropy condition, we see that  $ne_1$  and  $ne_3$  shocks violate this entropy condition.*

Now we give parameter representation for single non-entropy shocks. In the following lemma, we give a characterization for the case that the left state  $(p_-, u_-, n_-)$  can be connected with the right state  $(p_+, u_+, n_+)$  by a single  $ne_1$  shock or a single  $ne_3$  shock, respectively. The proof of the following lemma follows in the same way as the parametrization of entropy shocks given in Lemma 3.3.6.

**Lemma 6.2.3.** *Given are  $(p_{\pm}, u_{\pm}, n_{\pm}) \in \mathbb{R}^+ \times \mathbb{R} \times \mathbb{R}^+$ . Put  $\alpha := \frac{p_{\pm}}{p_-}$ ,  $\beta := \frac{\sqrt{1+u_+^2}-u_+}{\sqrt{1+u_-^2}-u_-}$*

*and  $\sigma := \sqrt{\frac{1-s}{1+s}}$ . Define  $u: \mathbb{R}^+ \rightarrow \mathbb{R}$  by  $u(w) = \frac{1}{2}(\frac{1}{w} - w)$ .*

(a) Assume that  $0 < p_+ < p_-$ , i.e.  $\alpha < 1$  and put  $p_* := p_+$  in (3.39). Then the following three conditions are equivalent:

1. The parametrizations given in equations (3.38)-(3.41) with the lower negative sign in (3.38) and (3.40).

2.

$$\beta = K_S(\alpha) \text{ and } n_{\pm} = n(p_{\pm}). \quad (6.3)$$

3. Using the abbreviations

$$w_- := \frac{\sigma}{L_s(\alpha)}, \quad w_+ := \frac{\sigma}{L_s(\frac{1}{\alpha})} \quad (6.4)$$

the conditions  $u_{\pm} = u(w_{\pm})$  and  $n_{\pm} = n(p_{\pm})$ .

Moreover, if these conditions are satisfied, then the lower state  $(p_-, u_-, n_-)$  can be connected with the upper state  $(p_+, u_+, n_+)$  by a single  $ne_1$ -shock.

(b) Assume that  $0 < p_- < p_+$ , i.e.  $\alpha > 1$  and put  $p_* := p_-$  in (3.39). Then the following three conditions are equivalent:

1. The parametrizations given in equations (3.38)-(3.41) with the upper positive sign in (3.38) and (3.40).

2.

$$\beta K_S(\alpha) = 1 \text{ and } n_{\pm} = n(p_{\pm}). \quad (6.5)$$

3. Using the abbreviations

$$w_- := \sigma \cdot L_s(\alpha), \quad w_+ := \sigma \cdot L_s\left(\frac{1}{\alpha}\right) \quad (6.6)$$

the conditions  $u_{\pm} = u(w_{\pm})$  and  $n_{\pm} = n(p_{\pm})$ .

Moreover, if these conditions are satisfied, then lower state  $(p_-, u_-, n_-)$  can be connected with the upper state  $(p_+, u_+, n_+)$  by a single  $ne_3$ -shock.

**Definition 6.2.4.**

- A  $g_1$ -shock is either a 1-shock or a  $ne_1$ -shock. We call it a generalized 1-shock.
- A  $g_3$ -shock is either a 3-shock or a  $ne_3$ -shock. We call it a generalized 3-shock.

**Lemma 6.2.5. Parametrizations of special non-entropy single shocks**

Given are the three states  $(p_j, u_j, n_j) \in \mathbb{R}^+ \times \mathbb{R} \times \mathbb{R}^+$ ,  $j = 1, 2, 3$ . For single non-entropy shocks with velocity zero on one side there hold the following equalities and inequalities given in Figure 6.3, where  $s_1, s_3$  are the velocities of the lower non-entropy 1 and 3-shocks, respectively, and  $\tilde{s}_1, \tilde{s}_3$  are the velocities of the upper non-entropy 1 and 3-shocks, respectively.

*Proof.* This lemma follows directly from the single non-entropy shock parametrizations given in Lemma 6.2.3. □

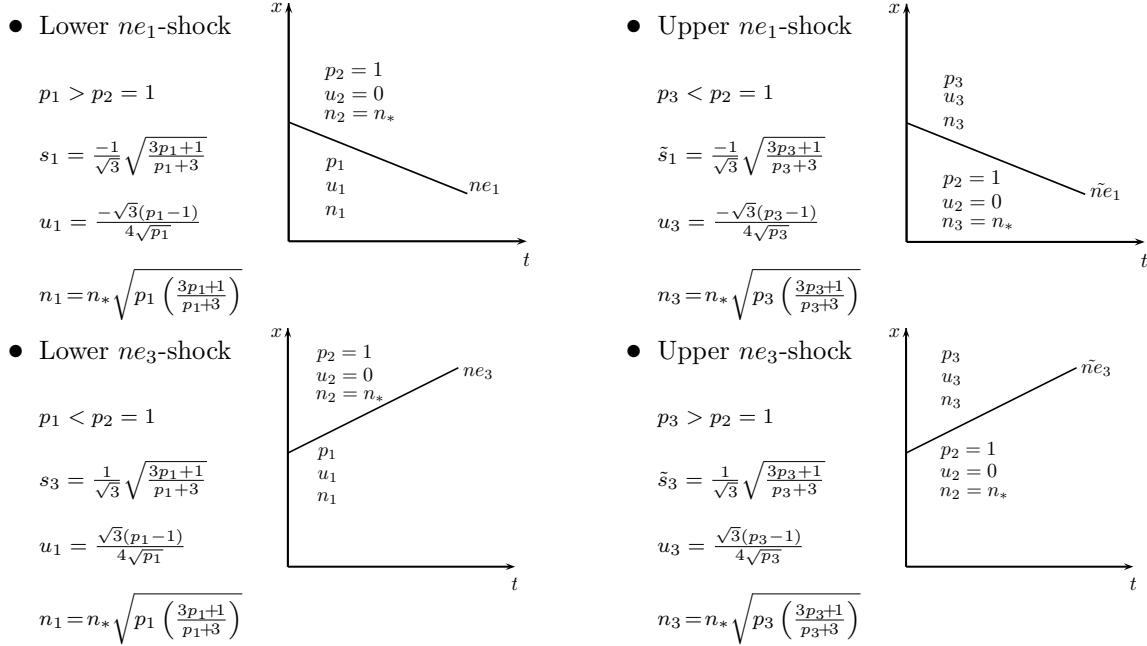


Figure 6.3: Classification of non-entropy shocks.

## 6.2.2 The discretization of rarefaction waves

In this section we give the front tracking discretization for 1 and 3-rarefaction waves. The discretization of a single rarefaction fan into a collection of finitely many non-entropy shocks with the same small strength, see Figures 6.4 and 6.5, is a basic building block for the front tracking Riemann solution presented in Subsection 6.2. Our discretization of rarefaction waves is restricted for the  $(p, u)$  system given in (3.6).

The following two lemmas enable the discretization of single 1- and 3-rarefaction waves, respectively. The following function  $\beta: \mathbb{R} \times \mathbb{R} \mapsto \mathbb{R}^+$  turns out to be very useful in order to perform these two lemmas in a completely unified way

$$\beta(u, v) := \frac{\sqrt{1+u^2} - u}{\sqrt{1+v^2} - v}.$$

### Lemma 6.2.6. Finite collection of non-entropy 1-shocks

Given are  $\tilde{p}_* > 0$ ,  $(p_-, u_-) \in \mathbb{R}^+ \times \mathbb{R}$  and  $N \in \mathbb{N}$ . Put  $\alpha := \frac{\tilde{p}_*}{p_-}$ ,  $\beta := K_S(\alpha^{\frac{1}{N}})^N$  and assume that  $\alpha < 1$ . Define the intermediate states  $\underline{U}_k := (p_k, u_k)$  for the indices  $k = 0, 1, \dots, N$  by

$$p_k := p_- \alpha^{\frac{k}{N}}, \quad u_k := \frac{1 - K_S(\alpha^{\frac{1}{N}})^{2k} \left( \sqrt{1+u_-^2} - u_- \right)^2}{2K_S(\alpha^{\frac{1}{N}})^k \left( \sqrt{1+u_-^2} - u_- \right)}. \quad (6.7)$$

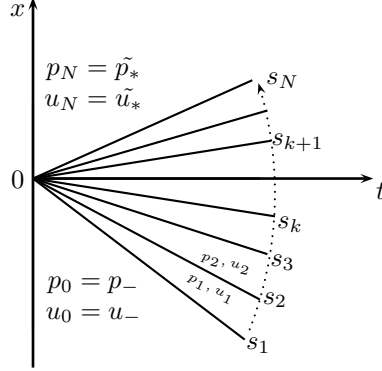


Figure 6.4: Discretization of 1-fan for non-entropy 1-shocks.

Then the initial data  $\underline{U}_0 = (p_-, u_-)$  and  $\underline{U}_N = (\tilde{p}_*, \tilde{u}_*)$  can be connected by a collection of  $N$  non-entropy 1-shocks with slopes  $s_1 < s_2 < \dots < s_N$ , such that each non-entropy shock with slope  $s_k$  connects the lower state  $\underline{U}_{k-1}$  with the upper state  $\underline{U}_k$  for  $k=1, 2, \dots, N$  due to the Rankine-Hugoniot jump conditions, see Figure 6.4.

*Proof.* We define the quantities  $w_k := \sqrt{1 + u_k^2} - u_k$  for  $k = 0, 1, \dots, N$ . Then, using (6.7) we have

$$w_k = w_0 K_S(\alpha^{\frac{1}{N}})^k. \quad (6.8)$$

Hence we have  $\beta(u_k, u_{k-1}) = \frac{w_k}{w_{k-1}} = K_S(\alpha^{\frac{1}{N}})$  for  $k = 1, \dots, N$ . From this relation, from  $\alpha < 1$  and part (a) of Lemma 6.2.3 we conclude that the lower state  $\underline{U}_{k-1}$  can be connected with the upper state  $\underline{U}_k$  by a non-entropy 1-shock with slope  $s_k$  for  $k = 1, \dots, N$ . Note that  $w_{k-1} > w_k$  and hence  $u_k > u_{k-1}$ , i.e. we have indeed  $N$  non-entropy 1-shocks. Define  $\sigma_k := \sqrt{\frac{1-s_k}{1+s_k}}$ . According to the parametrization of single  $ne_1$ -shocks (6.4) and (3.45) we have

$$w_k = \frac{\sigma_k}{L_S\left(\frac{1}{\alpha^{\frac{1}{N}}}\right)} = \frac{\sigma_{k+1}}{L_S(\alpha^{\frac{1}{N}})} \quad \text{implies} \quad \sigma_{k+1} = \sigma_k K_S(\alpha^{\frac{1}{N}}), \quad k = 1, 2, \dots, N-1. \quad (6.9)$$

According to (6.9) with  $\alpha < 1$  we have that the velocities of non-entropy 1-shocks satisfy the correct monotonicity conditions, namely

$$\sigma_1 > \sigma_2 > \dots > \sigma_N \quad \text{as well as} \quad s_1 < s_2 < \dots < s_N.$$

Hence the statement of the lemma follows.  $\square$

**Lemma 6.2.7. Finite collection of non-entropy 3-shocks**

Given are  $\tilde{p}_* > 0$ ,  $(p_+, u_+) \in \mathbb{R}^+ \times \mathbb{R}$  and  $M \in \mathbb{N}$ . Put  $\alpha := \frac{p_+}{\tilde{p}_*}$ ,  $\beta := K_S(\alpha^{\frac{1}{M}})^{-M}$  and assume that  $\alpha > 1$ . Define the intermediate states  $\underline{U}_k := (p_k, u_k)$  for the indices  $k = 0, 1, \dots, M$  by

$$p_k =: p_+ \left(\frac{1}{\alpha}\right)^{\frac{k}{M}}, \quad u_k := \frac{1 - K_S(\alpha^{\frac{1}{M}})^{2k} \left(\sqrt{1 + u_+^2} - u_+\right)^2}{2K_S(\alpha^{\frac{1}{M}})^k \left(\sqrt{1 + u_+^2} - u_+\right)}. \quad (6.10)$$

## CHAPTER 6. THE FRONT TRACKING SCHEME

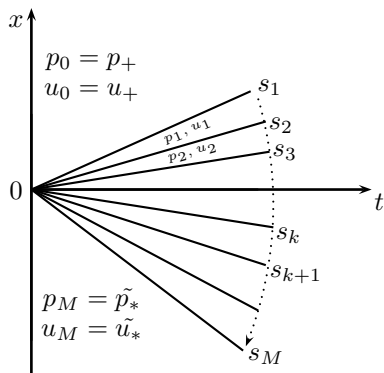


Figure 6.5: Discretization of 3-fan for non-entropy 3-shocks.

Then the initial data  $\underline{U}_0 = (p_+, u_+)$  and  $\underline{U}_M = (\tilde{p}_*, \tilde{u}_*)$  can be connected by a collection of  $M$  non-entropy 3-shocks with slopes  $s_1 > s_2 > \dots > s_M$ , such that each non-entropy shock with slope  $s_k$  connects the lower state  $\underline{U}_k$  with the upper state  $\underline{U}_{k-1}$  for  $k = 1, 2, \dots, M$  due to the Rankine-Hugoniot jump conditions, see Figure 6.5.

*Proof.* We define the quantities  $w_k := \sqrt{1 + u_k^2} - u_k$  for  $k = 0, 1, \dots, M$ . Then, using (6.10) we have

$$w_k = w_0 K_S(\alpha^{\frac{1}{M}})^k. \quad (6.11)$$

Hence we have  $\beta(u_{k-1}, u_k) = \frac{w_{k-1}}{w_k} = \frac{1}{K_S(\alpha^{\frac{1}{M}})}$  for  $k = 1, \dots, M$ . From this relation, from  $\alpha > 1$  and part (b) of Lemma 6.2.3 we conclude that the lower state  $\underline{U}_k$  can be connected with the upper state  $\underline{U}_{k-1}$  by a non-entropy 3-shock with slope  $s_k$  for  $k = 1, \dots, M$ . Note that  $w_k > w_{k-1}$  and hence  $u_{k-1} > u_k$ , i.e. we have indeed  $M$  non-entropy 3-shocks. According to the parametrization of single  $ne_3$ -shocks (6.6) and (3.45) we have

$$w_k = \sigma_k L_S(\alpha^{\frac{1}{M}}) = \sigma_{k+1} L_S\left(\frac{1}{\alpha^{\frac{1}{M}}}\right) \quad \text{implies} \quad \sigma_{k+1} = \sigma_k K_S(\alpha^{\frac{1}{M}}), \quad k = 1, 2, \dots, M-1. \quad (6.12)$$

According to (6.12) with  $\alpha > 1$  we have that the velocities of non-entropy 3-shocks satisfy the correct monotonicity conditions, namely

$$\sigma_1 < \sigma_2 < \dots < \sigma_M \quad \text{as well as} \quad s_1 > s_2 > \dots > s_M.$$

Hence the statement of the lemma follows.  $\square$

Straight calculations show the following result.

**Lemma 6.2.8.** *For all  $n \in \mathbb{N}$  and  $\alpha > 0$  we have*

$$\lim_{n \rightarrow \infty} K_S(\alpha^{\frac{1}{n}})^n = K_R(\alpha).$$



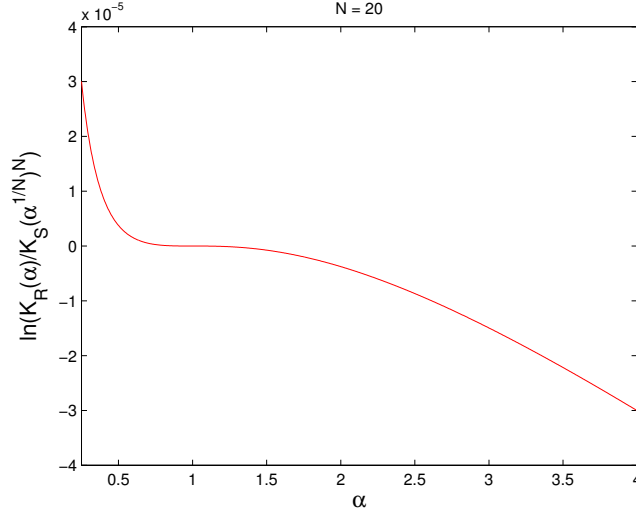


Figure 6.6: The difference between  $K_R(\alpha)$  and  $\left(K_S(\alpha^{\frac{1}{N}})\right)^N$ ,  $N = 20$ .

**Remark 6.2.9.** For the approximation of single 1-fans and single 3-fans by a collection of non-entropy shocks we subsequently replace  $K_R(\alpha)$  by  $K_S(\alpha^{\frac{1}{N}})^N$  and  $K_S(\alpha^{\frac{1}{M}})^M$ , respectively. In Figure 6.6 we see good coincidence between these two functions even for  $N = 20$ .

According to Lemma 6.2.8 we have that the discretized 1 and 3-rarefaction waves in Lemmas 6.2.6 and 6.2.7 tend to the 1 and 3-rarefaction waves described in Lemma 3.3.7.

### 6.2.3 Front tracking Riemann solution

In general the exact solution of (3.6) for given Riemannian initial data

$$p_0(x) = \begin{cases} p_-, & x \leq 0 \\ p_+, & x > 0 \end{cases}, \quad u_0(x) = \begin{cases} u_-, & x \leq 0 \\ u_+, & x > 0 \end{cases} \quad (6.13)$$

is not piecewise constant because of the presence of centered rarefaction waves. In the front tracking Riemann solution we approximate a continuous rarefaction wave according to Subsection 6.2.2 by a finite collection of non-entropy shocks. For more simplicity, we restrict the study of the front tracking Riemann solution to the  $(p, u)$  subsystem given in (3.6). However, it is not difficult to extend this solution to the full system (3.1) including the decoupled equation for the particle density  $n$  by using (3.39), which we will use for the numerical simulations in Section 6.3.

In [3, Section 3] we have formulated the Riemann solution for the subsystem (3.6) with initial data (6.13) in such a way that we can use it directly for the construction of the corresponding front tracking Riemann solution by using Lemmas 6.2.6 and 6.2.7. For this purpose we study the cases which contain continuous rarefaction waves. For each case we employ monotonicity arguments as well as the Intermediate Value Theorem in order to

## CHAPTER 6. THE FRONT TRACKING SCHEME

---

construct an intermediate state  $(\tilde{p}_*, \tilde{u}_*)$  in the so called “tilde-star-region”, which can be connected with a single shock or non-entropy shocks to the prescribed lower and upper Riemannian initial data. In view of Remark 6.2.9 the structure of the front tracking Riemann solution is quite similar to the exact Riemann solution.

**Lemma 6.2.10.** *For all  $n \in \mathbb{N}$  we have*

$K_S(\alpha^{\frac{1}{n}})^n > K_R(\alpha)$  for  $\alpha > 1$  as well as  $K_S(\alpha^{\frac{1}{n}})^n < K_R(\alpha)$  for  $\alpha < 1$ , otherwise equality for  $\alpha = 1$ .

*Proof.* See Lemma 5.2.3. □

In the following we use equation (3.43) and the exact Riemann solution given in Section 3.4, namely by  $p_*$  we denote the intermediate pressure in the star-region of this Riemann solution. For the construction of the corresponding front tracking Riemann solution we prescribe a sufficiently small parameter  $\varepsilon > 0$ , which controls the strength of each non-entropy shock. The approximate Riemann solution then depends on  $\varepsilon$ , and in the limit  $\varepsilon \downarrow 0$  it gives again the exact Riemann solution.

**Case 1:**  $\beta < K_S(\alpha)$  and  $\beta K_R(\alpha) > 1$ . We define

$$M := \left\lfloor \frac{1}{\varepsilon} \left| \ln \frac{p_+}{p_*} \right| \right\rfloor + 1, \quad (6.14)$$

where  $\lfloor x \rfloor$  is the largest integer smaller than or equal  $x$  and the parameter  $\varepsilon > 0$  introduced above. Using Lemma 6.2.10 with  $\alpha > 1$  we have

$$1 < \beta K_R(\alpha) < \beta K_S(\alpha^{\frac{1}{M}})^M < K_S(\alpha) K_S(\alpha^{\frac{1}{M}})^M. \quad (6.15)$$

We will show that the solution is composed on a single lower 1-shock and  $M$  upper  $ne_3$  shocks, where the intermediate pressure and velocity are determined by the implicit equations

$$K_S\left(\frac{\tilde{p}_*}{p_-}\right) K_S\left(\left(\frac{\tilde{p}_*}{p_+}\right)^{\frac{1}{M}}\right)^M = \beta, \quad \frac{\sqrt{1 + \tilde{u}_*^2} - \tilde{u}_*}{\sqrt{1 + u_-^2} - u_-} = K_S\left(\frac{\tilde{p}_*}{p_-}\right). \quad (6.16)$$

Since  $K_S\left(\frac{\tilde{p}_*}{p_-}\right) K_S\left(\left(\frac{\tilde{p}_*}{p_+}\right)^{\frac{1}{M}}\right)^M$  is strictly monotonically increasing in  $\tilde{p}_*$  with

$$\lim_{\tilde{p}_* \rightarrow 0} K_S\left(\frac{\tilde{p}_*}{p_-}\right) K_S\left(\left(\frac{\tilde{p}_*}{p_+}\right)^{\frac{1}{M}}\right)^M = 0, \quad \lim_{\tilde{p}_* \rightarrow \infty} K_S\left(\frac{\tilde{p}_*}{p_-}\right) K_S\left(\left(\frac{\tilde{p}_*}{p_+}\right)^{\frac{1}{M}}\right)^M = \infty,$$

we conclude that the implicit equation for  $\tilde{p}_* > 0$  and hence for  $\tilde{u}_*$  has a unique solution. Using (6.15) and

$$K_S\left(\frac{p_-}{p_-}\right) K_S\left(\left(\frac{p_-}{p_+}\right)^{\frac{1}{M}}\right)^M = \frac{1}{K_S(\alpha^{\frac{1}{M}})^M} < \beta, \quad K_S\left(\frac{p_+}{p_-}\right) K_S\left(\left(\frac{p_+}{p_+}\right)^{\frac{1}{M}}\right)^M = K_S(\alpha) > \beta,$$

## 6.2. FRONT TRACKING SCHEME

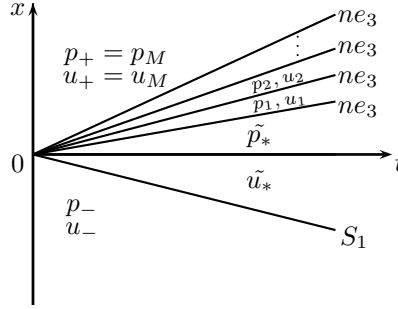


Figure 6.7: The wave family types of the front tracking Riemann solution in case 1.

we obtain from the Intermediate Value Theorem that  $p_- < \tilde{p}_* < p_+$ . This implies  $K_S\left(\frac{\tilde{p}_*}{p_-}\right) > 1$  and  $K_S\left(\frac{\tilde{p}_*}{p_+}\right) < 1$ . From the last two inequalities and (6.16) we obtain  $\tilde{u}_* < \min(u_-, u_+)$ .

We summarize these inequalities for the first case:

$$\alpha > 1, \quad p_- < \tilde{p}_* < p_+ \quad \text{and} \quad \tilde{u}_* < \min(u_-, u_+). \quad (6.17)$$

From (6.16), (6.17) and Lemmas 3.3.5, 6.2.7, respectively, we conclude that the states  $(p_-, u_-)$  and  $(\tilde{p}_*, \tilde{u}_*)$  can be connected by a 1-shock and the states  $(\tilde{p}_*, \tilde{u}_*)$  and  $(p_+, u_+)$  can be connected by  $M$  non-entropy 3-shocks.

In order to guarantee that the 1-shock with velocity  $v_s$  and the non-entropy 3-shocks fit together to a complete front tracking Riemann solution of (3.6) and (6.13), we only have to check that

$$v_s < s_M.$$

This inequality is valid in the special case  $\tilde{p}_* = 1$  and  $\tilde{u}_* = 0$  with velocity  $v_s = \frac{-1}{\sqrt{3}} \sqrt{\frac{1+3p_-}{3+p_-}} < 0$  and the velocity  $s_M = \frac{1}{\sqrt{3}} \sqrt{\frac{1+3p_{M-1}}{3+p_{M-1}}} > 0$ ,  $s_M$  is the slope of the lowest non-entropy 3-shock, see Figure 6.7 and hence valid in the general case, because any ordering of propagation velocities is invariant with respect to proper Lorentz-transformation (3.22).

**Case 2:**  $\beta > K_S(\alpha)$  and  $\beta K_S(\alpha) > 1$ .

Here the solution is composed on a lower 1-shock and an upper 3-shock. In this case we have no rarefaction wave, so  $\tilde{p}_* = p_*$  and  $\tilde{u}_* = u_*$ . Hence we obtain the exact Riemann solution with two entropy shocks in case 2. Note that on the boundary curves separating case 1 and case 2 and separating case 3 and case 2, respectively, we obtain a single entropy shock solution, which is also a front tracking Riemann solution.

**Case 3:**  $\beta > K_R(\alpha)$  and  $\beta K_S(\alpha) < 1$ . We define

$$N := \left\lfloor \frac{1}{\varepsilon} \left| \ln \frac{p_*}{p_-} \right| \right\rfloor + 1. \quad (6.18)$$

## CHAPTER 6. THE FRONT TRACKING SCHEME

---

We can show that the solution is composed on  $N$  lower  $ne_1$  shocks and a single upper 3-shock, where the intermediate pressure and velocity are determined by the implicit equations

$$K_S \left( \left( \frac{\tilde{p}_*}{p_-} \right)^{\frac{1}{N}} \right)^N K_S \left( \frac{\tilde{p}_*}{p_+} \right) = \beta, \quad \frac{\sqrt{1 + \tilde{u}_*^2} - \tilde{u}_*}{\sqrt{1 + u_-^2} - u_-} = K_S \left( \left( \frac{\tilde{p}_*}{p_-} \right)^{\frac{1}{N}} \right)^N. \quad (6.19)$$

Again the implicit equations have a unique solution for  $\tilde{p}_*$  and  $\tilde{u}_*$  and similar to the first case we obtain in the third case the inequalities

$$\alpha < 1, \quad p_- > \tilde{p}_* > p_+ \quad \text{and} \quad \tilde{u}_* > \max(u_-, u_+). \quad (6.20)$$

From (6.19), (6.20) and Lemmas 3.3.5, 6.2.6 we conclude that the states  $(p_-, u_-)$  and  $(\tilde{p}_*, \tilde{u}_*)$  can be connected by  $N$  non-entropy 1-shocks and the states  $(\tilde{p}_*, \tilde{u}_*)$  and  $(p_+, u_+)$  can be connected by a 3-shock. They form a complete front tracking Riemann solution because in the special case  $\tilde{p}_* = 1$  and  $\tilde{u}_* = 0$  the slope of the uppermost non-entropy 1-shock,  $s_N = \frac{-1}{\sqrt{3}} \sqrt{\frac{1 + 3p_{N-1}}{3 + p_{N-1}}}$  is negative, whereas the velocity of the upper 3-shock is positive.

**Case 4:**  $\beta < K_R(\alpha)$  and  $\beta K_R(\alpha) < 1$ .

We define the numbers  $N$  and  $M$  of fronts which discretize a lower 1-fan and upper 3-fan as in (6.18) and (6.14), respectively. We distinguish two further cases:

- If  $\alpha \leq 1$ , then we can assume the further condition that the number  $N$  is large enough such that

$$\beta < K_S(\alpha^{\frac{1}{N}})^N. \quad (6.21)$$

If this condition is not satisfied, then we either have  $\beta = K_S(\alpha^{\frac{1}{N}})^N$  and obtain a finite collection of non-entropy 1-shocks according to Lemma 6.2.6 or we have  $\beta > K_S(\alpha^{\frac{1}{N}})^N$ , in which case we proceed the construction of the front tracking Riemann solution exactly in the same way like in case 3.

- If  $\alpha > 1$ , then we can assume the further condition that the number  $M$  is large enough such that

$$\beta K_S(\alpha^{\frac{1}{M}})^M < 1. \quad (6.22)$$

If this condition is not satisfied, then we either have  $\beta K_S(\alpha^{\frac{1}{M}})^M = 1$  and obtain a finite collection of non-entropy 3-shocks according to Lemma 6.2.7 or we have  $\beta K_S(\alpha^{\frac{1}{M}})^M > 1$ , in which case we proceed the construction of the front tracking Riemann solution exactly in the same way like in case 1.

Using (6.21) for  $\alpha \leq 1$  and (6.22) for  $\alpha > 1$ , respectively, we can show that the front tracking solution is composed on  $N$  lower  $ne_1$  shocks and  $M$  upper  $ne_3$  shocks. For this purpose we define the intermediate pressure and velocity by the implicit equations

$$K_S \left( \left( \frac{\tilde{p}_*}{p_-} \right)^{\frac{1}{N}} \right)^N K_S \left( \left( \frac{\tilde{p}_*}{p_+} \right)^{\frac{1}{M}} \right)^M = \beta, \quad \frac{\sqrt{1 + \tilde{u}_*^2} - \tilde{u}_*}{\sqrt{1 + u_-^2} - u_-} = K_S \left( \left( \frac{\tilde{p}_*}{p_-} \right)^{\frac{1}{N}} \right)^N. \quad (6.23)$$

From  $\beta < K_S \left( \alpha^{\frac{1}{M}} \right)^M$  and  $\beta < \frac{1}{K_S \left( \alpha^{\frac{1}{M}} \right)^M} = K_S \left( \left( \frac{1}{\alpha} \right)^{\frac{1}{M}} \right)^M$  we conclude that  $\beta < 1$ , because one of the two numbers  $\alpha$  or  $\frac{1}{\alpha}$  is less than 1. Similar to the second case we obtain in the last case the inequalities

$$\beta < 1, \quad \tilde{p}_* < \min(p_-, p_+) \quad \text{and} \quad u_- < \tilde{u}_* < u_+. \quad (6.24)$$

From (6.23), (6.24) and Lemmas 6.2.6, 6.2.7 we conclude that the states  $(p_-, u_-)$  and  $(\tilde{p}_*, \tilde{u}_*)$  can be connected by  $N$  non-entropy 1-shocks and the states  $(\tilde{p}_*, \tilde{u}_*)$  and  $(p_+, u_+)$  can be connected by  $M$  non-entropy 3-shocks. They form a complete front tracking Riemann solution because in the special case  $\tilde{p}_* = 1$  and  $\tilde{u}_* = 0$  the slope of the uppermost non-entropy 1-shock is negative, whereas the velocity of the lowest non-entropy 3-shock is positive.

This completes the construction of the front tracking Riemann solution.

## 6.3 Numerical results

In this section we present numerical test cases for the solution of the ultra-relativistic Euler equations. For the comparison we use exact Riemann solution, cone-grid and front tracking schemes. The CFL condition in the ultra-relativistic case is very simple which is  $\Delta t = \frac{\Delta x}{2}$ . This CFL condition comes out automatically due to the structure of light cones, since every signal speed is bounded by the velocity of light, which is normalized to one in dimensionless form. In the following computations we have used the above CFL condition for the cone grid and front tracking schemes.

**Example 6.3.1.** *A numerical example for the Riemann solution.*

*We solve the weak form of the one-dimensional system of the ultra Euler equations*

$$\begin{aligned} (p(3 + 4u^2))_t + (4pu\sqrt{1 + u^2})_x &= 0, \\ (4pu\sqrt{1 + u^2})_t + (p(1 + 4u^2))_x &= 0, \\ (n\sqrt{1 + u^2})_t + (nu)_x &= 0, \end{aligned} \quad (6.25)$$

## CHAPTER 6. THE FRONT TRACKING SCHEME

---

for given Riemannian initial data at  $t=0$ , namely

$$p_0(x) = \begin{cases} 1, & x \leq 0 \\ 4, & x > 0 \end{cases}, \quad u_0(x) \equiv 0, \quad n_0(x) = \begin{cases} 3, & x \leq 0 \\ 1, & x > 0 \end{cases}. \quad (6.26)$$

We use the notation of Section 3.4 and obtain first that

$$\alpha = \frac{p_+}{p_-} = 4, \quad \beta = \frac{\sqrt{1+u_+^2} - u_+}{\sqrt{1+u_-^2} - u_-} = 1. \quad (6.27)$$

There holds  $\beta < K_S(\alpha)$  and  $\beta K_R(\alpha) > 1$  due to Case 1 for the classification of the Riemann solution, i.e. we have a lower 1-shock and an upper 3-fan. For the intermediate “star region” we obtain approximately the values

$$p_* = 1.99667361, \quad u_* = -0.30542181.$$

We define approximately the slopes

$$s_1 = -0.68287013, \quad s_2 = -0.29210155, \quad s_3 = 0.34311297, \quad s_4 = 0.57735026$$

and the constant

$$\delta_1 = 0.87424236, \quad \delta_2 = 0.31965308, \quad n_1 = 5.01387542, \quad n_2 = 0.59386169.$$

The slope  $s_1$  is the slope of the lower 1-shock,  $s_2$  is the slope of the contact discontinuity and the slopes  $s_3, s_4$  are the bounds for the upper 3-rarefaction fan. Then the Riemann solution at time  $t = 1$  is given by

$$p(1, x) = \begin{cases} 1, & x \leq s_1, \\ p_*, & s_1 < x \leq s_3, \\ \delta_1 \left( \frac{1+x}{1-x} \right)^{\frac{2}{\sqrt{3}}}, & s_3 < x \leq s_4, \\ 4, & x > s_4, \end{cases}$$

$$u(1, x) = \begin{cases} 0, & x \leq s_1, \\ u_*, & s_1 < x \leq s_3, \\ \sqrt{\frac{3}{2}} \frac{x - \frac{1}{\sqrt{3}}}{\sqrt{1-x^2}}, & s_3 < x \leq s_4, \\ 0, & x > s_4, \end{cases}$$

$$n(1, x) = \begin{cases} 3, & x \leq s_1, \\ n_1, & s_1 < x \leq s_2, \\ n_2, & s_2 < x \leq s_3, \\ \delta_2 \left( \frac{1+x}{1-x} \right)^{\frac{\sqrt{3}}{2}}, & s_3 < x \leq s_4, \\ 1, & x > s_4. \end{cases}$$

### 6.3. NUMERICAL RESULTS

Recall that we have constructed the front tracking Riemann solutions only for the  $(p, u)$ -subsystem in Subsection 6.2.3. Each such solution can be extended easily to the corresponding solution of the full system (3.1) using the parametrization of contact discontinuities in (3.42) as well as the parametrizations of single 1- and 3- shocks in Lemma 3.3.6 and of single non-entropy 1- and 3- shocks in Lemma 6.2.3, respectively.

The resulting front tracking Riemann solution for the complete initial data in this example is depicted in Figures 6.8 and A.0.1. In Figure A.0.1 we compare the cone-grid solution at time  $t = 1$  using a grid with  $Nt = 200$  time steps with the front tracking solution and the exact solution. Note that for the cone-grid scheme the resolution of the contact discontinuity is much worse than the resolution of corresponding lower 1-shock, whereas the front tracking scheme nearly coincides with the exact solution.

Due to the front tracking Riemann scheme, taking  $\varepsilon = 0.02$ , the strength of each non-entropy 3-shock. We find the number of fronts that discretize 3-fan  $M = 35$ . Also, due to the case 1 for the classification of the front tracking Riemann solution given in Subsection 6.2.3, i.e. we have a lower 1-shock and  $M$  of non-entropy 3 shocks. For the intermediate “tilde-star-region ” we obtain approximately the values

$$\tilde{p}_* = 1.99667644, \quad \tilde{u}_* = -0.30542246.$$

#### Experimental order of convergence in one space dimension

Here we check the EOC of the front tracking and cone-grid schemes. If  $h = \Delta x$  is the cells width then  $L^1$ -norm is given by

$$\| U(., t) - U_h(., t) \|_{L^1(\mathbb{R})} = ch^\alpha, \quad (6.28)$$

where  $\alpha$  is the order of the  $L^1$ -error. Here  $U$  denotes the exact solution and  $U_h$  the numerical solution. The  $L^1$ -error is defined as  $\| U(., t) - u_h(., t) \|_{L^1} = \Delta x \sum_{i=1}^N | U(x_i, t) - U_h(x_i, t) |$ , where  $N$  is the number of mesh points. Then (6.28) gives

$$EOC := \alpha = \ln \left( \frac{\| U(., t) - U_{\frac{h}{2}}(., t) \|_{L^1}}{\| U(., t) - U_h(., t) \|_{L^1}} \right) / \ln \left( \frac{1}{2} \right). \quad (6.29)$$

N	Front tracking scheme		Cone-grid scheme	
	$L^1$ -error	Eoc	$L^1$ -error	Eoc
25	0.016988		0.155429	
50	0.015598	0.1231	0.09984	0.6385
100	0.01549	0.01	0.061237	0.7052
200	0.013594	0.1883	0.036667	0.7399
400	0.012694	0.0988	0.021515	0.7691

Table 6.1:  $L^1$ -error and EOC for the cone-grid and the front tracking schemes

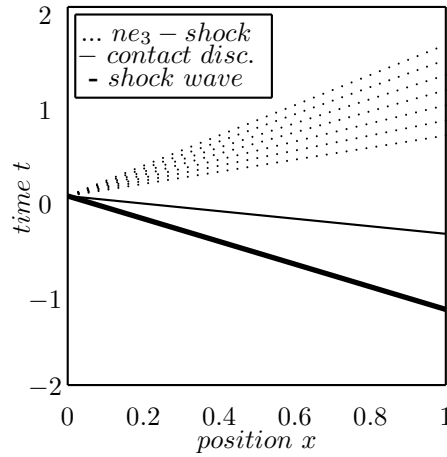


Figure 6.8: Structure of the front tracking solution in Example 6.3.1.

The table 6.1 gives the  $L^1$ -error and EOC for the front tracking and the cone-grid schemes.

**Example 6.3.2.** *Shock tube problem II.*

The initial data are

$$(p, u, n) = \begin{cases} (8.0, 0.0, 5.0), & x \leq 0.5, \\ (0.5, 0.0, 1.0), & x > 0.5. \end{cases}$$

The spatial domain is taken as  $[0, 1]$  with 500 mesh elements and the final time is  $t = 0.5$ . This problem involves the formation of an intermediate state bounded by a shock wave propagating to the right and a transonic rarefaction wave propagating to the left. The fluid in the intermediate state moves at a mildly relativistic speed ( $v = 0.54c$ ) to the right. Flow particles accumulate in a dense shell behind the shock wave compressing the fluid and heating it. The fluid is extremely relativistic from a thermodynamic point of view, but only mildly relativistic dynamically. Figure 6.10.

**Example 6.3.3.** *Shock tube problem III.*

The initial data are

$$(p, u, n) = \begin{cases} (3.0, 1.0, 1.0), & x \leq 0.5, \\ (2.0, -0.5, 1.0), & x > 0.5. \end{cases}$$

The spatial domain is taken as  $[0, 1]$  with 500 mesh elements and the final time is  $t = 0.5$ . The solution consist of left shock, a contact and a right shock. see Figure 6.11 presents plots for the pressure, velocity  $u$  and particle density.



### 6.3. NUMERICAL RESULTS

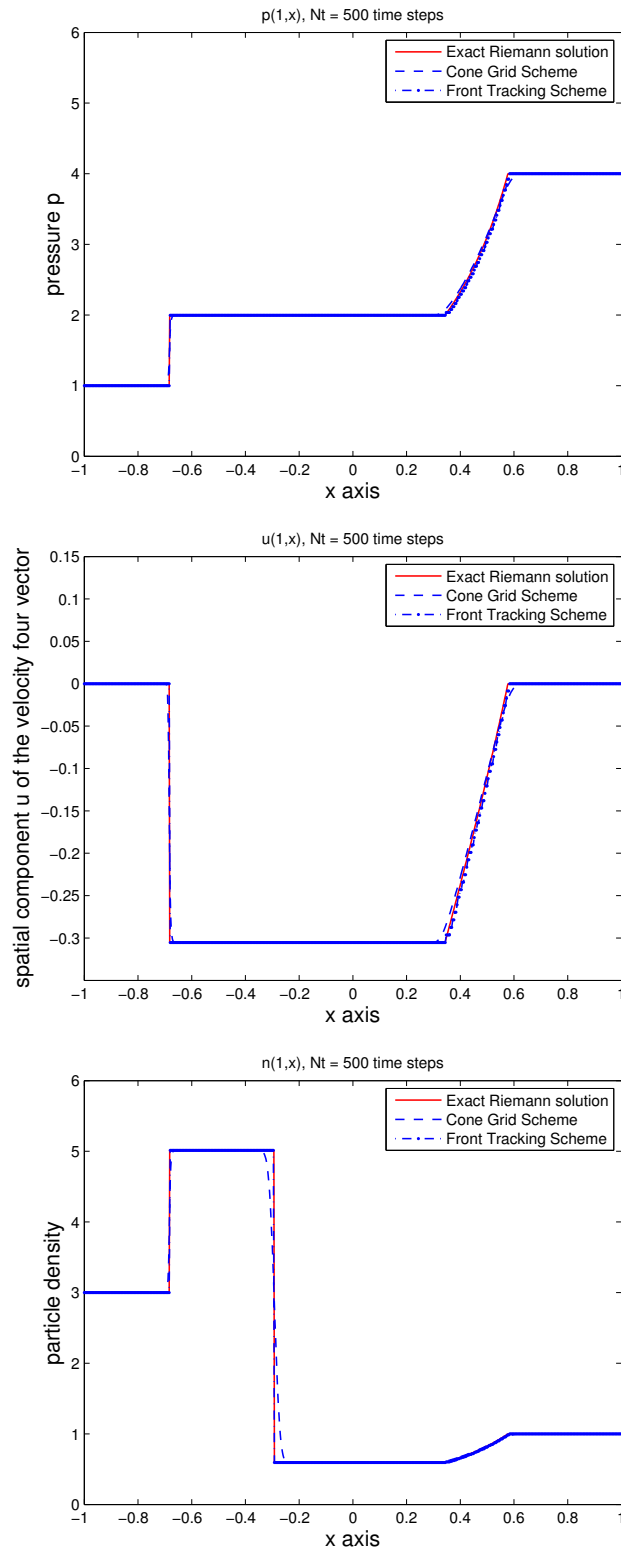


Figure 6.9: The front tracking and cone-grid schemes versus the Riemann solution at  $t = 1$ .

## CHAPTER 6. THE FRONT TRACKING SCHEME

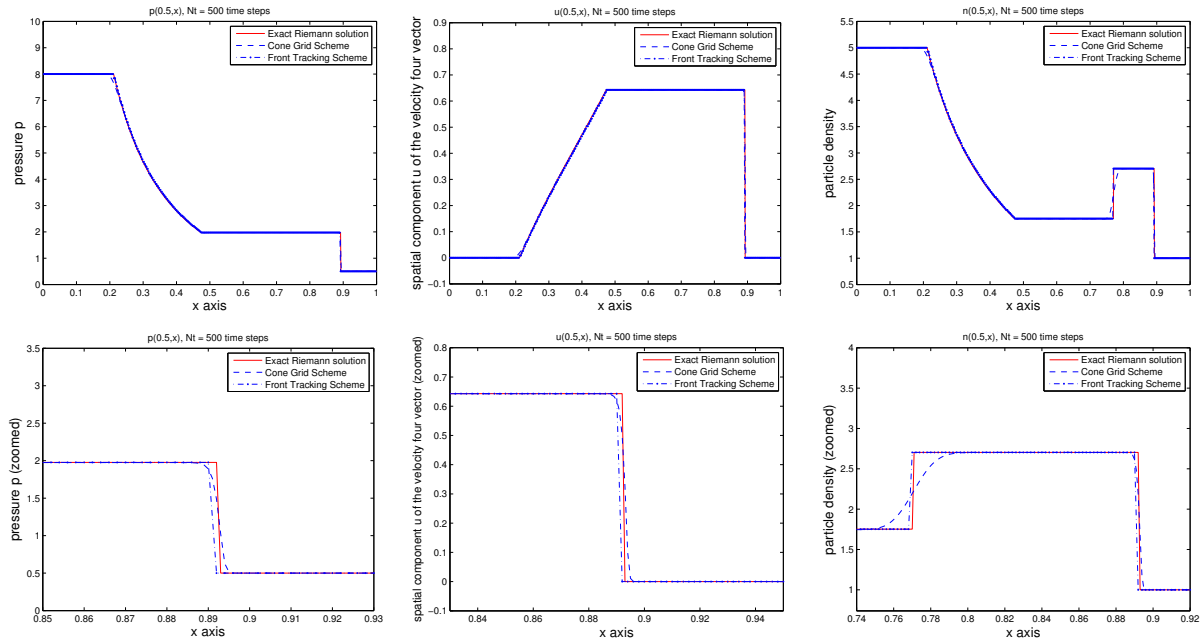


Figure 6.10: Comparison of the results from Example 6.3.1 at time  $t = 0.5$ .

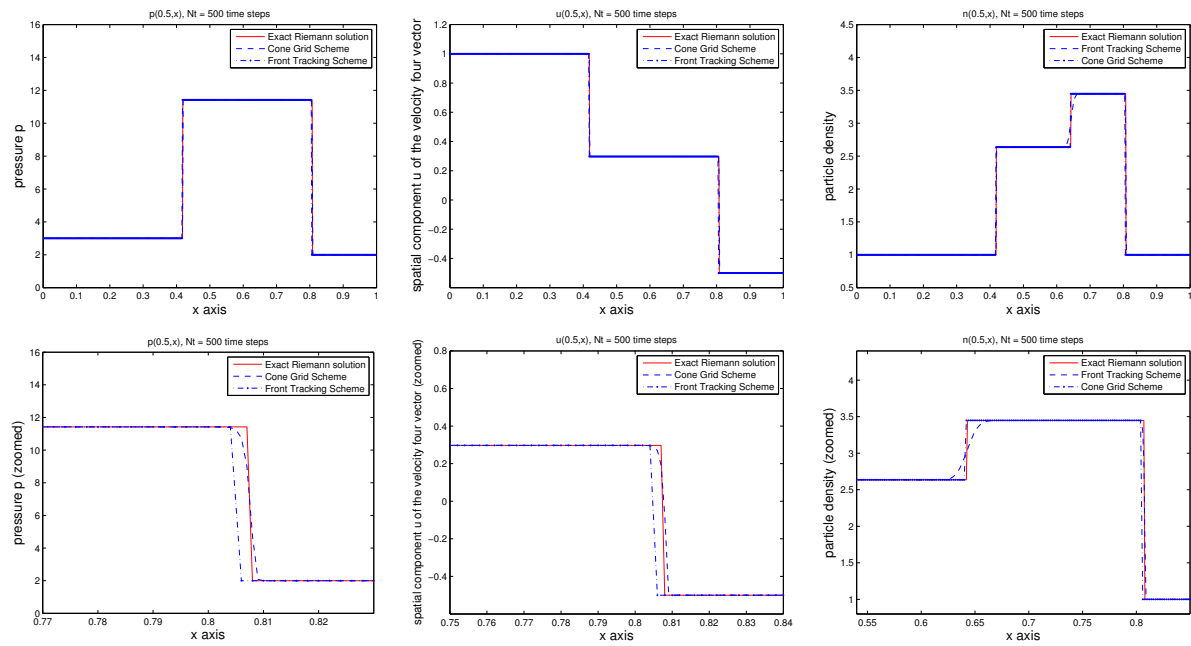


Figure 6.11: Comparison of the results for Example 6.3.2 at time  $t = 0.5$ .

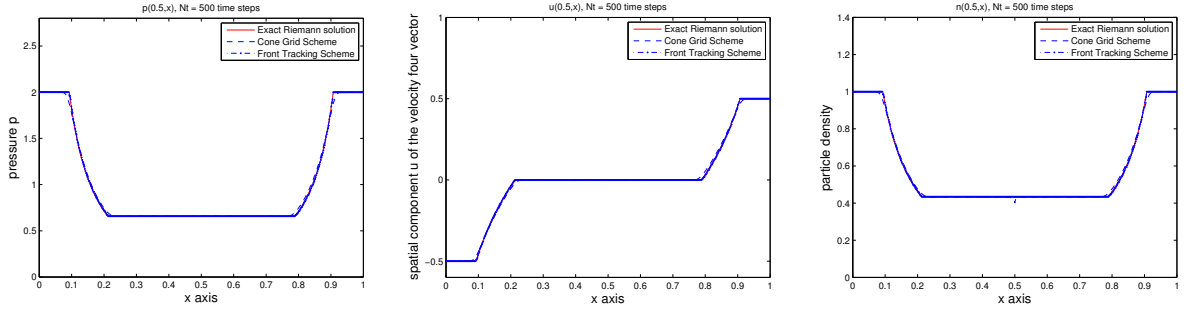


Figure 6.12: Comparison of the results for Example 6.3.3 at time  $t = 0.5$ .

**Example 6.3.4.** *Shock tube problem IV.*

The initial data are

$$(p, u, n) = \begin{cases} (2.0, -0.5, 1.0), & x \leq 0.5, \\ (2.0, 0.5, 1.0), & x > 0.5. \end{cases}$$

This problem has a solution consisting of two strong rarefactions and a trivial stationary contact discontinuity. The spatial domain is taken as  $[0, 1]$  with 500 mesh elements and the final time is  $t = 0.5$ . Figure 6.12 show the solution profiles.

**Example 6.3.5.** *Single shock solution of the Euler equations.*

In this example we test our cone-grid and front tracking schemes for a single shock problem. We supplied initial data to the program for which we know that a single shock solution results from the Rankine-Hugoniot jump conditions, see [47]. We select the initial data and the space-time range such that the shock exactly reaches the right lower corner at the time axis. Figure (6.13)<sub>1,2</sub> represent the plots of the particle density in the time range  $0 \leq t \leq 1.271$  and in the space range  $0 \leq x \leq 2$ . The figures shows that cone-grid and front tracking schemes captures this shock in exactly the same way as predicted by the RankineHugoniot jump conditions. The Figure 6.13<sub>3</sub> presents the particle density at the fixed time  $t = 0.635$  for the same initial data. The Riemannian initial data with a jump at  $x = 1$  are chosen as

$$(p, u, n) = \begin{cases} (1.0, 0.0, 1.0), & x \leq 1.0, \\ (4.0, -0.6495, 2.725), & x > 1.0, \end{cases}$$

where 500 mesh points are considered here. In this example we found that our cone-grid and front tracking schemes gives a sharp shock resolution. This is a good test for the front tracking scheme, and its success indicates that the conservation laws for mass, momentum and energy as well as the entropy inequality are satisfied.

## CHAPTER 6. THE FRONT TRACKING SCHEME

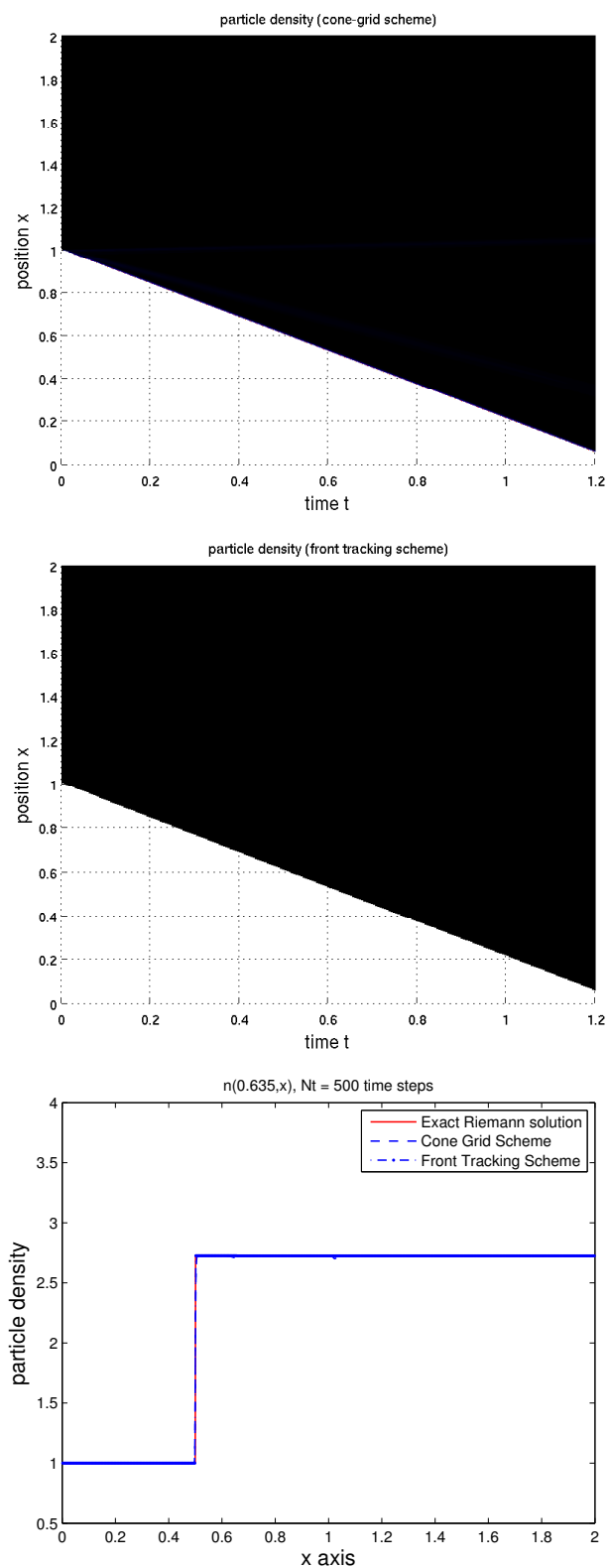


Figure 6.13: A single shock solution.

### 6.3. NUMERICAL RESULTS

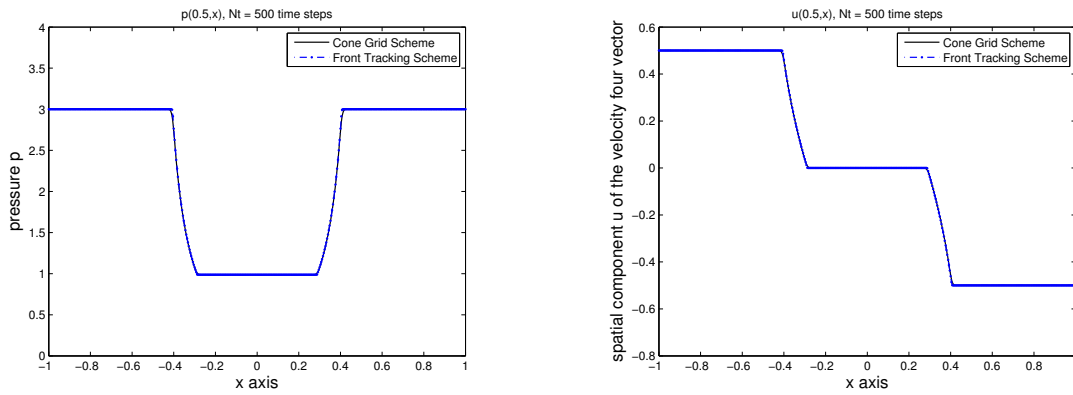


Figure 6.14: The front tracking versus cone-grid schemes corresponding to the first initial data at  $t = 0.5$ .

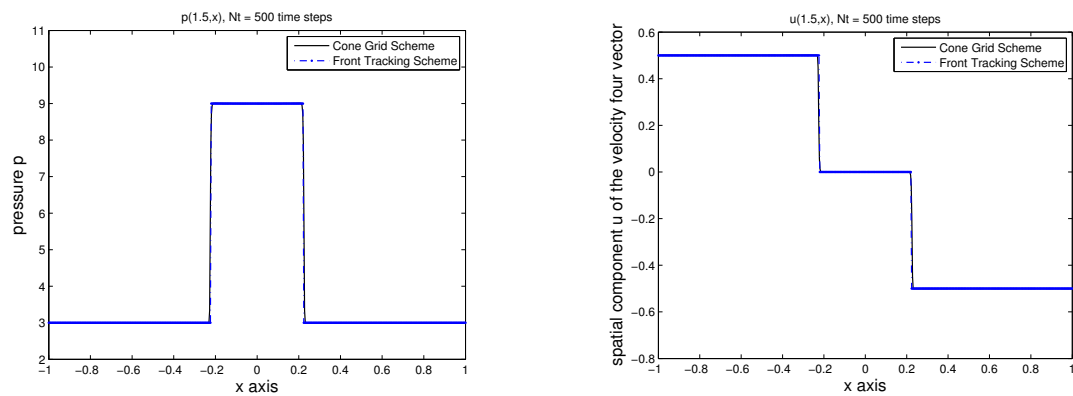


Figure 6.15: The front tracking versus cone-grid schemes corresponding to the first initial data at  $t = 1.5$ .

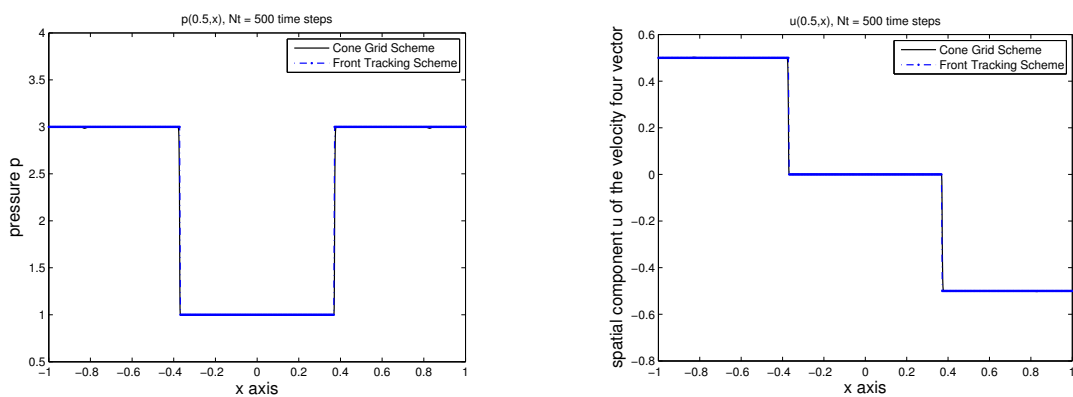


Figure 6.16: The front tracking versus cone-grid schemes corresponding to the second initial data at  $t = 0.5$ .

## CHAPTER 6. THE FRONT TRACKING SCHEME

---

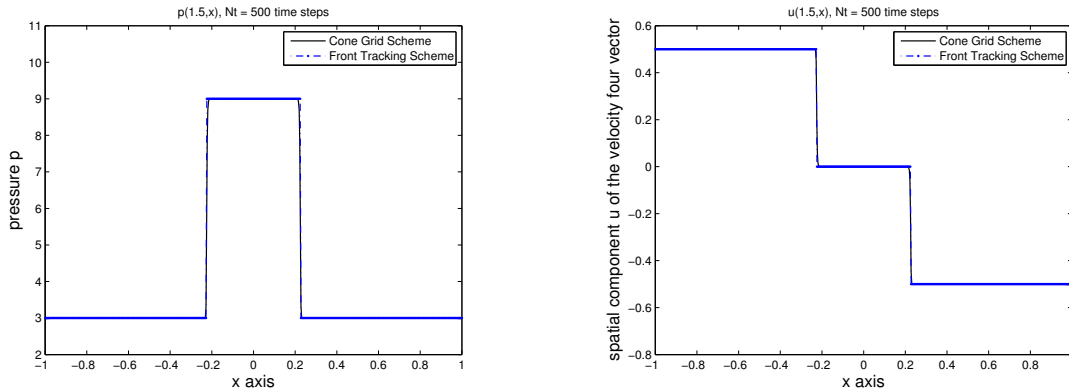


Figure 6.17: The front tracking versus cone-grid schemes corresponding to the second initial data at  $t = 1.5$ .

**Example 6.3.6.** *An example of non-backward uniqueness for the ultra-relativistic Euler system.*

*In this example we test our cone-grid and front tracking schemes for a non-backward uniqueness. We supplied initial data to the program for which we know that the following two initial data  $U_1(0, x) = (p_1(0, x), u_1(0, x))$  and  $U_2(0, x) = (p_2(0, x), u_2(0, x))$  of the system (3.6) for a given pressure  $p_0 > 1$  give the same solution at  $t = 1$ , which given in Section 4.4. Here we give the solution before and after interaction, see Figures 6.14, 6.15, 6.16 and 6.17.*

---

## Chapter 7

# Basic Estimates for the Front Tracking Algorithm for the Ultra-Relativistic Euler Equations

### 7.1 Introduction

In this chapter we study the interaction estimates of the generalized shocks (entropy and non-entropy shocks) of the ultra-relativistic Euler equations (3.6). We consider the interaction of generalized shocks and the outgoing asymptotic Riemann solution. Namely the interaction of two entropy shocks, of an entropy shock and a non-entropy shock and of two non-entropy shocks from different families is considered here, using our parametrizations of the generalized shocks. More precisely we give interaction estimates of the generalized shocks, using the function  $S(\alpha, \beta)$  given in Section 5.2.

**Definition 7.1.1.** *Two generalized shocks, located at points  $x_i < x_j$  and belonging to the characteristic families  $i, j \in \{1, 3\}$  respectively, are interacting if  $i > j$  or else if  $i = j$  and one of them is an entropy shock.*

**Lemma 7.1.2.** *The two non-entropy shocks of the same family are never interact.*

*Proof.* Assume that  $(p_-, u_-) = (p_1, u_1), (p_2, u_2)$  and  $(p_+, u_+) = (p_3, u_3)$  be the constant states of the solution to the lower of  $ne_1$  shock, between  $ne_1$  shock and  $\tilde{ne}_1$  shock, upper of  $\tilde{ne}_1$  shock with velocities  $s_1$  and  $\tilde{s}_1$  respectively such that

$$s_1 > \tilde{s}_1 \text{ i.e. } \sigma_1 < \tilde{\sigma}_1. \quad (7.1)$$

According to Lemmas 3.3.6 and Lemma 3.3.4, we have

$$L_s \left( \frac{p_1}{p_2} \right) < L_s \left( \frac{p_3}{p_2} \right) \text{ implies } p_1 < p_3. \quad (7.2)$$

But according to parametrization of non-entropy 1-shocks given in Lemma 6.2.3, we have

$$p_2 > p_3 \text{ and } p_1 > p_2 \text{ implies } p_1 > p_3. \quad (7.3)$$

## CHAPTER 7. BASIC ESTIMATES FOR THE FRONT TRACKING ALGORITHM FOR THE ULTRA-RELATIVISTIC EULER EQUATIONS

---

This contradicts (7.2). The excluding of the interaction of two non-entropy shocks  $ne_3$  and  $\tilde{n}e_3$  follows in the same way. This completes the proof of the lemma.  $\square$

In the following lemma we give an explicit form of the strength of the non-entropy shocks.

**Lemma 7.1.3.** *Given  $(p_{\pm}, u_{\pm}) \in \mathbb{R}^+ \times \mathbb{R}$ . Put  $\alpha := \frac{p_+}{p_-}$ ,  $\beta := \frac{\sqrt{1+u_+^2}-u_+}{\sqrt{1+u_-^2}-u_-}$ . Assume that, as depicted in Figure 7.1 the states  $(p_-, u_-)$  and  $(p_+, u_+)$  can be connected by a non-entropy shock. Then we have that the strength of non-entropy shocks is equal to the strength of the case four of the Riemann solution given as follows*

$$\text{Str}(ne_{1,3}) = \frac{4}{\sqrt{3}} |\ln \beta| = \frac{4}{\sqrt{3}} |\ln K_S(\alpha)|. \quad (7.4)$$

*Proof.* We consider the non-entropy 1-shock. According to parametrization of  $ne_1$ -shocks, given in Lemma 6.2.3, we have

$$\beta = K_S(\alpha), \quad \alpha = \frac{p_+}{p_-} < 1. \quad (7.5)$$

According to Lemma 5.2.3 (b) we have

$$\beta = K_S(\alpha) < K_R(\alpha) < 1 \implies \beta = \frac{\sqrt{1+u_+^2}-u_+}{\sqrt{1+u_-^2}-u_-} < 1 \implies u_- < u_+, \quad (7.6)$$

i.e. we have

$$u_- < u_+, \quad p_+ < p_- \quad (\text{necessary for case 4 but not sufficient}).$$

To justify case 4 we only have to check that  $\beta < K_R(\alpha)$ . But this follows directly from (7.6). Hence using (5.23) we have

$$\text{Str}(ne_{1,3}) = \ln \frac{p_-}{p_*} + \ln \frac{p_+}{p_*} = \frac{4}{\sqrt{3}} \ln \frac{1}{\beta} = \frac{4}{\sqrt{3}} \ln K_S \left( \frac{1}{\alpha} \right), \quad (7.7)$$

using  $p_* = p_- \alpha^{\frac{1}{2}} \beta^{\frac{2}{\sqrt{3}}}$  given in (3.80). The proof for a non-entropy 3-shock follows in the same way.  $\square$

Based on this lemma we give the strength of the discretized 1 and 3-rarefaction waves in Figure 6.4 by summing up the strengths of the non-entropy shocks. Here we consider the discretized 3-rarefaction wave and the discretized 1-rarefaction wave follows in the same way. Recall that  $\alpha_0 = \frac{p_k}{p_{k-1}}$ ,  $k=1,2,3,\dots,N$ . Then we have

$$\begin{aligned} & \text{Str}(ne_3^1) + \text{Str}(ne_3^2) + \dots + \text{Str}(ne_3^N) \\ &= \frac{4}{\sqrt{3}} \ln K_S \left( \frac{p_1}{p_0} \right) + \frac{4}{\sqrt{3}} \ln K_S \left( \frac{p_2}{p_1} \right) + \dots + \frac{4}{\sqrt{3}} \ln K_S \left( \frac{p_N}{p_{N-1}} \right) \\ &= \frac{4}{\sqrt{3}} \left( \ln K_S \left( \frac{p_1}{p_0} \right) + \ln K_S \left( \frac{p_2}{p_1} \right) + \dots + \ln K_S \left( \frac{p_N}{p_{N-1}} \right) \right) \\ &= \frac{4}{\sqrt{3}} \ln K_S (\alpha_0)^N = \frac{4}{\sqrt{3}} \ln K_S (\alpha^{\frac{1}{N}})^N. \end{aligned}$$



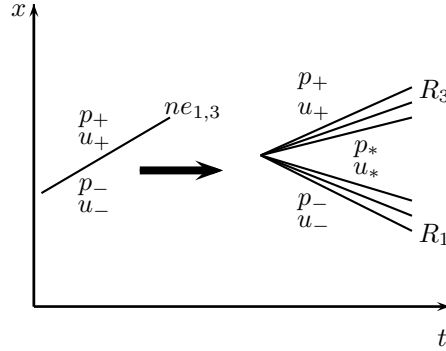


Figure 7.1: Strength of non entropy shocks.

Note that when  $N \rightarrow \infty$ , this strength tends to the strength of the classical rarefaction wave, which is  $\frac{4}{\sqrt{3}} \ln K_R(\alpha) = \ln \alpha$ .

At a fixed time  $t$ , let  $x_i$ ,  $i = 1, 3$ , be the locations of the generalized shocks in the front tracking approximation  $U(t, \cdot)$ . Moreover, let  $\epsilon_i$  be the strength of the wave-front at  $x_i$ , say of the family  $ne_1, ne_3, S_1$  or  $S_3$ . We introduce the two standard functionals  $V, Q : [0, \infty) \mapsto \mathbb{R}$  defined by

$$V(t) = V(U(t)) = \sum_i \epsilon_i \quad (7.8)$$

measuring the total strength of waves in  $U(t, \cdot)$ , and

$$Q(t) = Q(U(t)) = \sum_{(i,j) \in A} \epsilon_i \epsilon_j \quad (7.9)$$

measuring the wave interaction potential. In (7.9), the summation ranges over the set  $A$  of all couples of interacting generalized shocks.

## 7.2 Interaction estimates

In total there are ten possible incoming wave profiles see Figures 7.2, 7.3 and 7.4, corresponding to whether the two incoming waves are entropy shocks, entropy shock with non-entropy shock or two non-entropy shocks from different families. In this section we give the full information for each case including equalities and inequalities, which we will use in our interaction estimates. In Propositions 7.2.3, 7.2.4 and 7.2.5 we give the estimates of the difference between the strengths of the incoming and outgoing fronts. Especially for four cases of interaction of incoming generalized shocks we have the conservation of strength given in Proposition 7.2.2, and for other four cases of interaction of incoming generalized shocks we have that the strength is strictly decreasing given in Proposition 7.2.4. For the last two cases we obtain that the strength is increasing, but in the limit, these cases lead to conserved case given in Proposition 7.2.5.

CHAPTER 7. BASIC ESTIMATES FOR THE FRONT TRACKING ALGORITHM FOR THE ULTRA-RELATIVISTIC EULER EQUATIONS

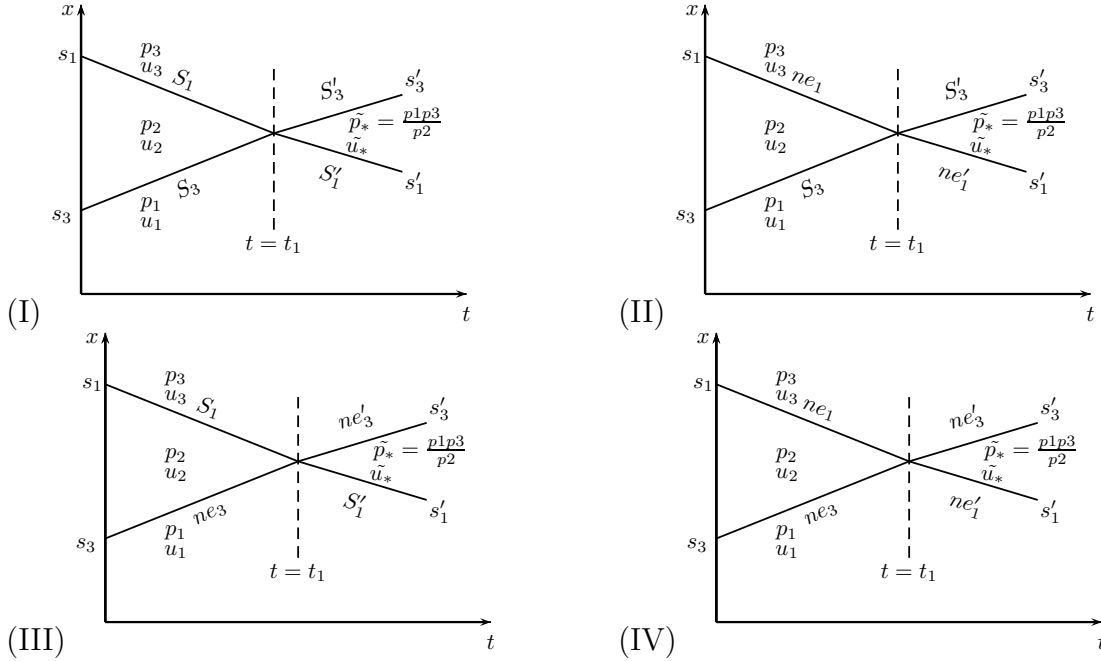


Figure 7.2: Interaction of generalized shocks of the different family.

### 7.2.1 The cases with conservation of strength

In this section we show that the strength is conserved for the interactions of generalized shocks of the different families. This means we prove that the strength of the incoming two generalized shocks is equal to the strength of the outgoing asymptotic front tracking Riemann solution, using the function  $S(\alpha, \beta)$  given in (5.15). Here we cover all cases, which give the conservation of strength.

Our study dealing with the cases of conservation of strength also allows us to determine the type of the outgoing front tracking Riemann solution. In Proposition 7.2.1 we will give the explicit form of the transmitted front tracking Riemann solution in the case of incoming waves with different families. Especially the pressure in the outgoing tilde-star region is given in simple algebraic terms of the pressures before interaction, which generalizes a result given in Proposition 4.3.1. This is important for the study of shock interactions, because in the general Riemann solution for the ultra-relativistic Euler equations the intermediate pressure is only given in implicit form. We start with the following three interactions of the different families. The first wave is the lower one and the second wave is the upper one, respectively.

- (i)  $S_3$  interacts with  $S_1$ , (ii)  $ne_3$  interacts with  $S_1$  and  $S_3$  interacts with  $ne_1$ , (iii)  $ne_3$  interacts with  $ne_1$ .

In Proposition 4.3.1 we described the interaction of two entropy shocks. We gave new explicit shock interaction formulas. In the next proposition we can follow the same line as Proposition 4.3.1 to the other incoming generalized shocks from different families.

## 7.2. INTERACTION ESTIMATES

**Proposition 7.2.1.** *Given  $p_1, p_2, p_3 > 0$ . The intermediate state  $(\tilde{p}_*, \tilde{u}_*)$  in the so called “tilde-star region”, which coming from the interaction of incoming generalized shocks from different families, namely*

(i)  $S_3 ne_1 \rightarrow ne_1 S_3$ , (ii)  $ne_3 ne_1 \rightarrow ne_1 ne_3$ , (iii)  $ne_3 S_1 \rightarrow S_1 ne_3$

can be connected with a single generalized shocks to the prescribed left and right Riemannian initial data. The intermediate pressure is given by

$$\tilde{p}_* = \frac{p_1 p_3}{p_2}. \quad (7.10)$$

**Proposition 7.2.2.** *Given are the three states  $(p_j, u_j) \in \mathbb{R}^+ \times \mathbb{R}$ ,  $j = 1, 2, 3$ . Assume that, as depicted in Figure 7.2, the states  $(p_1, u_1)$  and  $(p_2, u_2)$  as well as  $(p_2, u_2)$  and  $(p_3, u_3)$  can be connected by a lower generalized shocks and an upper generalized shocks, respectively, starting at  $t = 0$  on the  $t$ - $x$  plane which interact. Let the weak solution of (3.6) be continued across the point of intersection at time  $t = t_1$  of lower and upper generalized shocks. Then we have*

(a)<sub>1</sub>  $S_3 S_1 \rightarrow S'_1 S'_3$  with  $Str(S_3) + Str(S_1) = Str(S'_1) + Str(S'_3)$ ,

(b)<sub>1</sub>  $S_3 ne_1 \rightarrow ne'_1 S'_3$  with  $Str(S_3) + Str(ne_1) = Str(ne'_1) + Str(S'_3)$ ,

(c)<sub>1</sub>  $ne_3 S_1 \rightarrow S'_1 ne'_3$  with  $Str(ne_3) + Str(S_1) = Str(S'_1) + Str(ne'_3)$ ,

(d)<sub>1</sub>  $ne_3 ne_1 \rightarrow ne'_1 ne'_3$  with  $Str(ne_3) + Str(ne_1) = Str(ne'_1) + Str(ne'_3)$ ,

*Proof.* Put  $p_- = p_1$ ,  $p_+ = p_3$ ,  $u_- = u_1$ ,  $u_+ = u_3$  and recall  $\alpha = \frac{p_3}{p_1}$  and  $\beta = \frac{\sqrt{1+u_3^2}-u_3}{\sqrt{1+u_1^2}-u_1}$ .

The part (a)<sub>1</sub> depicted in Figure 7.2(I) is given in Proposition 5.3.4. We prove first part of (b)<sub>1</sub> where  $S_3$  interacts with  $ne_1$ , the interaction is depicted in Figure 7.2(II). One can follows the other cases similarly. According to Lemma 3.3.5 (2) and Lemma 6.2.3 (a) we have

$$\text{for } S_3 : \alpha_1 = \frac{p_2}{p_1} < 1, \text{ i.e. } p_2 < p_1, \quad \beta_1 = \frac{\sqrt{1+u_2^2}-u_2}{\sqrt{1+u_1^2}-u_1} = K_S\left(\frac{1}{\alpha_1}\right), \quad (7.11)$$

$$\text{for } ne_1 : \alpha_2 = \frac{p_3}{p_2} < 1, \text{ i.e. } p_3 < p_2, \quad \beta_2 = \frac{\sqrt{1+u_3^2}-u_3}{\sqrt{1+u_2^2}-u_2} = K_S(\alpha_2).$$

Hence  $p_1 > p_3$ , i.e.  $\alpha < 1$ . To prove this part we show that the initial data (6.13) satisfies the statements of case 3 of the front tracking Riemann solution. So we only have to check that

$$\beta > K_S(\alpha), \quad \beta K_S(\alpha) < 1. \quad (7.12)$$

Regarding  $p_1 > p_2 > p_3$ , we obtain from (7.11) and Lemma 5.3.2 (a)

$$\begin{aligned} \beta = \beta_2 \beta_1 &= K_S\left(\frac{p_1}{p_2}\right) K_S\left(\frac{p_3}{p_2}\right) > K_S\left(\frac{p_1}{p_2}\right) K_S\left(\frac{p_2}{p_1}\right) K_S\left(\frac{p_3}{p_1}\right) \\ &> K_S\left(\frac{p_3}{p_1}\right) = K_S(\alpha), \end{aligned}$$

**CHAPTER 7. BASIC ESTIMATES FOR THE FRONT TRACKING  
ALGORITHM FOR THE ULTRA-RELATIVISTIC EULER EQUATIONS**

---

$$\begin{aligned}\beta K_S(\alpha) &= K_S\left(\frac{p_1}{p_2}\right) K_S\left(\frac{p_3}{p_2}\right) K_S\left(\frac{p_3}{p_1}\right) \\ &< K_S\left(\frac{p_1}{p_2}\right) K_S\left(\frac{p_2}{p_1}\right) = 1.\end{aligned}$$

We prove second part of (b)<sub>1</sub>. Recall that  $Str(S_3) = \ln \frac{p_1}{p_2}$  along  $S_3$  and  $Str(ne_1) = \frac{4}{\sqrt{3}} \ln K_S\left(\frac{p_2}{p_3}\right)$  along  $ne_1$ . Hence we have before interaction:

$$Str(S_3) + Str(ne_1) = \ln \frac{p_1}{p_2} + \frac{4}{\sqrt{3}} \ln K_S\left(\frac{p_2}{p_3}\right),$$

$$Str(ne'_1) + Str(S'_3) = \frac{4}{\sqrt{3}} \ln K_S\left(\frac{p_1}{\tilde{p}_*}\right) + \ln \frac{\tilde{p}_*}{p_3} = \frac{4}{\sqrt{3}} \ln K_S\left(\frac{p_2}{p_3}\right) + \ln \frac{p_1}{p_2},$$

using Proposition 7.2.1. Then we get the statement in this case.

We prove first part of (c)<sub>1</sub> where  $ne_3$  interacts with  $S_1$ , the interaction is depicted in Figure 7.2(III). According to Lemma 6.2.3 (b) and Lemma 3.3.5 (1) we have

$$\text{for } ne_3 : \alpha_1 = \frac{p_2}{p_1} > 1, \text{ i.e. } p_2 > p_1, \quad \beta_1 = \frac{\sqrt{1+u_2^2} - u_2}{\sqrt{1+u_1^2} - u_1} = K_S\left(\frac{1}{\alpha_1}\right), \quad (7.13)$$

$$\text{for } S_1 : \alpha_2 = \frac{p_3}{p_2} > 1, \text{ i.e. } p_3 > p_2, \quad \beta_2 = \frac{\sqrt{1+u_3^2} - u_3}{\sqrt{1+u_2^2} - u_2} = K_S(\alpha_2).$$

Hence  $p_3 > p_1$ , i.e.  $\alpha > 1$ . To prove this part we show that the initial data (6.13) satisfies the statements of case 1 of the front tracking Riemann solution. So we only have to check that

$$\beta < K_S(\alpha), \quad \beta K_S(\alpha) > 1. \quad (7.14)$$

Regarding  $p_3 > p_2 > p_1$ , we obtain from (7.13) and Lemma 5.3.2 (a)

$$\begin{aligned}\beta = \beta_2 \beta_1 &= K_S\left(\frac{p_1}{p_2}\right) K_S\left(\frac{p_3}{p_2}\right) < K_S\left(\frac{p_1}{p_2}\right) K_S\left(\frac{p_3}{p_1}\right) K_S\left(\frac{p_2}{p_1}\right) \\ &< K_S\left(\frac{p_3}{p_1}\right) = K_S(\alpha),\end{aligned}$$

$$\begin{aligned}\beta K_S(\alpha) &= K_S\left(\frac{p_1}{p_2}\right) K_S\left(\frac{p_3}{p_2}\right) K_S\left(\frac{p_3}{p_1}\right) \\ &> K_S\left(\frac{p_1}{p_2}\right) K_S\left(\frac{p_2}{p_1}\right) = 1.\end{aligned}$$

## 7.2. INTERACTION ESTIMATES

We prove second part of (c)<sub>1</sub>. Recall that  $Str(ne_3) = \frac{4}{\sqrt{3}} \ln K_S \left( \frac{p_2}{p_1} \right)$  along  $ne_3$  and  $Str(S_1) = \ln \frac{p_3}{p_2}$  along  $S_1$ . Hence we have before interaction:

$$Str(ne_3) + Str(S_1) = \frac{4}{\sqrt{3}} \ln K_S \left( \frac{p_2}{p_1} \right) + \ln \frac{p_3}{p_2}, \quad (7.15)$$

we have after interaction:

$$Str(S'_1) + Str(ne'_3) = \ln \frac{p_*}{p_1} + \frac{4}{\sqrt{3}} \ln K_S \left( \frac{p_3}{p_*} \right) = \ln \frac{p_3}{p_2} + \frac{4}{\sqrt{3}} \ln K_S \left( \frac{p_2}{p_1} \right), \quad (7.16)$$

using Proposition 7.2.1. Then we get the statement in this case.

We prove first part of (d)<sub>1</sub> where  $ne_3$  interacts with  $ne_1$ , the interaction is depicted in Figure 7.2<sub>(IV)</sub>. According to Lemma 6.2.3 we have

$$\text{for } ne_3 : \alpha_1 = \frac{p_2}{p_1} > 1, \text{ i.e. } p_2 > p_1, \quad \beta_1 = \frac{\sqrt{1+u_2^2} - u_2}{\sqrt{1+u_1^2} - u_1} = K_S \left( \frac{1}{\alpha_1} \right), \quad (7.17)$$

$$\text{for } ne_1 : \alpha_2 = \frac{p_3}{p_2} < 1, \text{ i.e. } p_2 > p_3, \quad \beta_2 = \frac{\sqrt{1+u_3^2} - u_3}{\sqrt{1+u_2^2} - u_2} = K_S(\alpha_2).$$

To prove this part we show that the initial data (6.13) satisfies the statements of case 4 of the front tracking Riemann solution for  $\alpha > 1$  or  $\alpha < 1$ , where  $\alpha = \frac{p_3}{p_1}$ . So we only have to check that

$$\beta < K_S(\alpha), \quad \beta K_S(\alpha) < 1. \quad (7.18)$$

First for  $\alpha > 1$ , i.e.  $p_3 > p_1$ . Regarding  $p_2 > p_1$ ,  $p_2 > p_3$  and  $p_3 > p_1$  we obtain from (7.17)

$$\beta = \beta_2 \beta_1 = K_S \left( \frac{p_1}{p_2} \right) K_S \left( \frac{p_3}{p_2} \right) < K_S \left( \frac{p_3}{p_1} \right),$$

and from Lemma 5.3.2 (a)

$$\beta K_S(\alpha) = K_S \left( \frac{p_1}{p_2} \right) K_S \left( \frac{p_3}{p_2} \right) K_S \left( \frac{p_3}{p_1} \right) < K_S \left( \frac{p_1}{p_3} \right) K_S \left( \frac{p_3}{p_1} \right) = 1.$$

Second for  $\alpha < 1$ , i.e.  $p_3 < p_1$ . Regarding  $p_2 > p_1$ ,  $p_2 > p_3$  and  $p_3 < p_1$  we obtain from (7.17), Lemma 5.3.2 (a)

$$\beta = \beta_2 \beta_1 = K_S \left( \frac{p_1}{p_2} \right) K_S \left( \frac{p_3}{p_2} \right) < K_S \left( \frac{p_3}{p_1} \right) = K_S(\alpha),$$

$$\beta K_S(\alpha) = K_S \left( \frac{p_1}{p_2} \right) K_S \left( \frac{p_3}{p_2} \right) K_S \left( \frac{p_3}{p_1} \right) < 1.$$

**CHAPTER 7. BASIC ESTIMATES FOR THE FRONT TRACKING  
ALGORITHM FOR THE ULTRA-RELATIVISTIC EULER EQUATIONS**

---

We prove second part of  $(d)_1$ . Recall that  $Str(ne_3) = \frac{4}{\sqrt{3}} \ln K_S \left( \frac{p_2}{p_1} \right)$  along  $ne_3$  and  $Str(ne_1) = \frac{4}{\sqrt{3}} \ln K_S \left( \frac{p_2}{p_3} \right)$  along  $ne_1$ . Hence we have before interaction:

$$Str(ne_3) + Str(ne_1) = \frac{4}{\sqrt{3}} \ln K_S \left( \frac{p_2}{p_1} \right) + \frac{4}{\sqrt{3}} \ln K_S \left( \frac{p_2}{p_3} \right), \quad (7.19)$$

we have after interaction:

$$Str(ne'_1) + str(ne'_3) = \frac{4}{\sqrt{3}} \ln K_S \left( \frac{p_1}{p_*} \right) + \frac{4}{\sqrt{3}} \ln K_S \left( \frac{p_3}{p_*} \right) = \frac{4}{\sqrt{3}} \ln K_S \left( \frac{p_2}{p_3} \right) + \frac{4}{\sqrt{3}} \ln K_S \left( \frac{p_2}{p_1} \right), \quad (7.20)$$

using Proposition 7.2.1. Then we get the statement in this case.  $\square$

In the following proposition we show that the total strength and the interaction potential is conserved for the above interactions of waves of the different families.

**Proposition 7.2.3.** *For the above interaction cases given in Proposition 7.2.2, which are illustrated in Figure 7.2, we have*

$$\Delta V(t_1) = 0, \quad \Delta Q(t_1) = 0.$$

*Proof.* The first part  $\Delta V(t_1) = 0$  follows directly from Proposition 7.2.2. So we prove only the second part. Consider the case  $a_{(1)}$  in Proposition 7.2.2,  $S_3$  interacts with  $S_1$ . Recall that  $Str(S_3) = \ln \frac{p_1}{p_2}$  along  $S_3$  and  $Str(S_1) = \ln \frac{p_3}{p_2}$  along  $S_1$ .

$$Q_-(t_1) = Str(S_3) \cdot Str(S_1) = \ln \frac{p_1}{p_2} \cdot \ln \frac{p_3}{p_2},$$

$$Q_+(t_1) = Str(S'_1) \cdot Str(S'_3) = \ln \frac{\tilde{p}_*}{p_1} \cdot \ln \frac{\tilde{p}_*}{p_3} = \ln \frac{p_3}{p_2} \cdot \ln \frac{p_1}{p_2}.$$

Hence  $\Delta Q(t_1) = 0$ , which implies this part. Consider case  $(b)_1$ , where  $S_3$  interacts with  $ne_1$ . Recall that  $Str(S_3) = \ln \frac{p_1}{p_2}$  along  $S_3$  and  $Str(ne_1) = \frac{4}{\sqrt{3}} \ln K_S \left( \frac{p_2}{p_3} \right)$  along  $ne_1$ . Hence we have:

$$Q_-(t_1) = Str(S_3) \cdot Str(ne_1) = \ln \frac{p_1}{p_2} \cdot \frac{4}{\sqrt{3}} \ln K_S \left( \frac{p_2}{p_3} \right),$$

$$Q_+(t_1) = Str(ne'_1) \cdot Str(S'_3) = \frac{4}{\sqrt{3}} \ln K_S \left( \frac{p_1}{\tilde{p}_*} \right) \cdot \ln \frac{\tilde{p}_*}{p_3} = \frac{4}{\sqrt{3}} \ln K_S \left( \frac{p_2}{p_3} \right) \cdot \ln \frac{p_1}{p_2},$$

using Proposition 7.2.1. Hence  $\Delta Q(t_1) = 0$ , which implies this part. Consider case  $(c)_1$ , where  $ne_3$  interacts with  $S_1$ . Recall that  $Str(ne_3) = \frac{4}{\sqrt{3}} \ln K_S \left( \frac{p_2}{p_1} \right)$  along  $ne_3$  and  $Str(S_1) = \ln \frac{p_3}{p_2}$  along  $S_1$ . Hence we have:

$$Q_-(t_1) = Str(ne_3) \cdot Str(S_1) = \frac{4}{\sqrt{3}} \ln K_S \left( \frac{p_2}{p_1} \right) \cdot \ln \frac{p_3}{p_2},$$

## 7.2. INTERACTION ESTIMATES

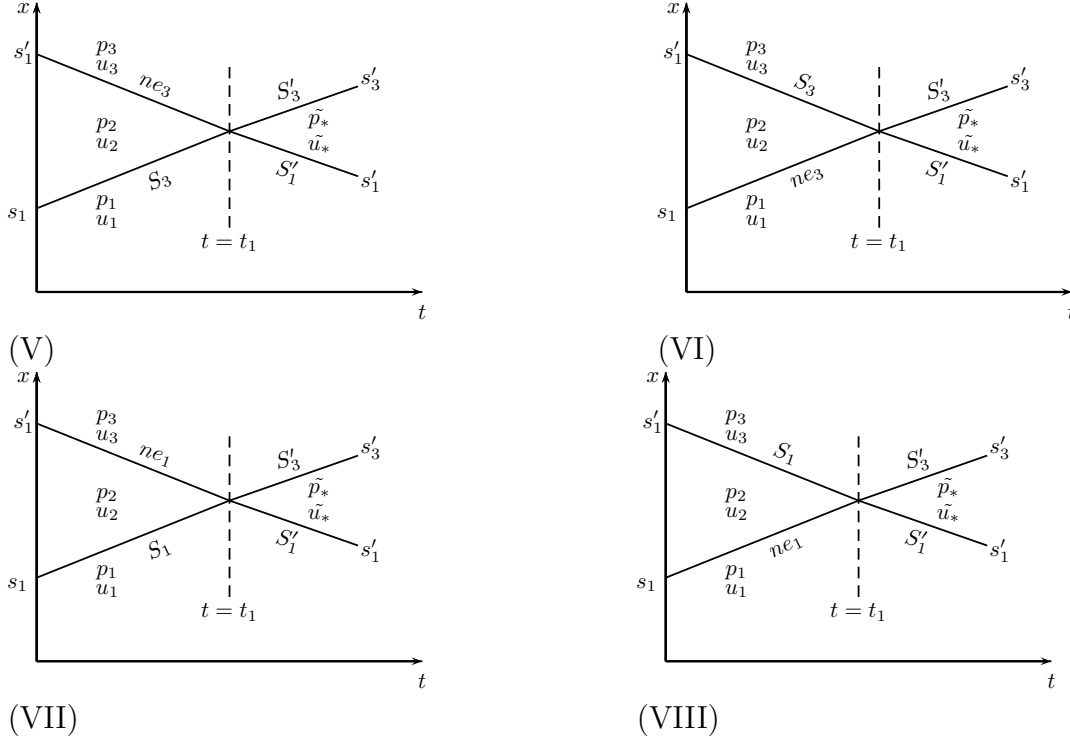


Figure 7.3: Interaction of generalized shocks of the same family.

$$Q_+(t_1) = Str(S'_1) \cdot Str(ne'_3) = \ln \frac{p_*}{p_1} \cdot \frac{4}{\sqrt{3}} \ln K_S \left( \frac{p_3}{p_*} \right) = \ln \frac{p_3}{p_2} \cdot \frac{4}{\sqrt{3}} \ln K_S \left( \frac{p_2}{p_1} \right),$$

using Proposition 7.2.1. Hence  $\Delta Q(t_1) = 0$ , which implies this part. Consider case  $(d)_1$ , where  $ne_3$  interacts with  $ne_1$ . Recall that  $Str(ne_3) = \frac{4}{\sqrt{3}} \ln K_S \left( \frac{p_2}{p_1} \right)$  along  $ne_3$  and  $Str(ne_1) = \frac{4}{\sqrt{3}} \ln K_S \left( \frac{p_2}{p_3} \right)$  along  $ne_1$ . Hence we have:

$$Q_-(t_1) = Str(ne_3) \cdot Str(ne_1) = \frac{4}{\sqrt{3}} \ln K_S \left( \frac{p_2}{p_1} \right) \cdot \frac{4}{\sqrt{3}} \ln K_S \left( \frac{p_2}{p_3} \right), \quad (7.21)$$

$$Q_+(t_1) = Str(ne'_1) \cdot Str(ne'_3) = \frac{4}{\sqrt{3}} \ln K_S \left( \frac{p_1}{p_*} \right) \cdot \frac{4}{\sqrt{3}} \ln K_S \left( \frac{p_3}{p_*} \right) = \frac{4}{\sqrt{3}} \ln K_S \left( \frac{p_2}{p_3} \right) \cdot \frac{4}{\sqrt{3}} \ln K_S \left( \frac{p_2}{p_1} \right), \quad (7.22)$$

using Proposition 7.2.1. Hence  $\Delta Q(t_1) = 0$ , which implies this part. Hence, this complete the proof of this proposition.  $\square$

### 7.2.2 The cases with strictly decreasing strength

Here we will study the cases for the interaction of the generalized shocks, which give a strictly decreasing strength. More precisely we study the interaction of entropy with non-entropy shocks belonging to the same family, namely  $ne_3 S_3$ ,  $S_3 ne_3$ ,  $ne_1 S_1$  and  $S_1 ne_1$ . We

## CHAPTER 7. BASIC ESTIMATES FOR THE FRONT TRACKING ALGORITHM FOR THE ULTRA-RELATIVISTIC EULER EQUATIONS

---

show that the strength is strictly decreasing, i.e. the strength after interaction is less than the strength before interaction. We consider the following cases of incoming generalized shocks and study their interactions.

- (i)  $ne_3$  interacts with  $S_3$  and  $S_3$  interacts with  $ne_3$ ,
- (ii)  $ne_1$  interacts with  $S_1$  and  $S_1$  interacts with  $ne_1$ .

We show that the strength is strictly decreasing for the interactions of fronts of the same families. Also we determine the type of the outgoing front tracking Riemann solution.

**Proposition 7.2.4.** *Given the three states  $(p_j, u_j) \in \mathbb{R}^+ \times \mathbb{R}$ ,  $j = 1, 2, 3$ . Assume that, as depicted in Figure 7.3, the states  $(p_1, u_1)$  and  $(p_2, u_2)$  as well as  $(p_2, u_2)$  and  $(p_3, u_3)$  can be connected by a lower generalized shocks and an upper generalized shocks, respectively as in (i), (ii), starting at  $t = 0$  on the  $t$ - $x$  plane which interact. Let the weak solution of (3.6) be continued across the point of intersection at time  $t = t_1$  of lower and upper generalized shocks. Define  $\alpha_1 = \frac{p_2}{p_1}$ ,  $\alpha_2 = \frac{p_3}{p_2}$ . Let the solution be extended across the point of intersection. Then the following estimates are valid for the corresponding interactions.*

(a)<sub>i</sub>  $S_3ne_3 \rightarrow S'_1S'_3$  with

(a)<sub>ii</sub>

$$\text{Str}(S_3) + \text{Str}(ne_3) < \text{Str}(S'_1) + \text{Str}(S'_3),$$

(a)<sub>iii</sub>

$$\Delta V(t_1) < \frac{4}{\sqrt{3}} \ln \frac{K_R\left(\frac{p_3}{p_2}\right)}{K_S\left(\frac{p_3}{p_2}\right)} < 0, \quad (7.23)$$

(a)<sub>iv</sub>

$$\Delta Q(t_1) < \ln\left(\frac{p_1}{p_2}\right) \cdot \frac{4}{\sqrt{3}} \ln \frac{K_R\left(\frac{p_3}{p_2}\right)}{K_S\left(\frac{p_3}{p_2}\right)} < 0, \quad (7.24)$$

(b)<sub>i</sub>  $ne_3S_3 \rightarrow S'_1S'_3$  with

(b)<sub>ii</sub>

$$\text{Str}(ne_3) + \text{Str}(S_3) < \text{Str}(S'_1) + \text{Str}(S'_3),$$

(b)<sub>iii</sub>

$$\Delta V(t_1) < \frac{4}{\sqrt{3}} \ln \frac{K_R\left(\frac{p_2}{p_1}\right)}{K_S\left(\frac{p_2}{p_1}\right)} < 0, \quad (7.25)$$

(b)<sub>iv</sub>

$$\Delta Q(t_1) < \ln\left(\frac{p_2}{p_3}\right) \cdot \frac{4}{\sqrt{3}} \ln \frac{K_R\left(\frac{p_2}{p_1}\right)}{K_S\left(\frac{p_2}{p_1}\right)} < 0, \quad (7.26)$$



## 7.2. INTERACTION ESTIMATES

(c)<sub>i</sub>  $S_1 ne_1 \rightarrow S'_1 S'_3$  with

(c)<sub>ii</sub>

$$\text{Str}(S_1) + \text{Str}(ne_1) < \text{Str}(S'_1) + \text{Str}(S'_3),$$

(c)<sub>iii</sub>

$$\Delta V(t_1) < \frac{4}{\sqrt{3}} \ln \frac{K_R\left(\frac{p_2}{p_3}\right)}{K_S\left(\frac{p_2}{p_3}\right)} < 0, \quad (7.27)$$

(c)<sub>iv</sub>

$$\Delta Q(t_1) < \ln\left(\frac{p_2}{p_1}\right) \cdot \frac{4}{\sqrt{3}} \ln \frac{K_R\left(\frac{p_2}{p_3}\right)}{K_S\left(\frac{p_2}{p_3}\right)} < 0, \quad (7.28)$$

(d)<sub>i</sub>  $ne_1 S_1 \rightarrow S'_1 S'_3$  with

(d)<sub>ii</sub>

$$\text{Str}(ne_1) + \text{Str}(S_1) < \text{Str}(S'_1) + \text{Str}(S'_3),$$

(d)<sub>iii</sub>

$$\Delta V(t_1) < \frac{4}{\sqrt{3}} \ln \frac{K_R\left(\frac{p_1}{p_2}\right)}{K_S\left(\frac{p_1}{p_2}\right)} < 0, \quad (7.29)$$

(d)<sub>iv</sub>

$$\Delta Q(t_1) < \ln\left(\frac{p_3}{p_2}\right) \cdot \frac{4}{\sqrt{3}} \ln \frac{K_R\left(\frac{p_1}{p_2}\right)}{K_S\left(\frac{p_1}{p_2}\right)} < 0. \quad (7.30)$$

*Proof.* Put  $p_- = p_1$ ,  $p_+ = p_3$ ,  $u_- = u_1$ ,  $u_+ = u_3$  and recall  $\alpha = \frac{p_3}{p_1}$  and  $\beta = \frac{\sqrt{1+u_3^2}-u_3}{\sqrt{1+u_1^2}-u_1}$ . We first consider the case where  $S_3$  interacts with  $ne_3$ , the interaction is depicted in Figure 7.3<sub>(V)</sub>. According to Lemma 3.3.5 (2) and Lemma 6.2.3 (b) we have

$$\text{for } S_3 : \alpha_1 = \frac{p_2}{p_1} < 1, \text{ i.e. } p_2 < p_1, \quad \beta_1 = \frac{\sqrt{1+u_2^2}-u_2}{\sqrt{1+u_1^2}-u_1} = K_S\left(\frac{1}{\alpha_1}\right), \quad (7.31)$$

$$\text{for } ne_3 : \alpha_2 = \frac{p_3}{p_2} > 1, \text{ i.e. } p_3 > p_2, \quad \beta_2 = \frac{\sqrt{1+u_3^2}-u_3}{\sqrt{1+u_2^2}-u_2} = K_S\left(\frac{1}{\alpha_2}\right).$$

Hence  $p_2 < \min(p_1, p_3)$  and  $p_1 > p_3$ , i.e.  $\alpha < 1$ . To prove this part we show that the initial data (6.13) satisfies the statements of case 2 of the front tracking Riemann solution. So we only have to check that

$$\beta > K_S(\alpha) \quad \text{and} \quad \beta K_S(\alpha) > 1. \quad (7.32)$$

**CHAPTER 7. BASIC ESTIMATES FOR THE FRONT TRACKING  
ALGORITHM FOR THE ULTRA-RELATIVISTIC EULER EQUATIONS**

---

Regarding  $p_2 < \min(p_1, p_3)$  and  $p_1 > p_3$ , we obtain from (7.31) and Lemma 5.3.2 (a)

$$\begin{aligned}\beta = \beta_2\beta_1 &= K_S\left(\frac{p_1}{p_2}\right) K_S\left(\frac{p_2}{p_3}\right) > K_S\left(\frac{p_1}{p_2}\right) K_S\left(\frac{p_2}{p_1}\right) K_S\left(\frac{p_3}{p_1}\right) \\ &= K_S\left(\frac{p_3}{p_1}\right) = K_S(\alpha),\end{aligned}$$

and from Lemma 5.3.1

$$\begin{aligned}\beta K_S(\alpha) &= K_S\left(\frac{p_1}{p_2}\right) K_S\left(\frac{p_2}{p_3}\right) K_S\left(\frac{p_3}{p_1}\right) \\ &> K_S\left(\frac{p_1}{p_2}\right) K_S\left(\frac{p_2}{p_1}\right) = 1.\end{aligned}$$

We prove part (a)<sub>ii</sub> corresponding to the interaction  $S_3 ne_3 \rightarrow S'_1 S'_3$ . The part (a)<sub>i</sub> gives the outgoing Riemann solution in region 2. Hence we use (3.76) and conclude that

$$p_2 < \min(p_1, p_3), \quad p_1 > p_3, \quad p_* > \max(p_1, p_3) \quad \text{and} \quad (7.33)$$

$$K_S\left(\frac{p_1}{p_2}\right) K_S\left(\frac{p_2}{p_3}\right) = K_S\left(\frac{p_*}{p_1}\right) K_S\left(\frac{p_*}{p_3}\right). \quad (7.34)$$

Using monotonicity of the function  $K_S$ , one can easily show

$$p_* < \frac{p_1 p_3}{p_2}. \quad (7.35)$$

Recall that  $Str(S_3) = \ln \frac{p_1}{p_2}$  along  $S_3$  and  $Str(ne_3) = \frac{4}{\sqrt{3}} \ln K_S\left(\frac{p_3}{p_2}\right)$  along  $ne_3$ . We want to prove

$$\ln \frac{p_1}{p_2} + \frac{4}{\sqrt{3}} \ln K_S\left(\frac{p_3}{p_2}\right) > \ln \frac{\tilde{p}_*}{p_1} + \ln \frac{\tilde{p}_*}{p_3}. \quad (7.36)$$

To justify this inequality, using Lemma 5.2.3 (a) and (7.35) we only have to check that

$$\begin{aligned}\ln \frac{p_1}{p_2} + \frac{4}{\sqrt{3}} \ln K_S\left(\frac{p_3}{p_2}\right) &> \ln \frac{\tilde{p}_*}{p_1} + \ln \frac{\tilde{p}_*}{p_3} \iff \\ \ln \frac{p_1}{p_2} + \ln \frac{p_3}{p_2} &> \ln \frac{\tilde{p}_*}{p_1} + \ln \frac{\tilde{p}_*}{p_3} \iff \\ \ln \frac{p_1 p_3}{p_2^2} &> \ln \frac{\tilde{p}_*^2}{p_1 p_3} \iff \\ \frac{p_1 p_3}{p_2} &> \tilde{p}_*.\end{aligned}$$

We prove part (a)<sub>iii</sub>, using (7.35)

$$\begin{aligned}
 \Delta V(t_1) &= \ln \frac{\tilde{p}_*}{p_1} + \ln \frac{\tilde{p}_*}{p_3} - \ln \frac{p_1}{p_2} - \frac{4}{\sqrt{3}} \ln K_S \left( \frac{p_3}{p_2} \right) \\
 &= \ln \frac{\tilde{p}_*^2 p_2}{p_1^2 p_3} - \frac{4}{\sqrt{3}} \ln K_S \left( \frac{p_3}{p_2} \right) \\
 &< \ln \frac{(p_1 p_3)^2 p_2}{p_2^2 p_1^2 p_3} - \frac{4}{\sqrt{3}} \ln K_S \left( \frac{p_3}{p_2} \right) \\
 &= \ln \frac{p_3}{p_2} - \frac{4}{\sqrt{3}} \ln K_S \left( \frac{p_3}{p_2} \right) \\
 &= \frac{4}{\sqrt{3}} \left( \frac{\sqrt{3}}{4} \ln \frac{p_3}{p_2} - \ln K_S \left( \frac{p_3}{p_2} \right) \right) \\
 &= \frac{4}{\sqrt{3}} \left( \ln K_R \left( \frac{p_3}{p_2} \right) - \ln K_S \left( \frac{p_3}{p_2} \right) \right) = \frac{4}{\sqrt{3}} \ln \frac{K_R \left( \frac{p_3}{p_2} \right)}{K_S \left( \frac{p_3}{p_2} \right)} < 0.
 \end{aligned}$$

We prove part (a)<sub>iv</sub>, using (7.35)

$$\begin{aligned}
 \Delta Q(t_1) &= \ln \frac{\tilde{p}_*}{p_1} \cdot \ln \frac{\tilde{p}_*}{p_3} - \ln \frac{p_1}{p_2} \cdot \frac{4}{\sqrt{3}} \ln K_S \left( \frac{p_3}{p_2} \right) \\
 &< \ln \frac{p_3}{p_2} \cdot \ln \frac{p_1}{p_2} - \ln \frac{p_1}{p_2} \cdot \frac{4}{\sqrt{3}} \ln K_S \left( \frac{p_3}{p_2} \right) \\
 &= \frac{4}{\sqrt{3}} \cdot \ln \frac{p_1}{p_2} \left( \frac{\sqrt{3}}{4} \ln \frac{p_3}{p_2} - \ln K_S \left( \frac{p_3}{p_2} \right) \right) \\
 &= \frac{4}{\sqrt{3}} \cdot \ln \frac{p_1}{p_2} \left( \ln K_R \left( \frac{p_3}{p_2} \right) - \ln K_S \left( \frac{p_3}{p_2} \right) \right) \\
 &= \ln \frac{p_1}{p_2} \cdot \frac{4}{\sqrt{3}} \ln \frac{K_R \left( \frac{p_3}{p_2} \right)}{K_S \left( \frac{p_3}{p_2} \right)} < 0.
 \end{aligned}$$

This complete the proof of this part. Second consider the case (b)<sub>i,ii,iii,iv</sub> where  $ne_3$  interacts with  $S_3$ , the interaction is depicted in Figure 7.3<sub>(V)</sub>. According to Lemma 6.2.3 (b) and Lemma 3.3.5 (2) we have

$$\text{for } ne_3 : \alpha_1 = \frac{p_2}{p_1} > 1, \text{ i.e. } p_2 > p_1, \quad \beta_1 = \frac{\sqrt{1+u_2^2} - u_2}{\sqrt{1+u_1^2} - u_1} = K_S \left( \frac{1}{\alpha_1} \right), \tag{7.37}$$

$$\text{for } S_3 : \alpha_2 = \frac{p_3}{p_2} < 1, \text{ i.e. } p_3 < p_2, \quad \beta_2 = \frac{\sqrt{1+u_3^2} - u_3}{\sqrt{1+u_2^2} - u_2} = K_S \left( \frac{1}{\alpha_2} \right).$$

Hence  $p_2 > \max(p_1, p_3)$  and  $p_1 > p_3$ , i.e.  $\alpha < 1$ . To prove this part we show that the initial data (6.13) satisfies the statements of case 2 of the front tracking Riemann solution.

**CHAPTER 7. BASIC ESTIMATES FOR THE FRONT TRACKING  
ALGORITHM FOR THE ULTRA-RELATIVISTIC EULER EQUATIONS**

---

So we only have to check that

$$\beta > K_S(\alpha) \quad \text{and} \quad \beta K_S(\alpha) > 1. \quad (7.38)$$

Regarding  $p_2 > \max(p_1, p_3)$  and  $p_1 > p_3$ , we obtain from (7.37) and Lemma 5.3.2 (a)

$$\begin{aligned} \beta = \beta_2 \beta_1 &= K_S\left(\frac{p_1}{p_2}\right) K_S\left(\frac{p_2}{p_3}\right) > K_S\left(\frac{p_3}{p_1}\right) K_S\left(\frac{p_3}{p_2}\right) K_S\left(\frac{p_2}{p_3}\right) \\ &= K_S\left(\frac{p_3}{p_1}\right) = K_S(\alpha), \end{aligned}$$

and from Lemma 5.3.1

$$\begin{aligned} \beta K_S(\alpha) &= K_S\left(\frac{p_1}{p_2}\right) K_S\left(\frac{p_2}{p_3}\right) K_S\left(\frac{p_3}{p_1}\right) \\ &> K_S\left(\frac{p_2}{p_3}\right) K_S\left(\frac{p_3}{p_2}\right) = 1. \end{aligned}$$

We prove part (b)<sub>ii</sub> corresponding to the interaction  $ne_3 S_3 \rightarrow S'_1 S'_3$ . The part (b)<sub>i</sub> gives the outgoing Riemann solution in region 2. Hence we use (3.76) and conclude that

$$p_2 > \max(p_1, p_3), \quad p_1 > p_3, \quad p_* > \max(p_1, p_3) \quad \text{and} \quad (7.39)$$

$$K_S\left(\frac{p_1}{p_2}\right) K_S\left(\frac{p_2}{p_3}\right) = K_S\left(\frac{\tilde{p}_*}{p_1}\right) K_S\left(\frac{\tilde{p}_*}{p_3}\right). \quad (7.40)$$

Using monotonicity of the function  $K_S$ , one can easily show

$$p_* < p_2. \quad (7.41)$$

Recall that  $Str(ne_3) = \frac{4}{\sqrt{3}} \ln K_S\left(\frac{p_2}{p_1}\right)$  along  $ne_3$  and  $Str(S_3) = \ln \frac{p_2}{p_3}$  along  $S_3$ . We want to prove

$$\frac{4}{\sqrt{3}} \ln K_S\left(\frac{p_2}{p_1}\right) + \ln \frac{p_2}{p_3} > \ln \frac{\tilde{p}_*}{p_1} + \ln \frac{\tilde{p}_*}{p_3}. \quad (7.42)$$

To justify this inequality, using Lemma 5.2.3 (a) and (7.41) we only have to check that

$$\begin{aligned} \frac{4}{\sqrt{3}} \ln K_R\left(\frac{p_2}{p_1}\right) + \ln \frac{p_2}{p_3} &> \ln \frac{\tilde{p}_*}{p_1} + \ln \frac{\tilde{p}_*}{p_3} &\iff \\ \ln \frac{p_2}{p_1} + \ln \frac{p_2}{p_3} &> \ln \frac{\tilde{p}_*}{p_1} + \ln \frac{\tilde{p}_*}{p_3} &\iff \\ \ln \frac{p_2^2}{p_1 p_3} &> \ln \frac{\tilde{p}_*^2}{p_1 p_3} &\iff \\ p_2 &> \tilde{p}_*. \end{aligned}$$

We prove part (b)<sub>iii</sub>, using (7.41)

$$\begin{aligned}
 \Delta V(t_1) &= \ln \frac{\tilde{p}_*}{p_1} + \ln \frac{\tilde{p}_*}{p_3} - \ln \frac{p_2}{p_3} - \frac{4}{\sqrt{3}} \ln K_S \left( \frac{p_2}{p_1} \right) \\
 &= \ln \frac{\tilde{p}_*^2}{p_1 p_2} - \frac{4}{\sqrt{3}} \ln K_S \left( \frac{p_2}{p_1} \right) \\
 &< \ln \frac{p_2^2}{p_1 p_2} - \frac{4}{\sqrt{3}} \ln K_S \left( \frac{p_2}{p_1} \right) \\
 &= \ln \frac{p_2}{p_1} - \frac{4}{\sqrt{3}} \ln K_S \left( \frac{p_2}{p_1} \right) \\
 &= \frac{4}{\sqrt{3}} \left( \frac{\sqrt{3}}{4} \ln \frac{p_2}{p_1} - \ln K_S \left( \frac{p_2}{p_1} \right) \right) \\
 &= \frac{4}{\sqrt{3}} \left( \ln K_R \left( \frac{p_2}{p_1} \right) - \ln K_S \left( \frac{p_2}{p_1} \right) \right) = \frac{4}{\sqrt{3}} \ln \frac{K_R \left( \frac{p_2}{p_1} \right)}{K_S \left( \frac{p_2}{p_1} \right)} < 0.
 \end{aligned}$$

We prove part (b)<sub>iv</sub>, using (7.41)

$$\begin{aligned}
 \Delta Q(t_1) &= \ln \frac{\tilde{p}_*}{p_1} \cdot \ln \frac{\tilde{p}_*}{p_3} - \ln \frac{p_2}{p_3} \cdot \frac{4}{\sqrt{3}} \ln K_S \left( \frac{p_2}{p_1} \right) \\
 &< \ln \frac{p_2}{p_1} \cdot \ln \frac{p_2}{p_3} - \ln \frac{p_2}{p_1} \cdot \frac{4}{\sqrt{3}} \ln K_S \left( \frac{p_2}{p_1} \right) \\
 &= \frac{4}{\sqrt{3}} \cdot \ln \frac{p_2}{p_3} \left( \frac{\sqrt{3}}{4} \ln \frac{p_2}{p_1} - \ln K_S \left( \frac{p_2}{p_1} \right) \right) \\
 &= \frac{4}{\sqrt{3}} \cdot \ln \frac{p_2}{p_3} \left( \ln K_R \left( \frac{p_2}{p_1} \right) - \ln K_S \left( \frac{p_2}{p_1} \right) \right) \\
 &= \ln \frac{p_2}{p_3} \cdot \frac{4}{\sqrt{3}} \ln \frac{K_R \left( \frac{p_2}{p_1} \right)}{K_S \left( \frac{p_2}{p_1} \right)} < 0.
 \end{aligned}$$

This complete the proof of this part. Third consider the case (c)<sub>i,ii,iii,iv</sub> where  $S_1$  interacts with  $ne_1$ , the interaction is depicted in Figure 7.3(VII). According to Lemma 3.3.5 (1) and Lemma 6.2.3 (a) we have

$$\text{for } S_1 : \alpha_1 = \frac{p_2}{p_1} > 1, \text{ i.e. } p_2 > p_1, \quad \beta_1 = \frac{\sqrt{1+u_2^2} - u_2}{\sqrt{1+u_1^2} - u_1} = K_S(\alpha_1), \tag{7.43}$$

$$\text{for } ne_1 : \alpha_2 = \frac{p_3}{p_2} < 1, \text{ i.e. } p_3 < p_2, \quad \beta_2 = \frac{\sqrt{1+u_3^2} - u_3}{\sqrt{1+u_2^2} - u_2} = K_S(\alpha_2).$$

Hence  $\max(p_1, p_3) < p_2$  and  $p_3 > p_1$ , i.e.  $\alpha > 1$ . To prove this part we show that the initial data (6.13) satisfies the statements of case 2 of the front tracking Riemann solution.

**CHAPTER 7. BASIC ESTIMATES FOR THE FRONT TRACKING  
ALGORITHM FOR THE ULTRA-RELATIVISTIC EULER EQUATIONS**

---

So we only have to check that

$$\beta > K_S(\alpha) \quad \text{and} \quad \beta K_S(\alpha) > 1. \quad (7.44)$$

Regarding  $\max(p_1, p_3) < p_2$  and  $p_3 > p_1$ , we obtain from (7.43) and Lemma 5.3.1

$$\begin{aligned} \beta = \beta_2 \beta_1 &= K_S\left(\frac{p_2}{p_1}\right) K_S\left(\frac{p_3}{p_2}\right) > K_S\left(\frac{p_2}{p_3}\right) K_S\left(\frac{p_3}{p_1}\right) K_S\left(\frac{p_3}{p_2}\right) \\ &= K_S\left(\frac{p_3}{p_1}\right) = K_S(\alpha), \end{aligned}$$

and from Lemma 5.3.2 (a)

$$\begin{aligned} \beta K_S(\alpha) &= K_S\left(\frac{p_2}{p_1}\right) K_S\left(\frac{p_3}{p_2}\right) K_S\left(\frac{p_3}{p_1}\right) \\ &> K_S\left(\frac{p_2}{p_3}\right) K_S\left(\frac{p_3}{p_2}\right) = 1. \end{aligned}$$

We prove part (c)<sub>ii</sub> corresponding to the interaction  $S_1 n e_1 \rightarrow S'_1 S'_3$ . The part (c)<sub>i</sub> gives the outgoing Riemann solution in region 2. Hence we use (3.76) and conclude that

$$\max(p_1, p_3) < p_2, \quad p_3 > p_1, \quad p_* > \max(p_1, p_3) \quad \text{and} \quad (7.45)$$

$$K_S\left(\frac{p_2}{p_1}\right) K_S\left(\frac{p_3}{p_2}\right) = K_S\left(\frac{\tilde{p}_*}{p_1}\right) K_S\left(\frac{\tilde{p}_*}{p_3}\right). \quad (7.46)$$

Using monotonicity of the function  $K_S$ , one can easily show

$$p_* < p_2. \quad (7.47)$$

Recall that  $Str(S_1) = \ln \frac{p_2}{p_1}$  along  $S_1$  and  $Str(n e_1) = \frac{4}{\sqrt{3}} \ln K_S\left(\frac{p_2}{p_3}\right)$  along  $n e_1$ . We want to prove

$$\ln \frac{p_2}{p_1} + \frac{4}{\sqrt{3}} \ln K_S\left(\frac{p_2}{p_3}\right) > \ln \frac{\tilde{p}_*}{p_1} + \ln \frac{\tilde{p}_*}{p_3}. \quad (7.48)$$

To justify this inequality, using Lemma 5.2.3 (a) and (7.47) we only have to check that

$$\begin{aligned} \ln \frac{p_2}{p_1} + \frac{4}{\sqrt{3}} \ln K_S\left(\frac{p_2}{p_3}\right) > \ln \frac{\tilde{p}_*}{p_1} + \ln \frac{\tilde{p}_*}{p_3} &\iff \\ \ln \frac{p_2}{p_1} + \ln \frac{p_2}{p_3} > \ln \frac{\tilde{p}_*}{p_1} + \ln \frac{\tilde{p}_*}{p_3} &\iff \\ \ln \frac{p_2^2}{p_1 p_3} > \ln \frac{\tilde{p}_*^2}{p_1 p_3} &\iff \\ p_2 > \tilde{p}_*. & \end{aligned}$$

We prove part (c)<sub>iii</sub>, using (7.47)

$$\begin{aligned}
 \Delta V(t_1) &= \ln \frac{\tilde{p}_*}{p_1} + \ln \frac{\tilde{p}_*}{p_3} - \ln \frac{p_2}{p_1} - \frac{4}{\sqrt{3}} \ln K_S \left( \frac{p_2}{p_3} \right) \\
 &= \ln \frac{\tilde{p}_*^2}{p_2 p_3} - \frac{4}{\sqrt{3}} \ln K_S \left( \frac{p_2}{p_3} \right) \\
 &< \ln \frac{p_2^2}{p_2 p_3} - \frac{4}{\sqrt{3}} \ln K_S \left( \frac{p_2}{p_3} \right) \\
 &= \ln \frac{p_2}{p_3} - \frac{4}{\sqrt{3}} \ln K_S \left( \frac{p_2}{p_3} \right) \\
 &= \frac{4}{\sqrt{3}} \left( \frac{\sqrt{3}}{4} \ln \frac{p_2}{p_3} - \ln K_S \left( \frac{p_2}{p_3} \right) \right) \\
 &= \frac{4}{\sqrt{3}} \left( \ln K_R \left( \frac{p_2}{p_3} \right) - \ln K_S \left( \frac{p_2}{p_3} \right) \right) = \frac{4}{\sqrt{3}} \ln \frac{K_R \left( \frac{p_2}{p_3} \right)}{K_S \left( \frac{p_2}{p_3} \right)} < 0.
 \end{aligned}$$

We prove part (c)<sub>iv</sub>, using (7.47)

$$\begin{aligned}
 \Delta Q(t_1) &= \ln \frac{\tilde{p}_*}{p_1} \cdot \ln \frac{\tilde{p}_*}{p_3} - \ln \frac{p_2}{p_1} \cdot \frac{4}{\sqrt{3}} \ln K_S \left( \frac{p_2}{p_3} \right) \\
 &< \ln \frac{p_2}{p_1} \cdot \ln \frac{p_2}{p_3} - \ln \frac{p_2}{p_1} \cdot \frac{4}{\sqrt{3}} \ln K_S \left( \frac{p_2}{p_3} \right) \\
 &= \frac{4}{\sqrt{3}} \cdot \ln \frac{p_2}{p_1} \left( \frac{\sqrt{3}}{4} \ln \frac{p_2}{p_3} - \ln K_S \left( \frac{p_2}{p_3} \right) \right) \\
 &= \frac{4}{\sqrt{3}} \cdot \ln \frac{p_2}{p_1} \left( \ln K_R \left( \frac{p_2}{p_3} \right) - \ln K_S \left( \frac{p_2}{p_3} \right) \right) \\
 &= \ln \frac{p_2}{p_1} \cdot \frac{4}{\sqrt{3}} \ln \frac{K_R \left( \frac{p_2}{p_3} \right)}{K_S \left( \frac{p_2}{p_3} \right)} < 0.
 \end{aligned}$$

This complete the proof of this part. □

Finally consider the case (d)<sub>i,ii,iii,iv</sub> where  $ne_1$  interacts with  $S_1$ , the interaction is depicted in Figure 7.3(VII). According to Lemma 6.2.3 (a) and Lemma 3.3.5 (1) we have

$$\text{for } ne_1 : \alpha_1 = \frac{p_2}{p_1} < 1, \text{ i.e. } p_2 < p_1, \quad \beta_1 = \frac{\sqrt{1+u_2^2} - u_2}{\sqrt{1+u_1^2} - u_1} = K_S(\alpha_1), \tag{7.49}$$

$$\text{for } S_1 : \alpha_2 = \frac{p_3}{p_2} > 1, \text{ i.e. } p_3 > p_2, \quad \beta_2 = \frac{\sqrt{1+u_3^2} - u_3}{\sqrt{1+u_2^2} - u_2} = K_S(\alpha_2).$$

## CHAPTER 7. BASIC ESTIMATES FOR THE FRONT TRACKING ALGORITHM FOR THE ULTRA-RELATIVISTIC EULER EQUATIONS

---

Hence  $p_2 < \min(p_1, p_3)$  and  $p_3 > p_1$ , i.e.  $\alpha > 1$ . To prove this part we show that the initial data (6.13) satisfies the statements of case 2 of the front tracking Riemann solution. So we only have to check that

$$\beta > K_S(\alpha) \quad \text{and} \quad \beta K_S(\alpha) > 1. \quad (7.50)$$

Regarding  $p_2 < \min(p_1, p_3)$  and  $p_3 > p_1$ , we obtain from (7.49) and Lemma 5.3.1

$$\begin{aligned} \beta = \beta_2 \beta_1 &= K_S\left(\frac{p_2}{p_1}\right) K_S\left(\frac{p_3}{p_2}\right) > K_S\left(\frac{p_2}{p_1}\right) K_S\left(\frac{p_3}{p_1}\right) K_S\left(\frac{p_1}{p_2}\right) \\ &= K_S\left(\frac{p_3}{p_1}\right) = K_S(\alpha), \end{aligned}$$

and from Lemma 5.3.2 (a)

$$\begin{aligned} \beta K_S(\alpha) &= K_S\left(\frac{p_2}{p_1}\right) K_S\left(\frac{p_3}{p_2}\right) K_S\left(\frac{p_3}{p_1}\right) \\ &> K_S\left(\frac{p_2}{p_1}\right) K_S\left(\frac{p_1}{p_2}\right) = 1. \end{aligned}$$

We prove part (d)<sub>ii</sub> corresponding to the interaction  $ne_1 S_1 \rightarrow S'_1 S'_3$ . The part (d)<sub>i</sub> gives the outgoing front tracking Riemann solution in region 2. Hence we use (3.76) and conclude that

$$p_2 < \min(p_1, p_3), \quad p_3 > p_1, \quad p_* > \max(p_1, p_3) \quad \text{and} \quad (7.51)$$

$$K_S\left(\frac{p_2}{p_1}\right) K_S\left(\frac{p_3}{p_2}\right) = K_S\left(\frac{\tilde{p}_*}{p_1}\right) K_S\left(\frac{\tilde{p}_*}{p_3}\right). \quad (7.52)$$

Using monotonicity of the function  $K_S$ , one can easily show

$$\tilde{p}_* < \frac{p_1 p_3}{p_2}. \quad (7.53)$$

Recall that  $Str(ne_1) = \frac{4}{\sqrt{3}} \ln K_S\left(\frac{p_1}{p_2}\right)$  along  $ne_1$  and  $Str(S_1) = \ln \frac{p_3}{p_2}$  along  $S_1$ . We want to prove

$$\frac{4}{\sqrt{3}} \ln K_S\left(\frac{p_1}{p_2}\right) + \ln \frac{p_3}{p_2} > \ln \frac{\tilde{p}_*}{p_1} + \ln \frac{\tilde{p}_*}{p_3}. \quad (7.54)$$

To justify this inequality, using Lemma 5.2.3 (a) and (7.53) we only have to check that

$$\begin{aligned} \frac{4}{\sqrt{3}} \ln K_R\left(\frac{p_1}{p_2}\right) + \ln \frac{p_3}{p_2} &> \ln \frac{\tilde{p}_*}{p_1} + \ln \frac{\tilde{p}_*}{p_3} &\iff \\ \ln \frac{p_1}{p_2} + \ln \frac{p_3}{p_2} &> \ln \frac{\tilde{p}_*}{p_1} + \ln \frac{\tilde{p}_*}{p_3} &\iff \\ \ln \frac{p_1 p_3}{p_2^2} &> \ln \frac{\tilde{p}_*^2}{p_1 p_3} &\iff \\ \frac{p_1 p_3}{p_2} &> \tilde{p}_*. \end{aligned}$$



We prove part (d)<sub>iii</sub>, using (7.53)

$$\begin{aligned}
 \Delta V(t_1) &= \ln \frac{\tilde{p}_*}{p_1} + \ln \frac{\tilde{p}_*}{p_3} - \ln \frac{p_3}{p_2} - \frac{4}{\sqrt{3}} \ln K_S \left( \frac{p_1}{p_2} \right) \\
 &= \ln \frac{\tilde{p}_*^2}{p_1 p_3} - \frac{4}{\sqrt{3}} \ln K_S \left( \frac{p_1}{p_2} \right) \\
 &< \ln \frac{p_1^2}{p_1 p_2} - \frac{4}{\sqrt{3}} \ln K_S \left( \frac{p_1}{p_2} \right) \\
 &= \ln \frac{p_1}{p_2} - \frac{4}{\sqrt{3}} \ln K_S \left( \frac{p_1}{p_2} \right) \\
 &= \frac{4}{\sqrt{3}} \left( \frac{\sqrt{3}}{4} \ln \frac{p_1}{p_2} - \ln K_S \left( \frac{p_1}{p_2} \right) \right) \\
 &= \frac{4}{\sqrt{3}} \left( \ln K_R \left( \frac{p_1}{p_2} \right) - \ln K_S \left( \frac{p_1}{p_2} \right) \right) = \frac{4}{\sqrt{3}} \ln \frac{K_R \left( \frac{p_1}{p_2} \right)}{K_S \left( \frac{p_1}{p_2} \right)} < 0.
 \end{aligned}$$

We prove part (d)<sub>iv</sub>, using (7.53)

$$\begin{aligned}
 \Delta Q(t_1) &= \ln \frac{\tilde{p}_*}{p_1} \cdot \ln \frac{\tilde{p}_*}{p_3} - \ln \frac{p_3}{p_2} \cdot \frac{4}{\sqrt{3}} \ln K_S \left( \frac{p_1}{p_2} \right) \\
 &< \ln \frac{p_3}{p_2} \cdot \ln \frac{p_1}{p_2} - \ln \frac{p_3}{p_2} \cdot \frac{4}{\sqrt{3}} \ln K_S \left( \frac{p_1}{p_2} \right) \\
 &= \frac{4}{\sqrt{3}} \cdot \ln \frac{p_3}{p_2} \left( \frac{\sqrt{3}}{4} \ln \frac{p_1}{p_2} - \ln K_S \left( \frac{p_1}{p_2} \right) \right) \\
 &= \frac{4}{\sqrt{3}} \cdot \ln \frac{p_3}{p_2} \left( \ln K_R \left( \frac{p_1}{p_2} \right) - \ln K_S \left( \frac{p_1}{p_2} \right) \right) \\
 &= \ln \frac{p_3}{p_2} \cdot \frac{4}{\sqrt{3}} \ln \frac{K_R \left( \frac{p_1}{p_2} \right)}{K_S \left( \frac{p_1}{p_2} \right)} < 0.
 \end{aligned}$$

This completes the proof of this part. Hence the proof of the proposition is completed.

### 7.2.3 The cases with conservation of strength in the limit

In this section we show that the strength is conserved in the limit for the interactions of entropy shocks of the same family:  $S_3 \tilde{S}_3$ ,  $S_1 \tilde{S}_1$ . In Proposition 5.3.4 we studied these two interaction. We show that these cases dealing with the cases of conservation of strength also we determine the type of the outgoing Riemann solution, namely  $S_3 \tilde{S}_3 \rightarrow R'_1 S'_3$  and  $S_1 \tilde{S}_1 \rightarrow S'_1 R'_3$ . Here the situation is different due to the discretization of rarefaction fans. It is well known that the total variation (strength) can increase as a result of wave interaction. However, if the total variation is small, this increase is compensated by the decrease of the wave interaction potential, as we will see in this section.

CHAPTER 7. BASIC ESTIMATES FOR THE FRONT TRACKING  
ALGORITHM FOR THE ULTRA-RELATIVISTIC EULER EQUATIONS

---

**Proposition 7.2.5.** *Given three states  $(p_j, u_j) \in \mathbb{R}^+ \times \mathbb{R}$ ,  $j = 1, 2, 3$ . Assume that, as depicted in Figure 7.4, the states  $(p_1, u_1)$  and  $(p_2, u_2)$  as well as  $(p_2, u_2)$  and  $(p_3, u_3)$  can be connected by a lower shock  $S_3$  (resp.  $S_1$ ) and an upper shock  $\tilde{S}_3$  (resp.  $\tilde{S}_1$ ), respectively, starting at  $t = 0$  on the  $t - x$  plane which interact. Let the weak solution of (3.6) be continued across the point of intersection at time  $t = t_1$  of lower and upper generalized shocks. Define  $\alpha_1 = \frac{p_2}{p_1}$ ,  $\alpha_2 = \frac{p_3}{p_2}$ . Let the solution be extended across the point of intersection. Then the following estimates are valid for the corresponding interactions.*

(a)<sub>I</sub>  $S_3\tilde{S}_3 \rightarrow ne'_1s$ ,  $ne'_1s$  is a family  $N$  of  $ne_1$  shocks with

(a)<sub>II</sub>

$$Str(S_3) + Str(\tilde{S}_3) < Str(S'_1) + \sum_{i=1}^N Str((ne'_1)_i),$$

(a)<sub>III</sub>

$$\Delta V(t_1) < \frac{4}{\sqrt{3}} N \ln \frac{K_R \left( \left( \frac{p_2}{p_1} \right)^{\frac{1}{N}} \right)}{K_S \left( \left( \frac{p_2}{p_1} \right)^{\frac{1}{N}} \right)} > 0, \quad (7.55)$$

(a)<sub>IV</sub>

$$\Delta Q(t_1) < \ln \frac{p_3}{p_2} \cdot \frac{4}{\sqrt{3}} N \ln \frac{K_R \left( \left( \frac{p_2}{p_1} \right)^{\frac{1}{N}} \right)}{K_S \left( \left( \frac{p_2}{p_1} \right)^{\frac{1}{N}} \right)} < 0, \quad (7.56)$$

(b)<sub>I</sub>  $S_1\tilde{S}_1 \rightarrow S'_1 ne'_3s$ ,  $ne'_3s$  is a family  $M$  of  $ne_3$  shocks with

(b)<sub>II</sub>

$$Str(S_1) + Str(\tilde{S}_1) < \sum_{i=1}^M Str((ne'_3)_i) + Str(S'_1),$$

(b)<sub>III</sub>

$$\Delta V(t_1) < \frac{4}{\sqrt{3}} M \ln \frac{K_R \left( \left( \frac{p_2}{p_3} \right)^{\frac{1}{M}} \right)}{K_S \left( \left( \frac{p_2}{p_3} \right)^{\frac{1}{M}} \right)} > 0, \quad (7.57)$$

(b)<sub>IV</sub>

$$\Delta Q(t_1) < \ln \frac{p_1}{p_2} \cdot \frac{4}{\sqrt{3}} M \ln \frac{K_R \left( \left( \frac{p_2}{p_3} \right)^{\frac{1}{M}} \right)}{K_S \left( \left( \frac{p_2}{p_3} \right)^{\frac{1}{M}} \right)} < 0. \quad (7.58)$$

## 7.2. INTERACTION ESTIMATES

*Proof.* We consider the case where  $S_3$  interacts with  $\tilde{S}_3$ , the interaction is depicted in Figure 7.4<sub>(IX)</sub>. According to Lemma 3.3.5 (2) we have

$$\text{for } S_3 : \alpha_1 = \frac{p_2}{p_1} < 1, \text{ i.e. } p_2 < p_1, \quad \beta_1 = \frac{\sqrt{1+u_2^2} - u_2}{\sqrt{1+u_1^2} - u_1} = K_S \left( \frac{1}{\alpha_1} \right), \quad (7.59)$$

$$\text{for } \tilde{S}_3 : \alpha_2 = \frac{p_3}{p_2} < 1, \text{ i.e. } p_3 < p_2, \quad \beta_2 = \frac{\sqrt{1+u_3^2} - u_3}{\sqrt{1+u_2^2} - u_2} = K_S \left( \frac{1}{\alpha_2} \right).$$

Hence  $p_1 > p_2 > p_3$ , i.e.  $\alpha < 1$ . To prove this part we show that the initial data (6.13) satisfies the statements of case 3 of the front tracking Riemann solution. So we only have to check that

$$\beta > K_S \left( \alpha^{\frac{1}{N}} \right)^N \quad \text{and} \quad \beta K_S(\alpha) < 1. \quad (7.60)$$

Regarding  $p_1 > p_2 > p_3$ , we obtain from (7.59) and Lemma 5.3.1

$$\beta = \beta_2 \beta_1 = K_S \left( \frac{p_1}{p_2} \right) K_S \left( \frac{p_2}{p_3} \right) > K_S \left( \alpha^{\frac{1}{N}} \right)^N,$$

$$\beta K_S(\alpha) = K_S \left( \frac{p_1}{p_2} \right) K_S \left( \frac{p_2}{p_3} \right) K_S \left( \frac{p_3}{p_1} \right) < K_S \left( \frac{p_1}{p_3} \right) K_S \left( \frac{p_3}{p_1} \right) = 1.$$

We prove part (a)<sub>II</sub>. The part (a)<sub>I</sub> gives the outcoming front tracking Riemann solution in region 3. Hence we use (6.20) and conclude that

$$p_1 > p_2 > p_3, \quad p_1 > p_* > p_3. \quad (7.61)$$

Recall that  $Str(S_3) = \ln \frac{p_1}{p_2}$  along  $S_3$  and  $Str(\tilde{S}_3) = \ln \frac{p_2}{p_3}$  along  $\tilde{S}_3$ . Regarding  $p_1 > p_* > p_3$  and Lemma 5.2.3 (a) We have

$$\begin{aligned} Str(S_3) + Str(\tilde{S}_3) &< Str(S'_1) + \sum_{i=1}^N Str((ne'_1)_i) \iff \\ \ln \frac{p_1}{p_2} + \ln \frac{p_2}{p_3} &< \ln \frac{\tilde{p}_*}{p_3} + \frac{4}{\sqrt{3}} \ln K_S \left( \left( \frac{p_1}{\tilde{p}_*} \right)^{\frac{1}{N}} \right)^N \iff \\ \ln \frac{p_1}{\tilde{p}_*} &< \frac{4}{\sqrt{3}} \ln K_S \left( \left( \frac{p_1}{\tilde{p}_*} \right)^{\frac{1}{N}} \right)^N \iff \\ \ln \left( \frac{p_1}{\tilde{p}_*} \right)^{\frac{\sqrt{3}}{4}} &< \ln K_S \left( \left( \frac{p_1}{\tilde{p}_*} \right)^{\frac{1}{N}} \right)^N \iff \\ K_R \left( \frac{p_1}{\tilde{p}_*} \right) &< K_S \left( \left( \frac{p_1}{\tilde{p}_*} \right)^{\frac{1}{N}} \right)^N \iff \\ K_R \left( \left( \frac{p_1}{\tilde{p}_*} \right)^{\frac{1}{N}} \right)^N &< K_S \left( \left( \frac{p_1}{\tilde{p}_*} \right)^{\frac{1}{N}} \right)^N. \end{aligned}$$

CHAPTER 7. BASIC ESTIMATES FOR THE FRONT TRACKING  
ALGORITHM FOR THE ULTRA-RELATIVISTIC EULER EQUATIONS

---

We prove part (a)<sub>III</sub>

$$\begin{aligned}
\Delta V(t_1) &= \ln \frac{\tilde{p}_*}{p_3} + \frac{4}{\sqrt{3}} \ln K_S \left( \left( \frac{p_1}{\tilde{p}_*} \right)^{\frac{1}{N}} \right)^N - \ln \frac{p_2}{p_3} - \ln \frac{p_1}{p_2} \\
&= \frac{4}{\sqrt{3}} \ln K_S \left( \left( \frac{p_1}{\tilde{p}_*} \right)^{\frac{1}{N}} \right)^N - \ln \frac{p_1}{\tilde{p}_*} \\
&< \frac{4}{\sqrt{3}} \ln K_S \left( \left( \frac{p_1}{p_2} \right)^{\frac{1}{N}} \right)^N - \ln \frac{p_1}{p_2} \\
&= \frac{4}{\sqrt{3}} \left( \ln K_S \left( \left( \frac{p_1}{p_2} \right)^{\frac{1}{N}} \right)^N - \frac{\sqrt{3}}{4} \ln \frac{p_1}{p_2} \right) \\
&= \frac{4}{\sqrt{3}} \left( \ln K_S \left( \left( \frac{p_1}{p_2} \right)^{\frac{1}{N}} \right)^N - \ln K_R \left( \frac{p_1}{p_2} \right) \right) \\
&= \frac{4}{\sqrt{3}} \left( \ln K_S \left( \left( \frac{p_1}{p_2} \right)^{\frac{1}{N}} \right)^N - \ln K_R \left( \left( \frac{p_1}{p_2} \right)^{\frac{1}{N}} \right)^N \right) \\
&= \frac{4}{\sqrt{3}} N \cdot \ln \frac{K_R \left( \left( \frac{p_2}{p_1} \right)^{\frac{1}{N}} \right)}{K_S \left( \left( \frac{p_2}{p_1} \right)^{\frac{1}{N}} \right)} > 0.
\end{aligned}$$

We prove part (a)<sub>IV</sub>

$$\begin{aligned}
\Delta Q(t_1) &= \ln \frac{\tilde{p}_*}{p_3} \cdot \frac{4}{\sqrt{3}} \ln K_S \left( \left( \frac{p_1}{\tilde{p}_*} \right)^{\frac{1}{N}} \right)^N - \ln \frac{p_2}{p_3} \cdot \ln \frac{p_1}{p_2} \\
&< \frac{4}{\sqrt{3}} \cdot \ln \frac{p_3}{p_2} \left( \ln K_S \left( \left( \frac{p_1}{p_2} \right)^{\frac{1}{N}} \right)^N - \frac{\sqrt{3}}{4} \ln \frac{p_1}{p_2} \right) \\
&= \frac{4}{\sqrt{3}} \cdot \ln \frac{p_3}{p_2} \left( \ln K_S \left( \left( \frac{p_1}{p_2} \right)^{\frac{1}{N}} \right)^N - \ln K_R \left( \frac{p_1}{p_2} \right) \right) \\
&= \frac{4}{\sqrt{3}} \cdot \ln \frac{p_3}{p_2} \left( \ln K_S \left( \left( \frac{p_1}{p_2} \right)^{\frac{1}{N}} \right)^N - \ln K_R \left( \left( \frac{p_1}{p_2} \right)^{\frac{1}{N}} \right)^N \right) \\
&= \ln \frac{p_3}{p_2} \cdot \frac{4}{\sqrt{3}} N \cdot \ln \frac{K_R \left( \left( \frac{p_2}{p_1} \right)^{\frac{1}{N}} \right)}{K_S \left( \left( \frac{p_2}{p_1} \right)^{\frac{1}{N}} \right)} < 0.
\end{aligned}$$

## 7.2. INTERACTION ESTIMATES

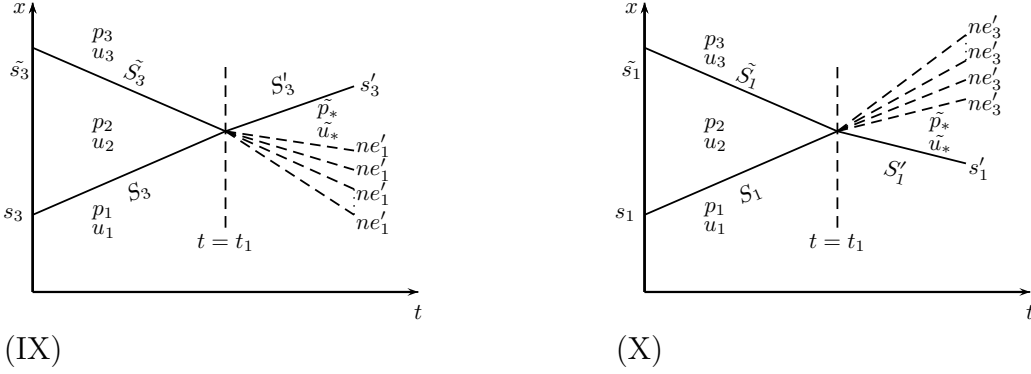


Figure 7.4: Interaction of entropy shocks of the same family.

This completes the proof of this part. We prove part (b)<sub>I</sub> where  $S_1$  interacts with  $\tilde{S}_1$ , the interaction is depicted in Figure 7.4<sub>(X)</sub>. According to Lemma 3.3.5 (1) we have

$$\text{for } S_1 : \alpha_1 = \frac{p_2}{p_1} > 1, \text{ i.e. } p_2 > p_1, \quad \beta_1 = \frac{\sqrt{1+u_2^2} - u_2}{\sqrt{1+u_1^2} - u_1} = K_S(\alpha_1), \quad (7.62)$$

$$\text{for } \tilde{S}_1 : \alpha_2 = \frac{p_3}{p_2} > 1, \text{ i.e. } p_3 > p_2, \quad \beta_2 = \frac{\sqrt{1+u_3^2} - u_3}{\sqrt{1+u_2^2} - u_2} = K_S(\alpha_2).$$

Hence  $p_3 > p_2 > p_1$ , i.e.  $\alpha > 1$ . To prove this part we show that the initial data (6.13) satisfies the statements of case 1 of the front tracking Riemann solution. So we only have to check that

$$\beta < K_S(\alpha) \quad \text{and} \quad \beta K_S\left(\alpha^{\frac{1}{M}}\right)^M > 1. \quad (7.63)$$

Regarding  $p_3 > p_2 > p_1$ , we obtain from (7.62) and from Lemma 5.3.1

$$\beta = \beta_2 \beta_1 = K_S\left(\frac{p_2}{p_1}\right) K_S\left(\frac{p_3}{p_2}\right) < K_S\left(\frac{p_3}{p_1}\right) = K_S(\alpha),$$

$$\beta K_S(\alpha^{\frac{1}{M}})^M = K_S\left(\frac{p_2}{p_1}\right) K_S\left(\frac{p_3}{p_2}\right) K_S\left(\alpha^{\frac{1}{M}}\right)^M > 1.$$

We prove part (b)<sub>II</sub>. The part (a)<sub>I</sub> gives the outgoing front tracking Riemann solution in region 1. Hence we use (6.17) and conclude that

$$p_3 > p_2 > p_1 \quad \text{and} \quad p_3 > p_* > p_1. \quad (7.64)$$

Recall that  $Str(S_1) = \ln \frac{p_2}{p_1}$  along  $S_1$  and  $Str(\tilde{S}_1) = \ln \frac{p_3}{p_2}$  along  $\tilde{S}_1$ . Regarding  $p_3 > p_* > p_1$

CHAPTER 7. BASIC ESTIMATES FOR THE FRONT TRACKING  
ALGORITHM FOR THE ULTRA-RELATIVISTIC EULER EQUATIONS

---

and Lemma 5.2.3 (a) We have

$$\begin{aligned}
Str(S_1) + Str(\tilde{S}1) &< \sum_{i=1}^M Str((ne'_3)_i) + Str(S'_3) \iff \\
\ln \frac{p_2}{p_1} + \ln \frac{p_3}{p_2} &< \ln \frac{\tilde{p}_*}{p_1} + \frac{4}{\sqrt{3}} \ln K_S \left( \left( \frac{p_3}{\tilde{p}_*} \right)^{\frac{1}{M}} \right)^M \iff \\
\ln \frac{p_3}{\tilde{p}_*} &< \frac{4}{\sqrt{3}} \ln K_S \left( \left( \frac{p_3}{\tilde{p}_*} \right)^{\frac{1}{M}} \right)^M \iff \\
\ln \left( \frac{p_3}{\tilde{p}_*} \right)^{\frac{\sqrt{3}}{4}} &< \ln K_S \left( \left( \frac{p_3}{\tilde{p}_*} \right)^{\frac{1}{M}} \right)^M \iff \\
K_R \left( \left( \frac{p_3}{\tilde{p}_*} \right)^{\frac{1}{M}} \right)^M &< K_S \left( \left( \frac{p_3}{\tilde{p}_*} \right)^{\frac{1}{M}} \right)^M \iff \\
K_R \left( \left( \frac{p_3}{\tilde{p}_*} \right)^{\frac{1}{M}} \right) &< K_S \left( \left( \frac{p_3}{\tilde{p}_*} \right)^{\frac{1}{M}} \right).
\end{aligned}$$

We prove part (b)<sub>III</sub>

$$\begin{aligned}
\Delta V(t_1) &= \ln \frac{\tilde{p}_*}{p_1} + \frac{4}{\sqrt{3}} \ln K_S \left( \left( \frac{p_3}{\tilde{p}_*} \right)^{\frac{1}{M}} \right)^M - \ln \frac{p_3}{p_2} - \ln \frac{p_2}{p_1} \\
&= \frac{4}{\sqrt{3}} \ln K_S \left( \left( \frac{p_3}{\tilde{p}_*} \right)^{\frac{1}{M}} \right)^M - \ln \frac{p_3}{\tilde{p}_*} \\
&< \frac{4}{\sqrt{3}} \ln K_S \left( \left( \frac{p_3}{p_2} \right)^{\frac{1}{M}} \right)^M - \ln \frac{p_3}{p_2} \\
&= \frac{4}{\sqrt{3}} \left( \ln K_S \left( \left( \frac{p_3}{p_2} \right)^{\frac{1}{M}} \right)^M - \frac{\sqrt{3}}{4} \ln \frac{p_3}{p_2} \right) \\
&= \frac{4}{\sqrt{3}} \left( \ln K_S \left( \left( \frac{p_3}{p_2} \right)^{\frac{1}{M}} \right)^M - \ln K_R \left( \frac{p_3}{p_2} \right) \right) \\
&= \frac{4}{\sqrt{3}} \left( \ln K_S \left( \left( \frac{p_3}{p_2} \right)^{\frac{1}{M}} \right)^M - \ln K_R \left( \left( \frac{p_3}{p_2} \right)^{\frac{1}{M}} \right)^M \right) \\
&= \frac{4}{\sqrt{3}} M \cdot \ln \frac{K_R \left( \left( \frac{p_2}{p_3} \right)^{\frac{1}{M}} \right)}{K_S \left( \left( \frac{p_2}{p_3} \right)^{\frac{1}{M}} \right)} > 0.
\end{aligned}$$

We prove part (b)<sub>IV</sub>

$$\begin{aligned}
 \Delta Q(t_1) &= \ln \frac{\tilde{p}_*}{p_1} \cdot \frac{4}{\sqrt{3}} \ln K_S \left( \left( \frac{p_3}{\tilde{p}_*} \right)^{\frac{1}{M}} \right)^M - \ln \frac{p_3}{p_2} \cdot \ln \frac{p_2}{p_1} \\
 &< \frac{4}{\sqrt{3}} \cdot \ln \frac{p_1}{p_2} \left( \ln K_S \left( \left( \frac{p_3}{p_2} \right)^{\frac{1}{M}} \right)^M - \frac{\sqrt{3}}{4} \ln \frac{p_3}{p_2} \right) \\
 &= \frac{4}{\sqrt{3}} \cdot \ln \frac{p_1}{p_2} \left( \ln K_S \left( \left( \frac{p_3}{p_2} \right)^{\frac{1}{M}} \right)^M - \ln K_R \left( \frac{p_3}{p_2} \right) \right) \\
 &= \frac{4}{\sqrt{3}} \cdot \ln \frac{p_1}{p_2} \left( \ln K_S \left( \left( \frac{p_3}{p_2} \right)^{\frac{1}{M}} \right)^M - \ln K_R \left( \left( \frac{p_3}{p_2} \right)^{\frac{1}{M}} \right)^M \right) \\
 &= \ln \frac{p_1}{p_2} \cdot \frac{4}{\sqrt{3}} M \cdot \ln \frac{K_R \left( \left( \frac{p_2}{p_3} \right)^{\frac{1}{M}} \right)}{K_S \left( \left( \frac{p_2}{p_3} \right)^{\frac{1}{M}} \right)} < 0.
 \end{aligned}$$

This completes the proof of the proposition. □





---

## Chapter 8

# Conclusions and Outlook

In this thesis, we studied the ultra-relativistic Euler equations for an ideal gas, which is a system of nonlinear hyperbolic conservation laws. The single shocks and rarefaction waves parametrizations and the Riemann solution were given. Especially we developed an own parametrization for single shocks, which used to derive a new explicit shock interaction formula. This shock interaction formula plays an important role in the study of the ultra-relativistic Euler equations.

We described the cone-grid scheme for the ultra-relativistic Euler equations numerically. This new scheme is based on the Riemann solution for the ultra-relativistic Euler system, it is unconditionally stable. The cone-grid scheme preserve the properties like conservations laws, entropy inequality, positivity.

We presented a system of hyperbolic system of conservation laws, which is equivalent to the ultra-relativistic Euler equations, which describes a phonon-Bose gas in terms of the energy density  $e$  and the heat flux  $Q$ . Then we given numerical test cases for the solution of the phonon-Bose equations, using cone-grid scheme.

We study the uniqueness problem of the Riemann solution. We also study the problem of the non-backward uniqueness of the ultra-relativistic Euler system (3.6). We give an interesting example to show that there is no backward uniqueness for our system.

We studied the interactions between nonlinear waves for the ultra-relativistic Euler equations (3.6) in its weak form (3.18), (3.19). More precisely, we study the interactions between shocks and rarefaction waves in terms of the new strength function  $S(\alpha, \beta)$  and obtain that the strength after interactions is non increasing. One basic ingredient of our analysis is the explicit algebraic formula for the intermediate pressure  $p_*$  in Propositions 4.3.1 and 5.3.3. This formula holds only for special kind of interactions which leads to a conserved strength after the interactions, whereas in the other cases we obtain algebraic inequalities for  $p_*$ , which are important as well. The cases where the strength is conserved after interaction is given in Proposition 5.3.4, whereas in the remaining cases the strength turns out to be strictly decreasing, see Proposition 5.3.5.

## CHAPTER 8. CONCLUSIONS AND OUTLOOK

---

The interpretation of the strength for the Riemann solution for system (3.6) is also given. This enables us to define a new kind of total variation of the approximate solutions of the ultra-relativistic Euler equations.

A new front tracking technique for the ultra-relativistic Euler equations (3.1) in one space dimension is presented. This method is based on the front tracking Riemann solution. In this Riemann solution we approximated a continuous rarefaction waves by a finite collection of discontinuities, so called non-entropy shocks (fronts). So this scheme is based on approximations to the solutions of the local Riemann problems, where the solution is represented by constant states separated by straight line shock segments. Now we give our algorithm, which can be simply reviewed as the following:

1. At the starting time  $t = 0$  the initial data is approximated by a piecewise constant function having a finite number of jumps. Then we solve the Riemann problems arising at each discontinuity point, which given in Section 6.2, where we replace the continuous rarefaction waves by a finite collection of discontinuities, called non-entropy shocks (fronts). Also we give all new states after these discretization in Section 6.2. The number of these discontinuities given in (6.18).
2. The solution procedure for an initial value problem takes care for the interaction of these shock segments of the neighboring local Riemann problems. At each intersection point the discontinuous solution is again equal to the initial conditions of a new local Riemann problem. The straight line shocks can again intersect with each other and so on.

We have numerically implemented the one-dimensional front tracking and cone-grid schemes. The CFL condition for both is very simple, which is  $\Delta x = 2\Delta t$ . This CFL condition comes out automatically due to the structure of light cones, since every signal speed is bounded by the velocity of light.

The theory presented in this thesis may give useful impacts for the analytical as well as the numerical study of more realistic gas dynamical models in relativity.

In the following we mention some of the future work and open problems in relation to our work, which we will study in the postdoctoral program.

- It would be interesting to implement the cone-grid scheme for the ultra-relativistic Euler equations in two and three dimensions.
- Using the new strength function  $S(\alpha, \beta)$  as a measure of wave strength and the results of interaction between nonlinear waves for the ultra-relativistic Euler equations (3.6) in Chapter 5, we can easily produce estimates on approximate solutions constructed using the Glimm scheme in the same way as in [67, 75, 81].

- 
- It is also so interesting to implement the front tracking scheme for the ultra-relativistic Euler equations in two dimensions.
  - Based on the interaction estimates of the generalized shocks given in Chapter 7 we can prove the existence of the approximate solution, which construct in Chapter 6.
  - Also, we plan to apply the front tracking scheme to the classical Euler equations, by construct a new function similar to  $S(\alpha, \beta)$ , which measures the strengths of the waves in the Riemann solution in a natural way.



---

# Appendix A

## The Lorentz Invariance of the Ultra-Relativistic Euler Equations

In this appendix we will give some basic facts about Lorentz transformations. This is needed for the derivation of the parametrization of single shocks. These facts also show the invariance of the ultra-relativistic Euler system (3.6) as well as the Rankine-Hugoniot conditions (3.23).

**Proposition A.0.6.** *For given  $u_0 \in \mathbb{R}$  we define the one-parameter group of spatial one-dimensional Lorentz-transformations (homogeneous)*

$$\Lambda(u_0) := \begin{pmatrix} \sqrt{1+u_0^2} & -u_0 \\ -u_0 & \sqrt{1+u_0^2} \end{pmatrix},$$

with  $\lambda(0) = \begin{pmatrix} 1 & 0 \\ 0 & 1 \end{pmatrix}$ ,  $\Lambda(-u_0) = \Lambda(u_0)^{-1}$  and the product

$$\Lambda(u_0) \cdot \Lambda(u_1) = \Lambda\left(u_1\sqrt{1+u_0^2} + u_0\sqrt{1+u_1^2}\right).$$

Let  $\alpha, \beta, \gamma, \delta \in \mathbb{R}$  and put

$$\begin{pmatrix} \alpha' \\ \beta' \end{pmatrix} = \Lambda(u_0) \begin{pmatrix} \alpha \\ \beta \end{pmatrix}, \quad \begin{pmatrix} \gamma' \\ \delta' \end{pmatrix} = \Lambda(u_0) \begin{pmatrix} \gamma \\ \delta \end{pmatrix}.$$

Then we obtain the following two Lorentz invariant quantities:

(ii) Invariance of  $\text{Det} \begin{pmatrix} \alpha & \gamma \\ \beta & \delta \end{pmatrix}$ :

$$\alpha\delta - \beta\gamma = \alpha'\delta' - \beta'\gamma'.$$

1. Invariance of Minkowski-metric:

$$\alpha^2 - \beta^2 = \alpha'^2 - \beta'^2,$$

and more general

$$\alpha\gamma - \beta\delta = \alpha'\gamma' - \beta'\delta'.$$

## APPENDIX A. THE LORENTZ INVARIANCE OF THE ULTRA-RELATIVISTIC EULER EQUATIONS

---

*Proof.* (i) We have in matrix-form

$$\begin{pmatrix} \alpha' & \gamma' \\ \beta' & \delta' \end{pmatrix} = \Lambda(u_0) \begin{pmatrix} \alpha & \gamma \\ \beta & \delta \end{pmatrix}$$

with

$$\text{Det } \Lambda(u_0) = \sqrt{1 + u_0^2}^2 - u_0^2 = 1,$$

and hence

$$\begin{aligned} \alpha'\delta' - \beta'\gamma' &= \text{Det} \begin{pmatrix} \alpha' & \gamma' \\ \beta' & \delta' \end{pmatrix} \\ &= \text{Det } \Lambda(u_0) \cdot \text{Det} \begin{pmatrix} \alpha & \gamma \\ \beta & \delta \end{pmatrix} \\ &= 1 \cdot (\alpha\delta - \beta\gamma). \end{aligned}$$

(ii)

$$\begin{pmatrix} \alpha' \\ \beta' \end{pmatrix} = \begin{pmatrix} \alpha \sqrt{1 + u_0^2} - \beta u_0 \\ -\alpha u_0 + \beta \sqrt{1 + u_0^2} \end{pmatrix}, \quad \begin{pmatrix} \gamma' \\ \delta' \end{pmatrix} = \begin{pmatrix} \gamma \sqrt{1 + u_0^2} - \delta u_0 \\ -\gamma u_0 + \delta \sqrt{1 + u_0^2} \end{pmatrix}.$$

Hence

$$\begin{aligned} \begin{pmatrix} \alpha' & \beta' \\ \delta' & \gamma' \end{pmatrix} &= \begin{pmatrix} \alpha \sqrt{1 + u_0^2} - \beta u_0 & -\alpha u_0 + \beta \sqrt{1 + u_0^2} \\ -\gamma u_0 + \delta \sqrt{1 + u_0^2} & \gamma \sqrt{1 + u_0^2} - \delta u_0 \end{pmatrix} \\ &= \begin{pmatrix} \alpha & \beta \\ \delta & \gamma \end{pmatrix} \cdot \begin{pmatrix} \sqrt{1 + u_0^2} & -u_0 \\ -u_0 & \sqrt{1 + u_0^2} \end{pmatrix}. \end{aligned}$$

Thus we have

$$\begin{aligned} \alpha'\gamma' - \beta'\delta' &= \text{Det} \begin{pmatrix} \alpha' & \beta' \\ \delta' & \gamma' \end{pmatrix} \\ &= \underbrace{\text{Det } \Lambda(u_0)}_{=1} \begin{pmatrix} \alpha & \beta \\ \delta & \gamma \end{pmatrix} \\ &= \alpha\gamma - \beta\delta. \end{aligned}$$

□

**Remark A.0.7.** We obtain a well defined abelian group  $(\Lambda(u_0), \cdot)$  for all  $u_0 \in \mathbb{R}$ .

**Definition A.0.8.** We say that a vector  $\begin{pmatrix} \alpha \\ \beta \end{pmatrix}$  with physical quantities  $\alpha, \beta$  given in a  $t, x$ -Lorentz-frame transforms like a Lorentz-vector, if  $\begin{pmatrix} \alpha' \\ \beta' \end{pmatrix} = \Lambda(u_0) \begin{pmatrix} \alpha \\ \beta \end{pmatrix}$  with the physical quantities  $\alpha', \beta'$  given in the new  $t', x'$ -Lorentz-frame, where  $\begin{pmatrix} t' \\ x' \end{pmatrix} = \Lambda(u_0) \begin{pmatrix} t \\ x \end{pmatrix} = \begin{pmatrix} t\sqrt{1 + u_0^2} - u_0x \\ -tu_0 + \sqrt{1 + u_0^2}x \end{pmatrix}$ .

---

**Remark A.0.9.** *Since we consider only homogeneous Lorentz-transformation here, the time-space vector  $\begin{pmatrix} t \\ x \end{pmatrix}$  is a Lorentz-vector by our definition.*

**Examples for Lorentz-vectors:**

**Example A.0.1.** *Any vector of the form  $\begin{pmatrix} \sqrt{1+u^2} \\ u \end{pmatrix}$ ,  $u \in \mathbb{R}$ , is a Lorentz-vector, since*

$$\Lambda(u_0) \begin{pmatrix} \sqrt{1+u^2} \\ u \end{pmatrix} = \begin{pmatrix} \sqrt{1+u_0^2}\sqrt{1+u^2} - u_0u \\ u\sqrt{1+u_0^2} - u_0\sqrt{1+u^2} \end{pmatrix} = \begin{pmatrix} \sqrt{1+u'^2} \\ u' \end{pmatrix}$$

with  $u' := u\sqrt{1+u_0^2} - u_0\sqrt{1+u^2}$ .

**Example A.0.2.** *If  $\begin{pmatrix} \alpha \\ \beta \end{pmatrix}$  is a Lorentz-vector, then also  $\begin{pmatrix} \beta \\ \alpha \end{pmatrix}$ .*

*Proof.*

$$\begin{pmatrix} \alpha' \\ \beta' \end{pmatrix} = \Lambda(u_0) \begin{pmatrix} \alpha \\ \beta \end{pmatrix} = \begin{pmatrix} \alpha\sqrt{1+u_0^2} - \beta u_0 \\ -\alpha u_0 + \beta\sqrt{1+u_0^2} \end{pmatrix},$$

and hence

$$\begin{pmatrix} \beta' \\ \alpha' \end{pmatrix} = \begin{pmatrix} \beta\sqrt{1+u_0^2} - \alpha u_0 \\ -\beta u_0 + \alpha\sqrt{1+u_0^2} \end{pmatrix} = \begin{pmatrix} \sqrt{1+u_0^2} & -u_0 \\ -u_0 & \sqrt{1+u_0^2} \end{pmatrix} \begin{pmatrix} \beta \\ \alpha \end{pmatrix} = \Lambda(u_0) \begin{pmatrix} \beta \\ \alpha \end{pmatrix}.$$

□

**Definition A.0.10.** *A matrix  $T \in \mathbb{R}^{2 \times 2}$  is called a  $2 \times 2$  Lorentz-tensor, if its entries are physical quantities given in a  $t, x$ -Lorentz-frame and if it transforms like*

$$T' = \Lambda(u_0)T\Lambda(u_0)$$

with  $T'$  given in the new  $t', x'$ -Lorentz-frame, where:

$$\begin{pmatrix} t' \\ x' \end{pmatrix} = \Lambda(u_0) \begin{pmatrix} t \\ x \end{pmatrix}.$$

**Example A.0.3.** *The matrix  $G := \begin{pmatrix} 1 & 0 \\ 0 & -1 \end{pmatrix}$  is a  $2 \times 2$  Lorentz-tensor with the same components in each Lorentz-frame, i.e.*

$$G' = \Lambda(u_0)G\Lambda(u_0) = G.$$

$G$  is called Einstein-Minkowski tensor.

## APPENDIX A. THE LORENTZ INVARIANCE OF THE ULTRA-RELATIVISTIC EULER EQUATIONS

---

*Proof.*

$$\begin{aligned} \begin{pmatrix} \sqrt{1+u_0^2} & -u_0 \\ -u_0 & \sqrt{1+u_0^2} \end{pmatrix} \begin{pmatrix} 1 & 0 \\ 0 & -1 \end{pmatrix} \begin{pmatrix} \sqrt{1+u_0^2} & -u_0 \\ -u_0 & \sqrt{1+u_0^2} \end{pmatrix} &= \\ \begin{pmatrix} \sqrt{1+u_0^2} & -u_0 \\ -u_0 & \sqrt{1+u_0^2} \end{pmatrix} \begin{pmatrix} \sqrt{1+u_0^2} & -u_0 \\ -u_0 & \sqrt{1+u_0^2} \end{pmatrix} &= \\ & \begin{pmatrix} 1 & 0 \\ 0 & -1 \end{pmatrix}. \end{aligned}$$

□

**Example A.0.4.** With the Lorentz-invariant pressure  $p$  and with the Lorentz-vector  $\begin{pmatrix} \sqrt{1+u^2} \\ u \end{pmatrix}$ , we form the energy-momentum tensor

$$T = p \begin{pmatrix} 3 + 4u^2 & 4u\sqrt{1+u^2} \\ 4u\sqrt{1+u^2} & 1 + 4u^2 \end{pmatrix}.$$

Then  $T$  is a  $2 \times 2$  Lorentz-tensor, i.e.

$$T' = \Lambda(u_0)T\Lambda(u_0)$$

with

$$T' = p \begin{pmatrix} 3 + 4u'^2 & 4u'\sqrt{1+u'^2} \\ 4u'\sqrt{1+u'^2} & 1 + 4u'^2 \end{pmatrix}$$

and

$$u' = u\sqrt{1+u_0^2} - u_0\sqrt{1+u^2}.$$

**Proposition A.0.11.** Given are the Lorentz-invariant pressure  $p$ , two Lorentz-vector  $\begin{pmatrix} \sqrt{1+u^2} \\ u \end{pmatrix}$ ,  $\begin{pmatrix} \sqrt{1+u_s^2} \\ u_s \end{pmatrix}$  and the energy-momentum tensor from example A.0.4

$$T = p \begin{pmatrix} 3 + 4u^2 & 4u\sqrt{1+u^2} \\ 4u\sqrt{1+u^2} & 1 + 4u^2 \end{pmatrix}.$$

Then the quantity

$$TG \begin{pmatrix} u_s \\ \sqrt{1+u_s^2} \end{pmatrix} = \begin{pmatrix} u_s p(3 + 4u^2) - 4pu\sqrt{1+u_s^2}\sqrt{1+u^2} \\ 4pu_s u\sqrt{1+u^2} - p\sqrt{1+u_s^2}(1 + 4u^2) \end{pmatrix}$$

is a Lorentz-vector.



---

*Proof.* From Examples A.0.2,A.0.3 and A.0.4 we obtain

$$\begin{aligned} T'G' \left( \frac{u'_s}{\sqrt{1+u'^2_s}} \right) &= \\ \Lambda(u_0)T\Lambda(u_0)G\Lambda(u_0) \left( \frac{u_s}{\sqrt{1+u^2_s}} \right) &= \\ \Lambda(u_0)TG \left( \frac{u_s}{\sqrt{1+u^2_s}} \right). \end{aligned}$$

□

### Invariance of the Rankine-Hugoniot conditions

Given are three Lorentz-vectors  $\begin{pmatrix} \sqrt{1+u^2_{\pm}} \\ u_{\pm} \end{pmatrix}$  and  $\begin{pmatrix} \sqrt{1+u^2_s} \\ u_s \end{pmatrix}$ . Put the Lorentz-tensor

$$T_{\pm} = p_{\pm} \begin{pmatrix} 3 + 4u^2_{\pm} & 4u_{\pm}\sqrt{1+u^2_{\pm}} \\ 4u_{\pm}\sqrt{1+u^2_{\pm}} & 1 + 4u^2_{\pm} \end{pmatrix},$$

where  $p_{\pm}$  are two Lorentz-invariant pressures. Then the statement

$$T_+G \left( \frac{u_s}{\sqrt{1+u^2_s}} \right) = T_-G \left( \frac{u_s}{\sqrt{1+u^2_s}} \right)$$

is Lorentz-invariant. This statement is either true in all Lorentz-frames or wrong in all Lorentz-frames.

**Remark A.0.12.** *This result will be used for the derivation of single shock parametrization.*



---

## Appendix B

# Mathematical Properties of the $3 \times 3$ Ultra-Relativistic Euler Equations

In order to investigate the mathematical properties of the system (3.1). We give the following proposition.

**Proposition B.0.13.** *The system (3.1) is strictly hyperbolic at  $(p, u, n)$  for  $p > 0$ ,  $u \in \mathbb{R}$  and  $n > 0$ . Furthermore, the first and third characteristic fields are genuinely non linear and the second is linearly degenerate.*

*Proof.* First we rewrite the conservation laws (3.1) as

$$W_t + D(W)W_x = 0, \tag{B.1}$$

then calculate the eigenvalues and eigenvectors in terms of these variables. These eigenvalues may first be obtained in the Lorentz rest frame where  $u = 0$ . To do this we rewrite (3.1) using the chain rule as

$$A(W)W_t + B(W)W_x = 0,$$

then we find  $D(W)$  by multiplying on the left by  $A^{-1}$  to get

$$W_t + [A^{-1}B](W)W_x = 0.$$

By the chain rule we have,

$$A(W) = \begin{pmatrix} 3 & 0 & 0 \\ 0 & 4p & 0 \\ 0 & 0 & 1 \end{pmatrix}$$

and

$$B(W) = \begin{pmatrix} 0 & 4p & 0 \\ 1 & 0 & 0 \\ 0 & n & 0 \end{pmatrix}.$$

## APPENDIX B. MATHEMATICAL PROPERTIES OF THE $3 \times 3$ ULTRA-RELATIVISTIC EULER EQUATIONS

---

Note that  $A(W)$  is invertible because for  $p > 0$ ,

$$\text{Det}[A(W)] = 12p \neq 0.$$

We have

$$A^{-1}(W) = \begin{pmatrix} \frac{1}{3} & 0 & 0 \\ 0 & \frac{1}{4p} & 0 \\ 0 & 0 & 1 \end{pmatrix}.$$

Therefore,

$$D(W) = [A^{-1}B](W) = \begin{pmatrix} 0 & \frac{4p}{3} & 0 \\ \frac{1}{4p} & 0 & 0 \\ 0 & n & 0 \end{pmatrix}.$$

We look for the roots of the characteristic polynomial,

$$\text{Det}[D(W) - \tilde{\lambda}I] = -\tilde{\lambda}(\tilde{\lambda}^2 - \frac{1}{3}) = 0.$$

There are three values of  $\lambda$ ,

$$\tilde{\lambda}_1 = \frac{-1}{\sqrt{3}} < \tilde{\lambda}_2 = 0 < \tilde{\lambda}_3 = \frac{1}{\sqrt{3}}.$$

Then using the relativistic additivity law for the velocities (2.21), we can easily obtain eigenvalues in the general Lorentz frame, which we rewrite as

$$\lambda_1 = \frac{2u\sqrt{1+u^2} - \sqrt{3}}{3+2u^2} < \lambda_2 = \frac{u}{\sqrt{1+u^2}} < \lambda_3 = \frac{2u\sqrt{1+u^2} + \sqrt{3}}{3+2u^2}.$$

Now, we show that the first and third characteristic fields are genuinely nonlinear and the second is linearly degenerate. To do this we need to find the eigenvectors of  $D(W)$ .

For  $\lambda_2$  we simply find

$$R_2(p, u, n) = (0, 0, 1).$$

After some calculation we get

$$R_1(p, u, n) = \left( \frac{4p}{3n}, \frac{-\sqrt{1+u^2}}{\sqrt{3}n}, 1 \right),$$

and

$$R_3(p, u, n) = \left( \frac{4p}{3n}, \frac{\sqrt{1+u^2}}{\sqrt{3}n}, 1 \right).$$

Computing the gradients of the characteristic fields with respect to  $W = (p, u, n)$ ,

---


$$\begin{aligned}\nabla\lambda_1 &= \left(0, \frac{2((\sqrt{1+u^2} + \sqrt{3}u)^2 + 2)}{\sqrt{1+u^2}(3+2u^2)^2}, 0\right), \\ \nabla\lambda_2 &= \left(0, \frac{1}{(1+u^2)^{\frac{3}{2}}}, 0\right), \\ \nabla\lambda_3 &= \left(0, \frac{2((\sqrt{1+u^2} - \sqrt{3}u)^2 + 2)}{\sqrt{1+u^2}(3+2u^2)^2}, 0\right).\end{aligned}\tag{B.2}$$

Thus

$$\begin{aligned}\nabla\lambda_1 \cdot R_1 &= -\frac{2}{\sqrt{3}} \frac{((\sqrt{1+u^2} + \sqrt{3}u)^2 + 2)}{n(3+2u^2)^2} \neq 0, \\ \nabla\lambda_2 \cdot R_2 &= 0, \\ \nabla\lambda_3 \cdot R_3 &= \frac{2}{\sqrt{3}} \frac{((\sqrt{1+u^2} - \sqrt{3}u)^2 + 2)}{n(3+2u^2)^2} \neq 0.\end{aligned}\tag{B.3}$$

This proves the genuine nonlinearity of the first and third characteristic fields and the linearly degenerate of the second one.  $\square$



---

# Appendix C

## Front Tracking Algorithm

We now describe an algorithm which generates approximate solutions of a front tracking scheme to the original Cauchy problem (3.6) with  $U(0, x) = U_0(x)$ . Having solved all the Riemann problems at time  $t = 0$ , the approximate solution  $U$  can be prolonged until a first time  $t_1$  is reached, when two wave-fronts interact. Since  $U(t_1, \cdot)$  is still piecewise constant function, the corresponding Riemann problems can again be approximately solved within the class of piecewise constant functions. The solution  $U$  is then continued up to a time  $t_2$  where a second interaction takes place, etc. We remark that, by an arbitrary small change in the speed of one of the wave fronts, it is not restrictive to assume that at most two incoming fronts collide, at each given time  $t < 0$ . This will considerably simplify all subsequent analysis, since we don't need to consider the case where three or more incoming fronts meet together.

Before we proceed further, we introduce some notation. Front tracking will produce piecewise constant function labeled  $U(t, x)$  that has, at least initially, some finite number  $N$  of fronts.

We calculated the intermediate states  $U_i = (p_i, u_i)$  in Section 6.2. In order to finish the

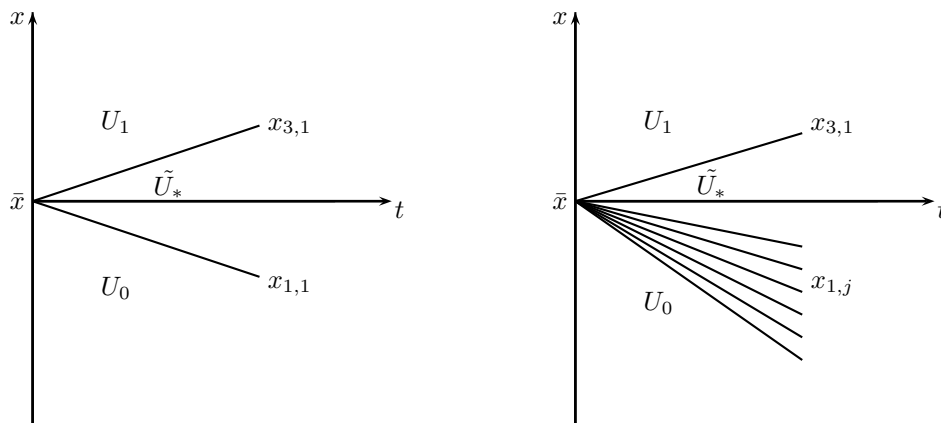


Figure C.1: Piecewise constant approximate solution to the Riemann problem.

## APPENDIX C. FRONT TRACKING ALGORITHM

---

construction of the approximate solutions for all  $t \geq 0$ , we calculate the locations  $x_{i,j}(t)$  of the fronts. At each point of interaction  $(\bar{t}, \bar{x})$  of the two generalized shocks we have two possibilities.

- (i) Let the interaction of two generalized shocks are of the different families  $i, j \in \{1, 3\}$  and entropy shock with non-entropy shock of the same family see Figures 7.3, 7.2, then we have the locations of the fronts

$$x_{k,1}(t) = s_k(t - \bar{t}) + \bar{x}, \quad k \in \{1, 3\} \quad \text{see Figure C.1 on the left.} \quad (\text{C.1})$$

- (ii) Let the interaction of two entropy shocks of the same family see Figure 7.4, then we have the locations of the fronts

$$x_{k,j}(t) = s_j(t - \bar{t}) + \bar{x}, \quad k \in \{1, 3\}, \quad j = 1, \dots, N, \quad \text{see Figure C.1 on the right,} \quad (\text{C.2})$$

where  $s_j$  is the speed of fronts, with  $s_k > s_{k+1}$ . As soon as the states  $(p_i, u_i)$  and the locations  $x_{i,j}(t)$  have been determined. Then we finish the front tracking algorithm to define an approximate solution.



---

# Bibliography

- [1] M.A.E. Abdelrahman and M. Kunik. The ultra-relativistic Euler equations. *Preprint No 11. Otto-von-Guericke University Magdeburg*, 2012.
- [2] M.A.E. Abdelrahman and M. Kunik. A new front tracking scheme for the ultra-relativistic Euler equations. *Preprint No 18. Otto-von-Guericke University Magdeburg*, 2013.
- [3] M.A.E. Abdelrahman and M. Kunik. The interaction of waves for the ultra-relativistic Euler equations. *J. Math. Anal. Appl*, 409(2):1140–1158, 2014.
- [4] H.D. Alber. Local existence of weak solutions to the quasilinear wave equation for large initial values. *Math. Z*, 190:249–276, 1985.
- [5] H.D. Alber. Global existence and large time behaviour of solutions for the equations of nonisentropic gas dynamics to initial values with unbounded support. *Preprint No. 15, Sonderforschungsbereich 256, Rheinische Friedrich-Wilhelms-Universität Bonn*, 1988.
- [6] F. Ancona and A. Marson. A wavefront tracking algorithm for  $n \times n$  nongenuinely nonlinear conservation laws. *J. Differential Equations*, 177:454–493, 2001.
- [7] F. Ancona and A. Marson. Basic estimates for a front tracking algorithm for general  $2 \times 2$  conservation laws. *12(2):155–182*, 2002.
- [8] F. Ancona and A. Marson. Well-posedness for general  $2 \times 2$  systems of conservation laws. *Mem. Amer. Math. Soc*, 169, 2004.
- [9] F. Ancona and A. Marson. Existence theory by front tracking for general nonlinear hyperbolic system. *Arch. Rational Mech. Anal*, 185:287–340, 2007.
- [10] P. Baiti and H.K. Jenssen. On the front tracking algorithm. *J. Math. Anal. Appl.*, 217:395–404, 1998.
- [11] P. Baiti and E.D. Santo. Front tracking for a  $2 \times 2$  system of conservation laws. *E. J. Diff. Equations*, 220:1–14, 2012.
- [12] A. Bressan. Global solutions to systems of conservation laws by wavefront tracking. *J. Math. Anal. Appl*, 170:414–432, 1992.
- [13] A. Bressan. Lecture notes on conservation laws. *S.I.S.S.A., Trieste*, 1995.
- [14] A. Bressan. *Hyperbolic Systems of Conservation Laws. The One Dimensional Cauchy Problem*. Springer-Verlag Berlin Heidelberg New York, 2000.

## BIBLIOGRAPHY

---

- [15] A. Bressan and R.M. Colombo. The semigroup generated by  $2 \times 2$  systems of conservation laws. *Arch. Rational Mech. Anal*, 133:1–75, 1995.
- [16] A. Bressan, G. Crasta, and B. Piccoli. Well-posedness of the cauchy problem for  $n \times n$  systems of conservation laws. *Mem. Am. Math. Soc., Providence*, 2000.
- [17] A. Bressan and P. LeFloch. Uniqueness of weak solution to systems of conservation laws. *Arch. Rational Mech. Anal*, 140:301–317, 1997.
- [18] T. Chang and L. Hsiao. *The Riemann problem and interaction of waves in gas dynamics*. Longman Scientific and Technical, Pitman Monographs and Surveys in Pure and Applied Mathematics, 1989.
- [19] J. Chen. Conservation laws for the relativistic p-system. *Comm. Partial Differential Equations*, 20:1602–1646, 1995.
- [20] I.L. Chern, J. Glimm, O. McBryan, B. Plohr, and S. Yaniv. Front tracking for gas dynamics. *J. Comput. Phys*, 62:83–110, 1986.
- [21] R. Courant and K.O. Friedrichs. *Supersonic flow and shock waves*. Springer, New York, 1999.
- [22] C.M. Dafermos. Polygonal approximations of solutions of the initial value problem for a conservation law. *J. Math. Anal. Appl*, 38:33–41, 1972.
- [23] C.M. Dafermos. The entropy rate admissibility criterion for solutions of hyperbolic conservation laws. *J. Diff. Eqs*, 14:202–212, 1973.
- [24] C.M. Dafermos. *Hyperbolic conservation laws in continuum physics*. Springer, Berlin, 2000.
- [25] R.J. Diperna. Global existence of solutions to nonlinear hyperbolic systems of conservation laws. *J. Comm. Differential Equations*, 20:187–212, 1976.
- [26] W. Dreyer, M. Herrmann, and M. Kunik. Kinetic solutions of the boltzmann-peierls equation and its moment systems. *Cont. Mech. Thermodyn*, 16:453–469, 2004.
- [27] W. Dreyer and M. Kunik. The maximum entropy principle revisited. *Cont. Mech. Thermodyn*, 10:331–347, 1998.
- [28] W. Dreyer and M. Kunik. Hyperbolic heat conduction. *Trends in applications of Mathematics to Mechanics, Chapman & Hall /CRC Monographs and Surveys in pure and applied Mathematics*, 106:127–137, 1999.
- [29] W. Dreyer and M. Kunik. Initial and boundary value problems of hyperbolic heat conduction. *Cont. Mech. Thermodyn*, 11.4:227–245, 1999.
- [30] W. Dreyer and H. Struchtrup. Heat pulse experiments revisited. *Cont.Mech.Thermodyn*, 5:1993, 3-50.
- [31] C. Eckart. "the thermodynamics of irreversible process I: The simple fluid". *Phys. Rev*, 58:267–269, 1940.

- 
- [32] C. Eckart. "the thermodynamics of irreversible process III: Relativistic theory of the simple fluid". *Phys. Rev*, 58:269–275, 1940.
- [33] C. Eckart. "the thermodynamics of irreversible process III: Relativistic theory of the simple fluid". *Phys.Rev*, 58:919–928, 1940.
- [34] L.C. Evans. *Partial Differential Equations*. Oxford University Press, 2000.
- [35] K.O. Friedrichs and P.D. Lax. Systems of conservation equations with a convex extension. *Proc. Acad. Sci. USA*, 68(8):1686–1688, 1971.
- [36] J. Glimm. Solution in the large for nonlinear hyperbolic systems of equations. *Comm. Pure. Appl. Math*, 18:697–715, 1965.
- [37] E. Godlewski and P.A. Raviart. *Numerical approximation of hyperbolic systems of conservation laws*. Springer, New York, 1996.
- [38] H. Holden, L. Holden, and R. Høegh-Krohn. A numerical method for first order nonlinear scalar conservation laws in one-dimension. *Comput. Math. Applic*, 15(6-8):595–602, 1988.
- [39] H. Holden and N.H. Risebro. *Front Tracking for Conservation Laws*. Springer-Verlag Berlin Heidelberg New York, 2000.
- [40] E. Isaacson and B. Temple. Convergence of the  $2 \times 2$  godunov method for a general resonant nonlinear balance law. *SIAM J. Appl. Math*, 55:625–640, 1995.
- [41] J.A. Font J.M. Martí, E. Müller and J.M. Ibáñez. Morphology and dynamics of highly supersonic relativistic jets. *Astrophysics. J*, 448:105–108, 1995.
- [42] F. Jüttner. Die relativistische quantentheorie des idealen gases. *Z. Phys*, 47:542–566, 1928.
- [43] B. Keyfitz and H.C. Kranzer. A viscosity approximation to a system of hyperbolic conservation laws with no classical riemann solution. in *Nonlinear hyperbolic problems, Carasso et al. (eds.)*, *Lecture notes in mathematics*, 1402:185–198, (1988).
- [44] D. Kröner. *Numerical schemes for conservation laws*. John Wiley and Sons, Chichester, 1997.
- [45] M. Kunik. *Selected Initial and Boundary Value Problems for Hyperbolic Systems and Kinetic Equations*. PhD thesis, Otto-von-Guericke University Magdeburg, 2005.
- [46] M. Kunik. *Lecture Note on Numerics for Hyperbolic Conservation Laws*. Otto-von-Guericke University Magdeburg, 2012.
- [47] M. Kunik, S. Qamar, and G. Warnecke. Kinetic schemes for the ultra-relativistic Euler equations. *J.Comput.Phys*, 187:572–596, 2003.
- [48] M. Kunik, S. Qamar, and G. Warnecke. Second-order accurate kinetic schemes for the ultra-relativistic Euler equations. *J. Comput. Phys*, 192:695–726, 2003.
- [49] M. Kunik, S. Qamar, and G. Warnecke. Kinetic schemes for the relativistic gas dynamics. *Numerische Mathematik*, 97:159–191, 2004.

## BIBLIOGRAPHY

---

- [50] P.D. Lax. Hyperbolic systems of conservation laws, ii,. *Comm. Pure Appl. Math*, 10:537–566, 1957.
- [51] P.D. Lax. *Hyperbolic systems of conservation laws and mathematical theory of shock waves*. SIAM Regional Conf. Ser. Appl. Math, 1972.
- [52] R.J. LeVeque. *Numerical methods for conservation laws*. Birkhäuser Verlag Basel, Switzerland, 1992.
- [53] R.J. LeVeque. *Finite Volume Methods for Hyperbolic Problems*. Cambridge University Press, 2002.
- [54] L. Lin. On the vacuum state for the equations of isentropic gas dynamics. *J. Math. Anal. Appl*, 121:406–425, 1987.
- [55] T.P. Liu. The riemann problem for general  $2 \times 2$  conservation laws. *Trans. Am. Math.Soc*, 199:89–112, 1974.
- [56] T.P. Liu. Existence and uniqueness theorems for riemann problems. *Trans. Am. Math.Soc*, 212:375–382, 1975.
- [57] T.P. Liu. The riemann problem for general systems of conservation laws. *J. Diff. Eqs*, 18:218–234, 1975.
- [58] T.P. Liu. The entropy condition and the admissibility of shocks. *J. Math. Anal. Appl*, 53:78–88, 1976.
- [59] T.P. Liu. Uniqueness of weak solutions of the cauchy problem for general  $2 \times 2$  conservation laws. *J. Diff. Equations*, 20:369–388, 1976.
- [60] T.P. Liu. Solutions in the large for the equations of nonisentropic gas dynamics. *Ind. Univ. Math. J.*, 26(1), 1977.
- [61] A. Majda. *Compressible Fluid Flow and Systems of Conservation Laws in Several Space Variables*. Appl. Mat. Sci, Springer, 1984.
- [62] J.M. Martí and E. Müller. Extension of the piecewise parabolic method to one-dimensional relativistic hydrodynamics. *J. Comp. Phys*, 123:1–14, 1996.
- [63] J.M. Martí and E. Müller. Numerical hydrodynamics in special relativity. *Living Rev*, 2:1–101, 1999.
- [64] T. Nishida and J. Smoller. Solutions in the large for some nonlinear hyperbolic conservation laws. *Comm. Pure Appl. Math*, 26:183–200, 1973.
- [65] H. Ohwa. On the wave-front tracking algorithm for  $2 \times 2$  hyperbolic system of conservation laws. *J. Math. Anal. Appl.*, 172:172–181, 2013.
- [66] O.A. Oleinik. Discontinuous solutions of nonlinear differential equations. *Amer. Math. Soc. Trans*, 26:95–172, 1957.

- 
- [67] V. Pant. Global entropy solutions for isentropic relativistic fluid dynamics. *Comm. Partial Diff. Eqs*, 21:1609–1641, 1996.
- [68] S. Qamar. *Kinetic schemes for the relativistic hydrodynamics*. PhD thesis, Faculty of Mathematics, Otto-von-Guericke University Magdeburg, 2003.
- [69] M. Reintjes. *Shock Wave Interactions in General Relativity and the Emergence of Regularity Singularities*. PhD thesis, University of California - Davis, September 2011.
- [70] N.H. Risebro. A front tracking alternative to the random choice method. *Proc. Am. Math. Soc*, 117:1125–1139, 1993.
- [71] N.H. Risebro and A. Tveito. Front tracking applied to a nonstrictly hyperbolic system of conservation laws. *SIAM J.Sci.Statist.Comput*, 12:1401–1419, 1991.
- [72] N.H. Risebro and A. Tveito. A front tracking method for conservation laws in one dimension. *J. Comput. Phys*, 101:130–139, 1992.
- [73] D. Serre. *Systems of conservation laws*. Cambridge University Press, Cambridge, 1999.
- [74] J. Smoller. *Shock Waves and Reaction-Diffusion Equations*. Springer-Verlag New York Heidelberg Berlin, 1994.
- [75] J. Smoller and B.Temple. Global solutions of the relativistic Euler equations. *Commun.Math.Phys*, 156:67–99, 1993.
- [76] B. Temple. Solutions in the large for the nonlinear hyperbolic conservation laws of gas dynamics. *J. Diff. Eqs*, 1:96161, 1981.
- [77] E.F. Toro. *Riemann Solvers and Numerical Methods for Fluid Dynamics*. Springer, Berlin, 1999.
- [78] R.M. Wald. *General Relativity*. The University of Chicago Press, Chicago and London, 1984.
- [79] S. Weinberg. *Gravitation and cosmology*. Wiley New York, 1972.
- [80] B. Wendroff. An analysis of front tracking for chromatography. *Acta Appl. Math*, 30:265–285, 1993.
- [81] B.D. Wissman. Global solutions to the ultra-relativistic Euler equations. *Commun. Math. Phys*, 306:831–851, 2011.
- [82] J.A.S. Witteveen. Second order front tracking for the Euler equations. *J.Comput.Phys*, 229(7):2719–2739, 2010.
- [83] J.A.S. Witteveen, B. Koren, and P.G. Bakker. An improved front tracking method for the Euler equations. *J.Comput.Phys*, 224:712–728, 2007.



# Curriculum Vitae

## Personal Information

Name	<b>Mahmoud Abdelaziz Elbiomy Abdelrahman</b>
Date of birth	26.02.1983
Nationality	Egyptian
Place of birth	Elmansoura, Egypt
Status	Married, two Children
Current job	Assistant Lecturer, Department of Mathematics Faculty of Science, Mansoura University
E-mail	mahmoud.abdelrahman@st.ovgu.de mahmoud.abdelrahman@mans.edu.eg mahmoud.abdelrahman1983@yahoo.de

## Education

2000 - 2003	Bachelor in Mathematics (Excellent With Honor), Department of Mathematics, Faculty of Science, Mansoura University, Egypt.
2005 - 2009	M.Sc. in Mathematic, Department of Mathematics, Faculty of Science, Mansoura University, Egypt.
2010 - 2013	PhD student, Institute for Analysis and Numerics, Faculty of Mathematics, Otto-von-Guericke University, Magdeburg, Germany.

## Academic Honors

- Scholarship from the Egyptian government in the Long Term Mission system (2010 - 2013).

## Work Experience

2003-2009	Teacher Instructor and Researcher. Department of Mathematics, Faculty of Science. University of Mansoura, Egypt.
-----------	---

## CURRICULUM VITAE

---

### References

- |   |  |
|---|--|
| Apl. Prof. Dr. Matthias Kunik               | Institute for Analysis and Numerics,<br>Otto-von-Guericke University Magdeburg,<br>Germany |
| Prof. Dr. Gerald Warnecke                   | Institute for Analysis and Numerics,<br>Otto-von-Guericke University Magdeburg,<br>Germany |
| Assistant. Prof. Dr. Magdi Hakeem Armanious | Department of Mathematics,<br>Faculty of Science, University of Mansoura,<br>Egypt         |

### Conference - Workshop

- 10th Workshop of Mathematical Theory and Numerical Analysis for Conservation Laws. 04-10 September 2011, Austria.
- 83rd Annual Scientific Conference of Applied Mathematics and Mechanics. 26-30 March 2012, Germany.
- 14th International Conference on Hyperbolic Problems: Theory, Numerics, Applications. 25-29 June 2012, Padova, Italy.
- International Conference on Applied Mathematics and Computational Science (AMMCS). 26-30 August 2013, Canada.
- 11th Workshop of Mathematical Theory and Numerical Analysis for Conservation Laws. 08-14 September 2013, Austria.

### List of Publication

- Mahmoud Abdelaziz Elbiomy Abdelrahman  
Constructions of Semi-Planar Steiner Quasigroups, Master Thesis, Department of Mathematics, Mansoura University (2007).
- M.H. Armanious, M.A. Elbiomy, On semi-planar Steiner quasigroups. *Discrete Mathematics* 309 (4): 686-692 (2009).
- Juergen Geiser , Mahmoud Elbiomy, Splitting Method of Convection-Diffusion Methods with Disentanglement methods. *Disentanglement Methods*, Preprint No 2. Humboldt-Universität zu Berlin, (2010).
- Mahmoud Abdelrahman, Matthias Kunik and Gerald Warnecke , On the Ultra-Relativistic Euler Equations. *Proc. Appl. Math. Mech.* 12, 597-598 (2012).
- Mahmoud A.E. Abdelrahman and M. Kunik. The ultra-relativistic Euler equations. Preprint No 11. Otto-von-Guericke University, (2012).



- Mahmoud A.E. Abdelrahman and M. Kunik. The interaction of waves for the ultra-relativistic Euler equations. In Press, Accepted Manuscript, Available online in Journal of Mathematical Analysis and Applications, (12 July 2013).
- Mahmoud A.E. Abdelrahman and Matthias Kunik, A new Front Tracking Scheme for the Ultra-Relativistic Euler Equations. Preprint No 18. Otto-von-Guericke University, (2013).

---

## Schriftliche Erklärung

Ich erkläre hiermit, dass ich die vorliegende Arbeit ohne unzulässige Hilfe Dritter und ohne Benutzung anderer als der angegebenen Hilfsmittel angefertigt habe. Die aus fremden Quellen direkt oder indirekt übernommenen Gedanken sind als solche kenntlich gemacht.

Insbesondere habe ich nicht die Hilfe einer kommerziellen Promotionsberatung in Anspruch genommen. Dritte haben von mir weder unmittelbar noch mittelbar geldwerte Leistungen für Arbeiten erhalten, die im Zusammenhang mit dem Inhalt der vorgelegten Dissertation stehen.

Die Arbeit wurde bisher weder im Inland noch im Ausland in gleicher oder ähnlicher Form als Dissertation, Diplom- oder ähnliche Prüfungsarbeit eingereicht und ist als Ganzes auch noch nicht veröffentlicht.

Mahmoud Abdelaziz Elbiomy Abdelrahman,  
Magdeburg, 22.08.2013.